



universidad  
de león

**INSTITUTO DE MEDIO AMBIENTE, RECURSOS  
NATURALES Y BIODIVERSIDAD**

**Grupo de Ingeniería Química, Ambiental y Bioprocesos**

**CONTRIBUTIONS TOWARDS PRACTICAL  
APPLICATION OF MICROBIAL  
ELECTROSYNTHESIS**

*Directores:*

*Tesis doctoral presentada por:*

*Antonio Morán Palao*

***Raúl Mateos González***

*Adrián Escapa González*

*Para optar al grado de Doctor*

*Ana Sotres Fernández*

León, Noviembre 2018



## *AGRADECIMIENTOS*

*Me gustaría agradecer a todas las personas que me han apoyado y han contribuido a este trabajo, por estar ahí en los buenos y en los malos momentos, y principalmente porque siento que este trabajo es en parte suyo también.*

*Como pilares fundamentales de este trabajo me gustaría dar las gracias a mis directores, que espero que estén orgullosos de mi trabajo, y de los que me gustaría destacar algunas de sus muchas virtudes. A Antonio Morán por llevar el peso de este grupo de investigación, por darme esta oportunidad, confiar en mí desde el primer momento y ejercer de mentor tanto para mí como para tantos otros compañeros. A Adrián Escapa por hacerme mejor investigador con su crítica constructiva y su exigencia, por complementar mis mayores defectos a lo largo de este trabajo, y por estar siempre dispuesto a solucionar cualquier problema. A Ana Sotres por aparecer y aportar un punto de vista diferente, y por pelear con fuerza para darle una calidad a esta tesis que yo no habría sido capaz de darle. En definitiva, muchas gracias a las tres personas a las que más me gustaría que agradara mi trabajo.*

*A mis compañeros del Instituto de Recursos Naturales y del grupo de investigación, que han sido muchos a lo largo de este tiempo, y con los que he compartido éxitos y fracasos durante muchas horas de trabajo. A Raúl, Guille, Gabriella, Christian, Judith G., Rubén M., Sergio, Benja, Graciela, Raquel P., Rebeca, Noemí, Marcia, Dani, Rubén G., Diego, Julio, Raquel B., Camilla, Natalia, y quizá en especial a Isa con la que he compartido este camino prácticamente de inicio a fin. También a los profesores Xiomar, Olegario, Marta Elena, Jorge, Fernando, Judith M., Camino y Guillermo R., así como a Juan, Carmen y Fernando por toda su ayuda. Soy consciente de que otra mucha gente ha pasado a mi lado a lo largo de esta tesis y les pido disculpas si no han sido nombrados.*

*También me gustaría agradecer al Ministerio de Educación, Cultura y Deporte por la beca predoctoral para formación de profesorado universitario FPU14/01573 en la que se enmarca esta tesis. También por concederme una ayuda complementaria a mi beca FPU para realizar una estancia breve en Bélgica.*

*I would like to thank Dr. Deepak Pant for giving me the opportunity to stay at VITO (Belgium) for three months, and for his supervision during this highly successful research visit. I would also like to thank all my colleagues there for their help and friendship.*

*Me gustaría hacer mención especial a mi familia ya que son los que han construido todo lo que soy hasta este momento. En especial a mis padres porque me lo han dado todo y me han empujado a conseguir todo lo que se ha puesto en mi camino desde que tengo un mínimo recuerdo. Y a mi hermano que siempre será una parte de mí en todo lo que haga a lo largo de mi vida.*

*Y por último gracias a Esther porque es quien a lo largo de estos años más ha sufrido conmigo los malos momentos, y más ha disfrutado conmigo de los buenos. Y además, y principalmente, por quererme como soy.*

*Gracias a todos.*

---

<b>TABLE OF CONTENTS</b> .....	I
<b>INDEX OF TABLES</b> .....	VII
<b>INDEX OF FIGURES</b> .....	IX
<b>TABLA DE CONTENIDOS</b> .....	XIII
<b>ÍNDICE DE TABLAS</b> .....	XIX
<b>ÍNDICE DE FIGURAS</b> .....	XXI
<b>ABSTRACT</b> .....	XXV
<b>RESUMEN</b> .....	XXVII
<b>LIST OF ABBREVIATIONS</b> .....	XXIX

## **TABLE OF CONTENTS**

### ***Chapter 1. Introduction***

<b><i>1.1 Microbial Electrochemical Technologies</i></b> .....	3
<b><i>1.2 Microbial Electrochemical Technologies for CO<sub>2</sub> Valorization - Microbial electrosynthesis</i></b> .....	5
<i>1.2.1 MES fundamentals and microbial ecology</i> .....	8
<i>1.2.2 Microbial electrosynthesis of chemicals and fuels</i> .....	11
<i>1.2.2.1 Key electro-biochemicals produced from CO<sub>2</sub></i> .....	11
<i>1.2.2.2 Electro-biofuels: electromethanogenesis and biogas upgrading</i> .....	13
<i>1.2.2.3 Product recovery</i> .....	14
<i>1.2.3 MES weaknesses and opportunities</i> .....	15
<b><i>1.3 References</i></b> .....	17

### ***Chapter 2. Objectives and thesis outline***

<b><i>2.1 Objectives</i></b> .....	33
------------------------------------	----

---

<i>2.2 Thesis outline</i> .....	33
---------------------------------	----

## ***Chapter 3. Materials and Methods***

<b><i>3.1 Experimental set-up</i></b> .....	39
3.1.1 <i>Conical test cell</i> .....	39
3.1.2 <i>Planar reactors</i> .....	39
3.1.3 <i>Bottle type reactors</i> .....	40
3.1.4 <i>H-type reactors</i> .....	41
<b><i>3.2 Inocula and culture media</i></b> .....	42
3.2.1 <i>Inocula</i> .....	42
3.2.2 <i>Culture media</i> .....	42
<b><i>3.3 Analytical and electrochemical techniques</i></b> .....	43
<b><i>3.4 Molecular biology techniques</i></b> .....	43
<b><i>3.5 Calculations</i></b> .....	44
<b><i>3.6 References</i></b> .....	45

## ***Chapter 4. Methodology for fast and facile characterisation of carbon-based electrodes focused on Bioelectrochemical Systems development and scale-up***

<b><i>4.1 Introduction</i></b> .....	50
<b><i>4.2 Experimental</i></b> .....	51
4.2.1 <i>Methodology proposal</i> .....	51
4.2.2 <i>Determination of electroactive area</i> .....	51
4.2.3 <i>Determination of fractal dimension (<math>D_f</math>)</i> .....	52
4.2.4 <i>Method validation</i> .....	53

---

---

4.2.5 Cell set-up and instrumentation.....	55
<b>4.3 Results and discussion .....</b>	<b>56</b>
4.3.1 Estimation of electroactive area .....	57
4.3.2 Determination of the fractal dimension.....	59
<b>4.4 Conclusions .....</b>	<b>63</b>
<b>4.5 References .....</b>	<b>64</b>
<b>Chapter 5. Impact of the start-up process on the microbial communities in biocathodes for electrosynthesis</b>	
<b>5.1 Introduction.....</b>	<b>72</b>
<b>5.2 Materials and Methods .....</b>	<b>74</b>
5.2.1 MES reactors set-up.....	74
5.2.2 Start-up strategies and operation .....	74
5.2.3 Influent and inocula .....	76
5.2.4 Measurements and analytical techniques .....	77
5.2.5 High throughput sequencing of massive 16S rRNA gene libraries.....	77
<b>5.3 Results.....</b>	<b>78</b>
5.3.1 Cell performance .....	78
5.3.1.1 Current production .....	78
5.3.1.2 Product formation.....	79
5.3.2 Microbial community assessment .....	81
5.3.2.1 Diversity indices analysis .....	81
5.3.2.2 Eubacterial community structure.....	83
5.3.2.3 Archaeal community structure .....	88

---

---

<i>5.4 Discussion</i> .....	89
<i>5.5 Conclusions</i> .....	93
<i>5.6 References</i> .....	94

***Chapter 6. Enhanced CO<sub>2</sub> conversion through MES by continuous headspace recirculation***

<i>6.1 Introduction</i> .....	104
<i>6.2 Materials and Methods</i> .....	105
<i>6.2.1 MES reactors set-up</i> .....	105
<i>6.2.2 Influent and inoculum</i> .....	106
<i>6.2.3 Experimental procedure</i> .....	107
<i>6.2.4 Measurements and analytical techniques</i> .....	107
<i>6.2.5 Microbial community analysis</i> .....	107
<i>6.3 Results</i> .....	108
<i>6.3.1 CO<sub>2</sub> recirculation effect on MES</i> .....	108
<i>6.3.2 Microbial communities involved in the process</i> .....	112
<i>6.4 Discussion</i> .....	116
<i>6.5 Conclusions</i> .....	119
<i>6.6 Bibliography</i> .....	120

***Chapter 7. Microbial electrosynthesis (MES) from CO<sub>2</sub> is resilient to fluctuations in renewable energy supply***

<i>7.1. Introduction</i> .....	128
<i>7.2. Materials and Methods</i> .....	129
<i>7.2.1 Microbial electrosynthesis reactor</i> .....	129



---

7.2.2 Carbon source, electrolyte and inoculum .....	130
7.2.3 Set-up .....	131
7.2.4 Bioelectrochemical analyses.....	131
7.2.5 Scanning electron microscopy (SEM).....	131
7.2.6 Microbial community analysis.....	132
<b>7.3. Results and discussion .....</b>	<b>132</b>
7.3.1 Current supply interruptions on H-Cell MES reactor .....	132
7.3.2 SEM.....	136
7.3.3 Microbial community analysis.....	137
7.3.3.1 Microbial diversity assessment .....	137
7.3.3.2 Microbial community composition.....	138
7.3.3.3 The role of main identified genera .....	140
7.3.4 Technological and commercial perspectives .....	141
<b>7.4. Conclusion.....</b>	<b>143</b>
<b>7.5. References .....</b>	<b>144</b>
<b>Chapter 8. Long-term open circuit MES system promotes methanogenesis</b>	
<b>8.1. Introduction.....</b>	<b>150</b>
<b>8.2. Materials and Methods .....</b>	<b>151</b>
8.2.1 MES reactors set up.....	151
8.2.2 Inoculum, influents and experimental procedure .....	151
8.2.3 Analytical techniques.....	152
8.2.4 Microbial community analysis.....	152

---

---

8.2.5 Scanning electron microscopy (SEM).....	153
<b>8.3. Results and discussion .....</b>	<b>153</b>
8.3.1 Previous operating history.....	153
8.3.2 Biocathode evolution and performance.....	154
8.3.3 Role of microbial communities involved in the process.....	156
<b>8.4. Conclusions .....</b>	<b>160</b>
<b>8.5. Bibliography.....</b>	<b>161</b>
 <b>Chapter 9. Conclusions and future work</b>	
<b>9.1 Conclusions.....</b>	<b>167</b>
<b>9.2 Future work.....</b>	<b>170</b>
 <b>Appendixes</b>	
<b>Appendix I.....</b>	<b>175</b>
<b>Appendix II.....</b>	<b>179</b>
<b>Appendix III.....</b>	<b>181</b>

---

## INDEX OF TABLES

### ***Chapter 4. Methodology for fast and facile characterisation of carbon-based electrodes focused on Bioelectrochemical Systems development and scale-up.....***

<i>Table 4.1: Material specification and coding.....</i>	54
<i>Table 4.2: Ohmic drop of each cell set-up. The standard error of the mean estimates the uncertainty associated to the determination of the ohmic drop.....</i>	57
<i>Table 4.3: Electroactive areas.....</i>	58
<i>Table 4.4: Fractal parameter comparison of different electrodes using CV measurements. The value presented alongside the fractal parameter <math>\alpha</math> represents the 90% confidence intervals for each estimated parameter.....</i>	60

### ***Chapter 5. Impact of the start-up process on the microbial communities in biocathodes for electrosynthesis***

<i>Table 5.1: Maximum recorded currents for each strategy and lag periods observed.....</i>	79
<i>Table 5.2: Cell performance for each start-up strategy.....</i>	81
<i>Table 5.3: Estimated richness (observed OTUs and Chao1) and diversity indexes (Shannon (<math>H'</math>) and 1/Simpson) for Eubacterial operational taxonomic units (OTUs), calculated with MOTHUR at the 3% distance level.....</i>	82
<i>Table 5.4: Estimated richness (observed OTUs and Chao1) and diversity indices (Shannon (<math>H'</math>) and 1/Simpson) for Archaeal operational taxonomic units (OTUs), calculated with MOTHUR at the 3% distance level.....</i>	83

### ***Chapter 6. Enhanced CO<sub>2</sub> conversion through MES by continuous headspace recirculation***

<i>Table 6.1: Acetic acid production summary, including averages for both MES and standard deviation.....</i>	111
<i>Table 6.2: Carbon balance and cathodic efficiency. Averages between both MES replicate reactors (MES1 and MES2) are shown.....</i>	111

---

## ***Chapter 7. Microbial electrosynthesis (MES) from CO<sub>2</sub> is resilient to fluctuations in renewable energy supply***

***Table 7.1: Average current density and recovery time comparison between MES fed with bicarbonate and fed with CO<sub>2</sub> gas .....*** 135

***Table 7.2: N° of sequences and OTUs, estimated richness (Chao1), diversity index (Shannon) and sample coverage values for Eubacterial operational taxonomic units (OTUs).....*** 138

## ***Chapter 8. Long-term open circuit MES system promotes methanogenesis***

***Table 8.1: Archaeal communities in the biofilm and supernatant at family level ..*** 159

---

## INDEX OF FIGURES

### ***Chapter 1. Introduction***

<b><i>Figure 1.1: Basic comparative diagrams for MFC, MEC and MES. ....</i></b>	<b>4</b>
<b><i>Figure 1.2: Current captured CO<sub>2</sub> uses. Figure based on NETL-CO<sub>2</sub> utilization original.....</i></b>	<b>6</b>
<b><i>Figure 1.3: General diagram of a potentiostatically controlled model MES system showing (I) direct electron transfer based product generation and (II) an example of hydrogen mediated product generation at the cathode. At the anode, water oxidation provides electrons for the cathode reactions. WE, CE and RE stand for working, counter and reference electrodes, respectively. ....</i></b>	<b>8</b>

### ***Chapter 2. Objectives and thesis outline***

<b><i>Figure 2.1: General overview of this thesis .....</i></b>	<b>36</b>
---	-----------

### ***Chapter 3. Materials and Methods***

<b><i>Figure 3.1: Conical test cell.....</i></b>	<b>39</b>
<b><i>Figure 3.2: Planar reactor .....</i></b>	<b>40</b>
<b><i>Figure 3.3: Bottle-type reactor. Real image and diagram. ....</i></b>	<b>41</b>
<b><i>Figure 3.4: H-type reactor .....</i></b>	<b>41</b>

### ***Chapter 4. Methodology for fast and facile characterisation of carbon-based electrodes focused on Bioelectrochemical Systems development and scale-up***

<b><i>Figure 4.1: 0.5cm-thick carbon felt (a), 0.25cm-thick carbon felt (b), carbon paper (c) and brush (d) electrodes.....</i></b>	<b>54</b>
<b><i>Figure 4.2: Carbon paper electrode with air bubbles after pre-treatment .....</i></b>	<b>55</b>
<b><i>Figure 4.3: Cell diagram (WE: Working electrode; RE: Reference electrode; CE: Counter electrode) and cell assembly.....</i></b>	<b>56</b>

---

<b>Figure 4.4:</b> Randles-Ševčík plot a: Thick felt (TF); b: Fine felt (FF); c: Paper (P); d: Brush (B).....	58
<b>Figure 4.5:</b> Linear trend in the logarithmic representation of $I_{pc}$ vs. $v$ .....	60
<b>Figure 4.6:</b> Fractal dimension of the electrodes tested. The values corresponding to Euclidean integer dimensions are shown as red solid lines. ....	61
<b>Figure 4.7:</b> Relationship between fractal dimension and EA/AS for each material tested. Black diamond points show the centroids of electrode clusters. ....	62
<b>Chapter 5. Impact of the start-up process on the microbial communities in biocathodes for electrosynthesis</b>	
<b>Figure 5.1.</b> Strategies overview.....	75
<b>Figure 5.2.</b> Averaged acetic acid concentration at the end of every batch cycle and for each strategy (error bars show standard deviation for three replicates). Day 0 corresponds to inoculation.....	80
<b>Figure 5.3:</b> Taxonomic classification of high throughput sequencing at phylum level. ....	84
<b>Figure 5.4:</b> Taxonomic classification of sequencing results of 16S rRNA gene from Eubacterial communities at a family level of a) samples from S2, b) samples from S3 and c) samples from S4. Groups accounting for less than 1% of the total number of sequences per sample were classified as 'others'. ....	85
<b>Figure 5.5:</b> Heatmap summarising the main genera present at the anode and cathode biofilms for the three strategies where a biofilm developed.....	87
<b>Figure 5.6:</b> Taxonomic assignment of Archaeal microbial communities of AD and RM inocula, and cathode samples taken from S2 and S3 strategies at a genus level. Groups accounting for less than 1% of the total number of sequences per sample were classified as 'others'. ....	89
<b>Chapter 6. Enhanced CO<sub>2</sub> conversion through MES by continuous headspace recirculation</b>	
<b>Figure 6.1:</b> Image and diagram of reactor set-up. CE: Counter electrode; RE: Reference electrode; WE: Working electrode. ....	106

---

---

<b>Figure 6.2:</b> Evolution of polarization curve currents along the experiment.....	109
<b>Figure 6.3:</b> Acetic acid concentration along the experimental period (Days 49-92). Current density is also shown along the whole period. The green area represents the 3 batch cycles with no gas headspace recirculation, while orange covers the 3 batches with recirculation. ....	110
<b>Figure 6.4:</b> Principal Component Analysis (PCA) of Eubacterial communities based on OTUs matrix. Microbial communities from the initial sludge (IS), enriched inoculum (EI), and samples from biofilm (B) and supernatant (S) along the experiment.....	113
<b>Figure 6.5:</b> Taxonomic classification of Eubacterial communities at family levels and the phyla to which these families belong. ....	114
<b>Figure 6.6:</b> Overlap of the four biofilm communities and the taxonomic identities of the shared OTUs. ....	115

## **Chapter 7. Microbial electrosynthesis (MES) from CO<sub>2</sub> is resilient to fluctuations in renewable energy supply**

<b>Figure 7.1:</b> Microbial electrosynthesis reactor (H-Cell MES) .....	130
<b>Figure 7.2:</b> H-Cell MES reactor performance under different current supply interruptions: Current density (CD), Inorganic carbon (IC) and Acetate (Ac) concentration .....	133
<b>Figure 7.3:</b> SEM at different magnification of control clean graphite felt (A and B) and enriched biofilm covering the electrode (C, D, E and F).....	137
<b>Figure 7.4:</b> Taxonomic classification of 16S rRNA gene from Eubacterial classification at a family level. Groups making up less than 1% of the total number of sequences per sample were classified as “others” .....	139
<b>Figure 7.5:</b> The most abundant genera identified in the supernatant and biofilm samples.....	140

## **Chapter 8. Long-term open circuit MES system promotes methanogenesis**

<b>Figure 8.1:</b> Schematic and image of cell assembly.....	151
--	-----

---

<b>Figure 8.2:</b> Substrate and acetic acid concentration in the liquid medium (Black and orange) and gaseous products proportion in the outlet gas (Blue and Green..	154
<b>Figure 8.3:</b> Methane production and efficiency. ....	155
<b>Figure 8.4:</b> SEM images belonging to control graphite felt (A and B) and biofilm covered graphite electrode (C, D, E and F) at different magnification.....	156
<b>Figure 8.5:</b> Inoculum, biofilm and supernatant Eubacterial composition at family level. ....	157
<b>Figure 8.6:</b> Biofilm and supernatant microbial community at genera level. ....	158
<b>Figure 8.7:</b> Tentative hypothetical mechanism. In yellow: main pathway suggested by physico-chemical and microbiological analyses.....	160



---

# TABLA DE CONTENIDOS

## **Capítulo 1. Introducción**

<b>1.1 Tecnologías electroquímicas microbianas .....</b>	<b>3</b>
<b>1.2 Tecnologías electroquímicas microbianas para valorización de CO<sub>2</sub> – Electrosíntesis microbiana.....</b>	<b>5</b>
1.2.1 Fundamentos de la MES y ecología microbiana .....	8
1.2.2 Electrosíntesis microbiana de productos químicos y combustibles .....	11
1.2.2.1 Electro-bioquímicos clave producidos a partir de CO <sub>2</sub> .....	11
1.2.2.2 Electro-biocombustibles: Electrometanogénesis y mejora de biogás .....	13
1.2.2.3 Recuperación de productos .....	14
1.2.3 Debilidades y oportunidades de la MES.....	15
<b>1.3 Referencias .....</b>	<b>17</b>

## **Capítulo 2. Objetivos y ámbito de la tesis**

<b>2.1 Objetivos .....</b>	<b>33</b>
<b>2.2 Ámbito de la tesis.....</b>	<b>33</b>

## **Capítulo 3. Materiales and Métodos**

<b>3.1 Montaje experimental.....</b>	<b>39</b>
3.1.1 Celda de test cónica.....	39
3.1.2 Reactores planos.....	39
3.1.3 Reactores de tipo botella .....	40
3.1.4 Reactores tipo H .....	41
<b>3.2 Inóculos y medios de cultivo.....</b>	<b>42</b>

---

3.2.1 Inóculos.....	42
3.2.2 Medios de cultivo.....	42
3.3 Técnicas analíticas y electroquímicas.....	43
3.4 Técnicas de biología molecular.....	43
3.5 Cálculos.....	44
3.6 Referencias.....	45

## **Capítulo 4. Metodología para la caracterización rápida y sencilla de electrodos de carbono para el desarrollo y escalado de sistemas bioelectroquímicos**

4.1 Introducción.....	50
4.2 Experimental.....	51
4.2.1 Propuesta de metodología.....	51
4.2.2 Determinación de área electroactiva.....	51
4.2.3 Determinación de la dimensión fractal ( $D_f$ ).....	52
4.2.4 Validación del método.....	53
4.2.5 Montaje de la celda e instrumentación.....	55
4.3 Resultados y discusión.....	56
4.3.1 Estimación del área electroactiva.....	57
4.3.2 Determinación de la dimensión fractal.....	59
4.4 Conclusiones.....	63
4.5 Referencias.....	64

## **Capítulo 5. Impacto del proceso de arranque sobre la comunidad microbiana en biocátodos para electrosíntesis.**

5.1 Introducción.....	72
-----------------------	----

---

---

<b>5.2 Materiales y Métodos .....</b>	<b>74</b>
5.2.1 Montaje de reactor MES.....	74
5.2.2 Estrategias de arranque y operación.....	74
5.2.3 Influentes e inóculos .....	76
5.2.4 Medidas y técnicas analíticas.....	77
5.2.5 Secuenciación masiva de librerías génicas del gen 16S rRNA.....	77
<b>5.3 Resultados.....</b>	<b>78</b>
5.3.1 Funcionamiento de la celda.....	78
5.3.1.1 Producción de corriente .....	78
5.3.1.2 Formación de producto.....	79
5.3.2 Evaluación de la comunidad microbiana .....	81
5.3.2.1 Análisis de índices de diversidad.....	81
5.3.2.2 Estructura de la comunidad de Eubacterias .....	83
5.3.2.3 Estructura de la comunidad de Archaeas.....	88
<b>5.4 Discusión.....</b>	<b>89</b>
<b>5.5 Conclusiones .....</b>	<b>93</b>
<b>5.6 Referencias .....</b>	<b>94</b>

## **Capítulo 6. Mejora de la conversión de CO<sub>2</sub> en MES por recirculación continua de la cabecera**

<b>6.1 Introducción.....</b>	<b>104</b>
<b>6.2 Materiales y Métodos .....</b>	<b>105</b>
6.2.1 Montaje de los reactores MES.....	105
6.2.2 Influentes e inóculos .....	106

---

---

6.2.3 Procedimiento experimental .....	107
6.2.4 Medidas y técnicas analíticas .....	107
6.2.5 Análisis de la comunidad microbiana.....	107
<b>6.3 Resultados.....</b>	<b>108</b>
6.3.1 Efecto de la recirculación de CO <sub>2</sub> en MES .....	108
6.3.2 Comunidades microbiana involucradas en el proceso .....	112
<b>6.4 Discusión .....</b>	<b>116</b>
<b>6.5 Conclusiones .....</b>	<b>119</b>
<b>6.6 Bibliografía.....</b>	<b>120</b>
<b>Capítulo 7. La electrosíntesis microbiana (MES) a partir de CO<sub>2</sub> es robusta frente a fluctuaciones en el suministro eléctrico por energía renovable</b>	
<b>7.1. Introducción.....</b>	<b>128</b>
<b>7.2. Materiales and Métodos.....</b>	<b>129</b>
7.2.1 Reactor de electrosíntesis microbiana.....	129
7.2.2 Fuente de carbono, electrolito e inóculo .....	130
7.2.3 Montaje .....	131
7.2.4 Análisis bioelectroquímicos.....	131
7.2.5 Microscopía electrónica de barrido (SEM).....	131
7.2.6 Análisis de la comunidad microbiana.....	132
<b>7.3. Resultados y discusión .....</b>	<b>132</b>
7.3.1 Cortes de corriente en el reactor MES .....	132
7.3.2 SEM.....	136
7.3.3 Análisis de la comunidad microbiana.....	137

---

---

7.3.3.1 Evaluación de la diversidad microbiana .....	137
7.3.3.2 Composición de la comunidad microbiana.....	138
7.3.3.3 Rol de los principales géneros identificados.....	140
7.3.4 Perspectivas comerciales y tecnológicas.....	141
<b>7.4. Conclusiones .....</b>	<b>143</b>
<b>7.5. Referencias.....</b>	<b>144</b>
<b>Capítulo 8. Un Sistema MES en circuito abierto por un periodo largo promueve la metanogénesis</b>	
<b>8.1. Introducción.....</b>	<b>150</b>
<b>8.2. Materiales and Métodos.....</b>	<b>151</b>
8.2.1 Montaje del reactor MES.....	151
8.2.2 Inóculo, influentes y procedimiento experimental.....	151
8.2.3 Técnicas analíticas .....	152
8.2.4 Análisis de comunidades microbianas.....	152
8.2.5 Microscopía electrónica de barrido (SEM).....	153
<b>8.3. Resultados y discusión .....</b>	<b>153</b>
8.3.1 Historia previa de operación.....	153
8.3.2 Evolución y funcionamiento del biocátodo.....	154
8.3.3 Rol de las comunidades microbianas involucradas en el proceso .....	156
<b>8.4. Conclusiones .....</b>	<b>160</b>
<b>8.5. Bibliografía.....</b>	<b>161</b>
<b>Capítulo 9. Conclusiones y trabajo futuro</b>	
<b>9.1 Conclusiones .....</b>	<b>167</b>

---

---

<i>9.2 Trabajo futuro .....</i>	170
---------------------------------	-----

***Apéndices***

<i>Apéndice I.....</i>	175
------------------------	-----

<i>Apéndice II .....</i>	179
--------------------------	-----

<i>Apéndice III.....</i>	181
--------------------------	-----

---

## ÍNDICE DE TABLAS

### **Capítulo 4. Metodología para la caracterización rápida y sencilla de electrodos de carbono para el desarrollo y escalado de sistemas bioelectroquímicos**

<b>Tabla 4.1:</b> Especificación del material y códigos.....	54
<b>Tabla 4.2:</b> Caída ohmica de cada montaje de celda. El error estándar de la media estima la incertidumbre asociada a la determinación de la caída óhmica..	57
<b>Tabla 4.3:</b> Área electroactiva.....	58
<b>Tabla 4.4:</b> Comparación de parámetros fractales de diferentes electrodos usando medidas de CV. El valor presentado junto al parámetro fractal $\alpha$ representa el intervalo de confianza del 90% para cada parámetro.....	60

### **Capítulo 5. Impacto del proceso de arranque sobre la comunidad microbiana en biocátodos para electrosíntesis.**

<b>Tabla 5.1:</b> Corrientes máximas para cada estrategia y periodos de latencia observados. ....	79
<b>Tabla 5.2:</b> Funcionamiento de celda para cada estrategia.....	81
<b>Tabla 5.3:</b> Riqueza estimada (OTUs observados and Chao1) e índices de diversidad (Shannon ( $H'$ ) y 1/Simpson) para OTUs de Eubacterias, calculados con MOTHUR al 3% de nivel de distancia. ....	82
<b>Tabla 5.4:</b> Riqueza estimada (OTUs observados and Chao1) e índices de diversidad (Shannon ( $H'$ ) y 1/Simpson) para OTUs de Archaeas, calculados con MOTHUR al 3% de nivel de distancia. ....	83

### **Capítulo 6. Mejora de la conversión de CO<sub>2</sub> en MES por recirculación continua de la cabecera**

<b>Tabla 6.1:</b> Resumen de producción de acético, incluyendo medias para ambas MES y desviación típica.....	111
<b>Tabla 6.2:</b> Balance de carbono y eficiencia catódica. Se muestran medias entre los dos reactores MES (MES1 and MES2). ....	111

---

**Capítulo 7. La electrosíntesis microbiana (MES) a partir de CO<sub>2</sub> es robusta frente a fluctuaciones en el suministro eléctrico por energía renovable**

**Tabla 7.1:** Densidad de corriente media y tiempo de recuperación entre MES alimentados con bicarbonato y con CO<sub>2</sub> gas ..... 135

**Tabla 7.2:** N° de secuencias y OTUs, riqueza estimada (Chao1), índice de diversidad (Shannon) and valores de cobertura de muestra para OTUs de Eubacteria..... 138

**Capítulo 8. Un Sistema MES en circuito abierto por un periodo largo promueve la metanogénesis**

**Tabla 8.1:** Comunidades de Archaeas en el biofilm y sobrenadante a nivel de familia ..... 159



---

# ÍNDICE DE FIGURAS

## **Capítulo 1. Introducción**

*Figura 1.1: Diagramas de comparativa básica entre MFC, MEC y MES.....* 4

*Figura 1.2: Usos actuales del CO<sub>2</sub>. Figura basada en un original de NETL-CO<sub>2</sub>.  
.....* 6

*Figura 1.3: Diagrama general de un modelo de Sistema MES controlado  
potenciostáticamente mostrando (I) generación de producto por transferencia de  
electrones directa y (II un ejemplo de generación de producto mediada por  
hidrógeno en el cátodo. En el ánodo, oxidación de agua genera los electrones  
necesarios para la reacción catódica. WE, CE y RE significan respectivamente  
Electrodo de trabajo, contraelectrodo y electrodo de referencia. ....* 8

## **Capítulo 2. Objetivos y ámbito de la tesis**

*Figura 2.1: Visión general del ámbito de la tesis .....* 36

## **Capítulo 3. Materiales and Métodos**

*Figura 3.1: Celda de test cónica.....* 39

*Figura 3.2: Reactor plano.....* 40

*Figura 3.3: Reactor tipo botella. Imagen real y diagrama.....* 41

*Figura 3.4: Reactor tipo H.....* 41

## **Capítulo 4. Metodología para la caracterización rápida y sencilla de electrodos de carbono para el desarrollo y escalado de sistemas bioelectroquímicos**

*Figura 4.1: Filtro de carbono de grosor 0.5cm (a) , filtro de carbono de grosor  
0.25cm (b), papel de carbono (c) y cepillo (d) .....* 54

*Figura 4.2: Electrodo de papel de carbono con burbujas de aire tras el  
pretratamiento.....* 55

*Figura 4.3: Diagrama y montaje de la celda.....* 56

---

<b>Figura 4.4:</b> Gráfica Randles-Ševčík. a: Fieltro grueso (TF); b: Fieltro fino (FF); c: Papel (P); d: Cepillo (B) .....	58
<b>Figura 4.5:</b> Tendencia lineal en la representación logarítmica de $I_{pc}$ vs. $v$ .....	60
<b>Figura 4.6:</b> Dimensión fractal de los electrodos evaluados. Valores correspondientes a dimensiones Euclídeas enteras se representan en líneas gruesas rojas. ....	61
<b>Figura 4.7:</b> Relación entre dimensión fractal y EA/AS para cada material evaluado. Rombos negros muestran el centroide para cada cluster de electrodos. ....	62

## **Capítulo 5. Impacto del proceso de arranque sobre la comunidad microbiana en biocátodos para electrosíntesis.**

<b>Figura 5.1.</b> Visión global de las estrategias.....	75
<b>Figura 5.2.</b> Media de la concentración de acético final para cada ciclo y cada estrategia (las barras de error muestran la desviación estándar de tres replicas) El día 0 corresponde a la inoculación. ....	80
<b>Figura 5.3:</b> Clasificación taxonómica de las secuencias a nivel de filo .....	84
<b>Figura 5.4:</b> Clasificación taxonómica para comunidades de Eubacterias a nivel de familia de a) muestras de S2, b) muestras de S3 y c) muestras de S4. Grupos por debajo del 1% del número total de secuencias se clasificaron como “otros”. ....	85
<b>Figura 5.5:</b> Heatmap resumiendo los principales géneros presentes en los biofilms de ánodos y cátodos para las tres estrategias desarrolladas. ....	87
<b>Figura 5.6:</b> Clasificación taxonómica para comunidades de Archaeas de los inóculos AD and RM y muestras de cátodo de S2 y S3 a nivel de género. Grupos por debajo del 1% del número total de secuencias se clasificaron como “otros”..	89

## **Capítulo 6. Mejora de la conversión de CO<sub>2</sub> en MES por recirculación continua de la cabecera**

<b>Figura 6.1:</b> Imagen y diagrama del montaje de reactor.. .....	106
---	-----

---

<b>Figura 6.2:</b> Evolución de la curva de polarización a lo largo del experimento. ...	109
<b>Figura 6.3:</b> Concentración de ácido acético a lo largo del periodo experimental (Días 49-92). La densidad de corriente también se muestra para el este periodo. El área verde representa los 3 ciclos sin recirculación mientras que el área naranja cubre los tres ciclos con recirculación. ....	110
<b>Figura 6.4:</b> PCA de las comunidades de Eubacterias basada en la matriz de OTUs. Comunidades microbianas del lodo inicial (IS), inóculo enriquecido (EI), y muestras del biofilm (B) y sobrenadante (S) a lo largo del experimento. ....	113
<b>Figura 6.5:</b> Clasificación taxonómica de la comunidad de Eubacterias a nivel de familia y el filo al que pertenecen .....	114
<b>Figura 6.6:</b> Superposición de las cuatro comunidades de biofilm y las identidades taxonómicas de los OTUs comunes. ....	115

## **Capítulo 7. La electrosíntesis microbiana (MES) a partir de CO<sub>2</sub> es robusta frente a fluctuaciones en el suministro eléctrico por energía renovable**

<b>Figura 7.1:</b> Reactor de electrosíntesis microbiana (MES tipo H) .....	130
<b>Figura 7.2:</b> Funcionamiento del reactor MES tipo H bajo diferentes cortes de suministro eléctrico: Densidad de corriente (CD), concentración de carbono inorgánico (IC) y ácido acético (Ac) .....	133
<b>Figura 7.3:</b> SEM a diferente magnificación del fieltro de grafito limpio de control (A y B) y del biofilm enriquecido cubriendo el electrodo (C, D, E y F). ....	137
<b>Figura 7.4:</b> Clasificación taxonómica de Eubacterias a nivel de familia. Grupos por debajo del 1% del número total de secuencias se clasificaron como “otros”. ....	139
<b>Figura 7.5:</b> Géneros más abundantes identificados en el sobrenadante y el biofilm. ....	140

## **Capítulo 8. Un Sistema MES en circuito abierto por un periodo largo promueve la metanogénesis**

<b>Figura 8.1:</b> Esquema e imagen del montaje de la celda .....	151
---	-----

---

<b>Figura 8.2:</b> Concentración de ácido acético y sustrato en el medio líquido (naranja y negro) y productos gaseosos en el gas de salida (azul y verde).....	154
<b>Figura 8.3:</b> Eficiencia y producción de metano. ....	155
<b>Figura 8.4:</b> Imágenes SEM pertenecientes al fieltro de grafito limpio de control (A and B) y del biofilm que cubre el electrodo (C, D, E and F) a diferente magnificación.....	156
<b>Figura 8.5:</b> Composición en Eubacterias del inoculo, biofilm y sobrenadante a nivel de familia.....	157
<b>Figura 8.6:</b> Comunidad microbiana en el biofilm y sobrenadante a nivel de género.....	158
<b>Figura 8.7:</b> Mecanismo hipotético. En Amarillo: ruta principal sugerida por los análisis físico-químicos y microbiológicos. ....	160

---

## ABSTRACT

The level of carbon dioxide has increased in the atmosphere during the past century, causing considerable public concern around climate change. Despite the efforts made to reduce this global environmental issue, its impact is expected to be intensified in the following years. Bioelectrochemical Systems (BES), and Microbial Electrosynthesis (MES) in particular, could be part of the solution, as this technology is capable of converting carbon dioxide into organics and fuels. However, MES is a recently born technology that still requires solving technological and economic issues before achieving practical application.

In this context, the main objective of this thesis is to give the initial steps to move MES from the proof of concept stage towards practical application by addressing some important issues that are limiting its development beyond the laboratory.

The first step was the development of a screening methodology for electrode materials. It is expected to become especially useful in the upscaling of BES as it provides a fast and cost-effective characterization method. This methodology relies on integrating the information provided by both, the electroactive area and the fractal dimension of carbonaceous materials.

Another source of concern in MES is the start-up process and how it influences the microbial communities that develop on the biofilm of acetogenic biocathodes. This thesis explores the suitability of two different start-up strategies and two different inocula, trying to assess their impact on microbial community evolution and products generation. The microbial structure that was finally present on the electrodes was highly dependent on the raw community present in the inoculum. Moreover, a highly specialised biofilm proved to be related to an improved performance in terms of consumed current and product generation.

In order to improve product generation on acetogenic MES systems, it is important to improve substrate availability to the biofilm. The approach used in this thesis to improve CO<sub>2</sub> availability is based on recirculating gas from the headspace of the cathode chamber. This provided an efficient and selective way of consuming CO<sub>2</sub> for

---

the production of acetic acid, showing 44% improvement in terms of production rate and over 80% in cathodic efficiency compared to the situation with no recirculation.

One of the key factors that need to be explored is MES resilience to fluctuations in operational conditions. For this purpose, acetogenic MES systems were subjected to short and long term interruptions in power supply with the aim of assessing their impact on performance and on microbial community dynamics. MES showed to be resilient to short power interruptions. In spite of a short period in which acetic acid concentration declined, the system fully recovered after the gaps achieving similar production rates than those found before the interruptions. Moreover, a well-established acetogenic MES recovered its electroactivity within two days after a long power interruption. However, this long supply gap drastically affected the end-products generated after reconnection.

---

## RESUMEN

Los niveles de dióxido de carbono en la atmósfera han crecido a lo largo del último siglo causando una alarma considerable en torno al cambio climático. A pesar de los esfuerzos en reducir este problema medioambiental global, se espera que su impacto se intensifique en los próximos años. Los sistemas bioelectroquímicos (BES), y la electrosíntesis microbiana (MES) en particular, pueden formar parte de la solución a este problema, ya que esta tecnología puede transformar el dióxido de carbono en compuestos orgánicos y combustibles. Sin embargo, la MES es una tecnología muy reciente y aún necesita resolver obstáculos tecnológicos y económicos antes de llegar a su aplicación práctica.

En este contexto, el objetivo principal de esta tesis es dar los primeros pasos para trasladar la tecnología MES de la prueba de concepto a su implementación práctica, y para ello resolver algunos de los factores más importantes que están limitando su desarrollo más allá del laboratorio.

El primer paso fue el desarrollo de una metodología para la selección de materiales para su uso como electrodos. Esta metodología puede ser especialmente interesante para el escalado de los BES ya que proporciona un método rápido y económico de caracterización. El resultado fundamenta en la integración de la información obtenida del área electroactiva y la dimensión fractal de los materiales carbonosos.

Otro punto problemático en MES es el proceso de arranque y cómo influye este en la comunidad microbiana que finalmente se desarrolla en un biocátodo acetogénico. Esta tesis explora la idoneidad de dos estrategias de arranque y dos inóculos diferentes, tratando de evaluar su impacto sobre la evolución de la comunidad microbiana y los productos generados. La estructura microbiológica que estaba finalmente presente en el electrodo fue muy dependiente de la comunidad original del inóculo. Además, se pudo probar que un *biofilm* muy especializado está ligado a una mejora en el funcionamiento en términos de corriente consumida y generación de productos.

Para incrementar la productividad de un sistema MES acetogénico, también es importante mejorar la disponibilidad que el *biofilm* tiene del sustrato. El planteamiento utilizado en esta tesis es el de mejorar la disponibilidad de CO<sub>2</sub> basada en la

---

recirculación del gas de cabecera de la cámara catódica. El resultado de utilizar esta recirculación es una mejora en la producción de acético, mostrando un incremento del 44% en términos de tasa de producción en comparación con la situación de no recirculación, y mostrando unas eficiencias catódicas por encima del 80%.

Uno de los factores clave que requiere ser explorado es la capacidad de adaptación de los sistemas MES frente a fluctuaciones en las condiciones de operación. Con este propósito, los sistemas MES fueron sometidos a cortes de suministro eléctrico de corta y larga duración con el objetivo de evaluar el impacto que generan sobre el funcionamiento de la celda y la dinámica microbiológica. El reactor mostró ser robusto frente a interrupciones de corta duración. A pesar de que la concentración de ácido acético decayó durante un breve periodo de tiempo, el sistema se recuperó totalmente llegando a producciones similares a las mostradas antes de estos cortes. Además, un reactor MES acetogénico estable pudo recuperar su electroactividad en dos días tras un largo corte de suministro eléctrico. Sin embargo, este corte de energía eléctrica afectó drásticamente a los productos finales tras la reconexión.



---

## LIST OF ABBREVIATIONS

<b>A</b>	Area
<b>AAB</b>	Acetic acid bacteria
<b>Ac</b>	Acetate
<b>AD</b>	Anaerobic digestion
<b>ARB</b>	Anode respiring bacteria
<b>AS</b>	Apparent surface
<b>BES</b>	Bioelectrochemical systems
<b>c</b>	concentration
<b>c.i.</b>	Confidence interval
<b>CA</b>	Chronoamperometry
<b>CCS</b>	Carbon capture and storage
<b>CD</b>	Current density
<b>CE</b>	Counter electrode
<b>CEM</b>	Cationic exchange membrane
<b>CV</b>	Cyclic voltammetry
<b>D</b>	Diffusion coefficient
<b>DET</b>	Direct electron transfer
<b>D<sub>f</sub></b>	Fractal dimension
<b>DNA</b>	Deoxyribonucleic acid
<b>DSA</b>	Dynamically stable anode
<b>EA</b>	Electroactive area
<b>E<sub>cat</sub></b>	Cathodic efficiency
<b>EI</b>	Enriched inoculum
<b>EIS</b>	Electrochemical impedance spectroscopy
<b>E<sub>we</sub></b>	Working electrode potential
<b>F</b>	Faraday's constant
<b>FF</b>	Fine felt
<b>GHGs</b>	Greenhouse gases
<b>H'</b>	Shannon index
<b>HAc</b>	Acetic acid
<b>HPLC</b>	High pressure liquid chromatography
<b>i</b>	Current
<b>IC</b>	Inorganic carbon
<b>I<sub>p</sub></b>	Peak current

---

<b>IS</b>	Initial Sludge
<b>MCFA</b>	Medium chain fatty acids
<b>MES</b>	Microbial electrochemical cell
<b>MES</b>	Microbial electrosynthesis
<b>MET</b>	Microbial electrochemical technologies
<b>MFC</b>	Microbial fuel cell
<b>n</b>	Number of electrons
<b>OTU</b>	Operational taxonomic unit
<b>PCA</b>	Principal components analysis
<b>PCR</b>	Polymerase chain reaction
<b>R</b>	Ideal gas constant
<b>RDP</b>	Ribosomal database project
<b>RE</b>	Reference electrode
<b>RM</b>	River mud
<b>RNA</b>	Ribonucleic acid
<b>S</b>	Supernatant
<b>SAO</b>	Syntrophic acetate oxidizers
<b>S<sub>c</sub></b>	Consumed substrate
<b>SEM</b>	Scanning electron microscopy
<b>S<sub>obs</sub></b>	Observed species. Richness estimator
<b>T</b>	Temperature
<b>t</b>	time
<b>TCD</b>	Thermal conductivity detector
<b>TF</b>	Thick felt
<b>TN</b>	Total nitrogen
<b>TOC</b>	Total organic carbon
<b>VFAs</b>	Volatile fatty acids
<b>WE</b>	Working electrode
<b>WWTP</b>	Wastewater treatment plant
<b>Z</b>	Impedance
<b>α</b>	Fractal parameter
<b>v</b>	Scan rate

---

# CHAPTER 1



## General Introduction

*Part of this chapter was adapted from:*

**Mateos, R.,** Escapa, A., Vanbroekhoven, K. , Patil, S.A., Morán, A. & Pant, D. (2018)  
Microbial Electrochemical Technologies for CO<sub>2</sub> and its Derived Products Valorization.  
In: *Biomass, Biofuels, Biochemicals: Microbial Electrochemical Technology: Sustainable Platform  
for Fuels, Chemicals and Remediation. 1st edition.*



## 1.1 MICROBIAL ELECTROCHEMICAL TECHNOLOGIES

Microbial electrochemistry, a field that has aroused to interests of scientists for a long time [1], studies the interaction between electrodes and living microorganisms [2]. Scientists involved in fundamental research have been interested on this field for a long time, and in the last two decades the involvement of applied research and engineering have promoted an increasing number of systems technically named as Microbial electrochemical technologies (MET) or bioelectrochemical systems (BES) [2]. This interlacing of engineering, electrochemistry and microbiology opens a wide and multidisciplinary field of research and technological developments that has rapidly grown [3–5]. Other disciplines, such as biochemistry, physics or mathematical modelling, have also showed growing interest on METs in the last years leading to an ever increasing number of applications [6–8]. All these applications share one core principle, in which microorganisms electrochemically interacts with a solid conductive surface (electrode) to catalyze a biochemical reaction, which could be oxidative or reductive depending on the electrode potential.

The history of METs began over a century ago when M.C. Potter discovered that certain bacteria are able to generate electric current associated to organic matter degradation [1]. After that momentous discovery only a few works explored this finding [9,10] until the late 1990's and the early 2000's when research on Microbial Fuel Cells (MFCs) was undertaken with a renewed interest [11–13]. Typically a MFC consists of two electrodes: an anode and a cathode (figure 1.1). The anode is colonized by microorganisms, and usually separated by an ion exchange membrane from the cathode. In the anode, electroactive bacteria degrade organic matter to produce electrons, protons and inorganic carbon. Protons and electrons are transferred to the cathode (through the ion exchange membrane and an external circuit respectively), where they typically react with oxygen to form water [14]. Further details on the fundamentals of MFC can be found elsewhere [14,15]. Although MFC have not gone beyond the pilot scale yet, electrical energy production in these systems has sharply increased during the past years from a few  $\text{mW}\cdot\text{m}^{-2}$  of electrode, up to over  $2.7\text{ W}\cdot\text{m}^{-2}$  [16], proving to be able to power lighting or small electronic devices at real field practical applications [17,18].

Around 2005 it was discovered that an MFC system could be operated in an electrolytic configuration, giving birth to the concept of Microbial Electrolysis Cells (MECs) [19,20]. MECs opened the opportunity of recovering energy in the form of chemicals, being hydrogen perhaps the most popular one [20,21]. In MECs exoelectrogenic microorganisms generate electrons from the oxidation of organic matter as in MFC; however, these electrons are forced to travel to the cathode by an applied potential where they recombine with protons to produce hydrogen (figure 1.1). In addition, the reductive power generated on the cathode can be used to other practical ends such as metal recovery [22], sulfate reduction [23] or hydrogen peroxide production [24]. Technological developments of MEC have mainly focused on devising systems for efficient organic wastes treatment in parallel to hydrogen gas production [3,25,26]. Moreover, pilot prototypes have been tested up to 1000L proving its feasibility for future practical application [27–29].

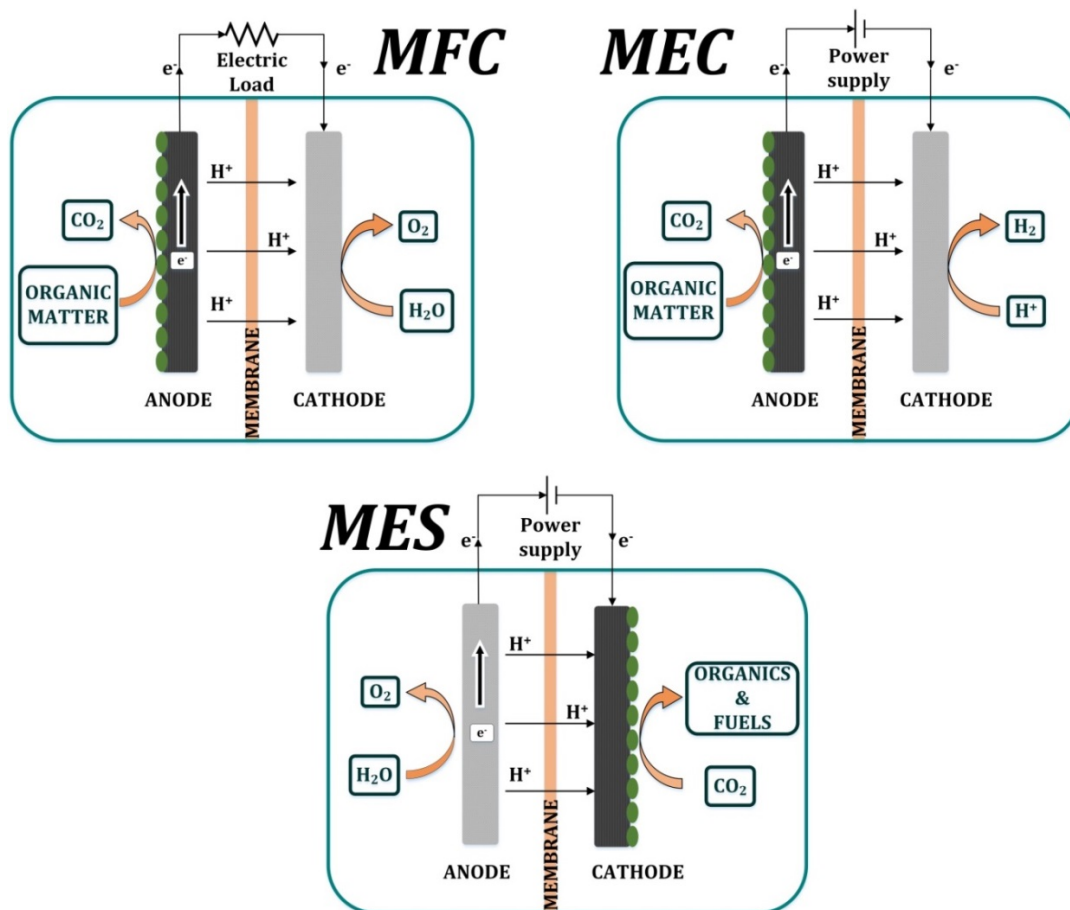


**Figure 1.1:** Basic comparative diagrams for MFC, MEC and MES.

In MFCs and MECs not only the anodic reaction but also the cathodic reaction can be bio-catalyzed. When the cathode is biologically catalyzed it is usually termed as biocathode, and it was Rozendal et. al in 2007 who operated a biocathode ( by reversing the potential of an acetate-oxidizing bioanode) for the first time [30]. This opened a new field in MET, and new applications for biocathodes rapidly emerged. Thus, in 2009 Clauwaert and Verstraete operated a biocathode specifically designed for methane production [31] and shortly after in 2010, Nevin and colleagues [32] demonstrated the generation of organic compounds from inorganic carbon giving birth to the concept of Microbial Electrosynthesis (MES). MES represents a novel technology, offering a wide range of opportunities in different industrial fields but also presenting a certain number of technical problems that must be overcome before achieving practical application. This thesis focuses precisely on gaining knowledge at how to overcome some of these difficulties paying special attention to critical aspects such as biocathode start-up, substrate availability and resilience against renewable energy supply. In the following sections of this introductory chapter I will go through fundamentals, state of the art and technical opportunities to provide a suitable framework for MES application.

## **1.2 MICROBIAL ELECTROCHEMICAL TECHNOLOGIES FOR CO<sub>2</sub> VALORIZATION – MICROBIAL ELECTROSYNTHESIS**

Global warming, caused by the emission of greenhouse gases (GHGs), has gathered major attention in the fields of energy and environmental engineering, and industrialized countries are urged to lower their emissions according to international environmental agreements [33–35]. However, as non-renewable fossil fuels are still the principal sources of energy, CO<sub>2</sub> emissions reduction targets are difficult to reach, even taking into account the major technological efficiency improvements reached in the recent years. Carbon capture and storage (CCS) is a process capable of massively reducing anthropogenic CO<sub>2</sub> releases into the atmosphere. It consists on capturing waste carbon dioxide streams from large scale industrial sources and transporting it to a geological deposit in which the CO<sub>2</sub> keeps isolated from the atmosphere. However, scepticism about the high cost of CCS, and increasing public concerns about safety risks around underground storing of carbon dioxide have discouraged some demonstration projects in the past few years [36].

Within this frame, value-added utilization of captured CO<sub>2</sub>, instead of massive storage, has become an interesting alternative recognized worldwide [37]. Its ubiquitousness, low toxicity to living organisms, and intensive production in factories or furnaces are some of the most relevant factors that make CO<sub>2</sub> an interesting precursor or feedstock for the industry. CO<sub>2</sub> utilization (figure 1.2) usually comprises its direct use in industry and/or its conversion into valuable chemicals or fuels. CO<sub>2</sub> can be directly utilized in the food and drink industry, as a propellant for fire extinguishers or even in sophisticated processes as supercritical solvent (figure 1.2) [38,39]. However, most of these applications make use of highly pure CO<sub>2</sub> that is difficult to obtain from intensive industrial processes such as fossil fuel combustion and agricultural or farming sites. In contrast, CO<sub>2</sub> conversion to chemicals or fuels, represents an interesting alternative because in general, and specially for fuels, the presence of impurities in the feedstock is less problematic [40,41]. This fact could potentially close carbon cycle in industry, and the generated revenue from marketable products could compensate for the CO<sub>2</sub> capture cost [42].

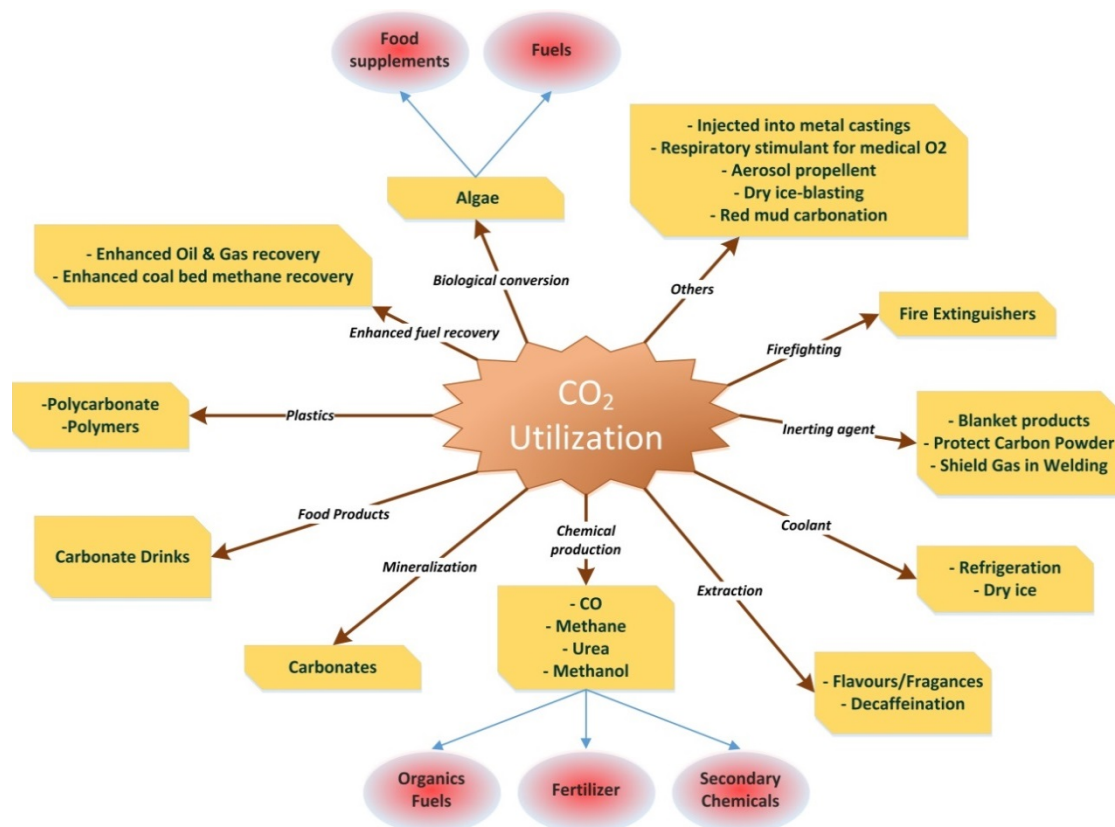


**Figure 1.2:** Current captured CO<sub>2</sub> uses. Figure based on NETL-CO<sub>2</sub> utilization original [38].



CO<sub>2</sub> as a feedstock for fuels and chemicals production gained increasing attention following the oil embargoes of the 1970s. Several organic and inorganic products such as formic acid (HCOOH), methanol (CH<sub>3</sub>OH), ethylene (C<sub>2</sub>H<sub>4</sub>), methane (CH<sub>4</sub>), and carbon monoxide (CO), have been obtained through electrocatalysis [43,44], which represents a suitable technology for CO<sub>2</sub> conversion as it can be operated at ambient pressure and room temperature, allows for modularity, is relatively easy to control and scale-up, and can be readily powered with renewable energies [45]. Moreover, the product formation is dependent mainly on the selected catalysts and electrode potentials. However, the electrochemical processes developed till date have to struggle with high overpotentials, low current efficiencies, kinetics or process stability, and a limited product profile [46].

As carbon in CO<sub>2</sub> is fully oxidized, CO<sub>2</sub> reduction to organic products is an energy consuming process [4,47,48] and therefore, developing efficient catalysts to overcome high energy cost is a fundamental issue. Traditionally, electrochemical processes have relay on novel metals such as gold, platinum, other novel metals or more complex composites [46] (which generally makes the process non-competitive in monetary terms) to drive the electrochemical reactions. Here is where biocatalysts can provide an alternative, as microorganisms represent a cheap and ubiquitous catalyst. Microbes such as acetogens and methanogens (usually found in MES biocathodes as biocatalysts) possess the natural capability of activating CO<sub>2</sub> to produce mono- and multi-carbon organics when provided with a reducing agent such as hydrogen, electrons from a cathode or other mediators [48,49] that will be discussed in following sections.

MES represents a recent technological development (that evolves from conventional electrochemical systems) for transforming CO<sub>2</sub> into valuable chemicals and fuels. Although MES is still in its early stages of development, striving to increase production rates and efficiency, it shows a great potential as evident from the progress made in a short period as will be discussed in this thesis. Moreover, MES fits the criteria of green chemical technologies as it uses bacteria and archaea as sustainable catalysts, operates at near ambient conditions and makes use of contaminants such as CO<sub>2</sub> as main raw material [4]. Furthermore, the chemical properties of CO<sub>2</sub> also favors its use as feedstock for MES as it is an extremely stable molecule [21] and represents a soluble gas that possesses pH buffering capacity and low toxicity.

### 1.2.1 MES fundamentals and microbial ecology

MES is a biocathode driven technology, taking advantage of electroactive microorganisms that catalyze inorganic carbon reduction to organics and fuels as shown in figure 1.3 [48,50]. Cathodes are usually made of carbon-based materials due to their high specific surface area, biocompatibility and chemical stability [51–53]. Other materials such as stainless steel and other metals have been used for its conductivity and mechanical strength [54].

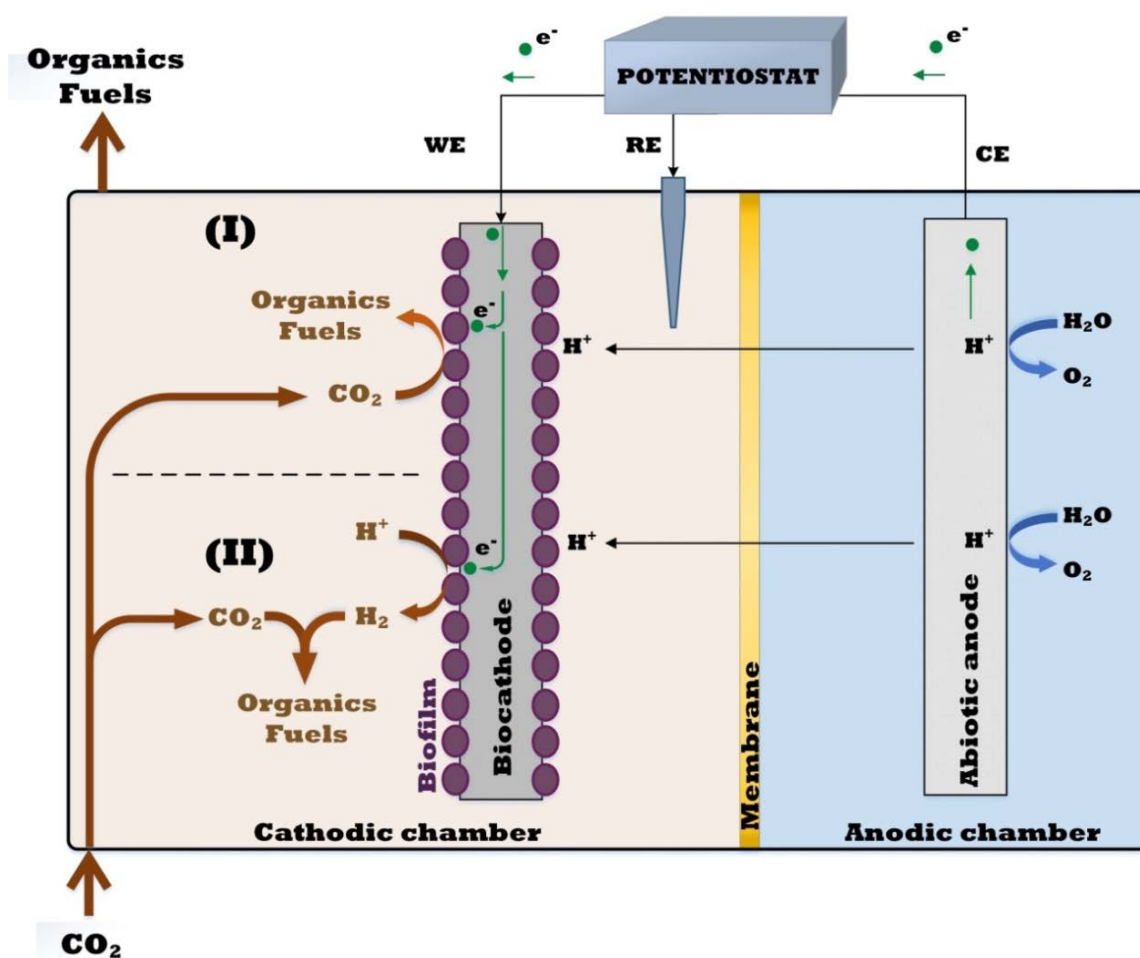


**Figure 1.3:** General diagram of a potentiostatically controlled model MES system showing (I) direct electron transfer based product generation and (II) an example of hydrogen mediated product generation at the cathode. At the anode, water oxidation provides electrons for the cathode reactions. WE, CE and RE stand for working, counter and reference electrodes, respectively.

Several anodic reactions, including microbial oxidation of organic matter [23,55], can be coupled with a biocathode. However, and for the sake of simplicity, water oxidation has become the most popular on basic research studies [51–53]. Moreover, water splitting using noble metals such as platinum, ensures that the counterelectrode is not the limiting factor and therefore cathode evaluation can be isolated. The ionic exchange membrane is another key aspect in MES as catholyte and anolyte cannot get in contact, while ions (mainly protons) must migrate from the anode to the cathode with the least possible impediments. Initially cationic exchange membranes such as Nafion 117 ® were used, but many others have been used for this purpose until date [56].

Although MES electron transfer mechanisms are not yet fully understood, they are usually classified as direct (the microorganism takes electrons directly from the cathode surface) and indirect (a chemical mediator is required to accomplish the electron transfer) [57,58] (figure 1.3). Direct electron transfer, in the absence of any mediator, requires physical contact between the microbial catalyst and the electrode surface. Several microorganisms have empirically proved to be able to drive this process although little information is known about how electrons are actually acquired by them [59]. C-type cytochromes have been proposed as responsible of this electron transfer for microorganisms such as *Geobacter sulfurreducens*, *Sporomusa Ovata* or *Shewanella oneidensis* [60,61]. However, the mechanisms for others like *Clostridium ljungdahlii* is expected to be extensively different as they lack c-type cytochromes [62].

A number of exogenous redox mediators have been proved to work as a shuttle for indirect electron transfer. Hydrogen, methyl viologen, neutral red, formate, ammonia, Fe (II) and others have been reported as mediators in MES systems [49,50,63]. Among these, hydrogen is the most common one as it can be biotically or abiotically produced in MES depending on the cathode potential. As an example, when hydrogen is present in the reaction chamber, it is likely that some reduction reactions, that for instance may involve *Desulfovibrio* sp. [64], are mediated by hydrogen [65]. However, microorganisms can also produce and release their own mediators to exchange electrons with the electrode. Flavins or phenazines have been reported as excreted electron mediators in microorganisms like *Pseudomonas* sp. or *Shewanella oneidensis* [66,67]. Moreover, these mediators have the advantage that can be used by

other microorganisms different than the producer, facilitating and boosting electron transfer in that case [49].

Focusing on the microorganisms responsible of MES, strong efforts have been made to optimize known electroactive microorganisms and screening new ones [68]. First studies were carried out using pure cultures and a wide range of different microorganisms proved to be capable of achieving CO<sub>2</sub> reduction into organics [59,69]. Those following the Wood-Ljungdahl pathway [70], and therefore producing acetate from CO<sub>2</sub>, are the most common and firstly studied microorganisms for MES. Both Gram positive, such as *Clostridium sp.* or *Moorella sp.*, and Gram negative, such as *Sporomusa sp.*, among many others [49,59,69], have been used in MES. Within all these, *Sporomusa Ovata* has been reported as the highest acetate producer [71]. Other pure cultures are capable of driving different reactions in MES from CO<sub>2</sub>, such as *Geobacter sp.*, capable of producing succinate from inorganic carbon [72] and extensively studied in bioanodes. Some ammonia oxidizing bacteria, photosynthesis bacteria or Fe (II) oxidizing bacteria can also grow on biocathodes [49]. In the case of methane production via direct MES, methanogenic Archaea, such as *Methanobacterium sp.*, are responsible of the process [73].

Although pure cultures are extremely interesting for fundamental knowledge, primary optimization and identification of reaction pathways, these are not applicable for most real applications. Mixed cultures offer the advantage of eliminating restrictive conditions required for pure cultures, and actually highest titers and production rates of acetate have been reported for these microbial communities [74–76]. In the recent years, most of the studies have been carried out using mixed cultures and in the vast majority of them they are collected from environmental sources such as anaerobic sludge [51], sediments [77,78] or brewery wastewater [79]. All these natural cultures come from different environments in terms of culture conditions, and therefore are expected to present a wide diversity of microorganisms [80]. In the case of sediment inoculated mixed culture biocathode, Zaybak and colleagues [78] reported that most of the microbial community contained in particular *Trichococcuspalustris sp.*, *Oscillibacter sp.*, *Clostridium sp.*, *Desulfotomaculum sp.*, *Tissella sp.* and others. Regarding to brewery wastewater, Marshall and colleagues [79] reported a community dominated by *Acetobacterium sp.* and others such as *Sulfurospirillum sp.* or

Rhodobacteraceae family. Regarding anaerobic sludge, the dominant communities were *Sporomusa sp.*, *Clostridium sp.* or *Desulfovibrio sp.* among many others.

It is also true that mixed community MES systems mainly produce acetate as in MES conditions acetogenic communities are quickly enriched [59], and also methanogenesis is often artificially inhibited [81,82]. The main drawback of using mixed cultures is the low selectivity [47,78,79] as hydrogen, other VFAs or alcohols can be easily found as byproducts.

## 1.2.2 Microbial electrosynthesis of chemicals and fuels

### 1.2.2.1 Key electro-biochemicals produced from CO<sub>2</sub>

Till now, target electro-biochemicals obtained through MES ranges from gas fuels to organic acids or alcohols, with the final end-product being strongly dependent on the microbial biocatalysts that develops on the biocathode, and the metabolic pathways that the biofilm can carry out [47]. This section covers rates and efficiencies for those chemicals that most frequently appear on biocathodes for both pure and mixed cultures.

#### Volatile fatty acids (VFAs):

VFAs has been the main focus of organic chemicals production in MES systems, as they are moderately oxidized and can be produced by several different electro-trophic microorganisms from CO<sub>2</sub>. Acetic acid is the most widely reported VFA, thanks to the versatility of homoacetogens [83], that can grow within a wide range of physico-chemical conditions, which usually involve simple gas atmospheres containing CO, CO<sub>2</sub> and/or hydrogen [84]. In addition, they can easily change from heterotrophic to autotrophic metabolism, being capable of withstanding severe conditions such as high or low temperatures and salinities. The CO<sub>2</sub> to acetate metabolic pathways mainly includes Wood-Ljungdahl pathway commonly found in the homoacetogenic microorganisms [47] such as *Sporomusa sp.* and *Clostridium sp.* The most optimized systems for acetate production have achieved production rates above 0.78 g·L<sup>-1</sup>·d<sup>-1</sup>, efficiencies of 99% in terms of current-to-acetate conversion and product titers up to 13.5 g·L<sup>-1</sup> [74–76].

Butyrate is another frequently reported carboxylic acid in MES reactors, as it can be produced from CO<sub>2</sub> at moderate negative potentials [85]. Moreover, it can also be obtained from acetate through chain elongation reaction [86] and so, butyrate has been usually observed as a co-product in acetate producing MES systems enriched with *Clostridium* sp. or *Moorella* sp. [52,69]. Few research groups have focused their work on obtaining butyrate as the only product; maximum titers of 5.5 g·L<sup>-1</sup> and production rates of up to 0.16 g·L<sup>-1</sup>·d<sup>-1</sup> have been reported so far [87]. Other VFAs such as propionate, isobutyrate or even medium chain fatty acids (MCFAs) have often been reported as by-products in acetate producing MES systems [85,86,88], although not targeted and at very low concentrations.

#### Alcohols:

Ethanol and longer chain alcohols are easily marketable chemicals as fuel and industrial feedstocks. Homoacetogens, which are responsible for the production of acetate, have been also identified as alcohol producers from CO<sub>2</sub>, provided that enough hydrogen or protons are present in the reaction media [63,89]. Ethanol can also be produced in MES systems from acetate, which is thermodynamically more favorable than starting from CO<sub>2</sub>. This suggests that using CO<sub>2</sub> as substrate probably involves a two-step mechanism. In this regard, the relevance of mediators such as methyl-viologen to favor acetate to ethanol has been reported [63].

Ethanol production is favored by slightly acidic pH when undissociated acetic acid is present in the reaction medium [86]. However, the ethanol titers in MES systems are relatively low (maximum 0.5 g·L<sup>-1</sup>), which may be due to the microbial utilization of ethanol to other processes, particularly when using mixed microbial culture [52,85].

Butanol production in MES follows a similar pattern compared to ethanol production. It is produced when butyrate accumulates in the reaction media, and sufficient hydrogen or protons are present to further reduce butyrate. Butanol has been found as a by-product but not targeted as the main product in MES experiments so far [47,85,90]. Recently, the production of secondary alcohol isopropanol has been reported in CO<sub>2</sub> continuous-fed MES systems inoculated with mixed microbial cultures [91]. Soussan et al. [72] reported the possibility of producing glycerol from the electroreduction of CO<sub>2</sub> when succinate was present in a biocathode. Titrers ranging

from 6.0 to 9.0 mM were reported in these experiments, achieving 100% CO<sub>2</sub>-glycerol selectivity.

### 1.2.2.2 *Electro-biofuels: electromethanogenesis and biogas upgrading*

Methane is frequently found in the off-gas of hydrogen-producing microbial electrolysis cells (MECs), usually as a result of the presence hydrogenotrophic methanogens in the catholyte of the MEC [92]. Early on, researchers took advantage of this observation to design bioelectrochemical systems with an aim to promote methane rather than hydrogen production [93,94]. Shortly thereafter, it was found that methane can be produced not only via hydrogen mediated mechanisms, but also via direct electron transfer mechanism (Eq. 1) [95,96], which makes methane production an autotrophic and electricity-driven biotransformation process.



The first study on electromethanogenesis from CO<sub>2</sub> was performed in a two chamber bioelectrochemical system that produced ~4.5 L-CH<sub>4</sub>·d<sup>-1</sup>·m<sup>-2</sup> with an 80% overall energy efficiency to methane [95]. In the following years, a number of works devoted to understanding the mechanism of bioelectrochemical methane production and to developing strategies to improve methane production [97] allowed to achieve up to 30.3 L<sub>CH<sub>4</sub></sub>·d<sup>-1</sup>·m<sup>-2</sup> [31] with current-to-methane efficiencies ranging from 23% [98] to ~100% [99,100]. According to recent studies, the energy consumed for methane generation via direct electron transfer at standard biological conditions is substantially lower than that required for the systems working with external hydrogen supply (11 vs. 25.5 kWh·m<sup>-3</sup> CH<sub>4</sub>) [47].

An interesting potential use of the electro-methanogenesis process is biogas upgrading. Biogas produced from the Anaerobic Digestion of organic wastes or energy crops can be a renewable and flexible source of energy. However, raw biogas contains a substantial amount of CO<sub>2</sub> (typically 30-40% CO<sub>2</sub>) and usually requires some kind of refinement to improve its energy value [101] to be thermally valorized or injected in natural gas grids. This CO<sub>2</sub> indeed represents a suitable feed for electromethanogenesis, which transforms CO<sub>2</sub> into methane, directly increasing fuel content and avoiding CO<sub>2</sub> side streams, which is the main disadvantage of traditional biogas up-grading approaches. Some studies have shown that directly implementing a pair of electrodes

inside a digester can improve COD removal, biogas production and methane content [94]. However, this effect cannot be attributed purely to electromethanogenesis, but to the combined effect of enhanced organic matter hydrolysis, additional electrons supplied by the cathode and improved syntrophic interactions within the immobilized biofilm [102].

There are two main strategies for integrating electromethanogenesis with AD. One of them consist of implementing the electrodes inside a traditional digester [103], which has proven to require fine control. The other alternative consists of using a bioelectrochemical system as a post-treatment to AD, which greatly simplifies the operation of both systems and leads to a more versatile assembly to optimize both processes. Recent studies on this approach succeeded to keep CO<sub>2</sub> content in biogas consistently below 10% while achieving coulombic efficiencies over 80% [98,104].

#### 1.2.2.3 *Product recovery*

Product inhibition and microbial tolerance towards a specific product represent one of the most important constraints of MES [47] as it limits titers and production rates [105]. Thus, the valorization of the resources obtained from MES requires the development, adaptation and/or optimization of separation technologies. A key aspect when dealing with separation technologies is that the target chemical should show a unique physicochemical property which differentiates it from the rest of the reaction medium [106]. Extraction, distillation, membranes, absorption, and adsorption are the main separation technologies in the fields of conventional fermentation processes and biorefineries [107]. Regarding MES, only a few studies have been published to date on integrating separation process in a working MES system [76,108,109]. Gildemyn et al. constructed an integrated production, extraction and concentration system for acetic acid production in MES [76]. This is a relevant study as it covers the full process from raw CO<sub>2</sub> to the final enriched product. This system consists of a three-chamber bioelectrochemical system in which acetate is produced from CO<sub>2</sub> in a biocathode chamber and migrates to a central chamber through an AEM. This whole process achieved an acetic acid production rate of 0.7 g·L<sup>-1</sup>·d<sup>-1</sup> reporting up to 73% coulombic efficiency and 99% extraction efficiency. Membrane fouling, system complexity and a high electric energy input are the major shortcomings of this approach [47]. Ion exchange resin adsorption is another demonstrated approach for integrated acetate



production and separation process [108,109]. Here, the catholyte containing acetate flows through an anion-exchange resin (Amberlite™ FPA53). Acetate sorption up to 20 mg·g<sub>resin</sub><sup>-1</sup> was reported from MES catholyte achieving a continued production rate of 0.5 g·L<sup>-1</sup>·d<sup>-1</sup> [109]. Main drawbacks of this approach are clogging of resin columns and the requirement of alkali for chemical resin regeneration.

Despite all these efforts, MES production rates and titers are still far from those achieved via conventional fermentation technologies. For instance, considering acetate recovery, which has been the main target product in MES so far, titers have not reached as high as in traditional fermentation (20-200 g·L<sup>-1</sup>), compromising product separation rates [105]. At such high titer levels, product inhibition would probably occur, which could be solved by implementing integrated product removal technologies.

### 1.2.3 MES weaknesses and opportunities

In the previous sections, fundamentals and merits of MES have been discussed showing facts and figures that allow for certain optimism. However, MES is still at a proof of concept stage, and has not left the laboratory scale. Practical application of MES will require extensive work to overcome current technological and economical barriers. Some of these limitations such as reactor design and robustness, electrodes and membranes cost and aging or biofouling are shared with the rest of METs. However, other major issues are intrinsic for MES including tedious and time consuming start-up procedures, substrate availability to microorganisms, or the effect of slight perturbances, like power fluctuations or minimum oxygen presence, on reactor performance.

Arduousness of biocathode start-up is a fact that is not reported for bioanodes [51,78]. Biocathodes are typically started-up by directly imposing reductive potentials to the electrode, but they have also been grown as bioanodes to reverse the potential when the biofilm is already formed [110,111]. In addition, different inocula and enrichment procedures have been tested to improve cathode start-up, but still further optimization and knowledge about microbial community optimization are required to reach standardized methodologies to start biocathodes for targeted products.

Feeding the substrate (CO<sub>2</sub>) to the MES reactor and its efficient dispersion and diffusion to reach the bioelectrode is another critical aspect. In reactors fed with gaseous

CO<sub>2</sub>, inorganic carbon availability for microorganisms usually becomes the limiting factor, even when supplying considerable excesses of CO<sub>2</sub> [52]. Mixers and impellers have been traditionally used in conventional bioreactors to improve gas dispersion in liquids [112], and in MES, adding excess of external bicarbonate [78] or bubbling excess of CO<sub>2</sub> [52] are frequent strategies to improve CO<sub>2</sub> bioavailability. However, stirring has a limit for bacterial cultures in terms of shear stress [113] and in the sparging method, most of the CO<sub>2</sub> is lost to the atmosphere, while pH must be continuously adjusted if bicarbonate is used as the substrate.

Linking MES to renewable power sources represents another key aspect in advancing this technology towards practical application. Moreover, MES is considered by several authors as an alternative for storing renewable energy surpluses [32,114,115]. However, this technology must prove to be able to withstand intrinsic unpredictable nature of renewable generators. Providing that the cathode as electron donor plays a critical point in MES, fluctuations or lack of supply is expected to appreciably affect reactor performance. To the best of my knowledge, although several studies have proposed MES and renewable energy combination, only one study has actually evaluated the influence of this unstable nature of renewable energy generator over MES reactors [116] before the work that is presented in this thesis. Therefore, gaining knowledge about this effect will extensively benefit the field of MES and will be an essential objective of this thesis.

### 1.3 REFERENCES

- [1] Potter MC. Electrical Effects Accompanying the Decomposition of Organic Compounds. *Proceedings of the Royal Society B: Biological Sciences* 1911;84:260–76. doi:10.1098/rspb.1911.0073.
- [2] Schröder U, Harnisch F, Angenent LT. Microbial electrochemistry and technology: terminology and classification. *Energy & Environmental Science* 2015;8:513–9. doi:10.1039/C4EE03359K.
- [3] Rozendal RA, Hamelers HVM, Rabaey K, Keller J, Buisman CJN. Towards practical implementation of bioelectrochemical wastewater treatment. *Trends in Biotechnology* 2008;26:450–9.
- [4] Desloover J, Arends JBABA, Hennebel T, Rabaey K. Operational and technical considerations for microbial electrosynthesis. *Biochemical Society Transactions* 2012;40:1233 LP-1238.
- [5] Pant D, Singh A, Van Bogaert G, Irving Olsen S, Singh Nigam P, Diels L, et al. Bioelectrochemical systems (BES) for sustainable energy production and product recovery from organic wastes and industrial wastewaters. *RSC Adv* 2012;2:1248–63. doi:10.1039/C1RA00839K.
- [6] Gadkari S, Gu S, Sadhukhan J. Towards automated design of bioelectrochemical systems: A comprehensive review of mathematical models. *Chemical Engineering Journal* 2018;343:303–16. doi:10.1016/J.CEJ.2018.03.005.
- [7] Wang H, Ren ZJ. A comprehensive review of microbial electrochemical systems as a platform technology. *Biotechnology Advances* 2013;31:1796–807. doi:10.1016/J.BIOTECHADV.2013.10.001.
- [8] Recio-Garrido D, Perrier M, Tartakovsky B. Modeling, optimization and control of bioelectrochemical systems. *Chemical Engineering Journal* 2016;289:180–90. doi:10.1016/J.CEJ.2015.11.112.
- [9] Potter MC. Electrical effects in relation to photosynthesis. *Zbl Bakteriol* 1929;78:56.

- [10] Cohen B. The bacterial culture as an electrical half-cell. *J Bacteriol* 1931;21:18–9.
- [11] Logan BE. Biologically extracting energy from wastewater: biohydrogen production and microbial fuel cells. *Environ Sci Technol* 2004;38:160–7.
- [12] Park DH, Laivenieks M, Guettler M V, Jain MK, Zeikus JG. Microbial utilization of electrically reduced neutral red as the sole electron donor for growth and metabolite production. *Applied and Environmental Microbiology* 1999;65:2912–7.
- [13] Kim BH, Kim HJ, Hyun MS, Park DH. Direct electrode reaction of Fe (III)-reducing bacterium, *Shewanella putrefaciens*. *Journal of Microbiology and Biotechnology* 1999;9:127–31.
- [14] Rabaey K, Verstraete W. Microbial fuel cells: novel biotechnology for energy generation. *Trends in Biotechnology* 2005;23:291–8. doi:10.1016/j.tibtech.2005.04.008.
- [15] Bruce E. Logan \*,‡, Bert Hamelers §, René Rozendal §,||, Uwe Schröder ⊥, Jürg Keller #, Stefano Freguia #, et al. *Microbial Fuel Cells: Methodology and Technology*† 2006. doi:10.1021/ES0605016.
- [16] Xing D, Zuo Y, Cheng S, Regan JM, Logan BE. Electricity Generation by *Rhodospseudomonas palustris* DX-1. *Environmental Science & Technology* 2008;42:4146–51. doi:10.1021/es800312v.
- [17] Ieropoulos IA, Stinchcombe A, Gajda I, Forbes S, Merino-Jimenez I, Pasternak G, et al. Pee power urinal - microbial fuel cell technology field trials in the context of sanitation. *Environ Sci: Water Res Technol* 2016;2:336–43. doi:10.1039/C5EW00270B.
- [18] Gajda I, Stinchcombe A, Greenman J, Melhuish C, Ieropoulos I. Ceramic MFCs with internal cathode producing sufficient power for practical applications. *International Journal of Hydrogen Energy* 2015;40:14627–31. doi:10.1016/J.IJHYDENE.2015.06.039.

- 
- [19] Liu H, Grot S, Logan BE. Electrochemically assisted microbial production of hydrogen from acetate. *Environmental Science & Technology* 2005;39:4317–20.
- [20] Rozendal RA, Hamelers HVM, Euverink GJW, Metz SJ, Buisman CJN. Principle and perspectives of hydrogen production through biocatalyzed electrolysis. *International Journal of Hydrogen Energy* 2006;31:1632–40.
- [21] Logan BE, Call D, Cheng S, Hamelers HVM, Sleutels THJA, Jeremiassi AW, et al. Microbial Electrolysis Cells for High Yield Hydrogen Gas Production from Organic Matter. *Environmental Science & Technology* 2008;42:8630–40. doi:10.1021/es801553z.
- [22] Jiang L, Huang L, Sun Y. Recovery of flakey cobalt from aqueous Co(II) with simultaneous hydrogen production in microbial electrolysis cells. *International Journal of Hydrogen Energy* 2014;39:654–63. doi:10.1016/J.IJHYDENE.2013.10.112.
- [23] Luo H, Fu S, Liu G, Zhang R, Bai Y, Luo X. Autotrophic biocathode for high efficient sulfate reduction in microbial electrolysis cells. *Bioresource Technology* 2014;167:462–8. doi:10.1016/J.BIORTECH.2014.06.058.
- [24] Ki D, Papat SC, Rittmann BE, Torres CI. H<sub>2</sub> O<sub>2</sub> Production in Microbial Electrochemical Cells Fed with Primary Sludge. *Environmental Science & Technology* 2017;51:6139–45. doi:10.1021/acs.est.7b00174.
- [25] Gil-Carrera L, Escapa A, Mehta P, Santoyo G, Guiot SR, Morán A, et al. Microbial electrolysis cell scale-up for combined wastewater treatment and hydrogen production. *Bioresource Technology* 2013;130:584–91. doi:10.1016/j.biortech.2012.12.062.
- [26] Escapa A, Mateos R, Martínez EJ, Blanes J. Microbial electrolysis cells: An emerging technology for wastewater treatment and energy recovery. From laboratory to pilot plant and beyond. *Renewable and Sustainable Energy Reviews* 2016;55:942–56. doi:10.1016/j.rser.2015.11.029.
- [27] Cusick RD, Bryan B, Parker DS, Merrill MD, Mehanna M, Kiely PD, et al. Performance of a pilot-scale continuous flow microbial electrolysis cell fed
-

- winery wastewater. *Applied Microbiology and Biotechnology* 2011;89:2053–63. doi:10.1007/s00253-011-3130-9.
- [28] Heidrich ES, Dolfing J, Scott K, Edwards SR, Jones C, Curtis TP. Production of hydrogen from domestic wastewater in a pilot-scale microbial electrolysis cell. *Applied Microbiology and Biotechnology* 2013;97:6979–89.
- [29] San-Martín MI, Mateos R, Carracedo B, Escapa A, Morán A. Pilot-scale bioelectrochemical system for simultaneous nitrogen and carbon removal in urban wastewater treatment plants. *Journal of Bioscience and Bioengineering* 2018. doi:10.1016/J.JBIOSEC.2018.06.008.
- [30] Rozendal RA, Jeremiassen AW, Hamelers HVM, Buisman CJN. Hydrogen Production with a Microbial Biocathode 2007. doi:10.1021/ES071720+.
- [31] Clauwaert P, Verstraete W. Methanogenesis in membraneless microbial electrolysis cells. *Applied Microbiology and Biotechnology* 2009;82:829–36. doi:10.1007/s00253-008-1796-4.
- [32] Nevin KP, Woodard TL, Franks AE, Summers ZM, Lovley DR. Microbial electrosynthesis: feeding microbes electricity to convert carbon dioxide and water to multicarbon extracellular organic compounds. *MBio* 2010;1:e00103--10.
- [33] Martínez Arranz A. Carbon capture and storage: Frames and blind spots. *Energy Policy* 2015;82:249–59. doi:10.1016/j.enpol.2015.03.018.
- [34] Rochedo PRR, Costa IVL, Império M, Hoffmann BS, Merschmann PR de C, Oliveira CCN, et al. Carbon capture potential and costs in Brazil. *Journal of Cleaner Production* 2016;131:280–95. doi:10.1016/j.jclepro.2016.05.033.
- [35] Oh TH. Carbon capture and storage potential in coal-fired plant in Malaysia—A review. *Renewable and Sustainable Energy Reviews* 2010;14:2697–709. doi:10.1016/j.rser.2010.06.003.
- [36] Stephens JC. Carbon capture and storage: a controversial climate mitigation approach. *The International Spectator* 2015;50:74–84.
- [37] Norhasyima RS, Mahlia TMI. Advances in CO<sub>2</sub> utilization technology: A patent

- landscape review. *Journal of CO<sub>2</sub> Utilization* 2018;26:323–35. doi:10.1016/J.JCOU.2018.05.022.
- [38] NETL. CO<sub>2</sub>-utilization - National Energy Technology Laboratory n.d. <https://www.netl.doe.gov/research/coal/carbon-storage/research-and-development/co2-utilization> (accessed August 1, 2017).
- [39] Huang C-HH, Tan C-SS. A review: CO<sub>2</sub> utilization. *Aerosol and Air Quality Research* 2014;14:480–99. doi:10.4209/aaqr.2013.10.0326.
- [40] Moss M, Reed DG, Allen RWK, others. Integrated CO<sub>2</sub> Capture and Utilisation using Non-Thermal Plasmolysis. *Frontiers in Energy Research* 2017;5:20.
- [41] Kang D, Lee M-G, Jo H, Yoo Y, Lee S-Y, Park J. Carbon capture and utilization using industrial wastewater under ambient conditions. *Chemical Engineering Journal* 2017;308:1073–80. doi:10.1016/j.cej.2016.09.120.
- [42] Psarras PC, Comello S, Bains P, Charoensawadpong P, Reichelstein S, Wilcox J. Carbon Capture and Utilization in the Industrial Sector. *Environmental Science & Technology* 2017;51:11440–9. doi:10.1021/acs.est.7b01723.
- [43] Qiao J, Liu Y, Hong F, Zhang J, Sridhar N, Shin W, et al. A review of catalysts for the electroreduction of carbon dioxide to produce low-carbon fuels. *Chem Soc Rev* 2014;43:631–75. doi:10.1039/C3CS60323G.
- [44] Whipple DT, Kenis PJA. Prospects of CO<sub>2</sub> Utilization via Direct Heterogeneous Electrochemical Reduction. *The Journal of Physical Chemistry Letters* 2010;1:3451–8. doi:10.1021/jz1012627.
- [45] Lee S, Lee J. Electrode Build-Up of Reducible Metal Composites toward Achievable Electrochemical Conversion of Carbon Dioxide. *ChemSusChem* 2016;9:333–44. doi:10.1002/cssc.201501112.
- [46] Halmann MM, Steinberg M. Chapter 12 - Electrochemical reduction of CO<sub>2</sub>. *Greenhouse gas carbon dioxide mitigation: science and technology*, CRC press; 1998, p. 411–516.
- [47] Bajracharya S, Srikanth S, Mohanakrishna G, Zacharia R, Strik DP, Pant D.

- Biotransformation of carbon dioxide in bioelectrochemical systems: State of the art and future prospects. *Journal of Power Sources* 2017;356:256–73. doi:10.1016/j.jpowsour.2017.04.024.
- [48] Rabaey K, Rozendal RA. Microbial electrosynthesis—revisiting the electrical route for microbial production. *Nature Reviews Microbiology* 2010;8:706–16.
- [49] Rosenbaum M, Aulenta F, Villano M, Angenent LT. Cathodes as electron donors for microbial metabolism: Which extracellular electron transfer mechanisms are involved? *Bioresource Technology* 2011;102:324–33. doi:10.1016/j.biortech.2010.07.008.
- [50] Lovley DR, Nevin KP. Electrobiocommodities: Powering microbial production of fuels and commodity chemicals from carbon dioxide with electricity. *Current Opinion in Biotechnology* 2013;24:385–90.
- [51] Bajracharya S, ter Heijne A, Dominguez Benetton X, Vanbroekhoven K, Buisman CJNN, Strik DPBTBBTB, et al. Carbon dioxide reduction by mixed and pure cultures in microbial electrosynthesis using an assembly of graphite felt and stainless steel as a cathode. *Bioresource Technology* 2015;195:14–24. doi:http://dx.doi.org/10.1016/j.biortech.2015.05.081.
- [52] Bajracharya S, Yuliasni R, Vanbroekhoven K, Buisman CJN, Strik DPBTB, Pant D. Long-term operation of microbial electrosynthesis cell reducing CO<sub>2</sub> to multi-carbon chemicals with a mixed culture avoiding methanogenesis. *Bioelectrochemistry* 2017;113:26–34. doi:10.1016/j.bioelechem.2016.09.001.
- [53] Jourdin L, Freguia S, Donose BC, Chen J, Wallace GG, Keller J. A novel carbon nanotube modified scaffold as an efficient biocathode material for improved microbial electrosynthesis. *J Mater Chem A* 2014;2. doi:10.1039/C4TA03101F.
- [54] Guo K, PrévotEAU A, Patil SA, Rabaey K. Engineering electrodes for microbial electrocatalysis. *Current Opinion in Biotechnology* 2015;33:149–56. doi:10.1016/J.COPBIO.2015.02.014.
- [55] Bouchez T, Bridier A, Le Quéméner E. Method and device for controlling the activity of a bioelectrochemical system comprising both a bioanode and a



- biocathode 2017.
- [56] Sleutels THJA, ter Heijne A, Kuntke P, Buisman CJN, Hamelers HVM. Membrane Selectivity Determines Energetic Losses for Ion Transport in Bioelectrochemical Systems. *ChemistrySelect* 2017;2:3462–70. doi:10.1002/slct.201700064.
- [57] Kracke F, Vassilev I, Kromer JO. Microbial electron transport and energy conservation - the foundation for optimizing bioelectrochemical systems. *Frontiers in Microbiology* 2015;6:575. doi:10.3389/fmicb.2015.00575.
- [58] Choi O, Sang B-I. Extracellular electron transfer from cathode to microbes: application for biofuel production. *Biotechnology for Biofuels* 2016;9:11. doi:10.1186/s13068-016-0426-0.
- [59] Tremblay PL, Zhang T. Electrifying microbes for the production of chemicals. *Front Microbiol* 2015.
- [60] Ross DE, Flynn JM, Baron DB, Gralnick JA, Bond DR. Towards Electrosynthesis in *Shewanella*: Energetics of Reversing the Mtr Pathway for Reductive Metabolism. *PLoS ONE* 2011;6:e16649. doi:10.1371/journal.pone.0016649.
- [61] Poehlein A, Gottschalk G, Daniel R. First Insights into the Genome of the Gram-Negative, Endospore-Forming Organism *Sporomusa ovata* Strain H1 DSM 2662. *Genome Announcements* 2013;1:e00734-13. doi:10.1128/genomeA.00734-13.
- [62] Köpke M, Held C, Hujer S, Liesegang H, Wiezer A, Wollherr A, et al. *Clostridium ljungdahlii* represents a microbial production platform based on syngas. *Proceedings of the National Academy of Sciences of the United States of America* 2010;107:13087–92. doi:10.1073/pnas.1004716107.
- [63] Steinbusch KJJ, Hamelers HVM, Schaap JD, Kampman C, Buisman CJN. Bioelectrochemical ethanol production through mediated acetate reduction by mixed cultures. *Environmental Science & Technology* 2009;44:513–7.
- [64] Kim BH, Lim SS, Daud WRW, Gadd GM, Chang IS. The biocathode of

- microbial electrochemical systems and microbially-influenced corrosion. *Bioresource Technology* 2015;190:395–401. doi:10.1016/j.biortech.2015.04.084.
- [65] Patil SA, Gildemyn S, Pant D, Zengler K, Logan BE, Rabaey K. A logical data representation framework for electricity-driven bioproduction processes. *Biotechnology Advances* 2015;33:736–44.
- [66] Marsili E, Baron DB, Shikhare ID, Coursolle D, Gralnick JA, Bond DR. *Shewanella* secretes flavins that mediate extracellular electron transfer. *Proceedings of the National Academy of Sciences of the United States of America* 2008;105:3968–73. doi:10.1073/pnas.0710525105.
- [67] Venkataraman A, Rosenbaum M, Arends JBA, Halitschke R, Angenent LT. Quorum sensing regulates electric current generation of *Pseudomonas aeruginosa* PA14 in bioelectrochemical systems. *Electrochemistry Communications* 2010;12:459–62. doi:10.1016/J.ELECOM.2010.01.019.
- [68] de Campos Rodrigues T, Rosenbaum MA. Microbial Electroreduction: Screening for New Cathodic Biocatalysts. *ChemElectroChem* 2014;1:1916–22. doi:10.1002/CELC.201402239.
- [69] Nevin KP, Hensley SA, Franks AE, Summers ZM, Ou J, Woodard TL, et al. Electrosynthesis of organic compounds from carbon dioxide is catalyzed by a diversity of acetogenic microorganisms. *Applied and Environmental Microbiology* 2011;77:2882–6. doi:10.1128/AEM.02642-10.
- [70] Ragsdale SW, Pierce E. Acetogenesis and the Wood–Ljungdahl pathway of CO<sub>2</sub> fixation. *Biochimica et Biophysica Acta (BBA) - Proteins and Proteomics* 2008;1784:1873–98. doi:10.1016/J.BBAPAP.2008.08.012.
- [71] Zhang T, Nie H, Bain TS, Lu H, Cui M, Snoeyenbos-West OL, et al. Improved cathode materials for microbial electrosynthesis. *Energy Environ Sci* 2013;6:217–24. doi:10.1039/C2EE23350A.
- [72] Soussan L, Riess J, Erable B, Delia M-L, Bergel A. Electrochemical reduction of CO<sub>2</sub> catalysed by *Geobacter sulfurreducens* grown on polarized stainless steel cathodes. vol. 28. 2013. doi:10.1016/j.elecom.2012.11.033.

- [73] Zhen G, Kobayashi T, Lu X, Xu K. Understanding methane bioelectrosynthesis from carbon dioxide in a two-chamber microbial electrolysis cells (MECs) containing a carbon biocathode. *Bioresource Technology* 2015;186:141–8. doi:10.1016/J.BIORTECH.2015.03.064.
- [74] Jourdin L, Lu Y, Flexer V, Keller J, Freguia S. Biologically Induced Hydrogen Production Drives High Rate/High Efficiency Microbial Electrosynthesis of Acetate from Carbon Dioxide. *ChemElectroChem* 2016. doi:10.1002/celc.201500530.
- [75] LaBelle E V., May HD. Energy Efficiency and Productivity Enhancement of Microbial Electrosynthesis of Acetate. *Frontiers in Microbiology* 2017;8:756. doi:10.3389/fmicb.2017.00756.
- [76] Gildemyn S, Verbeeck K, Slabbinck R, Andersen SJ, PrévotEAU A, Rabaey K. Integrated Production, Extraction, and Concentration of Acetic Acid from CO<sub>2</sub> through Microbial Electrosynthesis. *Environmental Science & Technology Letters* 2015;2:325–8. doi:10.1021/acs.estlett.5b00212.
- [77] Pisciotta JM, Zaybak Z, Call DF, Nam J-Y, Logan BE. Enrichment of microbial electrolysis cell biocathodes from sediment microbial fuel cell bioanodes. *Applied and Environmental Microbiology* 2012;78:5212–9. doi:10.1128/AEM.00480-12.
- [78] Zaybak Z, Pisciotta JM, Tokash JC, Logan BE. Enhanced start-up of anaerobic facultatively autotrophic biocathodes in bioelectrochemical systems. *Journal of Biotechnology* 2013;168:478–85. doi:10.1016/j.jbiotec.2013.10.001.
- [79] Marshall CW, Ross DE, Fichot EB, Norman RS, May HD. Electrosynthesis of commodity chemicals by an autotrophic microbial community. *Applied and Environmental Microbiology* 2012;78:8412–20.
- [80] Chabert N, Amin Ali O, Achouak W. All ecosystems potentially host electrogenic bacteria. *Bioelectrochemistry* 2015;106:88–96. doi:10.1016/J.BIOELECHEM.2015.07.004.
- [81] Modestra JA, Mohan SV. Microbial electrosynthesis of carboxylic acids through

- CO<sub>2</sub> reduction with selectively enriched biocatalyst: Microbial dynamics. *Journal of CO<sub>2</sub> Utilization* 2017;20:190–9. doi:10.1016/j.jcou.2017.05.011.
- [82] Mohanakrishna G, Seelam JS, Vanbroekhoven K, Pant D. An enriched electroactive homoacetogenic biocathode for the microbial electrosynthesis of acetate through carbon dioxide reduction. *Faraday Discussions* 2015;183:445–62. doi:10.1039/C5FD00041F.
- [83] May HD, Evans PJ, LaBelle E V. The bioelectrosynthesis of acetate. *Current Opinion in Biotechnology* 2016;42:225–33. doi:10.1016/j.copbio.2016.09.004.
- [84] Wood HG. Life with CO or CO<sub>2</sub> and H<sub>2</sub> as a source of carbon and energy. *The FASEB Journal* 1991;5:156–63.
- [85] Ganigué R, Puig S, Batlle-Vilanova P, Balaguer MD, Colprim J. Microbial electrosynthesis of butyrate from carbon dioxide. *Chemical Communications* 2015;51:3235–8.
- [86] Steinbusch KJJ, Hamelers HVM, Plugge CM, Buisman CJN. Biological formation of caproate and caprylate from acetate: fuel and chemical production from low grade biomass. *Energy Environ Sci* 2011;4:216–24. doi:10.1039/C0EE00282H.
- [87] Batlle-Vilanova P, Ganigué R, Ramió-Pujol S, Bañeras L, Jiménez G, Hidalgo M, et al. Microbial electrosynthesis of butyrate from carbon dioxide: Production and extraction. *Bioelectrochemistry* 2017. doi:10.1016/j.bioelechem.2017.06.004.
- [88] Annie Modestra J, Navaneeth B, Venkata Mohan S. Bio-electrocatalytic reduction of CO<sub>2</sub>: Enrichment of homoacetogens and pH optimization towards enhancement of carboxylic acids biosynthesis. *Journal of CO<sub>2</sub> Utilization* 2015;10:78–87. doi:10.1016/j.jcou.2015.04.001.
- [89] Ammam F, Tremblay P-L, Lizak DM, Zhang T. Effect of tungstate on acetate and ethanol production by the electrosynthetic bacterium *Sporomusa ovata*. *Biotechnology for Biofuels* 2016;9:163. doi:10.1186/s13068-016-0576-0.

- 
- [90] Blanchet E, Duquenne F, Rafrafi Y, Etcheverry L, Erable B, Bergel A. Importance of the hydrogen route in up-scaling electrosynthesis for microbial CO<sub>2</sub> reduction. *Energy & Environmental Science* 2015;8:3731–44.
- [91] Arends JBA, Patil SA, Roume H, Rabaey K. Continuous long-term electricity-driven bioproduction of carboxylates and isopropanol from CO<sub>2</sub> with a mixed microbial community. *Journal of CO<sub>2</sub> Utilization* 2017;20:141–9. doi:10.1016/j.jcou.2017.04.014.
- [92] Wang A, Liu W, Cheng S, Xing D, Zhou J, Logan BE. Source of methane and methods to control its formation in single chamber microbial electrolysis cells. *International Journal of Hydrogen Energy* 2009;34:3653–8. doi:10.1016/j.ijhydene.2009.03.005.
- [93] Molenaar S, Saha P, Mol A, Sleutels T, ter Heijne A, Buisman C. Competition between Methanogens and Acetogens in Biocathodes: A Comparison between Potentiostatic and Galvanostatic Control. *International Journal of Molecular Sciences* 2017;18:204. doi:10.3390/ijms18010204.
- [94] Moreno R, San-Martín MI, Escapa A, Morán A. Domestic wastewater treatment in parallel with methane production in a microbial electrolysis cell. *Renewable Energy* 2016;93:442–8. doi:10.1016/j.renene.2016.02.083.
- [95] Cheng S, Xing D, Call DF, Logan BE. Direct biological conversion of electrical current into methane by electromethanogenesis. *Environmental Science & Technology* 2009;43:3953–8.
- [96] Fu Q, Kuramochi Y, Fukushima N, Maeda H, Sato K, Kobayashi H. Bioelectrochemical analyses of the development of a thermophilic biocathode catalyzing electromethanogenesis. *Environmental Science & Technology* 2015;49:1225–32.
- [97] Geppert F, Liu D, van Eerten-Jansen M, Weidner E, Buisman C, ter Heijne A. Bioelectrochemical Power-to-Gas: State of the Art and Future Perspectives. *Trends in Biotechnology* 2016;34:879–94. doi:10.1016/j.tibtech.2016.08.010.
- [98] Eerten-Jansen V, Mieke CAA, Heijne A Ter, Buisman CJN, Hamelers HVM.
-

- Microbial electrolysis cells for production of methane from CO<sub>2</sub>: long-term performance and perspectives. *International Journal of Energy Research* 2012;36:809–19.
- [99] Van Eerten-Jansen MCAA, Veldhoen AB, Plugge CM, Stams AJM, Buisman CJN, Ter Heijne A. Microbial community analysis of a methane-producing biocathode in a bioelectrochemical system. *Archaea* 2013;2013.
- [100] Kuramochi Y, Fu Q, Kobayashi H, Ikarashi M, Wakayama T, Kawaguchi H, et al. Electromethanogenic CO<sub>2</sub> Conversion by Subsurface-reservoir Microorganisms. *Energy Procedia* 2013;37:7014–20. doi:10.1016/j.egypro.2013.06.636.
- [101] das Neves LC, Converti A, Vessoni Penna TC. Biogas production: new trends for alternative energy sources in rural and urban zones. *Chemical Engineering & Technology* 2009;32:1147–53.
- [102] Modin O. Integrating bioelectrochemical systems with anaerobic digestion. IWA Leading Edge Technologies conference, Bordeaux, France, June 2-6, 2013.
- [103] Energy recovery evaluation in an up flow microbial electrolysis coupled anaerobic digestion (ME-AD) reactor: Role of electrode positions and hydraulic retention times. *Applied Energy* 2017;206:1214–24. doi:10.1016/J.APENERGY.2017.10.026.
- [104] Xu H, Wang K, Holmes DE. Bioelectrochemical removal of carbon dioxide (CO<sub>2</sub>): An innovative method for biogas upgrading. *Bioresource Technology* 2014;173:392–8. doi:10.1016/j.biortech.2014.09.127.
- [105] López-Garzón CS, Straathof AJJ. Recovery of carboxylic acids produced by fermentation. *Biotechnology Advances* 2014;32:873–904. doi:10.1016/j.biotechadv.2014.04.002.
- [106] Roy S, Schievano A, Pant D. Electro-stimulated microbial factory for value added product synthesis. *Bioresource Technology* 2016;213:129–39. doi:10.1016/j.biortech.2016.03.052.

- 
- [107] Huang H-J, Ramaswamy S, Tschirner UW, Ramarao BV. A review of separation technologies in current and future biorefineries. *Separation and Purification Technology* 2008;62:1–21. doi:10.1016/j.seppur.2007.12.011.
- [108] Bajracharya S, Vanbroekhoven K, De Wever H, Strik D, Buisman C, Pant D. Integrated Product Separation in Bioelectrochemical CO<sub>2</sub> Reduction for Improved Process Efficiency. *Chemie Ingenieur Technik* 2016;88:1255–6.
- [109] Bajracharya S, van den Burg B, Vanbroekhoven K, De Wever H, Buisman CJN, Pant D, et al. In situ acetate separation in microbial electrosynthesis from CO<sub>2</sub> using ion-exchange resin. *Electrochimica Acta* 2017;237:267–75. doi:10.1016/j.electacta.2017.03.209.
- [110] Hartline RM, Call DF. Substrate and electrode potential affect electrotrophic activity of inverted bioanodes. *Bioelectrochemistry* 2016;110:13–8. doi:10.1016/j.bioelechem.2016.02.010.
- [111] Geelhoed JS, Stams AJM. Electricity-assisted biological hydrogen production from acetate by *Geobacter sulfurreducens*. *Environmental Science & Technology* 2010;45:815–20.
- [112] Bakker A, Smith J, Myers K. How to disperse gases in liquids. *Chem Eng* 1994:101.
- [113] Ercan D, Demirci A. Current and future trends for biofilm reactors for fermentation processes. *Critical Reviews in Biotechnology* 2015;35:1–14. doi:10.3109/07388551.2013.793170.
- [114] Abate S, Lanzafame P, Perathoner S, Centi G. New Sustainable Model of Biorefineries: Biofactories and Challenges of Integrating Bio-and Solar Refineries. *ChemSusChem* 2015;8:2854–66.
- [115] Perathoner S, Centi G. CO<sub>2</sub> Recycling: A Key Strategy to Introduce Green Energy in the Chemical Production Chain. *ChemSusChem* 2014;7:1274–82. doi:10.1002/cssc.201300926.
- [116] Anzola Rojas M del P, Zaiat M, Gonzalez ER, De Wever H, Pant D. Effect of the
-

electric supply interruption on a microbial electrosynthesis system converting inorganic carbon into acetate. *Bioresource Technology* 2018;266:203–10. doi:10.1016/J.BIORTECH.2018.06.074.



## CHAPTER 2

# Incentives

## Objectives and thesis outline

Taxes have no impact. CO<sub>2</sub> utilizing technology just needs to be competitive.

TAX EXHAUST ISO INTAKE

IF OUR CLOS ARE TAXED IMPORTED PRODUCTS AS WELL

A CO<sub>2</sub> TAX ONLY POSSIBLE IF THE EU CAN DO THE SAME

Emitting too cheap the more

Product consumption should be taxed irrespective of source

COMPETITIVE & RESOURCES ARE ALSO ELIGIBLE

MAKING IT FAIR

Price for CO<sub>2</sub>?

ISSIONS

Tax

A S... LCA

Should encourage/discourage, but not be the driver. CCU technologies should be self-sustainable.

CO<sub>2</sub> price

NEXT TO A CARBON TAX, HOW ABOUT A RESOURCE TAX? C IS NOT THE ONLY ONE!

SMART, UNRESTRAINABLE & FAIR POLICIES WOULD MAKE THE DIFFERENCE

Individual meat tax

Individual meat tax

LCA is key INCENTIVE

Real price of transport (with CO<sub>2</sub>)

Embodied



## 2.1 OBJECTIVES

The main objective of this thesis is to give the initial steps to move MES from the proof of concept stage (in which it currently is) towards practical application by addressing some important issues that are limiting its development beyond the laboratory. For this purpose, the following specific goals are proposed:

- a) Development of a methodology for fast (preliminary) screening of electrode materials for biocathodes.
- b) Assessment of different start-up strategies to obtain productive biocathodes, in order to gain insight about microbial communities developed on the biofilms.
- c) Enhancing biocathodes productivity to acetic acid by improving substrate (CO<sub>2</sub>) availability to microorganisms.
- d) Assessment of acetogenic biocathodes resilience to short power gaps as a first step towards MES - Renewable energy coupling.
- e) Assessment of the impact of long-term power interruptions on acetogenic biocathodes performance and on the structure of microbial communities.

## 2.2 THESIS OUTLINE

MES is currently at a laboratory or proof of concept stage and further development is still being hampered by the many factors that remain uncertain, including optimization, technical and economic feasibility or scaling-up. This thesis tries to provide an answer to some of these questions. It begins by paying attention to the core of MES technology: the cathode and the microbial communities associated to it. In this regard, a methodology to electrochemically characterize electrode materials capable of supporting electroactive biofilms is developed. In addition, and given the important role the later plays on MES performance, several start-up strategies are tested and compared in an effort to obtain a biocathode for chemical production (acetic acid in particular). This work ends by addressing other practical aspects such as improving CO<sub>2</sub> availability to microorganisms and testing how power fluctuations affect acetogenic biocathodes, as preliminary steps before undertaking the scale-up.

The present document is divided into 9 chapters, which are detailed below.

### ***Chapter 1: General introduction***

This chapter provides a general overview regarding the fundamental topics of the thesis. First, this chapter offers a general outlook on bioelectrochemical systems (BES). Secondly, a main body deals with the background and state of the art of the Microbial Electrosynthesis (MES) from CO<sub>2</sub>, including physico-chemical, technical and microbiological information. Finally, a summary gathering the main weaknesses and opportunities of MES is provided.

### ***Chapter 2: Objectives and thesis outline***

Objectives, thesis outline, scope and structure are presented in this chapter.

### ***Chapter 3: Materials and Methods***

The configuration of the BES used on this thesis, as well as technical and analytical conditions and methods, are summarized in this chapter. Specific information is further given on each experimental chapter.

### ***Chapter 4: Methodology for fast and facile characterisation of carbon-based electrodes focused on BES development and scale up***

In this chapter, an easy and simple methodology for a preliminary characterization and screening of electrode materials is presented. This method is based on basic electroanalytical techniques to give a fast and reliable estimation of the most suitable electrode for BES applications. The idea in this chapter is intended to provide researchers with a rapid tool for electrode screening.

### ***Chapter 5: Impact of the start-up process on the microbial communities in biocathodes for electrosynthesis***

This chapter aims at gaining knowledge on how the inoculation and start-up process influences the microbial communities present on the biocathode. This is performed following different start-up strategies with different inocula, and assessing differences in terms of microbial diversity, richness and composition as well as physicochemical performance of each MES system during the start-up.

---

***Chapter 6: Enhanced CO<sub>2</sub> conversion through MES by continuous headspace gas recirculation***

This chapter targets at gaining knowledge on how CO<sub>2</sub> availability to microorganisms can be improved through continuous gas recirculation and how it impacts on MES performance. Moreover, this chapter is also focused on elucidating which are the microorganisms responsible for the process and how their presence correlates with MES performance.

***Chapter 7: Microbial Electrosynthesis (MES) from CO<sub>2</sub> is resilient to fluctuations in renewable energy supply***

This chapter tries to gain knowledge on how short-term power fluctuations (in the range of hours) affect an acetogenic MES system fed with gaseous CO<sub>2</sub>.

***Chapter 8: Long-term open circuit MES system promotes methanogenesis***

This chapter focuses on how a long-term absence of power affects a MES system. Moreover, as extensive microbial community evolution can be expected after a change in the operating conditions, this chapter assesses microbiological and physicochemical effects on a well-established MES reactor.

***Chapter 9: General conclusions and future research suggestion***

The general conclusions of this PhD thesis are provided in this chapter. Furthermore, some personal recommendations are proposed for future investigations.

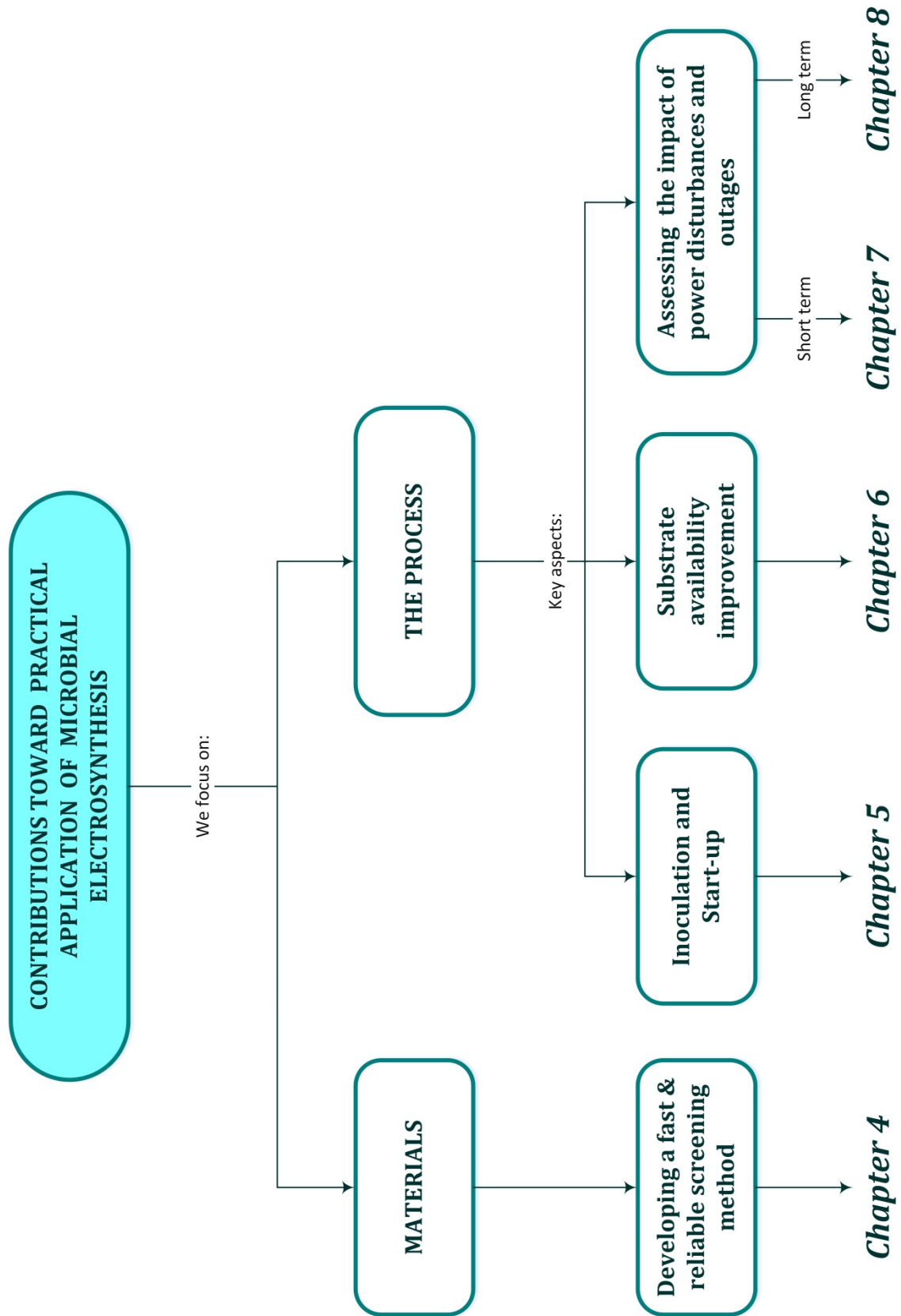


Figure 2.1: General overview of this thesis

## CHAPTER 3

### Materials and Methods

$$P = \frac{C_{end} - C_{ini}}{t_{end} - t_{ini}} \quad Q = \int i dt$$

$$V = I \cdot R$$





In this section, a general description of common experimental set-ups, inocula and culture media, analytical and electrochemical techniques and calculations are presented. Detailed information can be found on each chapter.

### 3.1 EXPERIMENTAL SET-UP

#### 3.1.1 Conical test cell

A 100mL single-chamber conical cell (Metrohm 6.1415.210) was used to develop the methodology proposed in **Chapter 4** (Figure 3.1). The commercial electrochemical cell offered enough access locations at top sealing to allow working and counter electrode connections, reference electrode, nitrogen bubbling for inertization and an extra sampling port.



**Figure 3.1:** Conical test cell.

#### 3.1.2 Planar reactors

Two-chambered 50 mL planar cells were used for the evaluation of biocathodes start-up in **Chapter 5**. This reactor was built of methacrylate and consists of two empty 3cm-thick bodies, acting as anodic and cathodic chambers, closed in both sides by other two 5mm-thick layers. Rubber joints were used as seals in between methacrylate pieces. A glass tube was attached to the top of the cathodic chamber as gas sample collector.

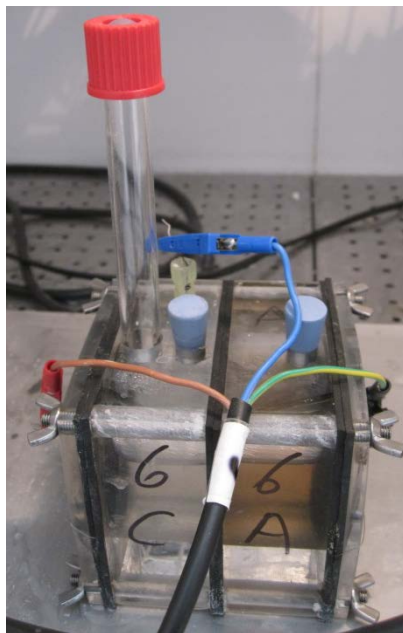


**Figure 3.2:** Planar reactor

### **3.1.3 Bottle type reactors**

500 mL modified Duran® bottles were used as reactors for **Chapter 6**. In this case a 20 mL semi-cylindrical glass chamber was design to be placed in the middle of the reactor to contain the anode as anodic chamber. The rest of the bottle acted as cathodic chamber with a cylindrical cathode attached to the bottle walls. Appropriate caps and connections were designed for headspace gas recirculation, reference electrode, sampling, feeding and electrical connections.

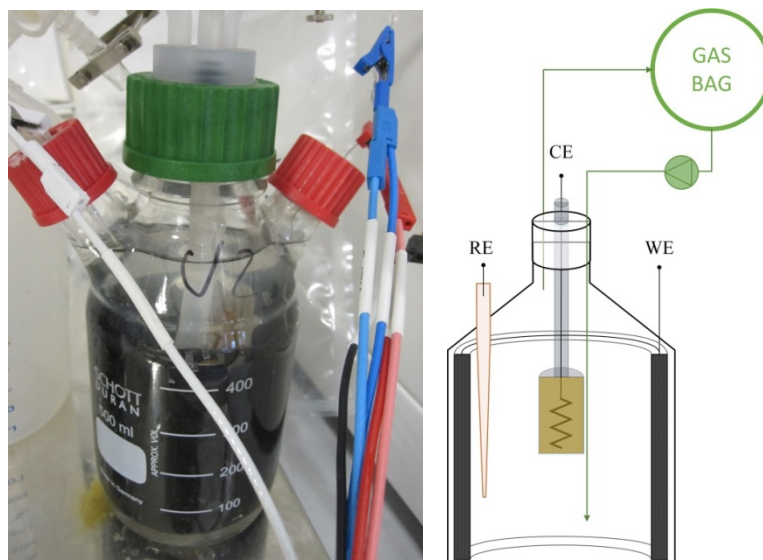


**Figure 3.3:** Bottle-type reactor. Real image and diagram.

### 3.1.4 H-type reactors

Standard H-type reactors were used in **Chapters 7 and 8** with 250 mL and 500 mL per chamber respectively. As it was foreseen in the case of bottle type reactors, appropriate connections and sealing were designed for connections sampling and substrate supply.



**Figure 3.4:** H-type reactor

Further information about reactor materials, set-up, operation and management will be provided in detail on each experimental chapter.

## 3.2 INOCULA AND CULTURE MEDIA

### 3.2.1 Inocula

For the experiments carried out in **Chapters 5, 6, 7 and 8**, anaerobic sludge was used as primary inoculum. This mixed culture was directly used as cell inoculum in the case of Chapter 5, and previously enriched to promote acetogens in Chapter 6. In the case of Chapters 7 and 8, the biocathode was inoculated with the supernatant of a previously existing cell, which was in turn started using anaerobic sludge as initial source of microorganisms. Details of enrichment and initial microbial community can be found in the corresponding chapters.

River mud was also used as primary source of microorganisms in **Chapter 5** with the aim of establishing a comparison against anaerobic sludge.

### 3.2.2 Culture media

In **chapters 5 and 6**, the culture medium used for the working electrode (WE) chamber consisted of a nutrient solution with the following composition (in  $\text{g}\cdot\text{L}^{-1}$ ): 0.87  $\text{K}_2\text{HPO}_4$ ; 0.68  $\text{KH}_2\text{PO}_4$ ; 0.25  $\text{NH}_4\text{Cl}$ ; 0.1  $\text{KCl}$ ; 0.04  $\text{CaCl}_2\cdot 2\text{H}_2\text{O}$ ; 0.45  $\text{MgCl}_2\cdot 6\text{H}_2\text{O}$  and 10 ml per litre of a mineral solution containing (in  $\text{g}\cdot\text{L}^{-1}$ ): 6  $\text{MgSO}_4\cdot 7\text{H}_2\text{O}$ , 1  $\text{MnSO}_4\cdot \text{H}_2\text{O}$ , 2  $\text{NaCl}$ , 0.2  $\text{FeSO}_4\cdot 7\text{H}_2\text{O}$ , 0.3  $\text{CoCl}_2\cdot 6\text{H}_2\text{O}$ , 0.2  $\text{CaCl}_2\cdot 2\text{H}_2\text{O}$ , 0.17  $\text{ZnCl}_2$ , 0.02 of  $\text{CuSO}_4\cdot 5\text{H}_2\text{O}$ , 0.02  $\text{H}_3\text{BO}_3$ , 0.04  $\text{Na}_2\text{MoO}_4\cdot 2\text{H}_2\text{O}$ , 0.06  $\text{NiCl}_2\cdot 6\text{H}_2\text{O}$ , 0.6 mg  $\text{Na}_2\text{SeO}_4$  and 0.8 mg  $\text{Na}_2\text{WO}_4\cdot 2\text{H}_2\text{O}$  as described in Marshall and colleagues (2012) [1].

In **chapter 5** when the WEs were operated as bioanodes, the carbon source consisted of a mixture of sodium acetate  $0.5 \text{ g}\cdot\text{L}^{-1}$ , sodium propionate  $0.1 \text{ g}\cdot\text{L}^{-1}$  and glucose  $0.1 \text{ g}\cdot\text{L}^{-1}$ . When they operated as biocathodes, the carbon source was  $2.5 \text{ g}\cdot\text{L}^{-1}$  sodium bicarbonate. The electrolyte used in the counter electrode (CE) chamber was a phosphate 0.1 M buffer solution. For CEs operating as chemical anodes, the initial pH was slightly alkaline (7.8) to counteract their natural tendency towards acidification. For similar reasons, the initial pH of CEs operating as chemical cathodes was slightly acidic (6.8).

In the case of **chapter 6**, the electrolyte used in the CE chamber was a pH 7.8 0.1 M phosphate buffer solution, and the source of carbon was gaseous  $\text{CO}_2$ .

---

For **chapters 7 and 8**, the catholyte consisted of a similar nutrient solution with the following composition:  $\text{KH}_2\text{PO}_4$  monobasic ( $0.33 \text{ g L}^{-1}$ );  $\text{K}_2\text{HPO}_4$  dibasic ( $0.45 \text{ g L}^{-1}$ );  $\text{NH}_4\text{Cl}$  ( $1 \text{ g L}^{-1}$ );  $\text{KCl}$  ( $0.1 \text{ g L}^{-1}$ );  $\text{NaCl}$  ( $0.8 \text{ g L}^{-1}$ );  $\text{MgSO}_4 \cdot 7\text{H}_2\text{O}$  ( $0.2 \text{ g L}^{-1}$ ); vitamin solution DSMZ 141 ( $1 \text{ mL L}^{-1}$ ), and trace solution DSMZ 141 ( $10 \text{ mL L}^{-1}$ ) [2]. In the case of **chapter 7**, pure gaseous  $\text{CO}_2$  was provided as the sole carbon source keeping the inflow at  $10 \text{ mL} \cdot \text{min}^{-1}$ . For **chapter 8**, inorganic carbon was provided in the form of bicarbonate.

### 3.3 ANALYTICAL AND ELECTROCHEMICAL TECHNIQUES

Liquid samples were analyzed in terms of total organic carbon (TOC), total inorganic carbon (IC) and total nitrogen (TN), volatile fatty acids (VFAs) from C2 to C6, alcohols from C1 to C4. Conductivity and pH were measured following standard methodologies. Further information of these analytical techniques and the equipment used for each case will be provided on each chapter.

Gas samples were measured in terms of composition targeting hydrogen, methane, carbon dioxide, carbon monoxide, oxygen and nitrogen by gas chromatography. Gas flow was also measured with appropriate using liquid displacing devices. Detailed information on equipment will be provided for each chapter.

Analytical electrochemistry, such as chronoamperometry (CA), cyclic voltammetry (CV) and Electrochemical Impedance Spectroscopy (EIS), was performed using a commercial potentiostat (VMP3, Biologic Science Instruments, France) in **chapters 4, 5, 6, 7 and 8**. Basic data treatment (i.e. transferred charge or peak analysis) was carried out with the software associated to this equipment (EC-Lab®). Further information about the electrochemical techniques applied on each chapter is given on each one. **Chapter 4** specially details analytical electrochemistry as it entails a different methodology than the rest of the chapters.

### 3.4 MOLECULAR BIOLOGY TECHNIQUES

Microbial communities present on **chapters 5 to 8** were analyzed and followed along the experimental time by high throughput sequencing of massive *16S rRNA gene* libraries. Total Eubacteria, and Archaea in some studies, were analyzed. In the case of solid samples from bioelectrodes thin pieces of approximately  $2 \times 2 \text{ mm}$  were cut off for

DNA extraction. Liquid samples, from inocula and supernatants, were directly used for DNA extraction. Genomic DNA was extracted with a PowerSoil® DNA Isolation Kit (MoBio Laboratories Inc., Carlsbad, CA, USA) or a Soil DNA Isolation Plus Kit® (Norgen Biotek Corp.) according to manufacturer's instructions. PCRs were carried out in a Mastercycler (Eppendorf, Hamburg, Germany) and these samples were checked for size of the product. Information about compilation, bioinformatics and other treatment of raw data is detailed on each chapter.

Scanning Electron Microscopy (SEM) images were used to verify biofilm formation on the electrodes. For electrode sampling, 0.5cm x 0.5cm thin pieces of graphite electrode were taken at the beginning and end of the experiments carried out in **chapters 7 and 8**. Samples were prepared following a methodology described previously [2] by fixing the biofilm in sterile phosphate buffer solution with 4% glutaraldehyde for 1 hour at ambient temperature; samples were rinsed with phosphate buffer and stored overnight at 4°C. After that, samples were dehydrated by subsequent immersion in alcohol 20%, 30%, 50%, 70%, 90% and 100% for 10 minutes. Finally the samples were dried at CO<sub>2</sub> critical point for three hours, and gold coated.

### 3.5 CALCULATIONS

Cell performance was assessed in terms of production rate (Eq. 1) and cathodic efficiency (Eq. 2) as main parameter in **chapters 5, 6, 7 and 8**. Other parameters such as substrate consumption rate (Eq. 3) were calculated when appropriate.

$$P = \frac{C_{end} - C_{ini}}{t_{end} - t_{ini}} \quad (\text{Eq. 1})$$

Where P is volumetric production rate in mg·L<sup>-1</sup>·d<sup>-1</sup>, C<sub>end</sub> and C<sub>ini</sub> are final and initial product concentration in mg·L<sup>-1</sup> and, t<sub>end</sub> and t<sub>ini</sub> are the final and initial experimental time in days.

$$E_{cat} = \frac{F \cdot M_p \cdot \Delta e}{\int i \cdot dt} \quad (\text{Eq. 2})$$

Where E<sub>cat</sub> is the cathodic efficiency in percentage, F in the Faraday constant in C·mol<sup>-1</sup>, M<sub>p</sub> is the generated product in mol, Δe is the number of electrons exchanged

per produced molecule in the reaction (8 electrons in the case of acetic acid and methane),  $i$  is the current in A and  $t$  is the experimental time in s.

$$S_c = \frac{C_{ini} - C_{end}}{t_{end} - t_{ini}} \quad (\text{Eq. 3})$$

Where  $S_c$  is the volumetric substrate consumption rate in  $\text{mg}\cdot\text{L}^{-1}\text{d}^{-1}$ ,  $C_{ini}$  and  $C_{end}$  are initial and final substrate concentration in  $\text{mg}\cdot\text{L}^{-1}$  and,  $t_{end}$  and  $t_{ini}$  are the final and initial experimental time in days.

Other particular calculations are described on each chapter. **Chapter 4** in particular develops and follows a different calculations methodology, as it is not a production study, which is covered in detail in the chapter itself.

### 3.6 REFERENCES

- [1] Marshall CW, Ross DE, Fichot EB, Norman RS, May HD. Electrosynthesis of commodity chemicals by an autotrophic microbial community. *Applied and Environmental Microbiology* 2012;78:8412–20.
- [2] Bajracharya S, ter Heijne A, Dominguez Benetton X, Vanbroekhoven K, Buisman CJN, Strik DPBTB, et al. Carbon dioxide reduction by mixed and pure cultures in microbial electrosynthesis using an assembly of graphite felt and stainless steel as a cathode. *Bioresource Technology* 2015;195:14–24. doi:10.1016/j.biortech.2015.05.081.





## CHAPTER 4

Methodology for fast and facile characterisation of carbon-based electrodes focused on bioelectrochemical systems development and scale-up

*Chapter adapted from:*

**Mateos, R.,** Alonso, R. M., Escapa, A., & Morán, A. (2017). Methodology for fast and facile characterisation of carbon-based electrodes focused on Bioelectrochemical Systems development and scale-up. *Materials*, 10 (1), 79.



---

**ABSTRACT**

The development and practical implementation of bioelectrochemical systems (BES) requires an in-depth characterisation of their components. The electrodes, which are critical elements, are usually built from carbon-based materials due to their high specific surface area, biocompatibility and chemical stability. In this study a simple methodology to electrochemically characterise carbon-based electrodes has been developed, derived from conventional electrochemical analyses. Combined with classical electrochemical theory and the more innovative fractal geometry approach, our method is aimed at comparing and characterising the performance of carbon electrodes through the determination of the electroactive surface and its fractal dimension. Overall, this methodology provides a quick and easy method for the screening of suitable electrode materials to be implemented in BES.

## 4.1 INTRODUCTION

Bioelectrochemical systems (BES) (an innovative technology in the fields of electrochemistry and bioprocessing technologies [1]) have undergone rapid development, breaking through as promising alternatives in the fields of wastewater treatment [2], bioremediation [3], biosensors construction [4] and chemicals recovery [5].

For wastewater treatment and chemicals recovery applications in particular, BES have reached a degree of maturity that has allowed researchers and engineers to bring about the first pilot-scale experiences [6,7]. These experiences provide valuable information on chemical, process engineering or durability issues (among many others), all of which helps to pave the way to practical implementation [8,9]. However, to optimize the reactors performance, BES developers often have to face the challenge of selecting the most appropriate electrode materials, since they play a vital role on bioelectrochemical reaction rates or energy losses. This is not always a straight forward issue since there are a wide variety of potential electrode materials [10]. Thus, when developing new BES, having a fast and easy method for the screening and characterization of electrode materials could become a powerful tool that can result in substantial time and resources savings.

The presence of surface patterns on electrodes is a key aspect when selecting electrode materials for BES, as it has a significant effect on their electrochemical performance [11]. The electroactive area (EA) of an electrode is a parameter clearly related to its surface structure, and its determination represents an essential step in characterising the electrochemical behaviour of electrodes in electrochemical systems in general [12] and BES in particular [13]. By combining EA determination with other analyses such as stochastic geometrical pattern characterisation, the three-dimensional structure of a porous electrode and its performance can be accurately estimated. Some studies make use of complex numerical treatments focused on a specific porous electrode type which provide accurate results [14,15]. Still, these approaches require the development of “tailor-made” analysis strategies for each individual porous electrode, which usually results in time-consuming analysis methods, and complicates comparison between electrodes.

In this paper we present an easy and simple method for a preliminary characterisation of electrode materials for BES. It is based on conventional electrochemical techniques and allows for fast and reliable estimation of the active area and electrode surface configuration of electrode materials. The method here proposed is intended to provide researchers and engineers with a tool for a rapid and easy characterization of potentially suitable electrode materials for BES applications.

## 4.2 EXPERIMENTAL

### 4.2.1 Methodology proposal

The core of this methodology relies on the determination of two basic parameters: the Electroactive area (EA) and Fractal dimension ( $D_f$ ) whose calculation is detailed in sections 2.2 and 2.3 respectively. While the EA provides a fairly good approximation to the equivalent surface area of a flat electrode (which is related to electrochemical reaction rates), the fractal dimension highlights the presence of three-dimensional patterns on the surface of the electrode (electrodes with three-dimensional structure tend to facilitate the settling and proliferation of electroactive microorganisms). Therefore, the information provided by these two parameters is complementary, and can be combined for preselecting the most suitable electrode material for a particular BES design.

The main advantage of this method, aside from its simplicity and promptness, is that it only requires performing basic electrochemical analytical techniques which are available on every electrochemical laboratory. These techniques are described in the Appendix I.

### 4.2.2 Determination of electroactive area

A direct method for the determination of the electroactive area is evaluation of the peak current in a set of cyclic voltammetry (CV) experiments using a well-known redox couple and cell set-up [16] (in this study  $K_3Fe(CN)_6 / K_4Fe(CN)_6$ ), that usually requires ohmic drop compensation to obtain suitable data for further analysis [17]. In our particular case, the ohmic drop is calculated by averaging the results obtained from CI and EIS (See appendix I).

The EA can be determined from Eq. 1 for a Nernstian system. Peak current ( $I_p$ ) can be calculated in a CV according to the Randles-Ševčík equation:

$$I_p = 0.4463 \left( \frac{F^3}{RT} \right)^{1/2} A C n^{3/2} (D v)^{1/2} \quad (1)$$

Where  $I_p$  is the peak current in A,  $F$  is the Faraday's constant in  $C \cdot mol^{-1}$ ,  $R$  is the ideal gas constant in  $J \cdot K^{-1} \cdot mol^{-1}$ ,  $T$  is the absolute temperature in K (298K in this study),  $A$  is the electroactive area in  $cm^2$ ,  $D$  is the diffusion coefficient of the electroactive specie in  $cm^2 \cdot s^{-1}$ ,  $n$  is the number of electron transferred in the redox reaction,  $C$  is the bulk concentration of the electroactive compound in solution in  $mol \cdot cm^{-3}$  and  $v$  is the scan rate in  $V \cdot s^{-1}$  [18]. The value of the diffusion coefficient is  $0.76 \cdot 10^5 \text{ cm}^2 \cdot \text{s}^{-1}$  at the experimental temperature of 25°C in KCl 0.1M and it was obtained from bibliographic data [19].

Cathodic peak currents ( $I_{pc}$ ) can be obtained from CV experiments using the decaying anodic current as baseline [18]. From the slope of the linear fit between  $I_{pc}$  and the square root of the scan rate, the electroactive area can be determined, following Eq. 1. This approach can be only applied in the experimental range in which a linear trend is observed between  $I_{pc}$  and  $v^{1/2}$ . The described approach is used for comparative purposes, keeping in mind that this model applies for flat electrodes [18].

Although more accurate numeric treatments have been developed [14], this study implements a simple model for the wide range of materials tested.

### 4.2.3 Determination of fractal dimension ( $D_f$ )

Roughness is a key parameter in electrode behaviour because it can condition mass transfer [20] and biofilm development [21]. Our method relies on the use of a fractal geometry approach to characterise electrode surface properties related to self-similarity.

Since B. Mandelbrot carried out his work on fractal geometry [22], it has been used to model different systems in science and technology [23], and especially in electrochemistry due to the importance of electrode surface characteristics [14,15,24].  $D_f$  is a quantitative parameter that can be used to analyse the rough surface structures of an electrode [15,17,24].

A method for determining  $D_f$  from CV data was proposed in [14,25]. This method consists of estimating the value of the fractal parameter ( $\alpha$ ) from the peak current of a set of voltammograms considering that:

$$I_{pc} \propto v^\alpha \quad (2)$$

As a consequence, by plotting the peak current vs.  $v$  on a logarithmic scale the fractal parameter can be estimated from the slope of the fitted linear model. Ohmic losses must be negligible in order to apply this methodology.

The fractal parameter is related to the fractal dimension through:

$$D_f = 2\alpha + 1 \quad (3)$$

$D_f$  values higher than 2 imply rough three-dimensional electrode surfaces whose macroscopic areas are lower than their microscopic areas [26]. In the case of a flat electrode the  $D_f$  value is expected to be 2, corresponding to a fractal parameter of 0.5. Lower values of  $D_f$  can be attributed to inactive surface regions that lower the electroactive surface area below the equivalent flat area.

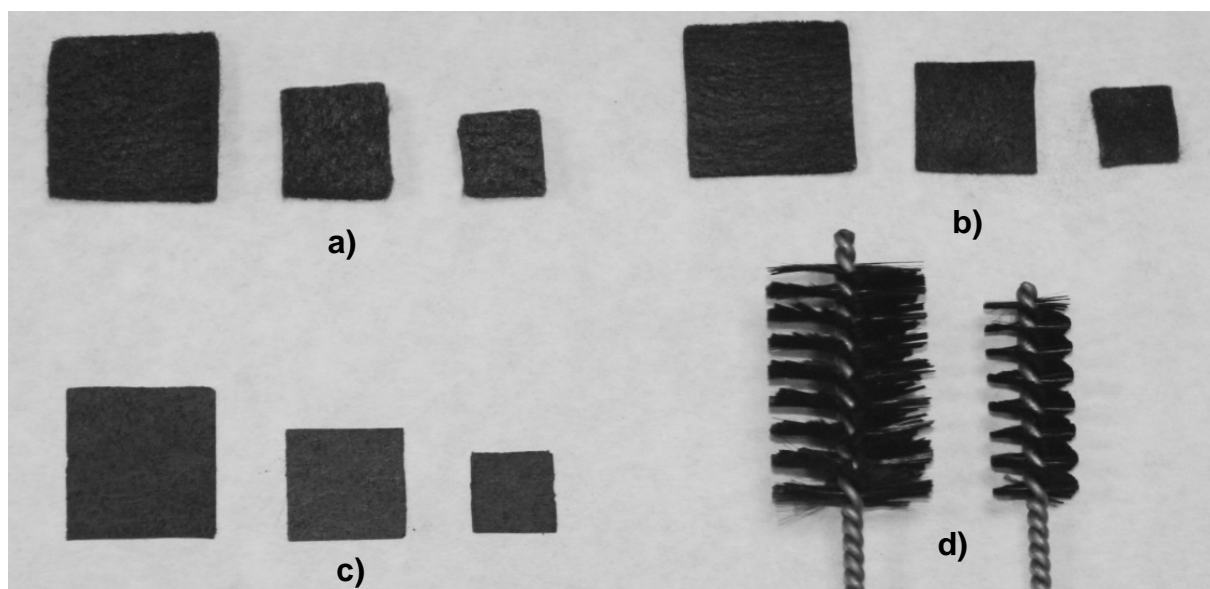
An uncertainty estimation for  $D_f$  can be provided via the confidence intervals of the slope parameter obtained from the fitted linear model, once the normality of the residuals has been checked.

#### 4.2.4 Method validation

The characterisation method described above was validated on four different types of carbon-based materials: Carbon felt of two different thicknesses (SGL Group), carbon paper (SGL Group) and carbon brush (Millrose Co.). All of these materials were tested in different widths and lengths. The materials are specified in table 4.1. See Appendix I for apparent surface determination of carbon brush.

**Table 4.1:** Material specification and coding

Code	Material	Size	Apparent surface (cm <sup>2</sup> )
TF1	Thick carbon felt	1cm Width; 1cm Length; 5mm Thickness	1
TF2	Thick carbon felt	1.5cm Width; 1.5cm Length; 5mm Thickness	2.25
TF3	Thick carbon felt	2cm Width; 2cm Length; 5mm Thickness	4
FF1	Fine carbon felt	1cm Width; 1cm Length; 2mm Thickness	1
FF2	Fine carbon felt	1.5cm Width; 1.5cm Length; 2mm Thickness	2.25
FF3	Fine carbon felt	2cm Width; 2cm Length; 2mm Thickness	4
P1	Carbon paper	1cm Width; 1cm Length	1
P2	Carbon paper	1.5cm Width; 1.5cm Length	2.25
P3	Carbon paper	2cm Width; 2cm Length	4
B1	Carbon brush	1cm Diameter; 2.5cm Height	1.87
B2	Carbon brush	2cm Diameter; 3cm Height	5.33

**Figure 4.1:** 0.5cm-thick carbon felt (a), 0.25cm-thick carbon felt (b), carbon paper (c) and brush (d) electrodes

Most of these materials present unacceptable initial wettability which may distort the analytical results, meaning that a pre-treatment to mitigate this problem is necessary [27,28]. The pre-treatment consists of sequentially immersing the electrode into 1M nitric acid, acetone and ethanol solutions with concentrations for 12 hours, 30 minutes and 30 minutes, respectively [27]. These parameters were established based on



previous experiments carried out on carbon felt materials, but proved to be ineffective for air removal from carbon paper electrodes, as shown in figure 4.2.



**Figure 4.2:** Carbon paper electrode with air bubbles after pre-treatment

#### 4.2.5 Cell set-up and instrumentation

The electrodes described in section 2.4 were characterised in a 100 mL conical cell (Metrohm 6.1415.210), using a three-electrode configuration with an Ag/AgCl reference electrode (Bioblock Scientific), as shown in figure 4.3. A solution containing 0.1M KCl was used as the electrolyte and 3.4 mM  $K_3Fe(CN)_6$  as the electroactive species. The reaction medium was previously sparged for 10 min with pure nitrogen to remove dissolved oxygen that interferes in the CV. The working and counter electrodes were identical in each test.

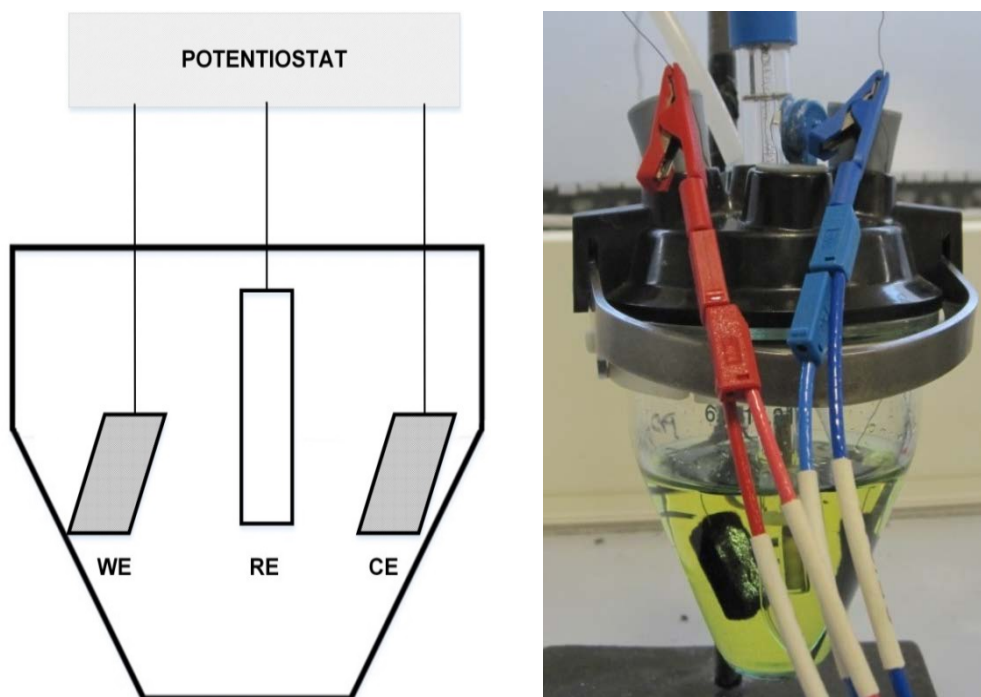


**Figure 4.3:** Cell diagram (WE: Working electrode; RE: Reference electrode; CE: Counter electrode) and cell assembly

The analytical electrochemistry (CV, Electrochemical Impedance Spectroscopy (EIS) and Current Interrupt (CI); see Appendix I) was performed using a BioLogic VSP potentiostat. The peak analysis was carried out using the software associated with the equipment (EC-Lab<sup>®</sup> V10.40). The ohmic drop is compensated by an in-built method in the EC-Lab<sup>®</sup> software in order to avoid undesirable peak displacement and current underestimates in the CV at relatively high currents.

### 4.3 RESULTS AND DISCUSSION

In this section we test and validate the methodology described in section 4.2 on the materials shown in table 4.1. Prior to its application, the ohmic drop was determined (table 4.2) based on CI and EIS techniques repeated 10 times each (see appendix I). As expected, samples made of the same material yielded lower resistance as the geometric surface area increases. This highlights the need of compensating for the ohmic drop in the CV.

**Table 4.2:** Ohmic drop of each cell set-up. The standard error of the mean estimates the uncertainty associated to the determination of the ohmic drop.

Electrodes	Mean ohmic drop ( $\Omega$ )	Standard error
TF1	22.50	0.010
TF2	16.65	0.011
TF3	10.09	0.012
FF1	34.08	0.011
FF2	18.05	0.011
FF3	20.02	0.013
P1	18.29	0.011
P2	14.05	0.010
P3	9.81	0.012
B1	13.71	0.009
B2	8.16	0.010

### 4.3.1 Estimation of electroactive area

As discussed in section 4.2, the first step in the proposed methodology is to determine the electroactive surface area, which is a critical parameter for the electrodes characterisation since it has a definite impact on the electrochemical reaction rate. figure 4.4 illustrates the peak reduction currents ( $I_p$ ) versus the square root of the scan rate ( $v^{0.5}$ ), which defines the Randles-Ševčík curves for the selected electrode material (see section 4.2.3). As can be observed, for scan rates below  $100 \text{ mVs}^{-1}$  ( $v^{0.5}=10$ ) the trend is linear, being indicative of a semi-infinite diffusion regime. However, at scan rates above  $100 \text{ mVs}^{-1}$  the current falls below the linear trend, which indicates the existence of irreversibilities [18]. Interestingly, this behaviour slightly differs for the carbon brush electrodes, where irreversibilities only appears at scan rates above  $200 \text{ mVs}^{-1}$  ( $v^{0.5}=14.1$ ), which seems to be indicative of enhanced electrode kinetics.

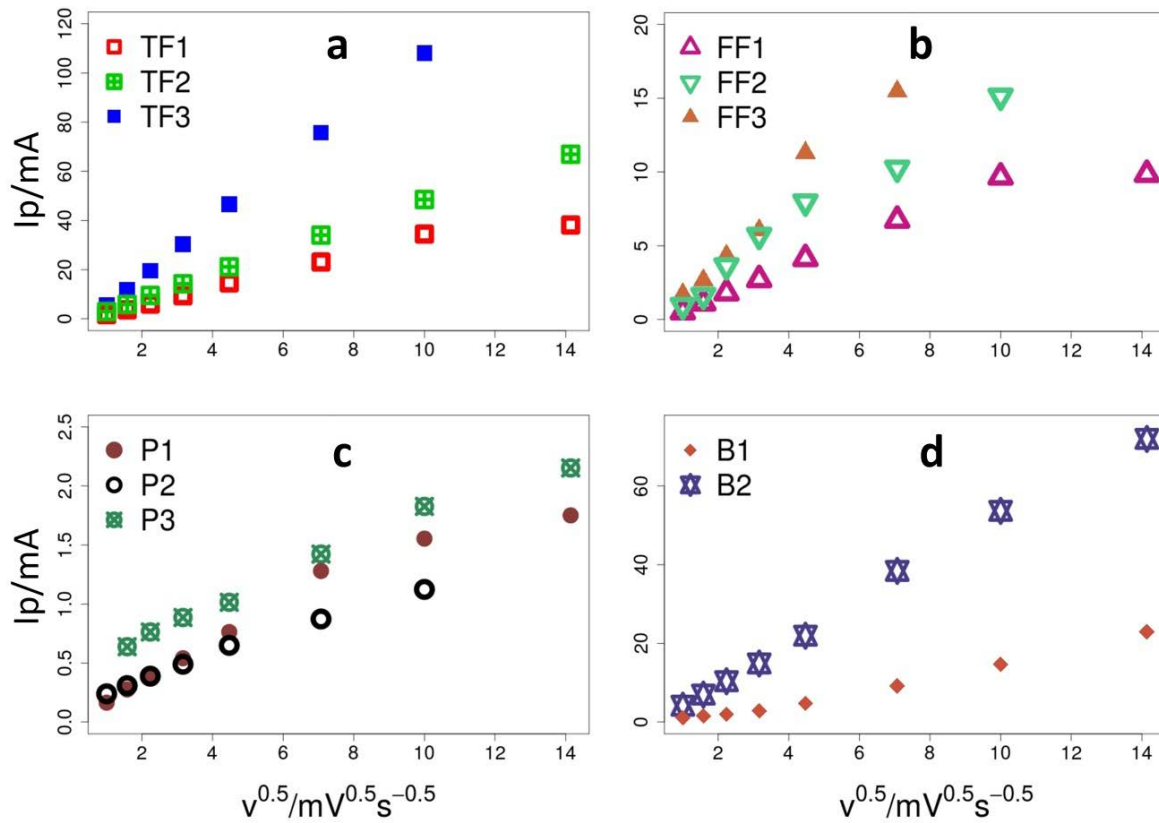


**Figure 4.4:** Randles-Ševčík plot a: Thick felt (TF); b: Fine felt (FF); c: Paper (P); d: Brush (B)

The EAs can be estimated from the slope of the Randles-Ševčík profiles as shown in table 4.3. This table also provides the ratio between the evaluated EA and the apparent surface of the electrodes (AS), which normalises the EA to the electrode size.

**Table 4.3:** Electroactive areas

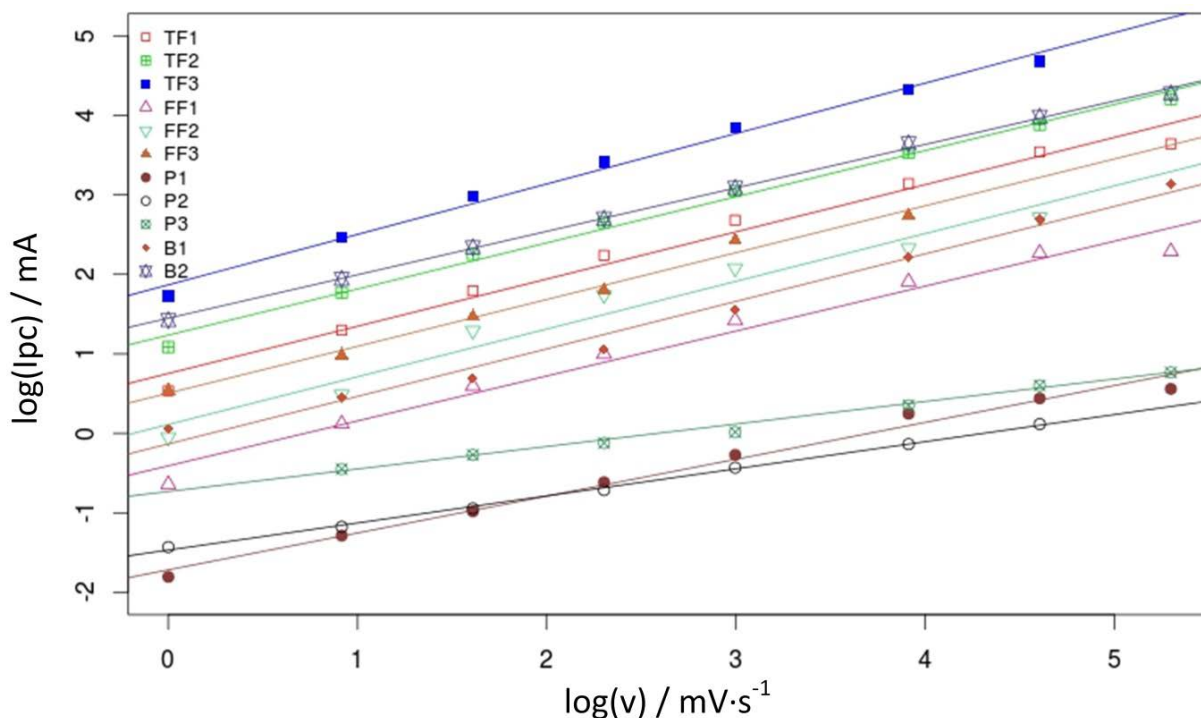
Material	Slope	Electroactive area ( $cm^2$ )	Electroactive area per apparent surface area ratio (EA/AS)
TF1	$9.44 \cdot 10^{-2}$	37.16	37.2
TF2	$1.55 \cdot 10^{-1}$	61.03	27.1
TF3	$3.62 \cdot 10^{-1}$	142.47	35.6
FF1	$2.47 \cdot 10^{-2}$	9.73	9.73
FF2	$4.85 \cdot 10^{-2}$	19.10	8.49
FF3	$7.53 \cdot 10^{-2}$	29.66	7.42
P1	$4.07 \cdot 10^{-3}$	1.60	1.60
P2	$3.11 \cdot 10^{-3}$	1.22	0.54
P3	$3.91 \cdot 10^{-3}$	1.54	0.39
B1	$5.31 \cdot 10^{-2}$	20.91	11.2
B2	$1.68 \cdot 10^{-1}$	65.97	12.4

Table 4.3 shows that for electrodes made of the same material, the EA/AS ratio is very similar regardless of the size of the electrode (see estimation of apparent surface area on appendix I), which also proves that the EA/AS ratio can be safely used to compare electrodes with different geometries.

Interestingly, carbon paper electrodes shown an EA/AS far below those observed on the other electrodes (See table 4.3). This is indeed a noteworthy observation, for a rough carbonaceous material would be expected to display high EA/AS ratios (as with the other carbonaceous electrodes). An unexpected low EA/AS is explained by an unusually low EA, most probably due the presence of electrochemically inactive areas within the surface of the electrode. These inactive areas can be caused by partial fouling, chemical inactivation or catalyst poisoning among others. Therefore, when comparing different electrode materials, the EA/AS can be used to detect irregularities attributable to the electrode surface deficiencies. In our particular case, we attribute this relatively low EA/AS for the paper electrodes (at least in part) to the embedded air that could not be removed in the pre-treatment process.

### 4.3.2 Determination of the fractal dimension

This section deals with the evaluation of  $D_f$ , a parameter that provides information about the relationship between the macroscopic and microscopic structure of an electrode, thus complementing the information provided by the EA. Following the procedure described in section 4.2.3,  $I_{pc}$  has been plotted against  $v$  in figure 4.5 on a logarithmic basis. This figure shows that all of the evaluated materials follow a linear model, indicating that  $I_{pc}$  follows a power-law dependency versus the scan rate in the considered range. Fractal dimension can be calculated from this slope as described in section 4.2.3.



**Figure 4.5:** Linear trend in the logarithmic representation of  $I_{pc}$  vs.  $v$

The slope of the linear fits shown in figure 4.5 corresponds to the parameter  $\alpha$  in eq 3. It is referred in table 4.4 and allows to calculate  $D_f$  (figure 4.6) (See section 4.2.3).

**Table 4.4:** Fractal parameter comparison of different electrodes using CV measurements. The value presented alongside the fractal parameter  $\alpha$  represents the 90% confidence intervals for each estimated parameter.

Electrode	Experimental range $v$ ( $\text{mV}\cdot\text{s}^{-1}$ )	Fractal parameter ( $\alpha$ )	Correlation coefficient ( $R^2$ )
TF1	1-200	$0.594 \pm 0.066$	0.981
TF2	1-200	$0.580 \pm 0.039$	0.993
TF3	1-100	$0.634 \pm 0.052$	0.992
FF1	1-200	$0.565 \pm 0.072$	0.975
FF2	1-200	$0.600 \pm 0.108$	0.961
FF3	1-50	$0.589 \pm 0.066$	0.989
P1	1-200	$0.464 \pm 0.042$	0.987
P2	1-100	$0.341 \pm 0.014$	0.998
P3	2.5-200	$0.283 \pm 0.026$	0.998
B1	1-200	$0.598 \pm 0.056$	0.986
B2	1-200	$0.547 \pm 0.015$	0.999

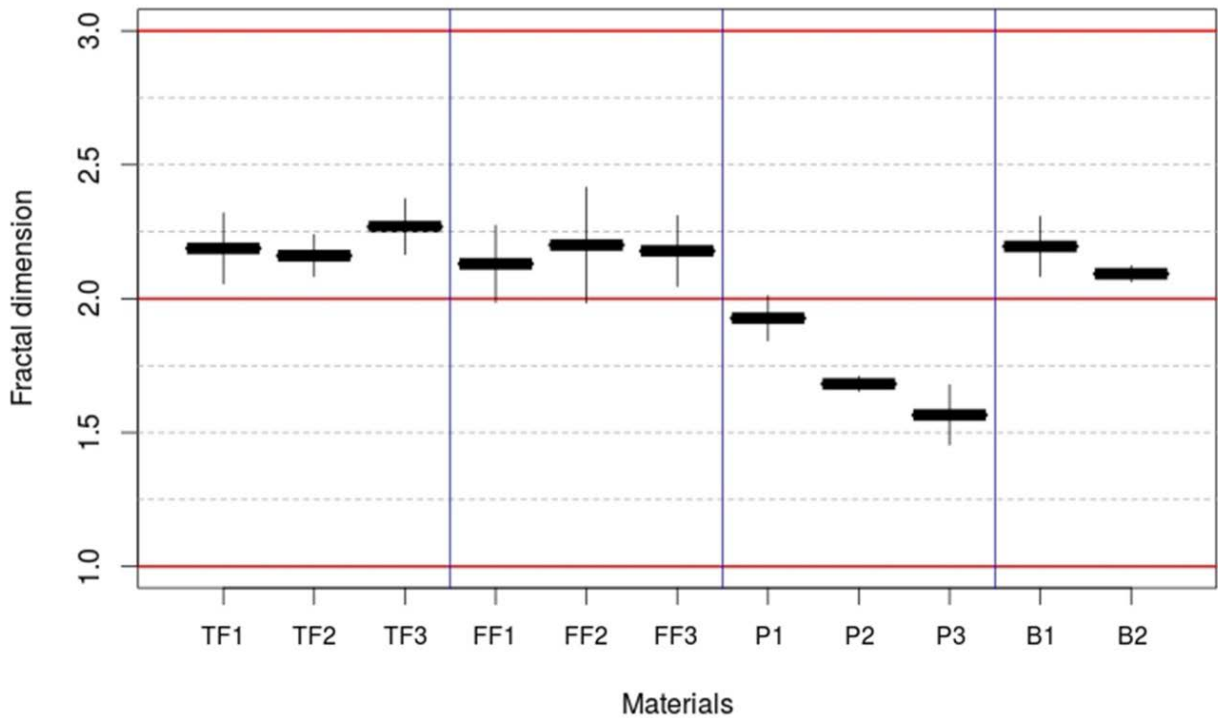


**Figure 4.6:** Fractal dimension of the electrodes tested. The values corresponding to Euclidean integer dimensions are shown as red solid lines.

The felt and brush electrodes showed a  $D_f > 2$ , which indicates that the surfaces present an intrinsic three-dimensional structure. This feature is expected to be uniformly distributed in the electrode principal plane according to its scaling properties [26]. However, the  $D_f$  found for carbon paper electrodes was even lower than the value expected for a completely smooth surface, which is  $D_f = 2$ . This may be caused by the accumulation of gas bubbles on the surface of the electrodes that could not be removed in the pre-treatment process. This result corroborates the unexpected EA/AS observed for these electrodes (see section 4.3.1). Interestingly, figure 4.6 shows that as electrode size increases from P1 to P3  $D_f$  gets further reduced, which can be attributed to a higher proportion of air bubbles in larger size electrodes (air bubbles tend to accumulate in central region of the electrode and far from the edges). This fact enforces the information given by low EA/AS values about the presence of “irregularities/impurities” that inactivate certain sections of the electrodes.

The information provided by the  $D_f$  can be integrated with the information provided by EA/AS as shown in figure 4.7. In our particular case, the different electrodes tested have been arranged in three different groups (classified via k-means

algorithm with C1, C2 and C3 representing the centroids) for each electrode material and electrode size. An efficient electrode should have a high EA/AS and a fractal dimension greater than 2 and as close to 3 as possible. Therefore, this electrode should appear within the region dominated by C3. Moreover, a high fractal dimension points to the existence of a three-dimensional subjacent structure which often results in high EA/AS. Thus it is unlikely to find materials below the main diagonal in figure 4.7, which results in a forbidden area.

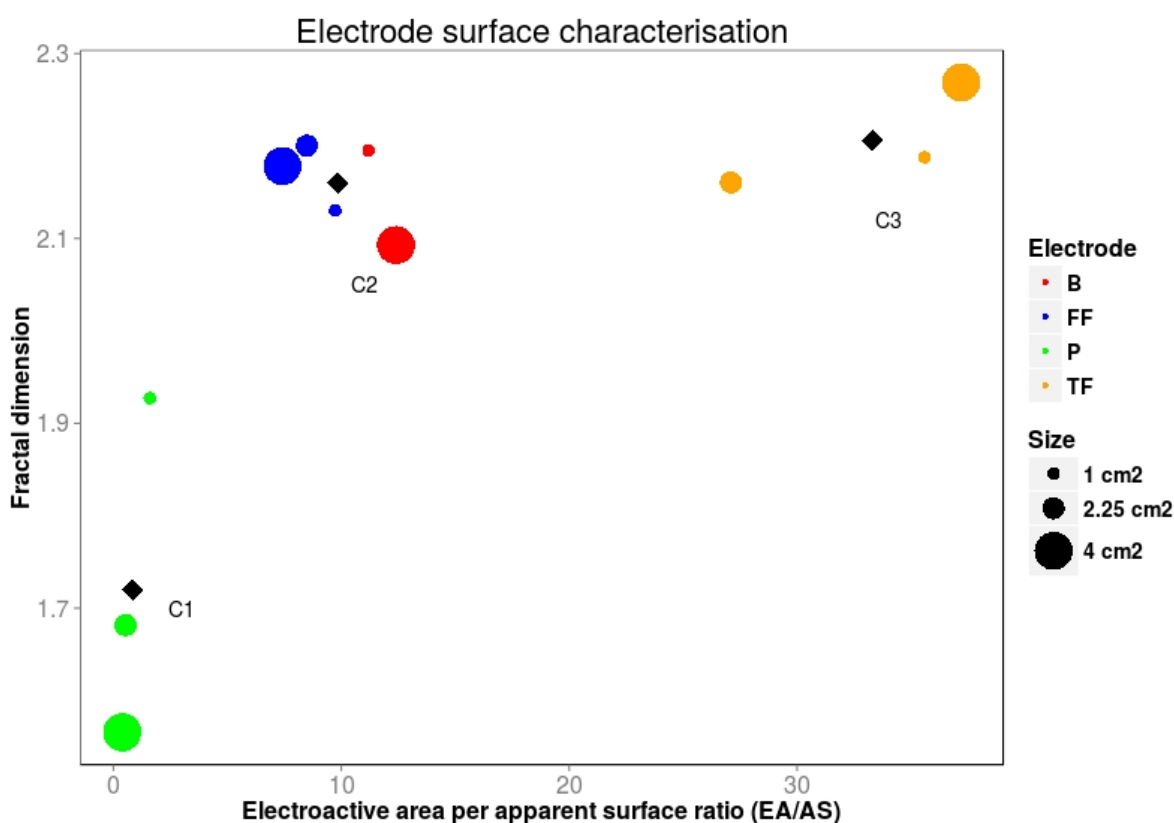


**Figure 4.7:** Relationship between fractal dimension and EA/AS for each material tested. Black diamond points show the centroids of electrode clusters.

It is also interesting to point out that by graphically integrating the information provided by the electroactive area and the fractal dimension, we can easily uncover unexpected behaviours of the materials under examination. For example, materials with quite different morphologies such as FF and B can surprisingly display similar electrochemical performance as they fall within the same region (C2) in figure 4.7. In contrast, materials with an a priori “enhanced” three-dimensional structure such as TF and B that would be expected to perform similarly, they actually fall within different



regions in figure 4.7. Although they show comparable fractal dimensions, their electroactive area differs significantly. Therefore, in this particular case, EA would become the key parameter in a potential screening process.

Overall, the described approach combines graphically two estimators (EA/AS and  $D_f$ ) derived from a common experimental procedure that provides complementary information useful, not only for quantifying the merit of electrode materials according to their reactive area, but also to highlight unexpected behaviours of the materials under test.

#### 4.4 CONCLUSIONS

An experimental framework for comparing the surface properties and electrochemical efficiency of carbon electrodes, focused on BES development, is proposed. The usual evaluation of electrochemical active area alone does not provide sufficient information to estimate the performance of an electrode. Here we also calculate the fractal dimension to account for the 3D structure of the material. By combining the information provided by these two complementary parameters we can have an estimation of the behaviour of electrode materials. The results obtained during the validation of the method show its suitability at least to characterise and compare carbonaceous electrode materials, offering an alternative metric for surface evaluation. Moreover, by graphically integrating the information provided by the electroactive area and the fractal dimension, this method makes easy to highlight unexpected behaviours of the materials under examination. Although it does not substitute accurate characterisation methods, it provides a suitable platform for easy comparison of a wide variety of different carbon-based materials which are the most common electrode materials used in BES. For researchers and developers with limited budgets, it represents a cost-effective methodology since it can be performed using a standard potentiostat that is present in most of bioelectrochemistry laboratories. Therefore, this method can become a useful tool for the screening and preliminary selection of available electrode materials during BES scale-up processes.

#### 4.5 REFERENCES

- [1] Butti SK, Velvizhi G, Sulonen MLK, Haavisto JM, Oguz Koroglu E, Yusuf Cetinkaya A, et al. Microbial electrochemical technologies with the perspective of harnessing bioenergy: Maneuvering towards upscaling. *Renewable and Sustainable Energy Reviews* 2016;53:462–76. doi:10.1016/j.rser.2015.08.058.
- [2] Escapa A, San-Martín MI, Mateos R, Morán A. Scaling-up of membraneless microbial electrolysis cells (MECs) for domestic wastewater treatment: Bottlenecks and limitations. *Bioresource Technology* 2015;180:72–8. doi:10.1016/j.biortech.2014.12.096.
- [3] Modin O, Wang X, Wu X, Rauch S, Fedje KK. Bioelectrochemical recovery of Cu, Pb, Cd, and Zn from dilute solutions. *Journal of Hazardous Materials* 2012;235–236:291–7. doi:10.1016/j.jhazmat.2012.07.058.
- [4] Webster DP, TerAvest MA, Doud DFR, Chakravorty A, Holmes EC, Radens CM, et al. An arsenic-specific biosensor with genetically engineered *Shewanella oneidensis* in a bioelectrochemical system. *Biosensors & Bioelectronics* 2014;62:320–4. doi:10.1016/j.bios.2014.07.003.
- [5] Marshall CW, Ross DE, Fichot EB, Norman RS, May HD. Electrosynthesis of commodity chemicals by an autotrophic microbial community. *Applied and Environmental Microbiology* 2012;78:8412–20. doi:10.1128/AEM.02401-12.
- [6] Heidrich ES, Dolfing J, Scott K, Edwards SR, Jones C, Curtis TP. Production of hydrogen from domestic wastewater in a pilot-scale microbial electrolysis cell. *Applied Microbiology and Biotechnology* 2013;97:6979–89.
- [7] Ieropoulos IA, Stinchcombe A, Gajda I, Forbes S, Merino-Jimenez I, Pasternak G, et al. Pee power urinal--microbial fuel cell technology field trials in the context of sanitation. *Environmental Science: Water Research & Technology* 2016;2:336–43.
- [8] ElMekawy A, Srikanth S, Vanbroekhoven K, De Wever H, Pant D. Bioelectrocatalytic valorization of dark fermentation effluents by acetate oxidizing bacteria in bioelectrochemical system (BES). *Journal of Power Sources* 2014;262:183–91.

- doi:10.1016/j.jpowsour.2014.03.111.
- [9] Rabaey K. Bioelectrochemical systems: from extracellular electron transfer to biotechnological application. IWA publishing; 2010.
- [10] Escapa A, Mateos R, Martínez EJ, Blanes J. Microbial electrolysis cells: An emerging technology for wastewater treatment and energy recovery. From laboratory to pilot plant and beyond. *Renewable and Sustainable Energy Reviews* 2016;55:942–56. doi:10.1016/j.rser.2015.11.029.
- [11] Cui H-F, Du L, Guo P-B, Zhu B, Luong JHT. Controlled modification of carbon nanotubes and polyaniline on macroporous graphite felt for high-performance microbial fuel cell anode. *Journal of Power Sources* 2015;283:46–53. doi:10.1016/j.jpowsour.2015.02.088.
- [12] Bagotsky VS. Fundamentals of electrochemistry. vol. 44. John Wiley & Sons; 2005.
- [13] Guo K, PrévotEAU A, Patil SA, Rabaey K. Engineering electrodes for microbial electrocatalysis. *Current Opinion in Biotechnology* 2015;33:149–56. doi:10.1016/j.copbio.2015.02.014.
- [14] Strømme M, Niklasson GA, Granqvist CG. Voltammetry on fractals. *Solid State Communications* 1995;96:151–4. doi:10.1016/0038-1098(95)00363-0.
- [15] Kant R, Singh MB. Generalization of Randles-Ershler admittance for an arbitrary topography electrode: application to random finite fractal roughness. *Electrochimica Acta* 2015;163:310–22. doi:10.1016/j.electacta.2015.02.107.
- [16] Pacios M, del Valle M, Bartroli J, Esplandiu MJ. Electrochemical behavior of rigid carbon nanotube composite electrodes. *Journal of Electroanalytical Chemistry* 2008;619–620:117–24.
- [17] Neves S, Polo Fonseca C. Determination of fractal dimension of polyaniline composites by SAXS and electrochemical techniques. *Electrochemistry Communications* 2001;3:36–43. doi:10.1016/S1388-2481(00)00148-X.
- [18] Bard AJ, Faulkner LR. *Electrochemical methods: fundamentals and applications*.

- vol. 2. Wiley New York; 1980.
- [19] Zoski CGC. Handbook of Electrochemistry. vol. 5. Elsevier; 2007. doi:10.1016/B978-044451958-0.50000-8.
- [20] Panah NB, Mahjani MG, Jafarian M. Correlation between irregular surface geometry and certain electrochemical quantities in poly-ortho-aminophenol. Progress in Organic Coatings 2009;64:33–8. doi:10.1016/j.porgcoat.2008.07.009.
- [21] Ammar Y, Swailes D, Bridgens B, Chen J. Influence of surface roughness on the initial formation of biofilm. Surface and Coatings Technology 2015. doi:10.1016/j.surfcoat.2015.07.062.
- [22] Mandelbrot BB. The fractal geometry of nature/Revised and enlarged edition. New York, WH Freeman and Co, 1983, 495 P 1983;1.
- [23] Avnir D. Fractal approach to heterogeneous chemistry. Wiley; 1989.
- [24] Kant R. Theory for staircase voltammetry and linear scan voltammetry on fractal electrodes: Emergence of anomalous Randles–Sevik behavior. Electrochimica Acta 2013;111:223–33. doi:10.1016/j.electacta.2013.07.163.
- [25] Strømme M, Niklasson GA, Granqvist CG. Determination of fractal dimension by cyclic I - V studies: The Laplace-transform method. Physical Review B 1995;52:14192–7. doi:10.1103/PhysRevB.52.14192.
- [26] Go J-Y, Pyun S-I, Hahn Y-D. A study on ionic diffusion towards self-affine fractal electrode by cyclic voltammetry and atomic force microscopy. Journal of Electroanalytical Chemistry 2003;549:49–59. doi:10.1016/S0022-0728(03)00244-4.
- [27] Dhar BR, Gao Y, Yeo H, Lee H-S. Separation of competitive microorganisms using anaerobic membrane bioreactors as pretreatment to microbial electrochemical cells. Bioresource Technology 2013;148:208–14. doi:10.1016/j.biortech.2013.08.138.
- [28] Smith REG, Davies TJ, Baynes N de B, Nichols RJ. The electrochemical characterisation of graphite felts. Journal of Electroanalytical Chemistry

2015;747:29–38. doi:10.1016/j.jelechem.2015.03.029.



## CHAPTER 5

# Impact of the start-up process on the microbial communities in biocathodes for electrosynthesis

*Chapter adapted from:*

**Mateos, R.,** Sotres, A., Alonso, R. M., Escapa, A., & Morán, A. (2018). Impact of the start-up process on the microbial communities in biocathodes for electrosynthesis. *Bioelectrochemistry*, 121, 27-37.





---

## ABSTRACT

This study seeks to understand how the bacterial communities that develop on biocathodes are influenced by inocula diversity and electrode potential during start-up. Two different inocula are used: one from a highly diverse environment (river mud) and the other from a low diverse milieu (anaerobic digestion). In addition, both inocula were subjected to two different polarising voltages: oxidative (+0.2V vs. Ag/AgCl) and reductive (-0.8V vs. Ag/AgCl).

Bacterial communities were analysed by means of high throughput sequencing. Possible syntrophic interactions and competitions between Archaea and Eubacteria were described together with a discussion of their potential role in product formation and current production. The results confirmed that reductive potentials lead to an inconsistent start-up procedure regardless of the inoculum used. However, imposing oxidative potentials help to quickly develop an electroactive biofilm ready to withstand reductive potentials (i.e. biocathodic operation). The microbial structure that finally developed on them was highly dependent on the raw community present in the inoculum. Using a non-specialised inoculum resulted in a highly specialised biofilm, which was accompanied by an improved performance in terms of consumed current and product generation. Interestingly, a much more specialised inoculum promoted a rediversification in the biofilm, with a lower general cell performance.

## 5.1 INTRODUCTION

Most of the carbon-based chemicals and fuels currently produced throughout the world are derived from non-renewable sources (i.e. fossil resources). They are the basic feedstock for many industrial processes and are present in most human activities. Yet, their production, transformation and utilisation are usually accompanied by the release of large amounts of CO<sub>2</sub> into the atmosphere. In an effort to limit the burden that these commodities place on the environment, innovative technologies and novel industrial processes have emerged in recent years, including CO<sub>2</sub> capture and utilization technologies [1,2]. This has given birth to the concept of biorefinery [3], a term that encompasses those industrial activities that integrate biomass conversion and the production of fuels, energy and value-added chemicals, such as methane, ethylene, ethylene-glycol or monomers for plastics like acrylic acid [2]. Processes that use CO<sub>2</sub> rich streams as a feedstock are of special interest, as this contributes to further reduce their environmental impact. Microbial electrosynthesis (MES) is a novel technology that can be framed within this group [4], although the ability of MES to use organic compounds (e.g. acetate, ethanol) as a substrate, also opens the possibility to upgrade organic feedstocks.

MES is based on the ability of certain strains of electroactive bacteria to directly or indirectly take electrons from a solid surface (usually termed as biocathode) and use them in their metabolism to produce chemicals such as carboxylic acids or combustible gases [5], depending on process design and conditions. For more information on the basics of MES, we refer the reader elsewhere [6–9].

MES opens a wide variety of possibilities to produce valuable organic compounds. The range of target products attainable is mainly restricted by the substrate (CO<sub>2</sub> or organic compounds) and the operational conditions (culture medium, pH, electrode potential and the microbial community present on the electrodes (mixed or pure culture biofilms) [6]). For instance, pure cultures of species like *Sporomusa Ovata* [10] or *Clostridium Ljungdahlii* [11] have been reported to be efficient at producing commodity chemicals from inorganic carbon on biocathodes. On the other hand, mixed cultures harvested from sediments, sludge or other natural environments have proven to be more robust when fed with real waste streams. Although mixed

cultures provide lower efficiencies in product generation, they have a promising potential for practical applications [11,12] as they allow to operate in continuous conditions, can be fed with mixed (non-sterilized) substrates and display a better adaptive capacity [13]. Acetic acid is the most reported product from CO<sub>2</sub> bioelectroreduction; it is generated mainly following the Wood-Ljungdahl pathway [14], requiring the presence of homoacetogens such as *Sporomusa sp.* and *Clostridium sp.* These species are commonly found in mixed culture biocathodes, and are responsible for the production not only of acetic acid, but also some other organic products from mixtures of CO<sub>2</sub> and H<sub>2</sub> [15]. All these products can be obtained alone or simultaneously in biocathodes, giving way to mixtures of carboxylic acids [16]. Moreover, biocathodes are also capable of performing chain elongation reactions, using short chain carboxylic acids as building blocks [17].

Laboratory scale MES is typically carried out in three-electrode two-chamber arrangements, and for the cathodic reaction to proceed, moderate potentials (usually in the range of -0.6 V and -1.1 V vs. Ag/AgCl) are required depending on the system overpotentials [18] and the target products. The minimum feasible threshold potential is limited by the hydrogen evolution reaction. Unfortunately, and contrary to what happens to bioanodes, the inoculation and start-up of biocathodes is usually an inconsistent, tedious and time-consuming procedure [11,19,20]. Biocathodes are usually started up directly in a cathodic mode of operation (i.e. by imposing cathodic potentials) [11,19], but they can also be started-up in an anodic mode of operation (i.e. by imposing anodic potentials) and then converted into biocathodes by reversing the potential to typical cathodic values [21–23].

The present study aims at gaining knowledge on how the start-up process influences the microbial communities that develop on the biofilm of biocathodes. This is done by assessing the impact of the microbial diversity of the inoculum and the starting potential of the bioelectrode. For this purpose, we tested a highly diverse inoculum such as river mud (RM), and a less species richness one such as anaerobic digestate (AD). We also evaluated the impact of the starting potential by either operating the working electrode as an anode and then switching it to cathode, or directly operating the working electrode as a cathode. This approach resulted in four different start-up strategies, and for all of them, we provide an analysis of the evolution of

microbial communities together with information of the reactor performance (in terms of current production and product formation).

## 5.2 MATERIALS AND METHODS

### 5.2.1 MES reactors set-up

Twelve identical two-chambered planar cells were constructed with polycarbonate plates, providing a working cathodic volume of 50 mL and 15 mL of headspace. A pretreated Nafion 117 (Cation Exchange Membrane (CEM)) was used to separate the anodic and cathodic compartments. Both the working and counter electrodes (WE and CE, respectively) were made of carbon felt (SGL Group, Germany) due to the suitability of this material to work as cathode or anode, providing chemical stability in both cases. No specific current collectors were used in our set-up. To provide an intimate contact between the electrodes and titanium wire, it was sewed through the carbon felt. All assemblies provided a contact resistance  $< 2$  ohm. Electrodes were pretreated by subsequent immersion in nitric acid 1M, acetone 1M and ethanol 1M during 24h each to avoid hydrophobicity and impurities. Then, the electrodes were rinsed in demineralised water to ensure absence of organics from the pretreatment. The electrodes and the membrane had a projected surface area of 19.6 cm<sup>2</sup>. All cells worked on a three-electrode configuration using an Ag/AgCl reference electrode (0.20 vs. SHE; the stability of the reference electrode was checked prior to every batch cycle). The catholyte was continuously stirred using a magnetic stirrer at 200 rpm, and gas was collected from a built-in rubber septum.

### 5.2.2 Start-up strategies and operation

Four different start-up strategies (designated as **S1**, **S2**, **S3** and **S4**) were tested in triplicate, resulting in a total set of 12 cells (figure 5.1). Each strategy was characterised by the inoculum (**AD** or **RM**) and the start-up procedures (either operating the WE as an anode and then switching to a cathode or directly operating the WE as a cathode). Anodic potentials for three-electrodes configurations are usually in the range of -0.2V to +0.2V vs. Ag/AgCl. In our study, we selected a high potential (+0.2V vs. Ag/AgCl) to ensure favourable conditions for anodic biofilm formation. Cathodic potentials for three-electrodes configurations are usually in the range of -0.4V to -1.4V vs. Ag/AgCl.

Again to favour a cathodic biofilm formation and to avoid extensive electrolytic hydrogen production, a relatively low cathodic potential was selected (-0.8V vs. Ag/AgCl).

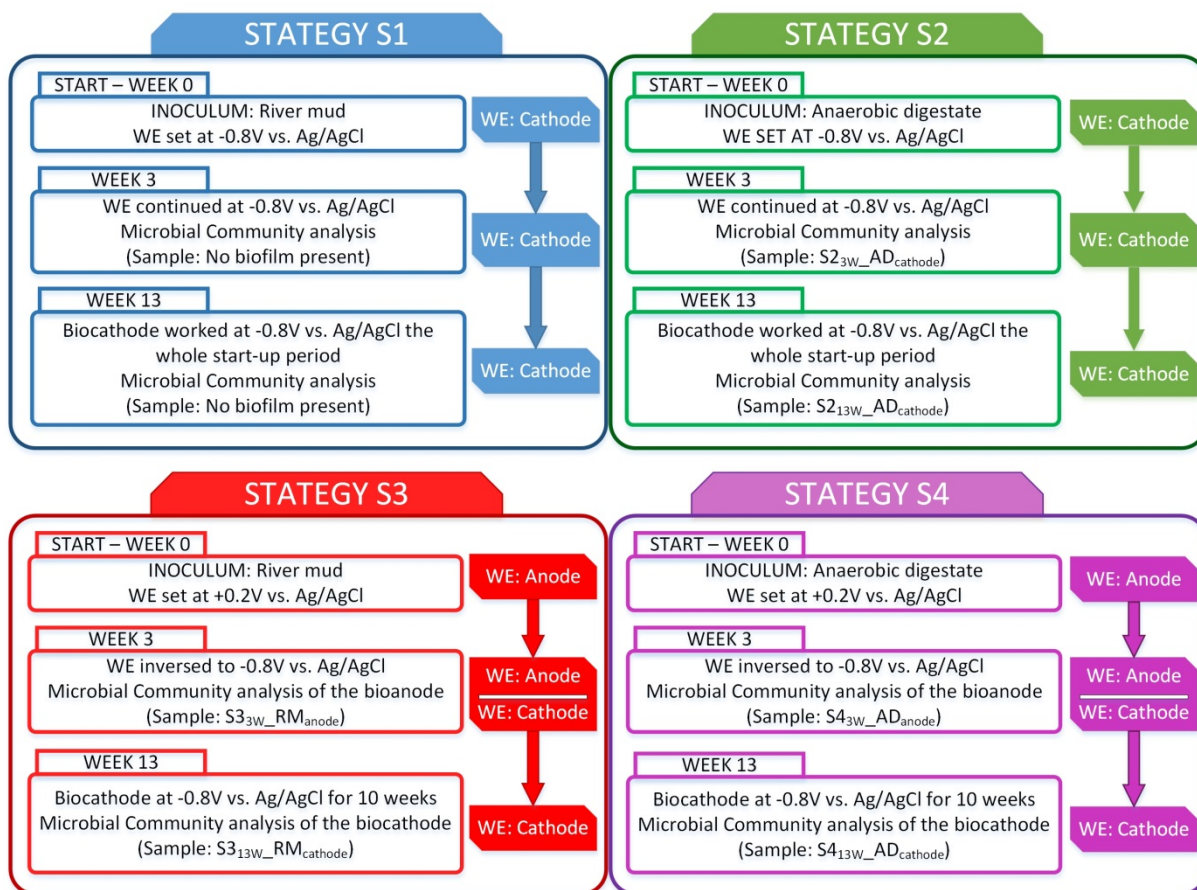


**Figure 5.1.** Strategies overview

For strategy **S1** the WE was started directly as a biocathode using RM as inoculum. The WE potential was set at -0.8 V vs. Ag/AgCl. Strategy **S2** was similar to **S1** but using AD as inoculum.

In strategy **S3**, the WE was started as a bioanode and was inoculated with RM. The WE potential was set at +0.2 V vs. Ag/AgCl. After a period of 3 weeks (following the start-up), once the anodes of the working cells had developed a clear current response, the electrode potential was poised at -0.8 V vs. Ag/AgCl to force them to operate as biocathodes. Strategy **S4** was similar to **S3** but with AD as inoculum.

Following the start-up, the cathodes were operated in batch mode. At the beginning of every batch cycle the WE and CE chamber were replenished with fresh culture medium/electrolyte. The duration of the batch cycles was fixed to 2 weeks to provide enough time for bacterial growth during the start-up period. The cells were maintained at 30 °C and initial pH of the catholyte was 7.4.

### 5.2.3 Influent and inocula

The culture medium used for the WE chamber consisted of a synthetic nutrient solution with a composition (in  $\text{g}\cdot\text{L}^{-1}$ ): 0.87  $\text{K}_2\text{HPO}_4$ ; 0.68  $\text{KH}_2\text{PO}_4$ ; 0.25  $\text{NH}_4\text{Cl}$ ; 0.1  $\text{KCl}$ ; 0.04  $\text{CaCl}_2\cdot 2\text{H}_2\text{O}$ ; 0.45  $\text{MgCl}_2\cdot 6\text{H}_2\text{O}$  and 10 ml per litre of a trace mineral solution containing (in  $\text{g}\cdot\text{L}^{-1}$ ): 6  $\text{MgSO}_4\cdot 7\text{H}_2\text{O}$ , 1  $\text{MnSO}_4\cdot \text{H}_2\text{O}$ , 2  $\text{NaCl}$ , 0.2  $\text{FeSO}_4\cdot 7\text{H}_2\text{O}$ , 0.3  $\text{CoCl}_2\cdot 6\text{H}_2\text{O}$ , 0.2  $\text{CaCl}_2\cdot 2\text{H}_2\text{O}$ , 0.17  $\text{ZnCl}_2$ , 0.02 of  $\text{CuSO}_4\cdot 5\text{H}_2\text{O}$ , 0.02  $\text{H}_3\text{BO}_3$ , 0.04  $\text{Na}_2\text{MoO}_4\cdot 2\text{H}_2\text{O}$ , 0.06  $\text{NiCl}_2\cdot 6\text{H}_2\text{O}$ , 0.6 mg  $\text{Na}_2\text{SeO}_4$  and 0.8 mg  $\text{Na}_2\text{WO}_4\cdot 2\text{H}_2\text{O}$  as described in [24]. When the WEs were operated as bioanodes, the carbon source consisted of a mixture of sodium acetate  $0.5\text{ g}\cdot\text{L}^{-1}$ , sodium propionate  $0.1\text{ g}\cdot\text{L}^{-1}$  and glucose  $0.1\text{ g}\cdot\text{L}^{-1}$ . When they operated as biocathodes, the carbon source was sodium bicarbonate  $2.5\text{ g}\cdot\text{L}^{-1}$ . All nutrient solutions were prepared immediately before each batch cycle to avoid microbial pre-contamination. The electrolyte used in the CE chamber was a phosphate 0.1 M buffer solution. For CE operating as chemical anodes, the pH was slightly alkaline (7.8) to counteract their natural tendency towards acidification. For similar reasons, the pH of CE operating as chemical cathodes was slightly acidic (6.8). Chemicals and reagents used were of analytical grade, and distilled water was used for medium preparation.

Two different inocula were used in this study: river mud taken from the sediments of a local river (Porma River, Province of Leon, Spain), and anaerobic digestate (AD) taken from the effluent of an anaerobic digester operating in the local wastewater treatment facility (Leon city WWTP, 200.000 i.e.). These inocula were diluted in oxygen-free culture medium (20/80 v/v) before being fed to the WE chamber. The cells were inoculated within a period of 3-4 hours after the inocula were collected.

#### 5.2.4 Measurements and analytical techniques

Liquid samples were collected from the cathodic and anodic chambers and analysed immediately afterwards. Gas samples were collected with a GASTIGHT 1001 (Hamilton Co., GR, Switzerland) syringe from a built-in rubber septum.

Total organic carbon (TOC) and total nitrogen (TN) content were measured using a thermocatalytic oxidation system Analytikjena Multi N/C\_3100. Volatile fatty acids (VFAs) were analysed using a gas chromatograph (Varian CP3800 GC) equipped with a thermal conductivity detector and a Nukol capillary column (30 m × 0.25 mm × 0.25 µm) from Supelco, using He as mobile phase as described by [25] (detection limit 5 mg·L<sup>-1</sup>). Conductivity and pH were determined using APHA standard methodologies as described by [26]. Conductivity was determined with a HACH CDC401 probe in a Hach HQ40d multimeter, while pH was determined with a HACH 5014T probe in a CRISON 20+ pH meter. Electrochemical tests were performed using a potentiostat (VMP3, Biologic Science Instruments).

#### 5.2.5 High throughput sequencing of massive *16S rRNA* gene libraries

Samples from microbial community analysis were taken from both inocula used, **AD inoculum** and **RM inoculum**, and from the biofilms after 3 and 13 weeks of operation for each working strategy (as the culture medium is completely replaced after every batch cycle, the influence of immobilised biofilm communities is much more relevant than planktonic communities). It is important to clarify the terminology for the samples taken for the strategy S2 (**S2<sub>3w</sub>\_AD<sub>cathode</sub>** and **S2<sub>13w</sub>\_AD<sub>cathode</sub>**), strategy S3 (**S3<sub>3w</sub>\_RM<sub>anode</sub>** and **S3<sub>13w</sub>\_RM<sub>cathode</sub>**) and strategy S4 (**S4<sub>3w</sub>\_AD<sub>anode</sub>** and **S4<sub>13w</sub>\_AD<sub>cathode</sub>**). A thin piece of electrode (2mm x 2mm) was cut off with a stainless steel surgical blade in sterile conditions in a laminar flow cabinet and genomic DNA was extracted with the PowerSoil<sup>®</sup> DNA Isolation Kit (MoBio Laboratories Inc., Carlsbad, CA, USA), following the manufacturer's instructions. All PCR reactions were carried out in a Mastercycler (Eppendorf, Hamburg, Germany) and PCR samples were checked for size of the product on a 1% agarose gel. The PCR conditions are described in detail in section S5.1 of Appendix II.

The entire DNA extract was used for high throughput sequencing of *16S-rRNA* gene-based massive libraries (total Eubacterial and Archaeal). Each sample was

amplified with *16S-rRNA* gene-based primers for Eubacteria and Archaea, respectively. The primer set used was 27Fmod (5'-AGRGTTTGATCMTGGCTCAG-3') / 519R modBio (5'-GTNTTACNGCGGCKGCTG-3') [27] and Arch 349F (5'-GYGCASCAGKCGMGAAW-3') / Arch 806R (5'-GGACTACVSGGGTATCTAAT-3') [28], respectively, for the Eubacterial and Archaeal analysis population. The obtained DNA reads were compiled in FASTq files for further bioinformatics processing and following the procedure described by [29]. Operational taxonomic units (OTUs) were then taxonomically classified using the Ribosomal Database Project (<http://rdp.cme.msu.edu>). Raw pyrosequencing data obtained from this analysis were deposited in the Sequence Read Archive (SRA) of the National Centre for Biotechnology Information (NCBI) under nucleotide sequence accession numbers SRP115155, for Eubacterial and Archaeal population.

Microbial richness estimators (*observed OTUs* and *Chao1*) and diversity indices estimators (Shannon ( $H'$ ) and  $1/Simpson$ ) were calculated using MOTHUR software, version 1.35.1, and normalizing the number of reads of all samples to those of the sample with the lowest number of reads. A heatmap for species abundance was completed using RStudio.

## 5.3 RESULTS

### 5.3.1 Cell performance

The results of cell performance for every strategy are reported in this section. Current production and product formation were selected as performance indicators.

#### 5.3.1.1 Current production

Important differences in the behaviour of the cells, in terms of current production, were observed depending on the start-up strategy. These differences are summarised in table 5.1, and for more detailed information about temporary current profiles on every replicate, we refer the reader to figure S5.1 in appendix II (section S5.2). For strategy S1, where the electrodes were operated at reductive potential (as cathodes) using RM as inoculum, no current production was observed in any of the three replicates.



**Table 5.1:** Maximum recorded currents for each strategy and lag periods observed.

Strategy	Maximum current (A/m <sup>2</sup> )		Comments
	3 weeks	13 weeks	
S1 (RM:cathode-cathode)	<0.01	<0.01	No current or products.
S2 (AD:cathode-cathode)	0.4 ± 0.1	0.5 ± 0.1	Initial lag period of 2 weeks.
S3 (RM:anode-cathode)	0.6 ± 0.1	1.0 ± 0.2	Initial lag period of 24 h. Biocathodes took 4 days to produce current.
S4 (AD:anode-cathode)	0.7 ± 0.1	0.4 ± 0.1	Initial lag period of 24 h. Biocathodes took 3 days to produce current.

In strategy S2, the electrodes were also operated as cathodes but AD was used as inoculum. In this situation, and after a lag-phase of 2 weeks, the cells produced a stable current of 0.4 A/m<sup>2</sup>, growing to 0.5 A/m<sup>2</sup> at the end of the experiment (13 weeks). For strategies S3 and S4 the electrodes were initially operated as anodes, using RM and AD, respectively, as inoculum. In both situations, an oxidative current was almost immediately produced (after a short lag-phase around 24 h; see figure S5.1, appendix II, section S5.2) reaching moderate and stable peak values at the end of the 3-week interval. After this period, the bioanodes were switched into biocathodes by imposing a reductive potential. For strategy S3, this inversion resulted in a lag-phase of 4 days, after which reduction currents started to grow steadily, stabilising at around 1 A/m<sup>2</sup> by the end of the test (week 13). The MECs in strategy S4 followed a similar pattern, although the currents at the end of week 13 were appreciably lower.

### 5.3.1.2 Product formation

Chemical production was measured at the end of every batch cycle and only acetic acid was detected in the electrolyte of all reactors (figure 5.2). Other volatile fatty acids (C2-C7) and alcohols (C1-C6) were not present above the detection limit of the chromatographs. Hydrogen was detected in the cathodic head-spaces in strategies S2, S3 and S4, while methane was detected only in strategy S2. However, total gas production could not be accurately quantified due to gas leakages detected in the set-up.

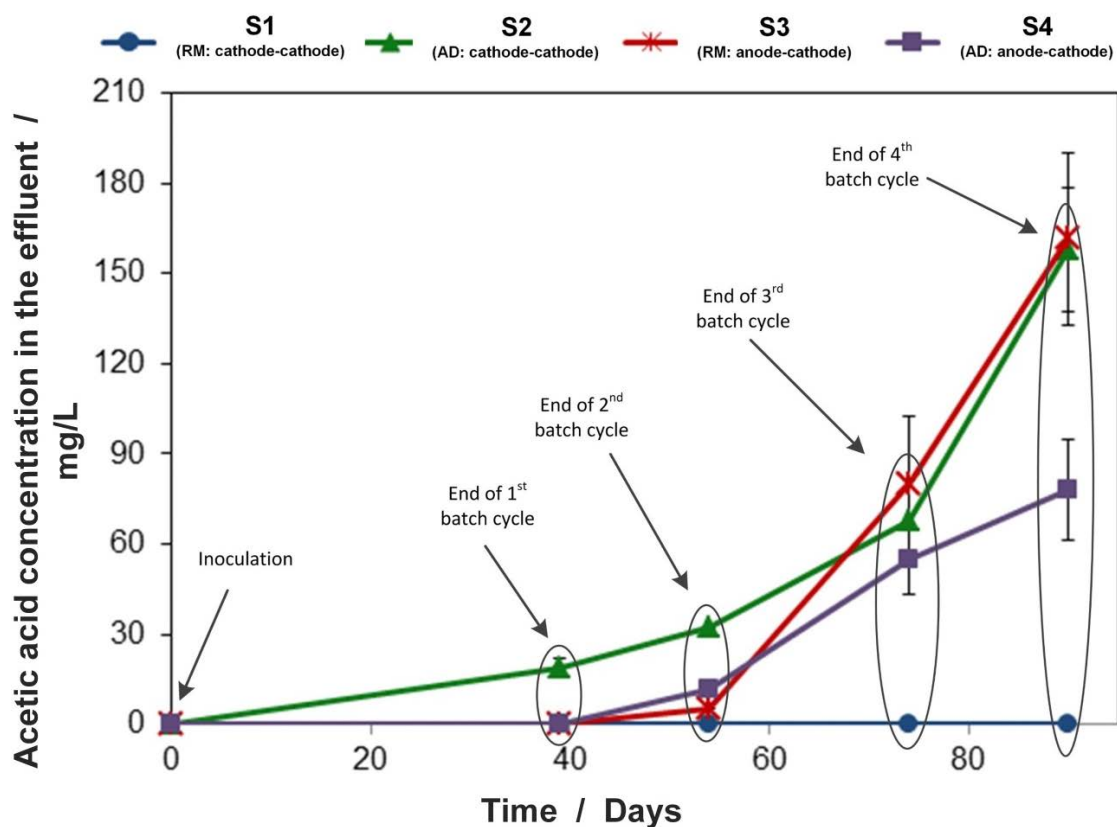


**Figure 5.2.** Averaged acetic acid concentration at the end of every batch cycle and for each strategy (error bars show standard deviation for three replicates). Day 0 corresponds to inoculation.

The absence of any measurable current in strategy S1 resulted in no acetate production (figure 5.2). For S2, some acetic acid was found from the beginning of the experiment, rising up to 158 mg/L at the end of the 13-week period. For S3, acetic acid production began to appear in small quantities at the end of week 7 after the first cathodic cycle, and rose sharply to 162 mg/L at the end of the final cycle. A similar behaviour was observed in S4, although the final acetate concentration was much lower (figure 5.2). Above all, figure 5.2 shows how titers consistently increase with every batch cycle for all strategies (except for S1), which might be indicative of a progressive acclimation and development of microbial communities.

**Table 5.2:** Cell performance for each start-up strategy

Strategy	Average current (A/m <sup>2</sup> )	Present in Off-gas		Coulombic efficiency (%)
		H <sub>2</sub>	CH <sub>4</sub>	
S1 (RM:cathode-cathode)	0	No	No	n.a.
S2 (AD:cathode-cathode)	0.45	Yes	Yes	9.5
S3 (RM:anode-cathode)	0.74	Yes	No	6.2
S4 (AD:anode-cathode)	0.37	Yes	No	5.7

The low coulombic efficiencies shown in table 5.2 indicate that a substantial amount of the electrons reaching the cathode are being diverted to other purposes rather than acetate production. The presence of methane and/or hydrogen in the off-gas clearly indicates that some of these electrons end up in those gases. Unfortunately, gas flowrates could not be measured accurately enough to provide a confident quantification of the incidence of those “electron sinks”. In addition, as the microbial communities are on the start-up and proliferation stage, it seems reasonable to think that a significant amount of electrons is also being diverted to biomass production, all of which could explain the relatively low coulombic efficiencies found in the present study.

### 5.3.2 Microbial community assessment

#### 5.3.2.1 Diversity indices analysis

The number of quality reads per sample ranged from 5430 to 104,398 for Eubacterial and from 1465 to 68,084 for Archaeal communities. No microbial analyses were performed for the strategy S1 due to the absence of biofilm. The rest of the samples were rarefied to 500 sequences for a good comparison in diversity analysis. Despite this reduction in sequence number, the richness and diversity of all samples were considered to be sufficiently covered. Regarding the Eubacterial community, wide differences both in species richness indicators (observed OTUs and Chao1), and in diversity indicators (Shannon (H') and 1/Simpson) were found between the AD and RM inoculum (table 5.3). Both indicators were much higher in the RM inoculum, as might be expected.

In S2, the diversity and richness indices decreased from **AD inoculum** (1/Simpson=33, Chao1=353) to **S2<sub>13w</sub>\_AD<sub>cathode</sub>** (1/Simpson=17, Chao1=243), and in the same way these indicators decreased in the S3 from **RM inoculum** (1/Simpson=174, Chao1=426) to **S3<sub>13w</sub>\_RM<sub>Cathode</sub>** (1/Simpson=3.0, Chao1=149). The same enrichment trend is observed in both cases, even sharper in the S3, due to the highly diversity of the **RM inoculum**.

However, in S4, the diversity remains constant from the **AD inoculum** (1/Simpson=33) to **S4<sub>13w</sub>\_AD<sub>cathode</sub>** (1/Simpson=34), while the richness is almost three-fold higher in the **AD inoculum** (Chao1=353) compared to the **S4<sub>13w</sub>\_AD<sub>cathode</sub>** biofilm (Chao1=141).

**Table 5.3:** Estimated richness (observed OTUs and Chao1) and diversity indices (Shannon (H') and 1/Simpson) for Eubacterial operational taxonomic units (OTUs), calculated with MOTHUR at the 3% distance level.

Samples	Observed OTUs	Chao1		Shannon (H')		1/Simpson	
		mean	(c.i.)*	mean	(c.i.)*	mean	(c.i.)*
<b>Strategy S2</b>							
<b>AD inoculum</b>	211	353	296-447	4.3	4.2-4.4	33	29-38
<b>S2<sub>3w</sub>_AD<sub>Cathode</sub></b>	112	163	136-223	3.4	3.3-3.5	13	11-15
<b>S2<sub>13w</sub>_AD<sub>Cathode</sub></b>	117	243	179-373	3.5	3.4-3.6	17	15-19
<b>Strategy S3</b>							
<b>RM inoculum</b>	351	426	398-470	5.5	5.4-5.6	174	145-217
<b>S3<sub>3w</sub>_RM<sub>Anode</sub></b>	184	315	259-414	4.3	4.2-4.3	38	34-43
<b>S3<sub>13w</sub>_RM<sub>Cathode</sub></b>	63	149	98-272	1.8	1.7-1.9	3.0	2.8-3.3
<b>Strategy S4</b>							
<b>AD inoculum</b>	211	353	296-447	4.3	4.2-4.4	33	29-38
<b>S4<sub>3w</sub>_AD<sub>Anode</sub></b>	225	351	301-436	4.6	4.5-4.6	46	41-54
<b>S4<sub>13w</sub>_AD<sub>Cathode</sub></b>	103	141	118-200	3.9	3.9-4.0	34	31-38

\*c.i. 95% confidence intervals

Results for Archaeal analysis indices are presented in table 5.4. Archaeal analysis was performed for the initial inocula and for the cathode biofilms at the end of the experiments. The numbers of sequences found were 52,490 and 68,084 for the **AD** and **RM inocula** samples, respectively, and the quantity of Archaeal decreases sharply to 1465 and 1473 sequences on the cathode biofilms for **S3<sub>13w</sub>\_AD<sub>cathode</sub>** and

**S2<sub>13w</sub>\_RM<sub>cathode</sub>**, respectively. However, it should be highlighted that just eight sequences were found on the **S4<sub>13w</sub>\_AD<sub>cathode</sub>**, indicating that the Archaea population was inhibited under this condition.

Similar results to those found in Eubacterial analysis were found for the Archaeal population. In both strategies (S2 and S3), the diversity is between a two and three-fold higher in the initial inocula (**AD** and **RM inocula**) and decrease in the cathode biofilms (**S2<sub>13w</sub>\_AD<sub>cathode</sub>** and **S3<sub>13w</sub>\_RM<sub>cathode</sub>**). The richness indicator for S2 is lower in the **S2<sub>13w</sub>\_AD<sub>cathode</sub>** (Chao1=35) than in the **AD inoculum** (Chao1=109), but in S3 this richness index is a four-fold increase over the **RM inoculum** (Chao1=322) than in the **S3<sub>13w</sub>\_RM<sub>cathode</sub>** (Chao1=81).

**Table 5.4:** Estimated richness (observed OTUs and Chao1) and diversity indices (Shannon (H') and 1/Simpson) for Archaeal operational taxonomic units (OTUs), calculated with MOTHUR at the 3% distance level.

Samples	Observed OTUs	Chao1		Shannon (H')		1/Simpson	
		mean	(c.i.)*	mean	(c.i.)*	mean	(c.i.)*
<b>Strategy S2</b>							
<b>AD inoculum</b>	61	109	80-183	2.2	2.1-2.3	4.2	4.0-4.6
<b>S2<sub>13w</sub>_AD<sub>Cathode</sub></b>	16	35	21-92	1.1	1.0-1.2	2.4	2.3-2.5
<b>Strategy S3</b>							
<b>RM inoculum</b>	132	322	231-497	3.0	2.9-3.2	6.1	5.4-7.0
<b>S3<sub>13w</sub>_RM<sub>Cathode</sub></b>	22	81	40-213	0.25	0.18-0.31	1.1	1.0-1.1
<b>Strategy S4</b>							
<b>AD inoculum</b>	61	109	80-183	2.2	2.2-2.3	4.2	4.0-4.6
<b>S4<sub>13w</sub>_AD<sub>Cathode</sub></b>	No Archaeal found						

\*c.i. 95% confidence intervals

### 5.3.2.2 Eubacterial community structure

Microbial community composition in the initial inocula used and growing on the surface of the carbon felt within the anode and cathode chamber were characterised by means of high throughput sequencing techniques.

**RM inoculum** presents a high diversity and it is composed of 12 different phyla, while in **AD inoculum**, which comes from a more specialised environment, *Firmicutes*

(46.1%) is the predominant phylum (figure 5.3). The predominant phyla in all electrodes were *Proteobacteria*, *Bacteroidetes* and *Firmicutes*.

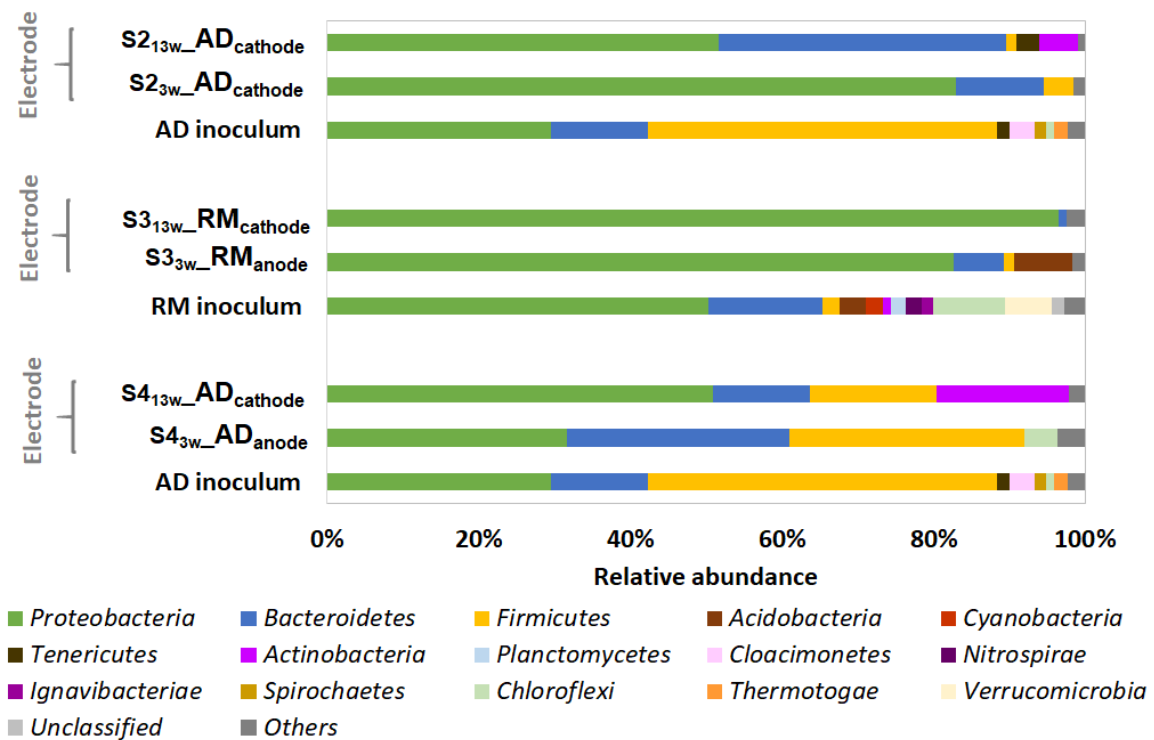


**Figure 5.3:** Taxonomic classification of high throughput sequencing at phylum level.

To better understand the microbial community evolution for each strategy, figure 5.4 compares the families on the initial inocula and those that develop on the anode and cathode biofilms. As already mentioned, no microbial analyses were performed for strategy S1. Additionally, and to have an overview of the main species present on the biofilms, a heatmap is shown (figure 5.5).

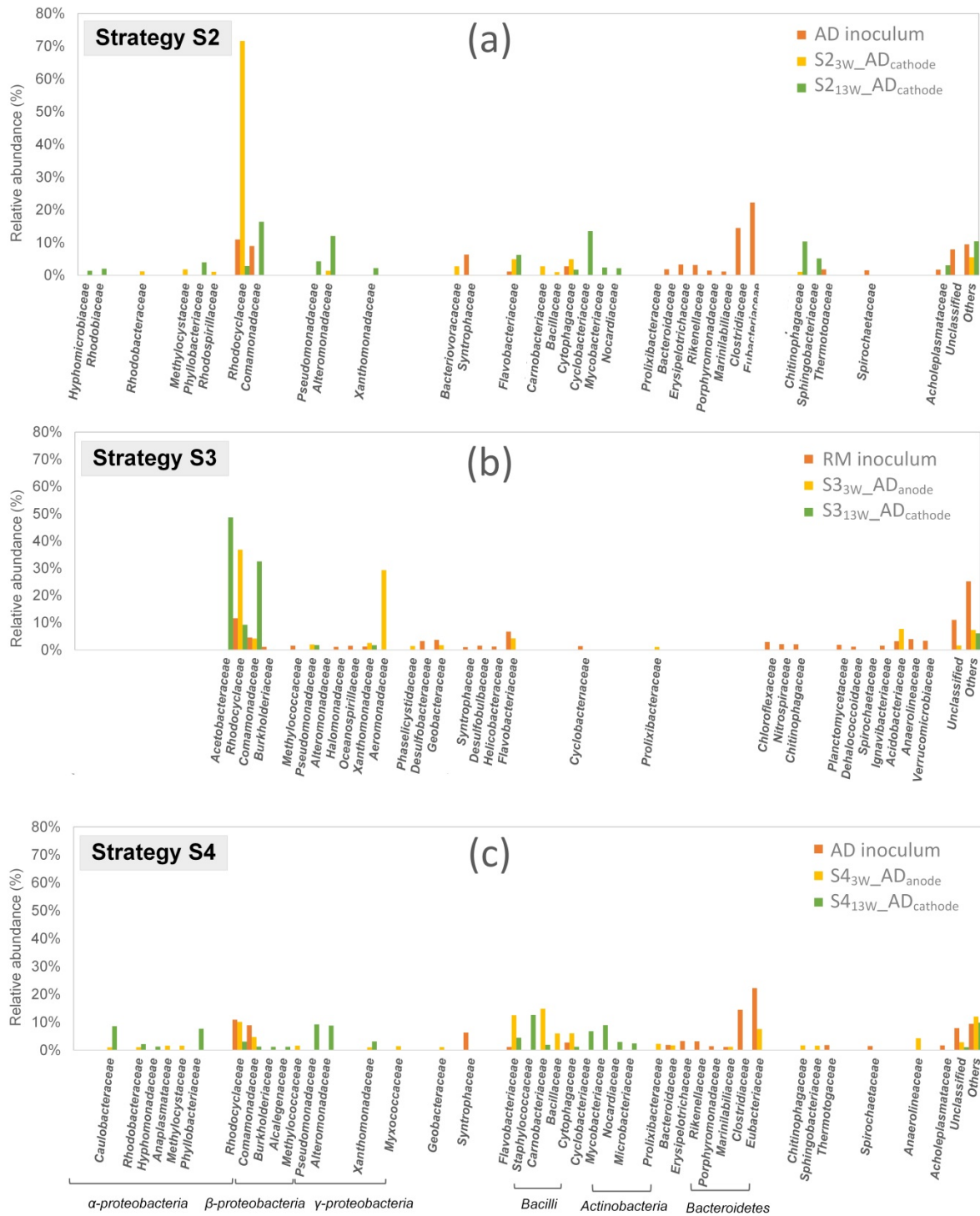


**Figure 5.4:** Taxonomic classification of sequencing results of *16S rRNA gene* from Eubacterial communities at a family level of a) samples from S2, b) samples from S3 and c) samples from S4. Groups accounting for less than 1% of the total number of sequences per sample were classified as ‘others’.

The anodic microbial populations were dominated by syntrophic interactions of fermenters, homoacetogens and anode respiring bacteria (ARB) (figures 5.4 and 5.5). Within the ARB, the well-known *Geobacter* is found in all anodic biofilms, independently of the inocula used (figure 5.5); however, after the polarity was inverted in S3 and S4, *Geobacter* was not identified. *Arcobacter*, a microaerobic electrogenic bacteria was found at the anode of S4 (first  $\epsilon$ -*proteobacteria* demonstrated to act as exoelectrogen [30]). Apart of these species, another important microorganism, *Desulfobulbus*, known as cable bacteria [31], which are directly related with current generation in BES, was found at all anodes biofilms. Some microorganisms which have been previously enriched and described at cathodic biofilms, such as *Alishewanella* [32], and *Rhodococcus* [33] were also found in the cathode biofilms of S2 and S4 (figure 5.5).

In S2, a sharp enrichment in *Rhodocyclaceae* (72%) (a hydrogen producing bacteria [34]) occurred in just 3 weeks (**S2<sub>3w</sub>\_AD<sub>cathode</sub>**). Our results showed that this family was mainly represented by two ribotypes, *Zooglea* (50%) and *Azoarcus* (19%) at week 3 of the experiment (figure 5.5). After 13 weeks of operation, the cathode microbial community becomes more diverse over time (**S2<sub>13w</sub>\_AD<sub>cathode</sub>**) (figure 5.4a). The *Rhodocyclaceae* family suffered a large decrease from 72% to 3%, while other families such as *Comamonadaceae*, *Alteromonadaceae*, *Pseudomonadaceae* and *Xanthomonadaceae* were enriched. The main genus of *Comamonadaceae* present was *Hydrogenophaga* (15%) (figure 5.5), which is an autotrophic hydrogen-oxidising bacteria [34]. Hydrogen-consuming microorganisms, such as *Hydrogenotropha* or *Thiobacillus*, electrotophic and also H<sub>2</sub> oxidising bacteria, were present.

For S3, where the electrodes were initially operated as anodes and inoculated with the highly diverse **RM inoculum**, the biofilms were swiftly enriched in nine anodophilic families (**S3<sub>3w</sub>\_RM<sub>anode</sub>**) (figure 5.4b). The two predominant families were also *Rhodocyclaceae* (37%) and *Aeromonadaceae* (29%). When the WEs were turned into cathode, the biofilm (**S3<sub>13w</sub>\_RM<sub>cathode</sub>**) became further specialised, with *Acetobacteraceae* (49.0%), *Comamonadaceae* (33.0%) and *Rhodocyclaceae* (9.2%) being the most abundant families. *Acetobacteraceae* belongs to the acetic acid bacteria (AAB), which can produce acetic acid using the Wood-Ljungdahl pathway oxidising H<sub>2</sub>



and using CO<sub>2</sub> as electron acceptor [35]. This family is represented by a single genus, *Acetobacter* (49%) (figure 5.5). *Acetobacterium* (a homoacetogenic non-electroactive bacteria) was found in much smaller abundance (0.2%).

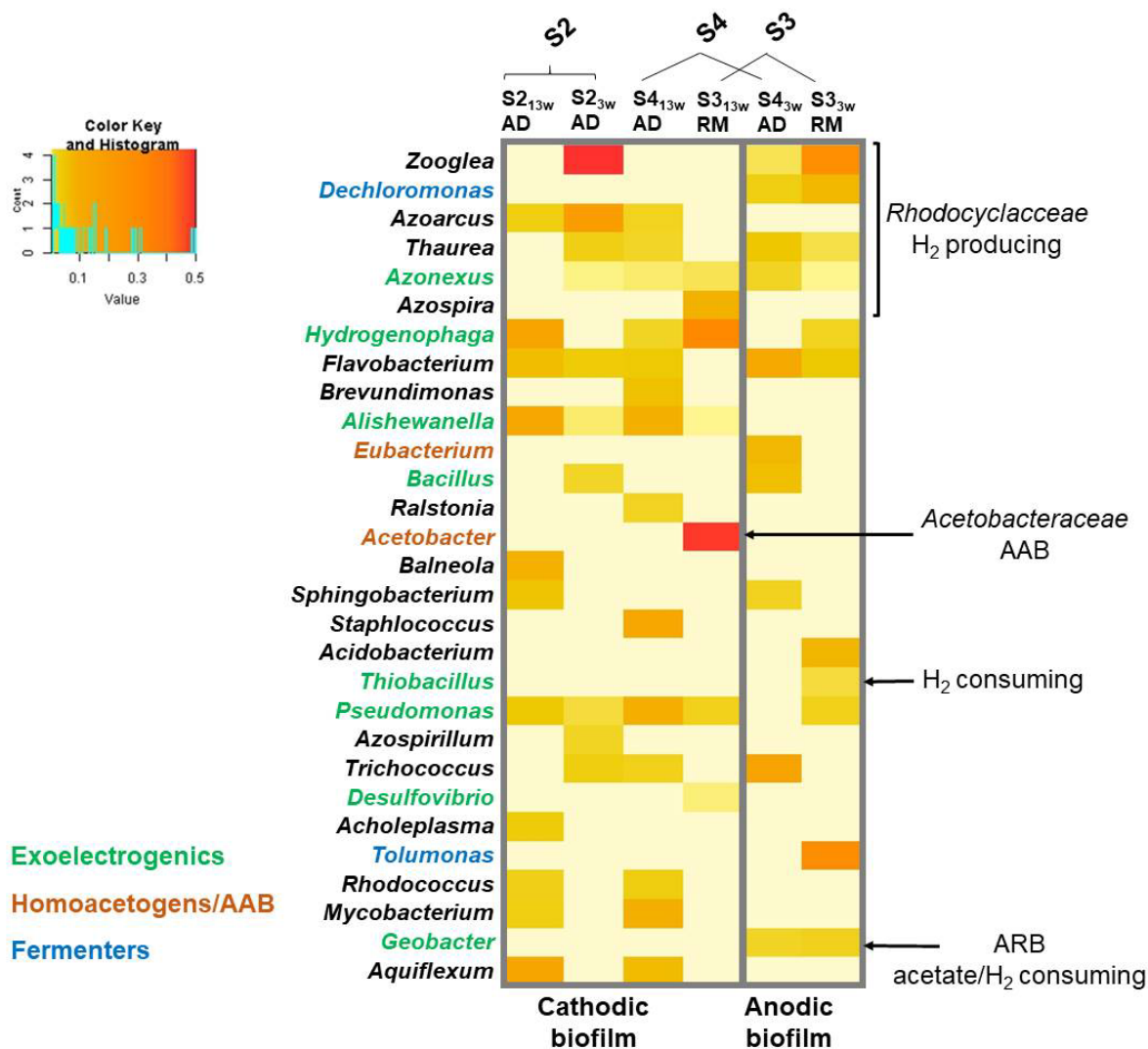


**Figure 5.5:** Heatmap summarising the main genera present at the anode and cathode biofilms for the three strategies where a biofilm developed.

In strategy S<sub>4</sub> (which followed the same start-up procedure as S<sub>3</sub>, but using **AD inoculum**), we found a drastically different scenario (figure 5.4c). A highly diverse biofilm was found in the anode (**S<sub>4</sub><sub>3w</sub>\_AD<sub>anode</sub>**), as well as when transformed into cathode (**S<sub>4</sub><sub>13w</sub>\_AD<sub>cathode</sub>**). Although **AD inoculum** is a highly specialised inoculum, the microbial community population that developed in the anodic biofilm sharply

changed. Furthermore, when the anode was turned into a cathode, the biofilm population was very diverse as well, but completely different from the anode and also the inoculum.

### 5.3.2.3 Archaeal community structure

In general, Archaeal communities display lower growth rates compared to Eubacteria; thus only initial inocula samples and cathode biofilms samples taken after 13 weeks of operation (once they were well stabilized) were analysed for Archaeal community structure.

In both inocula (**AD** and **RM**), the two predominant families were *Thermoplasmataceae* and *Methanosaetaceae*. Other families such as *Methanoregulaceae*, *Methanobacteriaceae*, *Crenarchaeota* and *Methanomassiliicoccaceae* were also found, although in a lower proportion (figure S5.2, Appendix II, section S5.3). Despite these similarities, the Archaeal communities that developed on the cathode biofilms were drastically different (figure 5.6 and figure S5.2, Appendix II). Cathode biofilm in the S2 (**S2<sub>13w</sub>\_AD<sub>cathode</sub>**), showed an important enrichment in the *Methanosaeta* (an acetoclastic methanogen belonging to the Methanosaetaceae family (49%)), and *Methanomassiliicoccus* (a methylotrophic H<sub>2</sub>-dependent methanogen [36] that belongs to the Methanomassiliicoccaceae family (44%)).

An important enrichment in the hydrogenotrophic methanogen *Methanobacterium*, which belongs to *Methanobacteriaceae* family, was observed on the cathode biofilm in S3 with respect to the **RM inoculum** (97% and 2.7%, respectively (figure 5.6)). As mentioned in the diversity indices section, no Archaeal population was found in S4.

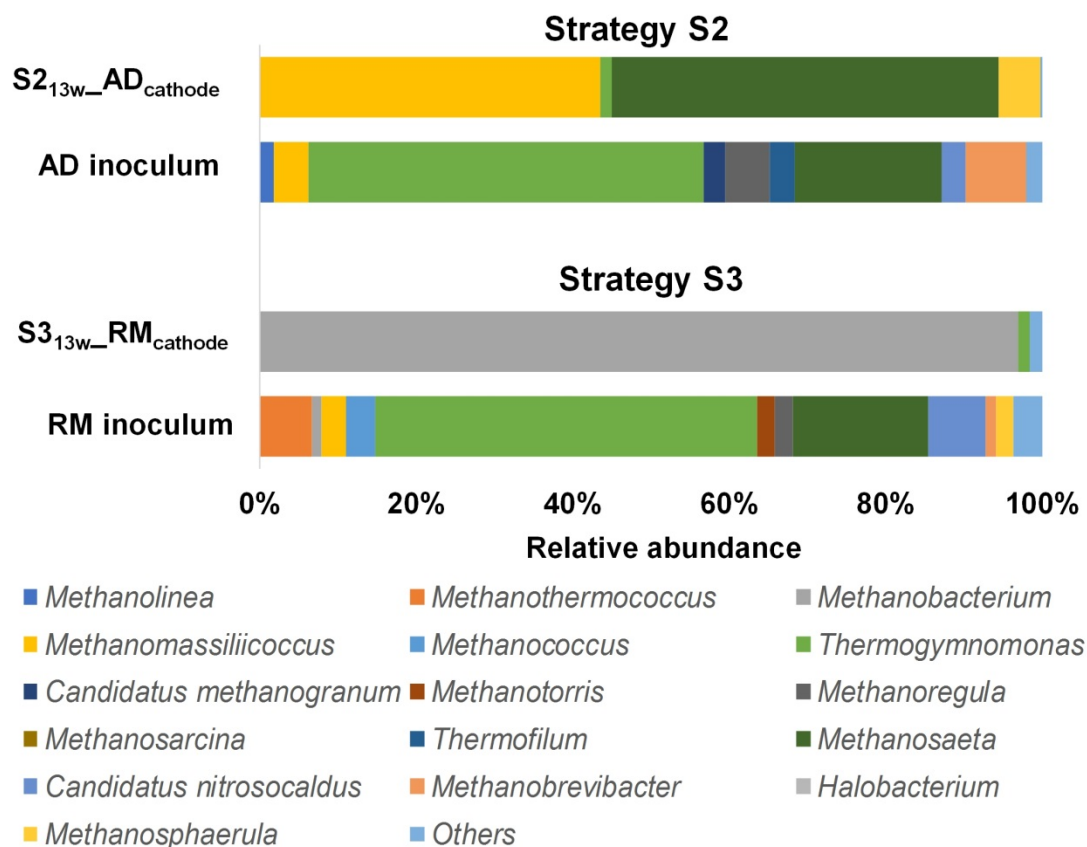


**Figure 5.6:** Taxonomic assignment of Archaeal microbial communities of AD and RM inocula, and cathode samples taken from S2 and S3 strategies at a genus level. Groups accounting for less than 1% of the total number of sequences per sample were classified as ‘others’.

## 5.4 DISCUSSION

The results presented in this article seem to confirm a usual finding reported by other authors when producing biocathodes for microbial electrosynthesis: biocathodes struggled to form a viable biofilm by merely imposing reductive potentials. In our particular case this was so, regardless of the characteristics of the inoculum being used: strategy S1 (from a diverse inoculum) totally failed to produce any biofilm in any of the three replicates, and strategy S2 (from a lower diverse inoculum) required a 2-week lag-phase to develop an electricity-producing biofilm. A drastically different behaviour was observed when the bioelectrodes were started-up with oxidative potentials (strategies S3 and S4). For both strategies, the bioelectrodes started to produce an oxidative current in about 24 hours, and peak currents stabilised just after two cycles. When converted to biocathodes (by imposing reductive potentials) they required 3 to 4 days to produce an appreciable cathodic current, although we believe this ‘lag-phase’ can be partially

explained by the microbial stress during microbiological sampling of the electrodes. Moreover, cathodic currents in strategies S3 and S4 tended to grow at a much higher rate than in S2. This promising behaviour observed in biocathodes started-up as bioanodes could be attributed to the rapid development of anode respiring bacteria (ARB) (*Geobacter* and *Thiobacillus*) and their subsequent syntrophic interactions with fermenters (*Dechloromonas* and *Tolumonas*) and homoacetogens (*Treponema*). These anodic microorganisms might be responsible for reaching a total degradation of the organic matter and obtaining good current production.

Interestingly, for all reactors and regardless of the inocula and the starting-up potential, the predominant phyla enriched in the electrode biofilms were *Proteobacteria*, *Bacteroidetes* and *Firmicutes*, which also confirms the observations made by other authors [34,37,38] (mainly in acetate fed MECs). *Proteobacteria* phylum contains well-known electrochemically active bacteria [39], and members of the classes  $\alpha$ ,  $\beta$ ,  $\gamma$  and  $\delta$ -*Proteobacteria* were identified in our electrodes. Furthermore, the proportion of this phylum tends to be raised in anode and cathode biofilms with respect to the initial inocula. To date, for *Bacteroidetes*, only two species have been claimed to be electroactive [40], and the vast majority of the species belonging to this phylum are not described as electrochemically active bacteria. However, its presence in BES is highly widespread, which suggests its importance for efficient biofilm function [37]. Despite these similarities at the phylum level, the results of this study indicated that greatly different Eubacterial phylotypes were identified in each strategy carried out. It is consistently highlighted that as the Archaeal community is quite similar in both inocula, the dominant families on the cathode biofilms were drastically different. Apparently, the results point to a quicker enrichment in electrotrophic Eubacterial communities using an anodic start-up. Below is a detailed summary of the main findings for each start-up strategy regarding biofilm development:

*Strategy S1: combining cathodic start-up potentials with a diverse inoculum.*

Although the inoculum contained various potentially electroactive bacteria, none of them succeeded in colonising the electrode. This is probably due to the fact that most of these bacteria oxidise organic chemical species and cannot modify their metabolic pathways to be viable at reductive potentials.

---

*Strategy S2: combining cathodic start-up potentials with a low diverse inoculum.*

This strategy showed a sharp enrichment during the first 3 weeks of operation, finding up to 70% of a H<sub>2</sub> producing family (*Rhodocyclaceae*). After 13 weeks, this family is still present in the biocathode, although its proportion is drastically reduced due to the proliferation of other cathodophilic families (*Hydrogenotropha* and *Thiobacillus*) responsible for H<sub>2</sub> oxidation and homacetogenesis. Regarding the Archaea population, acetoclastic and hydrogenotrophic communities are present in a similar proportion. This microbial community evolution, together with steadily growing current records during the start-up period, suggests that electrotrophic H<sub>2</sub> producing bacteria firstly spread on the biocathode, generating a suitable environment for other cathodophilic bacteria responsible for acetic acid production. The spread of H<sub>2</sub>-producing bacteria during the first phase of inoculation could also have paved the way for the proliferation of the H<sub>2</sub>-dependent methanogen *Methanomassiliicoccus*, which could explain, at least in part, the presence of methane in the off-gas.

*Strategy S3: combining anodic start-up potentials with a diverse inoculum.*

Despite using the same inoculum as in S1, the outcome of this strategy is totally different, probably as a result the oxidative potential imposed in S3. During the first 3 weeks of operation, the electrode community becomes highly specialised in certain ARB bacteria (*Geobacter*, *Desulfovibrio* and *Thiobacillus*), achieving a complete substrate degradation. Interestingly, when the electrode potential was inversed (cathode operation mode), some of these electrogenic bacteria were maintained, and acetic acid producing bacteria such as *Acetobacter* and *Acetobacterium* enriched over 50% of the total population. Presumably, the non-strictly anaerobic environment in our reactors can be responsible for the proliferation of these AAB against the typical homoacetogenic bacteria usually found in more strict anaerobic conditions [41,42]. It is important to note that this non-electroactive bacteria has been described as contributing to the microbial consortia via direct electron transfer (DET) [5], which could play an important role in the current production in this strategy.

Aside from ABB, acetate production could also be explained by the interaction between *Desulfovibrio* and *Acetobacterium*. *Desulfovibrio* belongs to  $\delta$ -*proteobacteria* class, and is known to use sulfate as an electron acceptor, and is also able to grow converting formate into H<sub>2</sub> [12]. *Desulfovibrio* was only identified on this strategy, probably in syntrophic conditions with *Acetobacterium*, and other microorganisms related to formate metabolism, since *Acetobacterium* can use formate to produce acetate [12]. *Desulfovibrio* can also act as acetogenic and produce acetate itself when the sulfate is in a low concentration and there is an H<sub>2</sub> / CO<sub>2</sub> atmosphere, as may be the case in our reactors. On the biocathode, biologically H<sub>2</sub> can also be generated by some bacteria identified in this strategy, which could favour the presence of hydrogenotrophic Archaea as well as H<sub>2</sub> consuming acetogens. The detected H<sub>2</sub> might cause strong competition from hydrogenotrophic methanogens. For this reason, it is not surprising that an important enrichment in the hydrogenotrophic methanogen *Methanobacterium*, which belongs to the *Methanobacteriaceae* family, is observed on the cathode biofilm with respect to the RM inoculum.

Overall, these findings suggest that it is possible to develop a robust acetate-producing biocathode in a shorter period of time (compared to S2) from a working bioanode. This rapid response seems to be related to the anodic potentials during the start-up and the high bacterial enrichment.

*Strategy S4: combining anodic start-up potentials with a low diverse inoculum.*

This strategy uses an inoculum obtained from an anaerobic digester, which represents a low diversity inoculum as the microbial communities have been previously adapted to the specific conditions of anaerobic digestion. Interestingly, the microbial structure drastically changes and diversifies when introduced to the particular environment of a bioanode. Interestingly, this population is rather different from the anode in S3 but shows comparably good results in terms of current production and substrate degradation. However, when the potential of the electrode is inverted, few microbial families resist on the biocathode, promoting a complete rediversified community with no single predominant family, which contrasts with the specific biocathode reached in S3. No Archaea were detected, which agrees with the absence of

detected methane. This non-specialised resulting community is capable of achieving a comparable but lower cathodic current than the previous S3; nevertheless, the lower acetic acid production found for this strategy suggests that a specialised biofilm is preferable.

## 5.5 CONCLUSIONS

This study elucidates the impact of the start-up strategies on the microbial communities that evolve on the biofilm of a biocathode. Using reductive start-up potentials and a highly diverse inoculum, this start-up failed to produce any biofilm. When a less species richness inoculum from an anaerobic environment was used with the same reductive initial potential, a specialised biofilm was formed and a highly productive biocathode was developed in terms of acetic acid and also current production. However, using oxidative start-up potential led to rapid electroactive biofilm development, although the final composition of the biofilm was highly dependent on the inoculum used. So, using the diverse RM inoculum, a final specialised biofilm grew on the electrode, also giving high acetate and current generation. However, when using the less species richness AD inoculum, it was found that a non-specialised biofilm was developed and lower acetic acid production was found.

Importantly, a higher specialisation of the biofilm leads to an improvement in acetate generation, probably due to lowered influence of undesirable secondary metabolic pathways. Moreover, it has been shown that the coupling of H<sub>2</sub> producing bacteria and acetic acid bacteria play an important role in acetate production.

## 5.6 REFERENCES

- [1] P.S. E. A. Quadrelli, K. Armstrong, Chapter 16 – Potential CO<sub>2</sub> Utilisation Contributions to a More Carbon-Sober Future: A 2050 Vision, in: Carbon Dioxide Util., 2015: pp. 285–302. doi:10.1016/B978-0-444-62746-9.00016-5.
- [2] E. Alper, O. Yuksel Orhan, CO<sub>2</sub> utilization: Developments in conversion processes, *Petroleum*. 3 (2017) 109–126. doi:10.1016/j.petlm.2016.11.003.
- [3] S. Venkata Mohan, J.A. Modestra, K. Amulya, S.K. Butti, G. Velvizhi, A Circular Bioeconomy with Biobased Products from CO<sub>2</sub> Sequestration, *Trends Biotechnol.* 34 (2016) 506–519. doi:10.1016/j.tibtech.2016.02.012.
- [4] J. Sadhukhan, J.R. Lloyd, K. Scott, G.C. Premier, E.H. Yu, T. Curtis, I.M. Head, A critical review of integration analysis of microbial electrosynthesis (MES) systems with waste biorefineries for the production of biofuel and chemical from reuse of CO<sub>2</sub>, *Renew. Sustain. Energy Rev.* 56 (2016) 116–132. doi:10.1016/j.rser.2015.11.015.
- [5] M. Kitching, R. Butler, E. Marsili, Microbial bioelectrosynthesis of hydrogen: Current challenges and scale-up, *Enzyme Microb. Technol.* 96 (2017) 1–13. doi:10.1016/j.enzmictec.2016.09.002.
- [6] T. Jafary, W.R.W. Daud, M. Ghasemi, B.H. Kim, J. Md Jahim, M. Ismail, S.S. Lim, Biocathode in microbial electrolysis cell; Present status and future prospects, *Renew. Sustain. Energy Rev.* 47 (2015) 23–33. doi:10.1016/j.rser.2015.03.003.
- [7] S. Bajracharya, M. Sharma, G. Mohanakrishna, X. Dominguez Benneton, D.P.B.T.B. Strik, P.M. Sarma, D. Pant, An overview on emerging bioelectrochemical systems (BESs): Technology for sustainable electricity, waste remediation, resource recovery, chemical production and beyond, *Renew. Energy*. (2016). doi:10.1016/j.renene.2016.03.002.
- [8] J. Desloover, J.B.A. Arends, T. Hennebel, K. Rabaey, Operational and technical considerations for microbial electrosynthesis, *Biochem. Soc. Trans.* 40 (2012) 1233 LP-1238. <http://www.biochemsoctrans.org/content/40/6/1233.abstract>.



- 
- [9] D.R. Lovley, Powering microbes with electricity: direct electron transfer from electrodes to microbes., *Environ. Microbiol. Rep.* 3 (2011) 27–35. doi:10.1111/j.1758-2229.2010.00211.x.
- [10] P.L. Tremblay, T. Zhang, Electrifying microbes for the production of chemicals, *Front Microbiol.* (2015).
- [11] S. Bajracharya, A. ter Heijne, X. Dominguez Benetton, K. Vanbroekhoven, C.J.N. Buisman, D.P.B.T.B. Strik, D. Pant, Carbon dioxide reduction by mixed and pure cultures in microbial electrosynthesis using an assembly of graphite felt and stainless steel as a cathode, *Bioresour. Technol.* 195 (2015) 14–24. doi:10.1016/j.biortech.2015.05.081.
- [12] H.D. May, P.J. Evans, E. V LaBelle, The bioelectrosynthesis of acetate, *Curr. Opin. Biotechnol.* 42 (2016) 225–233. doi:10.1016/j.copbio.2016.09.004.
- [13] R. Kleerebezem, M.C. van Loosdrecht, Mixed culture biotechnology for bioenergy production, *Curr. Opin. Biotechnol.* 18 (2007) 207–212. doi:10.1016/j.copbio.2007.05.001.
- [14] K. Schuchmann, V. Müller, Autotrophy at the thermodynamic limit of life: a model for energy conservation in acetogenic bacteria., *Nat. Rev. Microbiol.* 12 (2014) 809–821. <http://10.0.4.14/nrmicro3365>.
- [15] F.M. Liew, M. Köpke, S.D. Simpson, Gas fermentation for commercial biofuels production, INTECH Open Access Publisher, 2013. doi:10.5772/52164.
- [16] S. Bajracharya, R. Yuliasni, K. Vanbroekhoven, C.J.N. Buisman, D.P.B.T.B. Strik, D. Pant, Long-term operation of microbial electrosynthesis cell reducing CO<sub>2</sub> to multi-carbon chemicals with a mixed culture avoiding methanogenesis, *Bioelectrochemistry.* 113 (2017) 26–34. doi:10.1016/j.bioelechem.2016.09.001.
- [17] K.J.J. Steinbusch, H.V.M. Hamelers, C.M. Plugge, C.J.N. Buisman, Biological formation of caproate and caprylate from acetate: fuel and chemical production from low grade biomass, *Energy Environ. Sci.* 4 (2011) 216–224. doi:10.1039/C0EE00282H.
-

- [18] G. Mohanakrishna, K. Vanbroekhoven, D. Pant, Imperative role of applied potential and inorganic carbon source on acetate production through microbial electrosynthesis, *J. CO2 Util.* 15 (2016) 57–64. doi:10.1016/j.jcou.2016.03.003.
- [19] Z. Zaybak, J.M. Pisciotta, J.C. Tokash, B.E. Logan, Enhanced start-up of anaerobic facultatively autotrophic biocathodes in bioelectrochemical systems., *J. Biotechnol.* 168 (2013) 478–85. doi:10.1016/j.jbiotec.2013.10.001.
- [20] S.A. Patil, J.B.A. Arends, I. Vanwonterghem, J. Van Meerbergen, K. Guo, G.W. Tyson, K. Rabaey, Selective enrichment establishes a stable performing community for microbial electrosynthesis of acetate from CO<sub>2</sub>, *Environ. Sci. Technol.* 49 (2015) 8833–8843.
- [21] J.S. Geelhoed, A.J.M. Stams, Electricity-assisted biological hydrogen production from acetate by *Geobacter sulfurreducens*, *Environ. Sci. Technol.* 45 (2010) 815–820.
- [22] R.M. Hartline, D.F. Call, Substrate and electrode potential affect electrotrophic activity of inverted bioanodes, *Bioelectrochemistry.* 110 (2016) 13–18. doi:10.1016/j.bioelechem.2016.02.010.
- [23] H. Yun, B. Liang, D.-Y. Kong, H.-Y. Cheng, Z.-L. Li, Y.-B. Gu, H.-Q. Yin, A.-J. Wang, Polarity inversion of bioanode for biocathodic reduction of aromatic pollutants, *J. Hazard. Mater.* 331 (2017) 280–288. doi:10.1016/j.jhazmat.2017.02.054.
- [24] C.W. Marshall, D.E. Ross, E.B. Fichot, R.S. Norman, H.D. May, Electrosynthesis of commodity chemicals by an autotrophic microbial community, *Appl. Environ. Microbiol.* 78 (2012) 8412–8420.
- [25] E.J. Martínez, M. V Gil, J.G. Rosas, R. Moreno, R. Mateos, A. Morán, X. Gómez, Application of thermal analysis for evaluating the digestion of microwave pre-treated sewage sludge, *J. Therm. Anal. Calorim.* (2016). doi:10.1007/s10973-016-5460-4.
- [26] E.W. Rice, L. Bridgewater, A.P.H. Association, A.W.W. Association, W.E. Federation, *Standard Methods for the Examination of Water and Wastewater*,

- American Public Health Association, 2012.  
<https://books.google.dk/books?id=dd2juAAACAAJ>.
- [27] T.R. Callaway, S.E. Dowd, R.D. Wolcott, Y. Sun, J.L. McReynolds, T.S. Edrington, J. a Byrd, R.C. Anderson, N. Krueger, D.J. Nisbet, Evaluation of the bacterial diversity in cecal contents of laying hens fed various molting diets by using bacterial tag-encoded FLX amplicon pyrosequencing., *Poult. Sci.* 88 (2009) 298–302. doi:10.3382/ps.2008-00222.
- [28] K. Takai, K. Horikoshi, K.E.N. Takai, Rapid Detection and Quantification of Members of the Archaeal Community by Quantitative PCR Using Fluorogenic Probes Rapid Detection and Quantification of Members of the Archaeal Community by Quantitative PCR Using Fluorogenic Probes, *Appl. Environ. Microbiol.* 66 (2000) 5066–5072. doi:10.1128/AEM.66.11.5066-5072.2000.Updated.
- [29] A. Sotres, L. Tey, A. Bonmatí, M. Viñas, Microbial community dynamics in continuous microbial fuel cells fed with synthetic wastewater and pig slurry, *Bioelectrochemistry.* (2016).
- [30] H. Toh, V.K. Sharma, K. Oshima, S. Kondo, M. Hattori, F.B. Ward, A. Free, T.D. Taylor, Complete genome sequences of *Arcobacter butzleri* ED-1 and *Arcobacter* sp. Strain L, both isolated from a microbial fuel cell, *J. Bacteriol.* 193 (2011) 6411–6412. doi:10.1128/JB.06084-11.
- [31] R. Schauer, N. Risgaard-petersen, K.U. Kjeldsen, J.J.T. Bjerg, B.B. Jørgensen, A. Schramm, L.P. Nielsen, Succession of cable bacteria and electric currents in marine sediment, (2014) 1314–1322. doi:10.1038/ismej.2013.239.
- [32] J.M. Morris, S. Jin, B. Crimi, A. Pruden, Microbial fuel cell in enhancing anaerobic biodegradation of diesel, *Chem. Eng. J.* 146 (2009) 161–167.
- [33] R. Blasco-Gómez, P. Batlle-Vilanova, M. Villano, M.D. Balaguer, J. Colprim, S. Puig, On the Edge of Research and Technological Application: A Critical Review of Electromethanogenesis, *Int. J. Mol. Sci.* 18 (2017) 874.
- [34] L. Jourdin, S. Freguia, B.C. Donose, J. Keller, Autotrophic hydrogen-producing

- biofilm growth sustained by a cathode as the sole electron and energy source, *Bioelectrochemistry*. 102 (2015) 56–63. doi:10.1016/j.bioelechem.2014.12.001.
- [35] M.L.T. Cossio, L.F. Giesen, G. Araya, M.L.S. Pérez-Cotapos, R.L. VERGARA, M. Manca, R.A. Tohme, S.D. Holmberg, T. Bressmann, D.R. Lirio, J.S. Román, R.G. Solís, S. Thakur, S.N. Rao, E.L. Modelado, A.D.E. La, C. Durante, U.N.A. Tradición, M. En, E.L. Espejo, D.E.L.A.S. Fuentes, U.A. De Yucatán, C.M. Lenin, L.F. Cian, M.J. Douglas, L. Plata, F. Héritier, *Brock Biology of Microorganism*, 2012. doi:10.1007/s13398-014-0173-7.2.
- [36] G. Borrel, P.W. O’Toole, H.M.B. Harris, P. Peyret, J.F. Brugère, S. Gribaldo, Phylogenomic data support a seventh order of methylotrophic methanogens and provide insights into the evolution of methanogenesis, *Genome Biol. Evol.* 5 (2013) 1769–1780. doi:10.1093/gbe/evt128.
- [37] S. Ishii, S. Suzuki, T.M. Norden-krichmar, K.H. Nealson, Y. Sekiguchi, Y.A. Gorby, O. Bretschger, Functionally Stable and Phylogenetically Diverse Microbial Enrichments from Microbial Fuel Cells during Wastewater Treatment, 7 (2012). doi:10.1371/journal.pone.0030495.
- [38] G.T. Kim, G. Webster, J.W.T. Wimpenny, B.H. Kim, H.J. Kim, A.J. Weightman, Bacterial community structure, compartmentalization and activity in a microbial fuel cell, *J. Appl. Microbiol.* 101 (2006) 698–710. doi:10.1111/j.1365-2672.2006.02923.x.
- [39] C. Koch, F. Harnisch, Is there a Specific Ecological Niche for Electroactive Microorganisms?, *ChemElectroChem.* (2016) 1282–1295. doi:10.1002/celec.201600079.
- [40] P.P. Aparna, S. Meignanalakshmi, Comparison of power generation of electrochemically active bacteria isolated from the biofilm of single chambered multi-electrode microbial fuel cell developed using *Capra hircus* rumen fluid, *Energy Sources, Part A Recover. Util. Environ. Eff.* 38 (2016) 982–988.
- [41] E. V. LaBelle, C.W. Marshall, J.A. Gilbert, H.D. May, Influence of acidic pH on hydrogen and acetate production by an electrosynthetic microbiome, *PLoS One*.

- 
- 9 (2014) 1–10. doi:10.1371/journal.pone.0109935.
- [42] L. Jourdin, T. Grieger, J. Monetti, V. Flexer, S. Freguia, Y. Lu, J. Chen, M. Romano, G.G. Wallace, J. Keller, High Acetic Acid Production Rate Obtained by Microbial Electrosynthesis from Carbon Dioxide, *Environ. Sci. Technol.* 49 (2015) 13566–13574. doi:10.1021/acs.est.5b03821.



## CHAPTER 6

Enhanced CO<sub>2</sub> conversion  
through MES by continuous  
headspace gas recirculation

*Chapter adapted from:*

**Mateos, R.,** Sotres, A., Alonso, R. M., Escapa, A., & Morán, A. (n.a.). Enhanced CO<sub>2</sub> conversion through MES by continuous headspace recirculation.

Submitted to peer review.





## ABSTRACT

Bioelectrochemical systems (BESs) is a term that encompasses a group of novel technologies that are able to interconvert electrical energy and chemical energy by means of a bioelectroactive biofilm. Microbial Electrosynthesis (MES), which branch off from BES, are able to convert CO<sub>2</sub> into valuable organic chemicals and fuels. This study demonstrates that CO<sub>2</sub> reduction in MES can be enhanced by previously enriching the inoculum and improving CO<sub>2</sub> availability to the biofilm. The proposed system proves to be a repetitive, efficient and selective way of consuming CO<sub>2</sub> for the production of acetic acid, showing cathodic efficiencies over 55% and CO<sub>2</sub> conversions over 80%. Continuous recirculation of the gas headspace through the catholyte allowed to improve performance by 44%, achieving CO<sub>2</sub> fixation rates of 171 ml CO<sub>2</sub> · L<sup>-1</sup> · d<sup>-1</sup>, a maximum daily acetate production rate of 261 mg HAc · L<sup>-1</sup> · d<sup>-1</sup>, and a maximum acetate titer of 1957 mg · L<sup>-1</sup>. High-throughput sequencing revealed that CO<sub>2</sub> reduction was mainly driven by a mixed culture biocathode, in which *Sporomusa* and *Clostridium*, both bioelectrochemical acetogenic bacteria, were identified together with other species such as *Desulfovibrio*, *Pseudomonas*, *Arcobacter*, *Acinetobacter* or *Sulfurospirillum*, which are usually found in biocathode biofilms. Moreover, a connection was observed between cathodic microbial communities and reactor performance.

## 6.1 INTRODUCTION

Anthropogenic greenhouse gas emissions, among which CO<sub>2</sub> occupies a preeminent position, are widely considered as the main contributors to the global rise in temperature [1]. Thus, not surprisingly, increasing worldwide CO<sub>2</sub> emissions and their impact on climate change have become one of the main public concerns, and great efforts and investments are being made in the fields of science and engineering to reverse this situation [2].

In the last few years, the concept of carbon capture and utilization has become of great interest for the chemical industry, as it represents a technological solution that aims to prevent CO<sub>2</sub> emissions by converting them into value added chemicals [3]. Exploring ways to give added value to this CO<sub>2</sub> has gained attention during the last few years, and a wide range of chemical and biological methods have already been put forward for its valorization [4]. However, CO<sub>2</sub> is a highly oxidized molecule and its conversion into valuable molecules (e.g. fuels, solvents, precursors, etc.) requires a chemical reductant to provide the necessary electrons. Alternatively, an electrode (cathode) can also serve as an electron donor, thus avoiding the need for a chemical reductant [5]. This is the case for Microbial Electrosynthesis (MES), a relatively recent technology, which makes use of a bioelectrode to provide electrons for CO<sub>2</sub> reduction and generate multicarbon organics [6,7]. MES is rooted on the capability of some types of bacteria to electrically interact with a solid surface (cathode) that acts as an electron donor for their metabolism [8]. Several studies have been published in the last few years, studying different aspects of CO<sub>2</sub> bioelectroreduction, targeting acetate as an end-product [7,9,10], and using both mixed and pure culture electroactive biofilms. For instance, pure cultures of homoacetogenic bacteria such as *Sporomusa sp.* [11] or *Clostridium sp.* [12] have been used to understand and overcome fundamental challenges (e.g. characterizing electron transfer mechanisms), while enriched acetogenic biocathodes seem to be the key to achieving robust and inexpensive scalable systems [13]. Nevertheless, MES technology and bioelectrochemical systems in general are still a far from practical application and further research into basic operational variables, long-term stability, continuous production, repeatability and scalability is still necessary [14–16]. The need to improve CO<sub>2</sub> availability to microorganisms is particularly important; in this regard, CO<sub>2</sub> solubility issues play a vital role. This problem has

mainly been solved to date by sparging excess quantities of CO<sub>2</sub> in the culture medium [13], or directly adding inorganic carbon in the form of bicarbonate [17]. However, these approaches have some drawbacks: in the sparging method, most of the CO<sub>2</sub> is lost to the atmosphere, while pH must be continuously adjusted if bicarbonate is used as the substrate.

The present study aimed to gain knowledge on how improving CO<sub>2</sub> availability to the microbial communities of a MES, by continuous CO<sub>2</sub> recirculation, impacts on MES performance in terms of current density and product (acetic acid) formation. We also focused on elucidating which microorganisms are responsible for the process and how their temporal evolution correlates with the MES performance.

## 6.2 MATERIALS AND METHODS

### 6.2.1 MES reactors set-up

Two identical two-chambered cells built in a modified 500 mL Duran® bottle were constructed and named MES1 and MES2. The anodic chamber consisted of a 20 mL semi-cylindrical glass chamber containing a platinum counter electrode (CE) placed in the center of the bottle, and opened to the atmosphere through a multi-connection plastic cap. The rest of the bottle (Effective volume: 450 mL) acted as the cathodic chamber in which a cylindrical graphite felt electrode (Apparent area: 176 cm<sup>2</sup>; Thickness: 0.5cm) was fixed to the bottle wall and connected to the outside through a sewn titanium wire. A pretreated cationic exchange membrane (Membranes International Inc., USA) was used to separate both compartments. All electrode assemblies showed a contact resistance <2 Ω. Electrodes were pre-treated by subsequent immersion in nitric acid 1 M, acetone 1 M and ethanol 1 M for 24 h each to improve wettability and avoid impurities [18]. Electrodes were extensively rinsed in demineralized water to ensure absence of chemicals from the pretreatment. Both cells worked as replicates on a three-electrode configuration with an Ag/AgCl reference electrode (0.20 vs. SHE; the reference electrode was checked at the beginning of every batch cycle). The culture medium was continuously stirred using a magnetic stirrer at 200 rpm and maintained at 25°C.

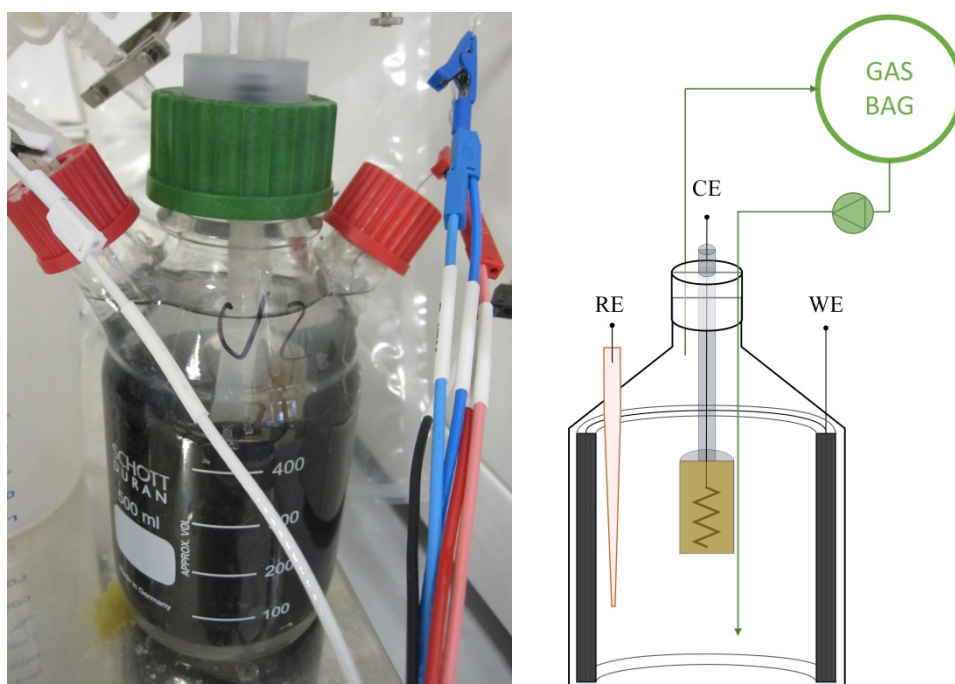


**Figure 6.1:** Image and diagram of reactor set-up. CE: Counter electrode; RE: Reference electrode; WE: Working electrode.

### 6.2.2 Influent and inoculum

The catholyte consisted of a synthetic nutrient solution with the following composition (in  $\text{g}\cdot\text{L}^{-1}$ ): 0.87  $\text{K}_2\text{HPO}_4$ ; 0.68  $\text{KH}_2\text{PO}_4$ ; 0.25  $\text{NH}_4\text{Cl}$ ; 0.1  $\text{KCl}$ ; 0.04  $\text{CaCl}_2\cdot 2\text{H}_2\text{O}$ ; 0.45  $\text{MgCl}_2\cdot 6\text{H}_2\text{O}$  and 10 ml per liter of a trace mineral solution containing (in  $\text{g}\cdot\text{L}^{-1}$ ): 6  $\text{MgSO}_4\cdot 7\text{H}_2\text{O}$ , 1  $\text{MnSO}_4\cdot \text{H}_2\text{O}$ , 2  $\text{NaCl}$ , 0.2  $\text{FeSO}_4\cdot 7\text{H}_2\text{O}$ , 0.3  $\text{CoCl}_2\cdot 6\text{H}_2\text{O}$ , 0.2  $\text{CaCl}_2\cdot 2\text{H}_2\text{O}$ , 0.17  $\text{ZnCl}_2$ , 0.02 of  $\text{CuSO}_4\cdot 5\text{H}_2\text{O}$ , 0.02  $\text{H}_3\text{BO}_3$ , 0.04  $\text{Na}_2\text{MoO}_4\cdot 2\text{H}_2\text{O}$ , 0.06  $\text{NiCl}_2\cdot 6\text{H}_2\text{O}$ , 0.6 mg  $\text{Na}_2\text{SeO}_4$  and 0.8 mg  $\text{Na}_2\text{WO}_4\cdot 2\text{H}_2\text{O}$  as described in [18]. The anolyte consisted of 0.1 M phosphate buffer (pH 7.8).

An enriched inoculum (EI) was used as the direct source of microorganisms for the biocathodes. An anaerobic culture enrichment procedure from Bajracharya et al. [13] was strictly followed, starting from an initial anaerobic sludge (IS) retrieved from a running continuous anaerobic digester operating in the local wastewater treatment plant (Leon city WWTP, 350.000 i.e.). An initial 20% inoculum / 80% culture medium mixture was used as the initial inoculation feed.

### 6.2.3 Experimental procedure

Both cells were inoculated and operated in the potentiostatic mode (-1 V vs. Ag / AgCl) until clear responses were found in terms of current consumption and acetic acid production. After acclimation, acetic acid titer was lowered to around 1000 mg·L<sup>-1</sup> by replacing part of the culture medium, as a starting point of the first and subsequent batches. This allowed to maintain conditions as constant as possible, and to avoid changes that could hide differences between batches. After each batch, part of the culture medium was replaced to maintain the same initial conditions in terms of titer throughout the whole experiment. Two sets of 3 batches each were planned in order to assess the effect of CO<sub>2</sub> recirculation in the system. In the first set, 500 mL of CO<sub>2</sub> was fed into the headspace of the reactor, while 600 mL of CO<sub>2</sub> was fed in the second set and continuously recirculated from the headspace to the bottom of the bottle at 120 mL·h<sup>-1</sup>.

### 6.2.4 Measurements and analytical techniques

Gas samples were collected from the headspace at the beginning and end of each cycle and analyzed immediately afterwards. These samples were collected with a GASTIGHT 1001 (Hamilton Co., GR, Switzerland) syringe from a built-in rubber septum.

Regarding liquid samples, Volatile fatty acids (VFAs) were measured using a gas chromatograph (Varian CP3800 GC) equipped with a Nukol capillary column and a thermal conductivity detector (30 m × 0.25 mm × 0.25 μm) from Supelco, using He as the mobile phase, as described by [19] (detection limit 5 mg·L<sup>-1</sup>). pH was determined using APHA standard methodologies, as described by [20]. pH was determined with a HACH 5014T probe in a CRISON 20+ pH meter. Electrochemical tests were performed using a potentiostat (VMP3, Biologic Science Instruments, France).

### 6.2.5 Microbial community analysis

Genomic DNA was extracted from the IS and from the EI which was used as an inoculum for the reactor biocathodes. Samples from the biofilm (B) and supernatant (S) in the reactors were also taken from both reactors (MES1 and MES2) at 49 and 92 days of operation. Therefore, for a better understanding, samples are named using the code

ReactorName\_SampleType\_Days. Microbiology samples in this experiment correspond to MES1\_B\_49d, MES1\_B\_92d, MES2\_S\_49d and MES1\_S\_92d for MES1; and MES2\_B\_49d, MES2\_B\_92d, MES2\_S\_49d and MES2\_S\_92d for MES2.

A thin piece of electrode (2 mm x 2 mm) was removed using a stainless steel surgical blade in sterile conditions in a laminar flow cabinet and total DNA was extracted from the biofilm. The DNA was extracted with the Soil DNA Isolation Plus Kit<sup>®</sup> (Norgen Biotek Corp.) following the manufacturer's instructions.

DNA was used for high throughput sequencing of *16S-rRNA* gene-based massive libraries for Eubacterial populations, using the primer set 27Fmod (5'-AGRGTTCGATCMTGGCTCAG-3') / 519R modBio (5'-GTNTTACNGCGGCKGCTG-3') [21]. The obtained DNA reads were compiled in FASTq files for further bioinformatics processing and operational taxonomic units (OTUs) were then taxonomically classified using the Ribosomal Database Project (<http://rdp.cme.msu.edu>).

Venn diagram analysis was performed using Mothur and Venny software. The XLSTAT package for multivariate analysis was used for performing a correspondence analysis on the OTU abundance matrix. The obtained samples and OTU scores were depicted in a 2D biplot, which represents the phylogenetic assignment of the predominant OTUs (relative abundance >0.5%).

## 6.3 RESULTS

### 6.3.1 CO<sub>2</sub> recirculation effect on MES

The two MES reactors (MES1 and MES2) were inoculated with an enriched inoculum as described in section 2.2. They were initially operated with a static CO<sub>2</sub> feed (i.e. the CO<sub>2</sub> fed was not recirculated) and once reactors developed a clear and stable response in terms of current and acetate production, the experimental period began. During this period, two sets of 3 batch cycles each were performed to assess the effect of headspace gas recirculation. The first set, in which the static feed was continued, comprised 21 days (from day 49 to 70). During the second set (from day 71 to 92) both reactors were provided with a recirculation loop to continuously recirculate the headspace gas.

Figure 6.2 represents a set of polarization curves obtained at different stages during both the acclimation and experimental periods, and shows how biocatalytic activity evolves over time. The biocathodes began to display a moderate current rise at about one month after inoculation (day 31) and consistently increased with time. This trend can be easily noticed at  $-0.8\text{V}$  vs.  $\text{Ag}/\text{AgCl}$ , becoming more apparent at  $-1\text{V}$  vs.  $\text{Ag}/\text{AgCl}$ , and being even higher at the end of the experiment (day 92) when  $\text{CO}_2$  was being bubbled into the culture medium. Although abiotic hydrogen could be theoretically produced at  $1\text{V}$  vs.  $\text{Ag}/\text{AgCl}$  on graphite electrodes, this can be ruled out due to the negligible currents registered with the graphite electrode before inoculation (day 0).

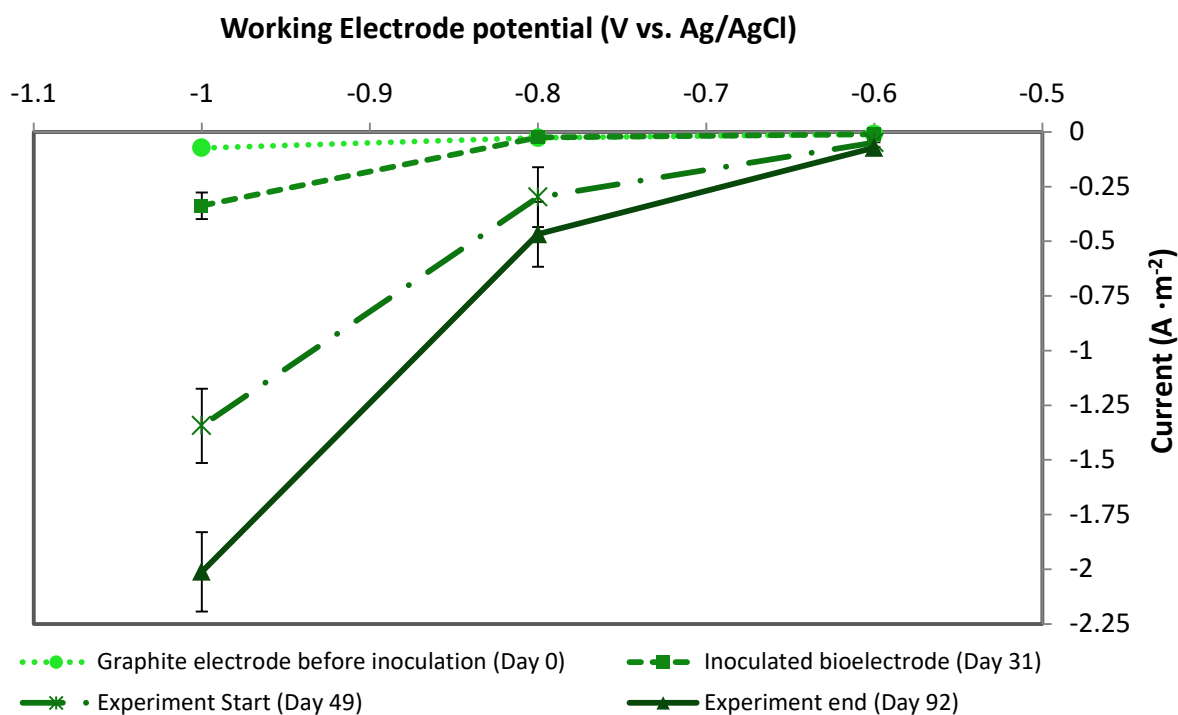


**Figure 6.2:** Evolution of polarization curve currents along the experiment.

Figure 6.3 represents the evolution of the two reactors during the six batch cycles (experimental period) in terms of acetate and current production. Both reactors showed good replicability, developing similar performances during the entire experimental period (separate data for MES1 and MES2 are shown in figure S6.1 and S6.2, section S6.1, appendix III). Furthermore, they displayed high selectivity to acetate

(>95%), only yielding other VFAs or alcohols at trace concentrations below the quantification limit.

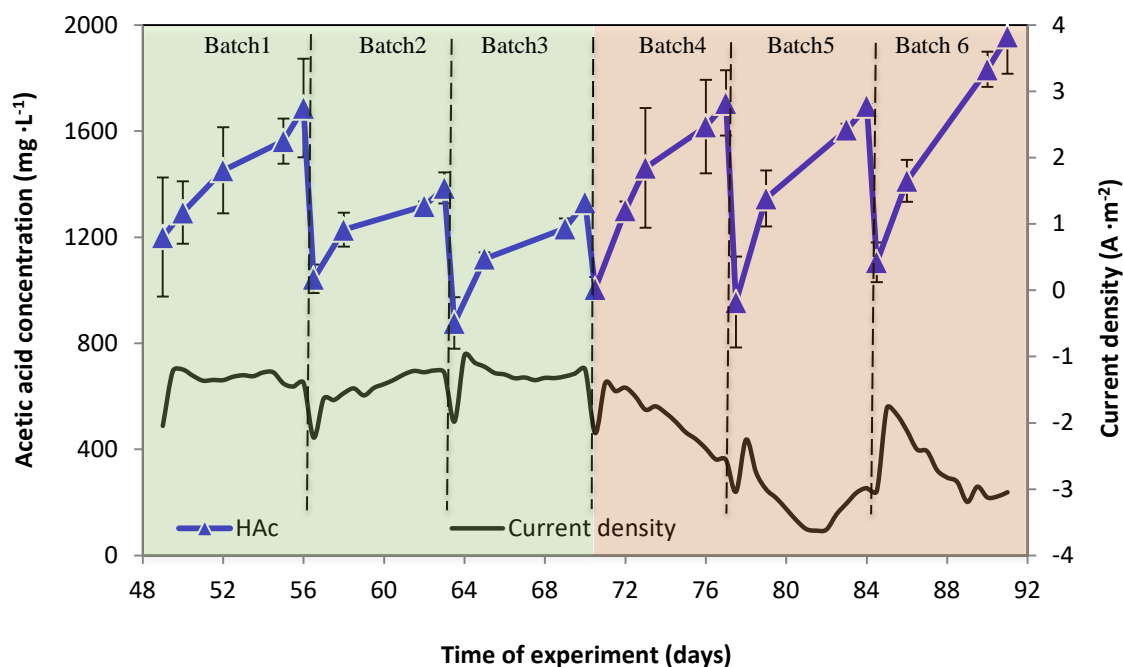


**Figure 6.3:** Acetic acid concentration along the experimental period (Days 49-92). Current density is also shown along the whole period. The green area represents the 3 batch cycles with no gas headspace recirculation, while orange covers the 3 batches with recirculation.

The average acetate production rate during the first period (with no recirculation) was  $61 \text{ mg}\cdot\text{L}^{-1}\cdot\text{d}^{-1}$ , reaching peak values of  $161 \text{ mg}\cdot\text{L}^{-1}\cdot\text{d}^{-1}$  and a maximum titer of  $1687 \text{ mg}\cdot\text{L}^{-1}$  (table 6.1). Once the recirculation loop was implemented, the average production rate increased to  $109 \text{ mg}\cdot\text{L}^{-1}\cdot\text{d}^{-1}$  reaching a peak value of  $261 \text{ mg}\cdot\text{L}^{-1}\cdot\text{d}^{-1}$ , and a maximum titer of  $1957 \text{ mg}\cdot\text{L}^{-1}$ . This corresponded to an increase of 44% in the average acetate production, 62% in the peak and 16% in the maximum titer.



**Table 6.1:** Acetic acid production summary, including averages for both MES and standard deviation.

Acetic acid production						
	Batch	MES1 Rate (mg·L <sup>-1</sup> ·d <sup>-1</sup> )	MES2 Rate (mg·L <sup>-1</sup> ·d <sup>-1</sup> )	MES average (mg·L <sup>-1</sup> ·d <sup>-1</sup> )	Std. dev. (mg·L <sup>-1</sup> ·d <sup>-1</sup> )	Period average (mg·L <sup>-1</sup> ·d <sup>-1</sup> )
Without recirculation	1	73.5	65.5	69.5	5.6	61.1
	2	49.5	48.4	48.9	0.7	
	3	55.3	74.7	65.0	13.8	
With recirculation	4	83.1	117.1	100.2	24.1	109.1
	5	122.0	89.1	105.6	23.3	
	6	115.0	128.25	121.6	9.4	

Table 6.2 summarizes CO<sub>2</sub> conversion, product formation and the corresponding cathodic efficiencies for each batch cycle. CO<sub>2</sub> conversion was found to be above 80% in all cases. Cathodic efficiencies were not as consistent as conversion values, showing a certain fluctuation in the range from 57–91%.

**Table 6.2:** Carbon balance and cathodic efficiency. Averages between both MES replicate reactors (MES1 and MES2) are shown.

	Batch	CO <sub>2</sub> input (mol C)	CO <sub>2</sub> output (mol C)	CO <sub>2</sub> consumption (%)	Acetate production (mol C)	Transferred charge (C)	Cathodic efficiency (%)
Without recirculation	1	0.022	0.006	98%	0.016	14230	89.8%
	2	0.022	0.008	81%	0.011	15670	57.4%
	3	0.022	0.006	93%	0.015	13790	86.7%
With recirculation	4	0.027	0.001	90%	0.023	20320	90.6%
	5	0.027	0.000	93%	0.025	33500	57.8%
	6	0.027	0.000	106%	0.028	28480	78.5%

### 6.3.2 Microbial communities involved in the process

The two MES reactors (MES1 and MES2) were inoculated with an enriched inoculum (EI) coming from anaerobic sludge (IS). Samples from EI and IS, along with samples from the biofilm (B) and supernatant (S), were taken from both reactors (MES1 and MES2) at 49 and 92 days of operation. The microbial communities of the six samples were compared using Principal Component Analysis (PCA), to get an overview of the global populations dynamics throughout the experiment based on the relative abundance of the OTU matrix (figure 6.4). Each point of the PCA plot represents a sample, and a closer distance between two points indicates smaller differences between the two microbial communities. A notable shift is observed after the enrichment procedure of the IS. This change should be attributed to enrichment in homoacetogenic microorganisms (as it is the objective of the enrichment), and death of others that were originally adapted to anaerobic digestion and are highly disfavored to the enrichment conditions. It is important to note that these enriched homoacetogenic microorganisms are not necessarily electroactive, so it is expected that the enriched population still shifts when introduced to a cell with a set potential as a result of changing of growth conditions. This is represented in figure 6.4 by a wide distance between EI and MES samples. The results also indicate that the EI and samples from the reactor were distinctively clustered based on operational days: MES\_B\_49d and MES\_S\_49d from MES\_B\_92d and MES\_S\_92d. It should also be indicated that there is a clear difference from the population of the biofilm compared to those of the supernatant at stage 92d (figure 6.4). Overall, PCA results confirmed that there has been an evolution of the microbial composition through the experiment, meaning that the biofilm also phylogenetically changed.

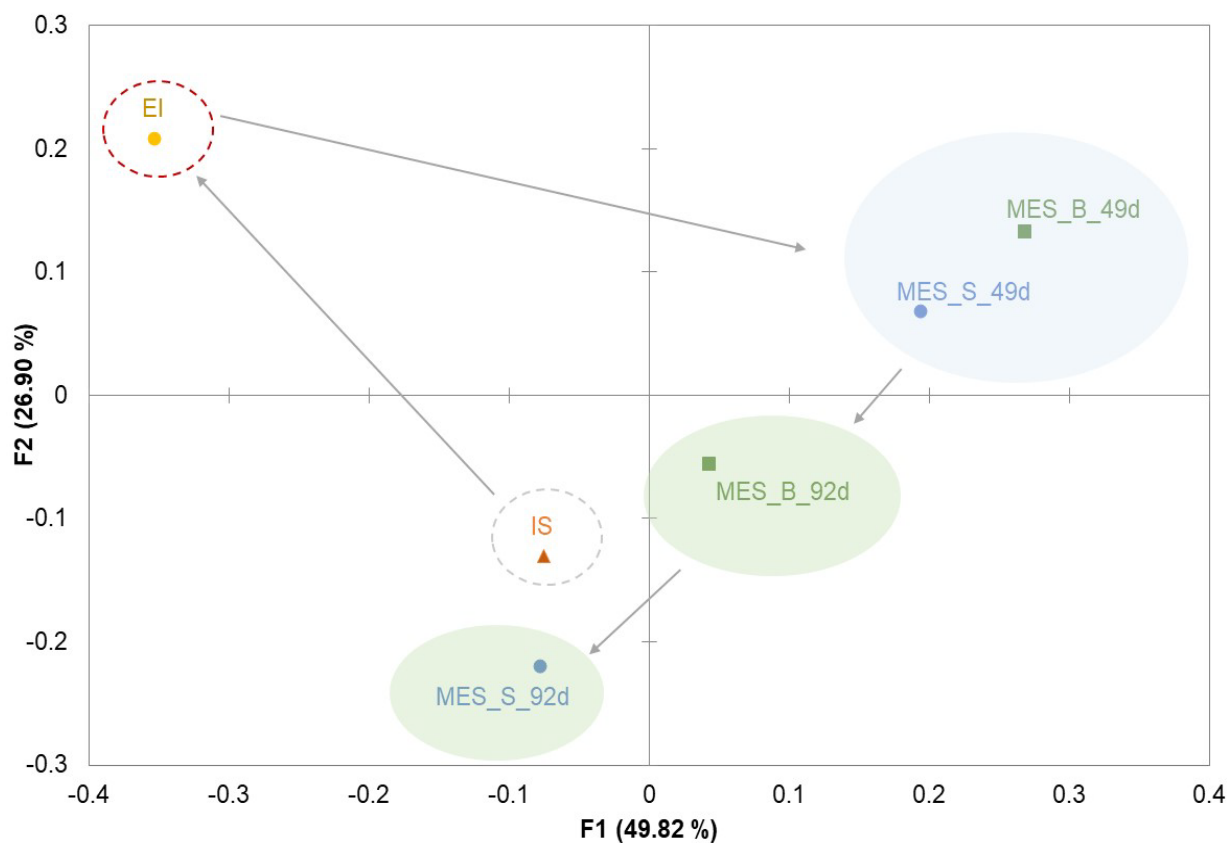


**Figure 6.4:** Principal Component Analysis (PCA) of Eubacterial communities based on OTUs matrix. Microbial communities from the initial sludge (IS), enriched inoculum (EI), and samples from biofilm (B) and supernatant (S) along the experiment.

The enrichment procedure (carried out according to Bajracharya et al. [13]) proved to be satisfactory, as the number of sequences identified was reduced from 67,168 in the IS to 24,387 in the EI; in total, 213 OTUs were found in the EI compared to 1690 in the IS (table S1, appendix III), indicating that the richness was considerably lower in the EI than in the IS. The observed OTUs are eight times lower in EI compared to the IS (figure S6.3, appendix III). Moreover, the enrichment was evident, as 94.0% of the 69 OTUs exclusively present in the EI are composed of only 5 OTUs identified as *Bacillaceae*, *Clostridiaceae*, *Sporolactobacillaceae* and *Peptostreptococcaceae* belonging to Firmicutes, and *Pseudomonadaceae* belonging to *Gammaproteobacteria* (figure 6.5). The main homoacetogenic family is *Clostridiaceae*, although *Peptostreptococcaceae* contains genera (as *Peptostreptococcus*) which have also been described as homoacetogenic bacteria. In contrast, the population is much less specific

in the IS (figure 6.5 and figure S6.3 (appendix III)), presenting high richness and diversity, and not finding any member that is predominant over the others.

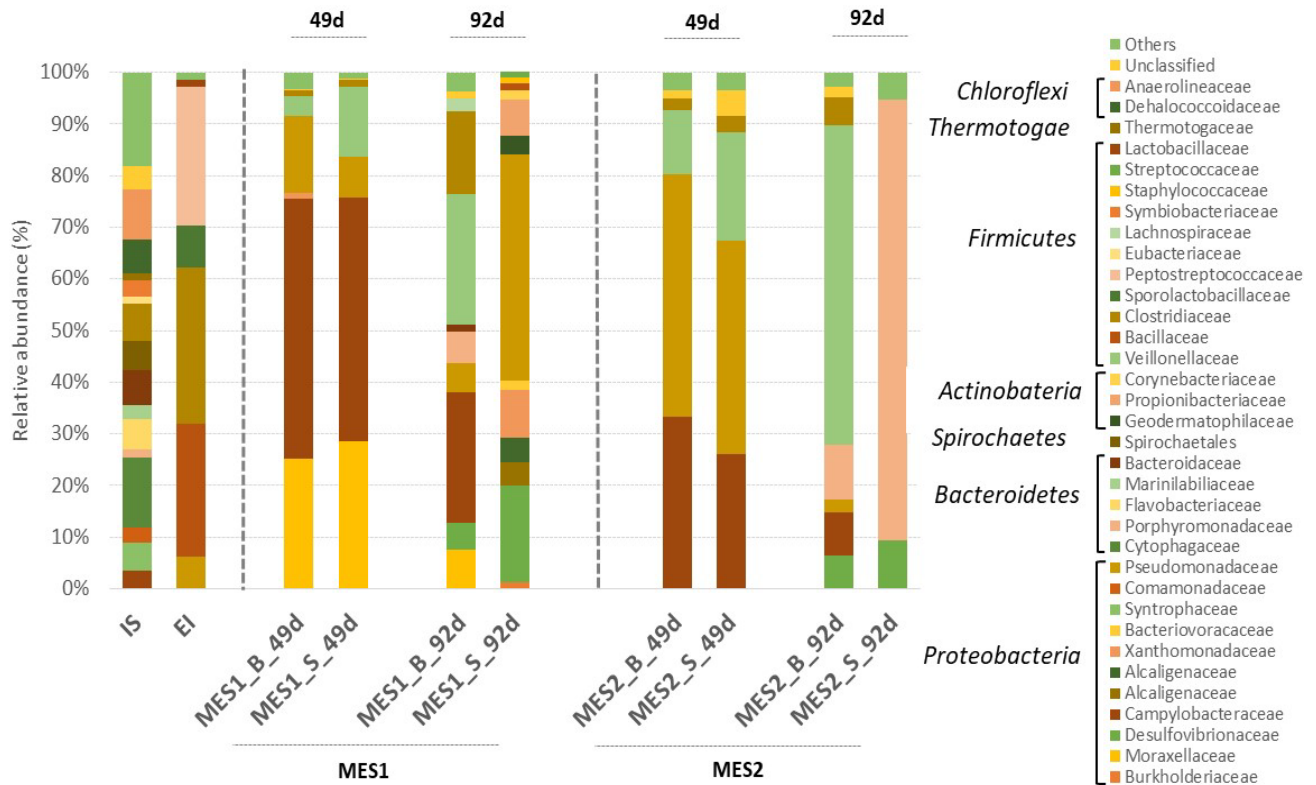


**Figure 6.5:** Taxonomic classification of Eubacterial communities at family levels and the phyla to which these families belong to.

After inoculation and 49d under acclimation conditions, which correspond to the conditions of the first 3 experimental batches (without recirculation, table 6.1), the biofilms of both MES were mainly composed of five families (figure 6.5), each represented by a main genus, *Campylobacteraceae* (*Sulfurospirillum*), *Pseudomonadaceae* (*Pseudomonas*) and *Moraxellaceae* (*Acinetobacter*) belonging to *Proteobacteria* phyla, and *Veillonellaceae* (*Sporomusa*) and *Clostridiaceae* (*Clostridium*) belonging to *Firmicutes*.

However, both biofilms were phylogenetically different after 92d of operation, which corresponds to the last three experimental batches (with recirculation, table 6.1; see also figure 6.4). Although it is true that the main groups found at 49d are still identified at 92d, other microorganisms that are usually found in MES systems, such as

*Porphyromonadaceae* and *Desulfovibrionadaceae*, were also identified. The two main families that were enriched from the first period (49d) to the last one (92d) were *Veillonellaceae*, exclusively composed of *Sporomusa*, and *Clostridiaceae*, mostly composed of *Clostridium*. These two families, which have been identified as acetogenic bacteria with bioelectrochemical activity [5], accounted for 41.5% and 67.5% of the total community attached to the biofilm and played an important role in acetate production within our system.

A Venn diagram was built for both initial and final biofilm samples, and for both MES1 and MES2 (figure 6.6) in order to identify the core microbiome attached onto the biofilm. Providing that the source of microorganisms is the same for all of the represented samples, some microorganisms that are really not favored in our experimental conditions might be present at trace proportions. For a screening of those irrelevant microorganisms at very low proportions, only OTUs with a contribution of over 0.1% to the relative abundance are present in the Venn diagram.

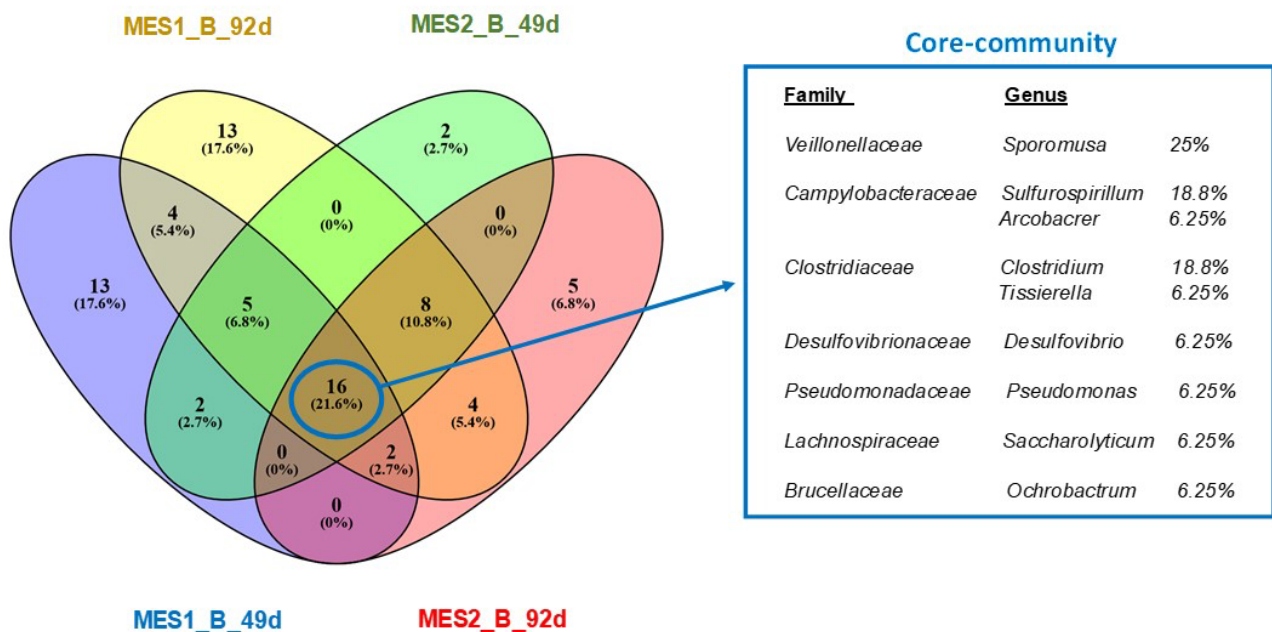


**Figure 6.6:** Overlap of the four biofilm communities and the taxonomic identities of the shared OTUs.

The results showed that 16 common OTUs (21.6% of the total OTUs) were shared by all biofilm samples over time. The taxonomic identities of these shared OTUs are represented in figure 6.6. This analysis shows that 6 genera composed the core community, represented mainly by *Sporomusa*, *Sulfurospirillum* and *Clostridium*,

followed by important microorganisms in MES systems like *Desulfovibrio*, *Arcobacter*, *Pseudomonas* and *Ochrobactrum*, among others (figure 6.6). This core community is composed of important genera that are usually present in acetogenic MES systems, which are most likely responsible for the conversion of CO<sub>2</sub> into acetate.

At 49d, the supernatant community is composed of the same families that are present in the biofilms. Nevertheless, this does not happen at the end of the experiment (92d) when the biofilm and supernatant populations considerably differ. The number of sequences identified in this period was between 4- and 7-fold increased in the biofilm compared to the supernatant, which indicates that the population attached onto the biofilm over time has a more important role in MES performance. The Venn diagram for the supernatant samples (See figure S6.4, section S2, appendix III) shows that only 2 OTUs are common in the microbial communities present at the beginning and end of the experiment. Interestingly, these two OTUs, which only account for 2.1%, correspond to *Pseudomonas* and *Desulfovibrio*; both also belong to the core microbiome found in the biofilm, suggesting their importance in MES systems.

#### 6.4 DISCUSSION

The inoculum enrichment succeeded in generating a stable, efficient and selective biofilm on the surface of the bioelectrodes, promoting the proliferation of certain families (both in the biofilm and the supernatant) such as *Clostridiaceae* and *Pseudomonadaceae*. These families and others groups have an important role in acetic acid production [22], favoring optimal conditions for the subsequent development of an acetogenic microbiome. Both replicate cells developed a similar electrical behavior during the start-up and acclimation period, reaching the starting point of the batch tests (day 49 of experiment), in a strongly repetitive state. This is supported by a low deviation between them in terms of the current consumption and product generation (figure 6.3). This trend (repetitive current and product generation) continued during the first three batch cycles (days 49 to 70); in addition, both MES showed little evolution between cycles. This behavior can be expected from a well-established biofilm enriched in important families that can undergo the proposed process: early colonizers in both biofilm and supernatant were dominated by *Arcobacter*, *Acinetobacter*, *Pseudomonas* and *Sulfurospirillum* [23] with a high relative abundance, which are responsible for the

current consumption from the first three batches. However, during these 3 batches, acetate production rates were below those reported by other researchers in MES operating under similar conditions [12,13,24,25]. Still, in the referred studies, the availability of CO<sub>2</sub> to acetogenic bacteria was improved by sparging an excess amount of CO<sub>2</sub> through the culture medium, or adding an excess amount of bicarbonate as feed. However, these methods might lead to an inefficient use of CO<sub>2</sub>. For instance, in the sparging method, most of the CO<sub>2</sub> is lost to the atmosphere, while pH must be continuously adjusted if bicarbonate is used as the substrate, and it is not applicable for real exhaust gas streams.

Our approach to solving this CO<sub>2</sub> availability issue without wasting an important part of our substrate, and therefore fixing the maximum of the whole CO<sub>2</sub> that is put in place, is to continuously recirculate through the culture medium the gas present in the headspace. This approach, used in the last 3 cycles (days 70-92), proved to be successful, leading to a 44% improvement in current consumption and product formation (tables 6.1 and 6.2). It must be highlighted that hydrogen, which is a reaction intermediate in this process, can also be recirculated along with the CO<sub>2</sub> throughout the experimental batch. As hydrogen is even less soluble than CO<sub>2</sub>, this might have also contributed to the reported improvement.

The recirculation of the gas from the headspace also seemed to have an effect on the cathodic microbial communities. At the end of the experiment (day 92), and after three batch cycles with recirculation, *Sporomusa* was identified as the most important family; some of these OTU sequences present 99% homology with *Sporomusa sphaeroides*, a homoacetogen which has been shown to be able to produce acetic acid, reducing inorganic carbon to the sole carbon source [8]. Although it is true that these OTUs were also present prior to recirculation (day 49), the relative abundance across biofilm showed that this genus increased from 4–12% without recirculation up to 25–59% with recirculation, which could explain the improvement in acetate production. Other OTUs that include members of *Clostridium* and *Desulfovibrio* were also enriched after implementing the recirculation. Both genera, described as electroactive species [8,26], might be responsible for the improved current density. Furthermore, the presence of *Desulfovibrio*, which is able to produce hydrogen on biocathodes [27] might enhance the availability of hydrogen to homoacetogens, like *Clostridium* and *Sporomusa*, thus

helping to explain improved performance. While both of the mentioned acetogens, *Clostridium* and *Sporomusa*, were enriched on the surface of electrodes, *Desulfovibrio* was identified at day 92 in the biofilm as well as in the supernatant at a slightly higher abundance. This result was in agreement with other works [28], where *Desulfovibrio* was present in a high relative abundance as a planktonic member, although the same authors also identified this genus on their enriched electrodes in previous works [29]. *Desulfovibrio* has been mainly described as a biological hydrogen production [27], and their presence with *Pseudomonas*, both belonging to *Proteobacteria* phylum, has been described in other MES systems [30]. Besides, it is well known as a shuttle, producing bacteria; therefore, its role in the biofilm, supernatant and bioelectrochemical systems in general is relevant [31]. The correlation of genera from OTUs showing both acetogenic and bioelectrochemical activity, with an improvement in acetate production (44% improvement), serves to corroborate the importance of this mixture of populations which reached 34–67% of the total community attached to the biofilm.

Despite changes in the microbial community across the experiment due to the different conditions applied, a core microbiome can be found, represented by a few dominant members as *Sporomusa*, *Sulfurospirillum*, *Arcobacter*, *Clostridium*, *Tissierella*, *Desulfovibrio*, *Pseudomonas*, *Sacharolyticum* and *Ochrobactrum*. These core communities are consistently associated with a microbial electrosynthesis biofilm that is well developed and commonly found in MES systems [17]. Regarding the supernatant population, it has been highlighted that the two common OTUs across the experiment belonged to *Pseudomonas* and *Desulfovibrio*, which are also identified within the biofilm core microbiome. This fact revealed the importance of these microorganisms in the acetogenic performance of the whole MES.

To sum up, it can be stated that our recirculation system improves system kinetics and therefore the performance of the previous non-recirculated one. Although it still does not reach the maximum production rates reported by other authors [13,24], this system is capable of consistently fixing around 100% of the CO<sub>2</sub> fed in an efficient way, showing cathodic efficiencies of 57–91%.



## 6.5 CONCLUSIONS

The inoculum enrichment procedure proved to be effective in developing a homoacetogenic community that is capable of producing a stable, replicable and selective biofilm. This biofilm was mainly composed of a core microbiome whose predominant genera, *Sporomusa*, *Sulfurospirillum*, *Arcobacter*, *Desulfovibrio*, *Pseudomonas* and *Clostridium*, are usually found in acetogenic biocathodes. The correlation of these phylotypes with acetate production and MES performance suggests the important role that this mixed community played across the experiment (e.g. a higher relative abundance of *Sporomusa* was found in correlation with higher acetate production). By continuously recirculating the gas headspace, it was possible to increase acetate production by 44%, increasing the acetate production rate up to  $261 \text{ mg HAc}\cdot\text{L}^{-1}\cdot\text{d}^{-1}$  (maximum titer:  $1957 \text{ mg}\cdot\text{L}^{-1}$ ). Cathodic efficiencies over 50% were found during the whole experiment, increasing to 91% with gas headspace recirculation. In addition, up to 100% of the  $\text{CO}_2$  fed was consumed, which represents up to  $171 \text{ ml CO}_2\cdot\text{L}^{-1}\cdot\text{d}^{-1}$ .

## 6.6 BIBLIOGRAPHY

- [1] R.J. Pearson, M.D. Eisaman, J.W.G. Turner, P.P. Edwards, Z. Jiang, V.L. Kuznetsov, K.A. Littau, L. Di Marco, S.R.G. Taylor, Energy Storage via Carbon-Neutral Fuels Made From CO<sub>2</sub>, Water, and Renewable Energy, *Proceedings of the IEEE*. 100 (2012) 440–460.
- [2] Z.A. Manan, W.N.R. Mohd Nawawi, S.R. Wan Alwi, J.J. Klemeš, Advances in Process Integration research for CO<sub>2</sub> emission reduction – A review, *Journal of Cleaner Production*. 167 (2017) 1–13. doi:10.1016/J.JCLEPRO.2017.08.138.
- [3] A. Otto, T. Grube, S. Schiebahn, D. Stolten, Closing the loop: captured CO<sub>2</sub> as a feedstock in the chemical industry, *Energy & Environmental Science*. 8 (2015) 3283–3297. doi:10.1039/C5EE02591E.
- [4] I.S. Thakur, M. Kumar, S.J. Varjani, Y. Wu, E. Gnansounou, S. Ravindran, Sequestration and utilization of carbon dioxide by chemical and biological methods for biofuels and biomaterials by chemoautotrophs: Opportunities and challenges, *Bioresource Technology*. 256 (2018) 478–490. doi:10.1016/J.BIORTECH.2018.02.039.
- [5] P.L. Tremblay, T. Zhang, Electrifying microbes for the production of chemicals, *Front Microbiol.* (2015).
- [6] K. Rabaey, R.A. Rozendal, Microbial electrosynthesis—revisiting the electrical route for microbial production, *Nature Reviews Microbiology*. 8 (2010) 706–716.
- [7] S. Bajracharya, S. Srikanth, G. Mohanakrishna, R. Zacharia, D.P. Strik, D. Pant, Biotransformation of carbon dioxide in bioelectrochemical systems: State of the art and future prospects, *Journal of Power Sources*. 356 (2017) 256–273. doi:10.1016/j.jpowsour.2017.04.024.
- [8] K.P. Nevin, S.A. Hensley, A.E. Franks, Z.M. Summers, J. Ou, T.L. Woodard, O.L. Snoeyenbos-West, D.R. Lovley, Electrosynthesis of organic compounds from carbon dioxide is catalyzed by a diversity of acetogenic microorganisms., *Applied and Environmental Microbiology*. 77 (2011) 2882–6. doi:10.1128/AEM.02642-10.

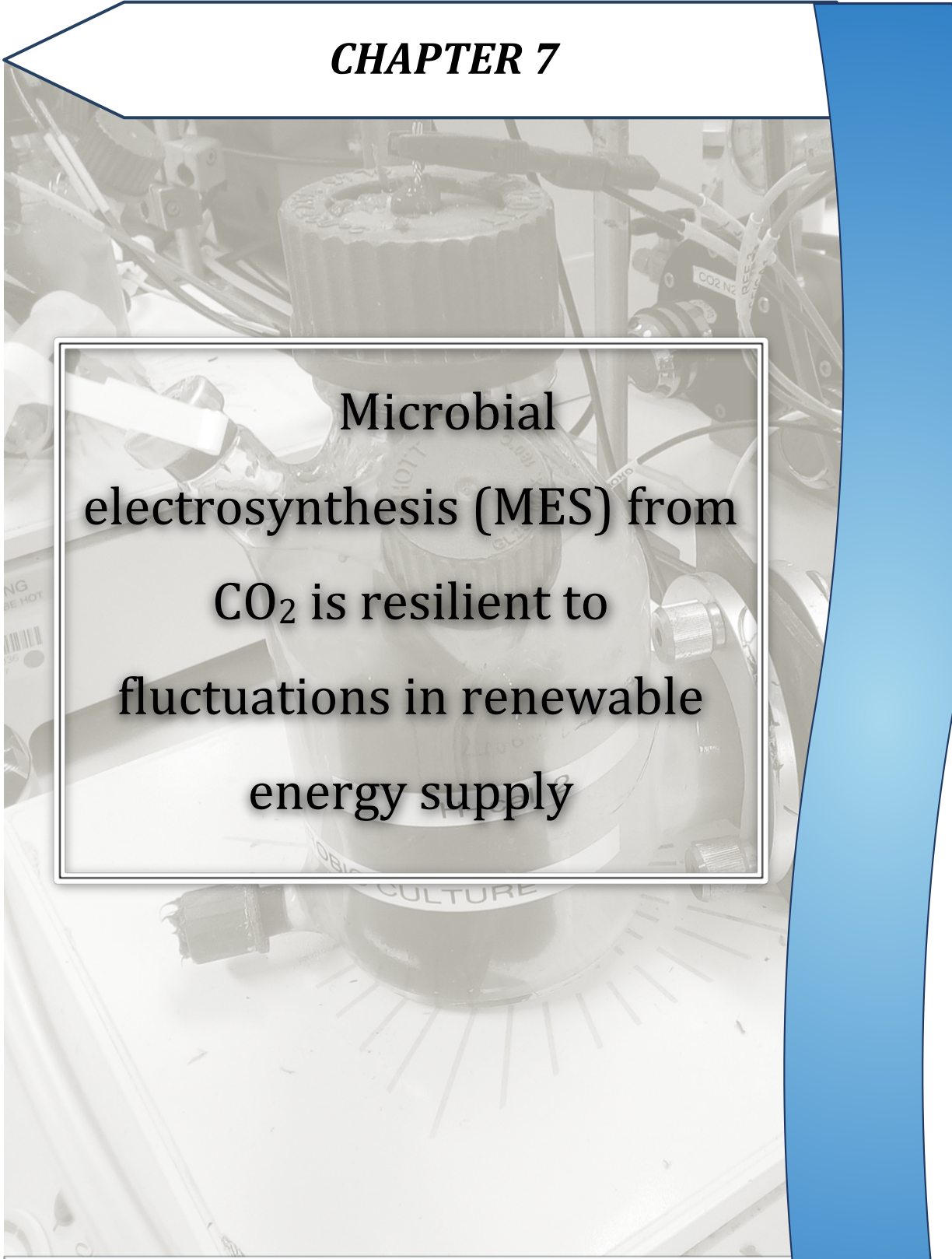
- 
- [9] T. Jafary, W.R.W. Daud, M. Ghasemi, B.H. Kim, J. Md Jahim, M. Ismail, S.S. Lim, Biocathode in microbial electrolysis cell; present status and future prospects, *Renewable and Sustainable Energy Reviews*. 47 (2015) 23–33. doi:10.1016/j.rser.2015.03.003.
- [10] H.D. May, P.J. Evans, E. V LaBelle, The bioelectrosynthesis of acetate, *Current Opinion in Biotechnology*. 42 (2016) 225–233. doi:10.1016/j.copbio.2016.09.004.
- [11] N. Aryal, P.-L. Tremblay, D.M. Lizak, T. Zhang, Performance of different *Sporomusa* species for the microbial electrosynthesis of acetate from carbon dioxide, *Bioresource Technology*. 233 (2017) 184–190. doi:10.1016/j.biortech.2017.02.128.
- [12] S. Bajracharya, A. ter Heijne, X. Dominguez Benetton, K. Vanbroekhoven, C.J.N. Buisman, D.P.B.T.B. Strik, D. Pant, Carbon dioxide reduction by mixed and pure cultures in microbial electrosynthesis using an assembly of graphite felt and stainless steel as a cathode, *Bioresource Technology*. 195 (2015) 14–24. doi:10.1016/j.biortech.2015.05.081.
- [13] S. Bajracharya, R. Yuliasni, K. Vanbroekhoven, C.J.N. Buisman, D.P.B.T.B. Strik, D. Pant, Long-term operation of microbial electrosynthesis cell reducing CO<sub>2</sub> to multi-carbon chemicals with a mixed culture avoiding methanogenesis, *Bioelectrochemistry*. 113 (2017) 26–34. doi:10.1016/j.bioelechem.2016.09.001.
- [14] J. Desloover, J.B.A. Arends, T. Hennebel, K. Rabaey, Operational and technical considerations for microbial electrosynthesis, *Biochemical Society Transactions*. 40 (2012) 1233 LP-1238.
- [15] T. Krieg, J.A. Wood, K.-M. Mangold, D. Holtmann, Mass transport limitations in microbial fuel cells: Impact of flow configurations, *Biochemical Engineering Journal*. 138 (2018) 172–178. doi:10.1016/J.BEJ.2018.07.017.
- [16] E. Martin, O. Savadogo, S.R. Guiot, B. Tartakovsky, The influence of operational conditions on the performance of a microbial fuel cell seeded with mesophilic anaerobic sludge, *Biochemical Engineering Journal*. 51 (2010) 132–
-

139. doi:10.1016/J.BEJ.2010.06.006.
- [17] Z. Zaybak, J.M. Pisciotta, J.C. Tokash, B.E. Logan, Enhanced start-up of anaerobic facultatively autotrophic biocathodes in bioelectrochemical systems., *Journal of Biotechnology*. 168 (2013) 478–85. doi:10.1016/j.jbiotec.2013.10.001.
- [18] R. Mateos, A. Sotres, R.M. Alonso, A. Escapa, A. Morán, Impact of the start-up process on the microbial communities in biocathodes for electrosynthesis, *Bioelectrochemistry*. 121 (2018) 27–37. doi:10.1016/j.bioelechem.2018.01.002.
- [19] E.J. Martínez, M. V Gil, J.G. Rosas, R. Moreno, R. Mateos, A. Morán, X. Gómez, Application of thermal analysis for evaluating the digestion of microwave pre-treated sewage sludge, *Journal of Thermal Analysis and Calorimetry*. (2016). doi:10.1007/s10973-016-5460-4.
- [20] E.W. Rice, L. Bridgewater, A.P.H. Association, A.W.W. Association, W.E. Federation, *Standard Methods for the Examination of Water and Wastewater*, American Public Health Association, 2012.
- [21] T.R. Callaway, S.E. Dowd, R.D. Wolcott, Y. Sun, J.L. McReynolds, T.S. Edrington, J. a Byrd, R.C. Anderson, N. Krueger, D.J. Nisbet, Evaluation of the bacterial diversity in cecal contents of laying hens fed various molting diets by using bacterial tag-encoded FLX amplicon pyrosequencing., *Poultry Science*. 88 (2009) 298–302. doi:10.3382/ps.2008-00222.
- [22] R.G. Saratale, G.D. Saratale, A. Pugazhendhi, G. Zhen, G. Kumar, A. Kadier, P. Sivagurunathan, Microbiome involved in microbial electrochemical systems (MESs): A review, *Chemosphere*. 177 (2017) 176–188. doi:10.1016/J.CHEMOSPHERE.2017.02.143.
- [23] E. V. LaBelle, C.W. Marshall, J.A. Gilbert, H.D. May, Influence of acidic pH on hydrogen and acetate production by an electrosynthetic microbiome, *PLoS ONE*. 9 (2014) 1–10. doi:10.1371/journal.pone.0109935.
- [24] S. Gildemyn, K. Verbeeck, R. Slabbinck, S.J. Andersen, A. PrévotEAU, K. Rabaey, Integrated production, extraction, and concentration of acetic acid from CO<sub>2</sub> through microbial electrosynthesis, *Environmental Science & Technology*

- Letters. 2 (2015) 325–328.
- [25] L. Jourdin, T. Grieger, J. Monetti, V. Flexer, S. Freguia, Y. Lu, J. Chen, M. Romano, G.G. Wallace, J. Keller, High Acetic Acid Production Rate Obtained by Microbial Electrosynthesis from Carbon Dioxide, *Environmental Science and Technology*. 49 (2015) 13566–13574. doi:10.1021/acs.est.5b03821.
- [26] M.J. Cooney, E. Roschi, I.W. Marison, C. Comminellis, U. von Stockar, Physiologic studies with the sulfate-reducing bacterium *Desulfovibrio desulfuricans*: Evaluation for use in a biofuel cell, *Enzyme and Microbial Technology*. 18 (1996) 358–365. doi:10.1016/0141-0229(95)00132-8.
- [27] F. Aulenta, L. Catapano, L. Snip, M. Villano, M. Majone, Linking Bacterial Metabolism to Graphite Cathodes: Electrochemical Insights into the H<sub>2</sub>-Producing Capability of *Desulfovibrio* sp., *ChemSusChem*. 5 (2012) 1080–1085.
- [28] J.B.A. Arends, S.A. Patil, H. Roume, K. Rabaey, Continuous long-term electricity-driven bioproduction of carboxylates and isopropanol from CO<sub>2</sub> with a mixed microbial community, *Journal of CO<sub>2</sub> Utilization*. 20 (2017) 141–149. doi:10.1016/j.jcou.2017.04.014.
- [29] S.A. Patil, J.B.A. Arends, I. Vanwonterghem, J. Van Meerbergen, K. Guo, G.W. Tyson, K. Rabaey, Selective enrichment establishes a stable performing community for microbial electrosynthesis of acetate from CO<sub>2</sub>, *Environmental Science & Technology*. 49 (2015) 8833–8843.
- [30] A.R. Hari, K. Venkidusamy, K.P. Katuri, S. Bagchi, P.E. Saikaly, Temporal microbial community dynamics in microbial electrolysis cells--influence of acetate and propionate concentration, *Frontiers in Microbiology*. 8 (2017) 1371.
- [31] C. Koch, F. Harnisch, Is there a specific ecological niche for electroactive microorganisms?, *ChemElectroChem*. (2016).



## CHAPTER 7



Microbial  
electrosynthesis (MES) from  
CO<sub>2</sub> is resilient to  
fluctuations in renewable  
energy supply

*Chapter adapted from:*

Anzola, M.P., **Mateos, R.**, Sotres, A., Zaiat M., González E.R., Escapa, A., De Wever H. & Pant D. (2018) Microbial electro-synthesis (MES) from CO<sub>2</sub> is resilient to fluctuations in renewable energy supply. *Energy Conversion and Management.* (177) 272-279





## ABSTRACT

Microbial electrosynthesis (MES) allow CO<sub>2</sub> capture and utilization for the electricity-driven bioproduction of organics such as acetic acid. Such systems can be coupled to any renewable electricity supply, especially those derived from solar and wind energy. However, fluctuations or even absence of electricity may cause damages or changes in the microbial community, and/or affect the performance and robustness of MES. Therefore, the transformation of gaseous CO<sub>2</sub> into organic products in a MES was assessed continuously during 120 days of operation. Time-increasing power outages, from 4 h to 64 h, were applied in order to evaluate the effects of electric energy (current) absence on microbial community, organics formation, production rates and product accumulation. Acetic acid was the main product observed before and after the power outages. A maximum titer and production rate of 6965 mg·L<sup>-1</sup> and 516.2 mg·L<sup>-1</sup>·d<sup>-1</sup> (35.8 g·m<sup>-2</sup>·d<sup>-1</sup>) of acetic acid were observed, respectively. During the absence of power supply, it was observed that acetic acid is oxidized back to CO<sub>2</sub> which suggests microbial activity and/or pathway reversal. However, the electro-autotrophic activity recovered after the power gaps, and acetic acid production was restored after reconnecting the energy supply, reaching a current density of -25 A m<sup>-2</sup>. The microbial community of the biofilm responsible for this behavior was characterized by means of high-throughput sequencing, revealing that *Clostridium*, *Desulfovibrio* and *Sporomusa* accounted for 93% of the total community attached onto the cathodic biofilm. Such resilience of electrotrophic microorganisms reinforces the opportunity to couple bioelectrochemical systems to renewable energy, overcoming the eventual electrical power fluctuations.

## 7.1. INTRODUCTION

In the past few years, renewable energy production has sharply increased together with public concerns for the environment in the developed world [1]. This increasing amount of installed renewable power usually produces energy surplus that can be used, stored or lost. Some alternatives such as batteries [2], water pumping storage [3] or hydrogen production by water splitting [4] have been proposed for the surplus electricity exploitation [5]. Recently, using excess electricity to convert CO<sub>2</sub> into organic chemicals and fuels has come up as a novel alternative for off-peak electrical overproduction, in which electrical energy is stored in the form of chemical energy [6,7]. MES is a recent technology, an offshoot of conventional bioelectrochemical systems (BESs) used for wastewater treatment and energy recovery, proposed in 2010 [8]. This technology is able to produce chemicals such as volatile fatty acids (VFAs) and/or alcohols from the bioelectrochemical reduction of CO<sub>2</sub> [9]. In this conversion approach, certain kinds of microorganisms can reduce CO<sub>2</sub> using a solid electrode (cathode), which besides to be electron donor for their electroautotrophic metabolism also serves as growth surface for the biofilm [6,10]. This systems offer a dual advantage, since excess of electrical energy can be stored into chemicals while CO<sub>2</sub> can be removed from the atmosphere or directly captured from heavy CO<sub>2</sub> sources [11]. This fact makes MES an environmental-friendly technology helping to mitigate greenhouse gas emissions in bulk atmosphere or generation source.

Therefore, MES seem to be an ideal option for the combined purpose of energy storage and CO<sub>2</sub> utilization, which has been purposed as a promising novel alternative for this issue [8,12,13]. However, renewable energy is intrinsically unpredictable due to fluctuations or lack of electrical supply which may affect the MES performance. As electrical electron supply plays the role of electron donor for the electroactive biofilm in MES, a lack of supply could drive the system to an unpredictable stand-by state in which the performance might be compromised or the biofilm altered.

To the best of our knowledge, some studies have indeed proposed MES technologies to take advantage of renewable energy surplus [8,12,13]; however, no studies have been made to test the influence of inconsistent nature of this kind of energy in CO<sub>2</sub> fed MES systems. Moreover, none of these studies have evaluated the influence of the microbial community present in the reaction chamber and electrode.

A preliminary study, using MES fed with sodium bicarbonate showed that absence of electricity during periods between 4 h and 64 h affected product formation, causing temporary pathway reversal and decrease in production rates [14]. Nevertheless, the same study indicates that the microbial community is able to recover after reconnection. However, as MES cells present different behavior while fed with dissolved bicarbonate or gas CO<sub>2</sub> [15], it is expected that the effect of power interruptions is also different in this case.

In that context, the aim of this study is to assess the effects of power supply interruptions on an acetogenic MES cell fed with gaseous CO<sub>2</sub>, and comparing these results with the behavior found in a previously bicarbonate fed system [14]. For this purpose, a MES system fed with pure CO<sub>2</sub> gas rather than bicarbonate was operated at fixed applied potential in a semi-continuous mode under a scheduled and increasing set of current interruptions from 4 to 64 hours. The system recovery was evaluated in terms of product generation and rate, and current consumption before, during and after power interruptions. The microbial biofilm and supernatant was analyzed before starting the interruptions and after the last one, allowing identifying which microorganisms were affected by power cuts or responsible of system performance changes along the experiment. Therefore, to the best of our knowledge, this is the first study presenting the alterations on the microbial community of MES submitted to electricity fluctuations.

## 7.2. MATERIAL AND METHODS

### 7.2.1 Microbial electrosynthesis reactor

Microbial electrosynthesis (MES) for producing organics from CO<sub>2</sub> was performed in a two-chambered H-cell reactor type previously described in [14]. H-cell reactor consisted of a cathodic and an anodic chamber with a volume of 250 mL each, separated by a Cation Exchange Membrane (CEM) Ion Power Nafion membrane N117, Germany (figure 7.1). Cathode, used as working electrode, was made of a graphite stick placed between two graphite felts (Mast Carbon, UK) with an effective surface area of 33 cm<sup>2</sup>. Anode electrode was a dynamically stable anode (DSA, Magneto Anodes, Netherlands), and reference electrode was an Ag/AgCl - 3M KCl electrode (Radiometer analytical, France), installed in the cathodic chamber in close proximity to the cathode.

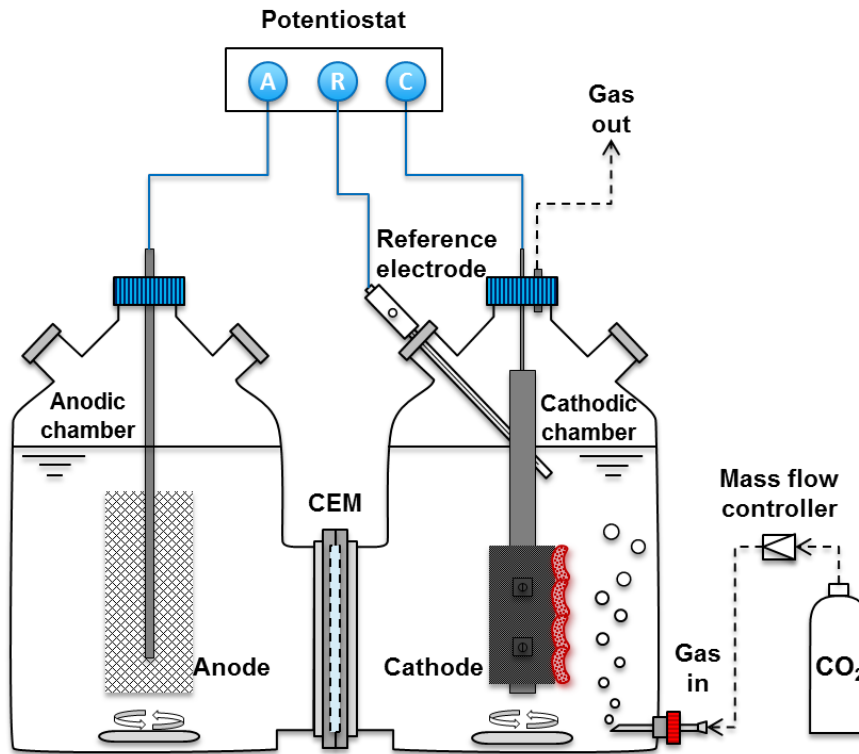


**Figure 7.1:** Microbial electrosynthesis reactor (H-Cell MES)

### 7.2.2 Carbon source, electrolyte and inoculum,

Pure CO<sub>2</sub> was provided as the sole carbon source. CO<sub>2</sub> gas was bubbled into the mineral medium by a needle placed in cathodic chamber (figure 7.1). A mass flow controller (Brooks instrument GF series) kept the CO<sub>2</sub> inflow at 10 mL·min<sup>-1</sup>. The composition of mineral medium of 2 mS/cm conductivity was: KH<sub>2</sub>PO<sub>4</sub> monobasic (0.33 g·L<sup>-1</sup>); K<sub>2</sub>HPO<sub>4</sub> dibasic (0.45 g·L<sup>-1</sup>); NH<sub>4</sub>Cl (1 g·L<sup>-1</sup>); KCl (0.1 g·L<sup>-1</sup>); NaCl (0.8 g·L<sup>-1</sup>); MgSO<sub>4</sub>·7H<sub>2</sub>O (0.2 g·L<sup>-1</sup>); vitamin solution DSMZ 141 (1 mL·L<sup>-1</sup>), and trace solution DSMZ 141 (10 mL·L<sup>-1</sup>) [16].

The biocathode was taken from an H-Cell MES reactor producing acetate from sodium bicarbonate (0.05 M), which was operated for approximately 210 days [14]. Such a biocathode was subjected to different current supply interruptions from 4 h to 64 h. Original electro-autotrophic microorganism culture was taken from the supernatant of a running acetogenic MES which was enriched from an anaerobic sludge following the protocol reported in [17].

### 7.2.3 Set-up

H-Cell MES reactor was operated during 116 days divided in two batches (54 and 62 days), and continuously fed with pure CO<sub>2</sub>. Each batch was referred to change of half of the electrolyte in order to dilute acetate concentration and avoid any possible product inhibition. H-Cell MES was subjected of energy supply interruptions of 4 h, 6 h, and 8 h during first batch, and 16 h, 32 h, and 64 h during second batch. Liquid sampling consisted of retrieving 5 mL of electrolyte from cathode chamber using a plastic syringe. Immediately after sampling, the same volume of fresh electrolyte was added in order to maintain constant effective volume. Gas samples of 1 mL were collected from headspace of cathode chamber before the liquid sampling.

### 7.2.4 Bioelectrochemical analyses

Volatile fatted acids (VFA) and ethanol were measured by high-performance liquid chromatography (HPLC) (Agilent 1200), equipped with an Agilent Hi-Plex H column and an Agilent 1260 infinity refractive index detector. Inorganic carbon in the liquid was measured in a total inorganic carbon analyzer (TOC 5050A – Shimadzu). Gas composition, i.e. hydrogen (H<sub>2</sub>), carbon dioxide (CO<sub>2</sub>), oxygen (O<sub>2</sub>), nitrogen (N<sub>2</sub>) and methane (CH<sub>4</sub>), were determined by a gas chromatographic (CTC Analytics model HXT Pal), equipped with a thermal conductivity detector (TCD).

Using a Biologic multichannel potentiostat (software EC Lab vs. 10.23), H-Cell MES reactor was poised at -1.0 V vs. Ag/AgCl - 3M KCl reference electrode on a three-electrode setup. The reduction current was recorded each 600 seconds by means of chronoamperometry.

Production rates, based on volumetric or effective surface area of the cathode, and Coulombic efficiencies, based on acetate and hydrogen, were estimated by the equations previously described in [14].

### 7.2.5 Scanning electron microscopy (SEM)

SEM images were taken to verify microorganism attachment on the biocathode. Towards this end, approximately 0.25 cm<sup>2</sup> of biocathode from H-Cell MES and control clean carbon felt were sampled at the end of the experiment. A comparison between images of both the H-Cell reactor and the control graphite felt was believed to confirm

the microorganism attachment in the biocathode. Preparation of samples was done as described previously [16] by fixing the microorganisms in 4% glutaraldehyde in sterile phosphate buffer solution for 1 hour at room temperature; samples were rinsed and stored at 4 °C overnight. Afterward, samples were dehydrated by series of 10 minutes with alcohol 20%, 30%, 50%, 70%, 90% and 100% and, then dried at CO<sub>2</sub> critical point for three hours, and gold coated.

### 7.2.6 Microbial community analysis

In order to analyze the microbial community present on the surface of the electrode, from supernatant at the end of the experiment and, from inoculum before starting power supply interruptions, genomic DNA was extracted using the Soil DNA Isolation Plus Kit<sup>®</sup> (Norgen Biotek Corp.), following the manufacturer's instructions. The entire DNA extracted was used for the pyrosequencing of Eubacteria *16S-rRNA* gene based massive library. The primer set used was 27Fmod (5'-AGRGTTTGATCMTGGCTCAG-3') /519R modBio (5'-GTNTTACNGCGGCKGCTG-3') [18]. The obtained DNA reads were compiled in FASTq files for further bioinformatics processing. The following steps were performed using QIIME: Denoising, using a Denoiser [19]. Operational Taxonomic Units (OTUs) were then taxonomically classified using the Ribosomal Database Project (RDP) Bayesian Classifier (<http://rdp.cme.msu.edu>).

Microbial richness estimators ( $S_{obs}$  and *Chao1*) and diversity index estimator (*Shannon*) were calculated with the defined OTUs table using MOTHUR software [20], version 1.35.1 at 3% distance level.

## 7.3. RESULTS AND DISCUSSION

### 7.3.1 Current supply interruptions on H-Cell MES reactor

Figure 7.2 shows that the production of acetate from CO<sub>2</sub> by MES was measurable from 5<sup>th</sup> day of operation, concomitantly with the increase in the reduction current. A continuous and uniform increase was observed until 26<sup>th</sup> day. During undisturbed period, maximum value of acetate concentration and rate before power interruptions reached 5656 mg·L<sup>-1</sup> and 516 mg·L<sup>-1</sup>·d<sup>-1</sup> (36 g·m<sup>-2</sup>·d<sup>-1</sup>) respectively, with reductive current density of around -27 A m<sup>-2</sup>. At the beginning of the experiment while

acetate was rapidly accumulating, the concentration of inorganic carbon fell from 324 mg·L<sup>-1</sup> to less than 30 mg·L<sup>-1</sup>, and it was maintained on this value. The low concentration of inorganic carbon in the culture medium while the acetate concentration was increasing can be an indication of microorganisms directly using the CO<sub>2</sub> in gaseous form as CO<sub>2</sub> was continuously fed, or immediate utilization of dissolved IC. It can also point out one of the main issues to solve in this kind of systems, which is the poor solubility of CO<sub>2</sub> in comparison with the organics production potential of this technology. This behavior was persistent during the whole experiment.

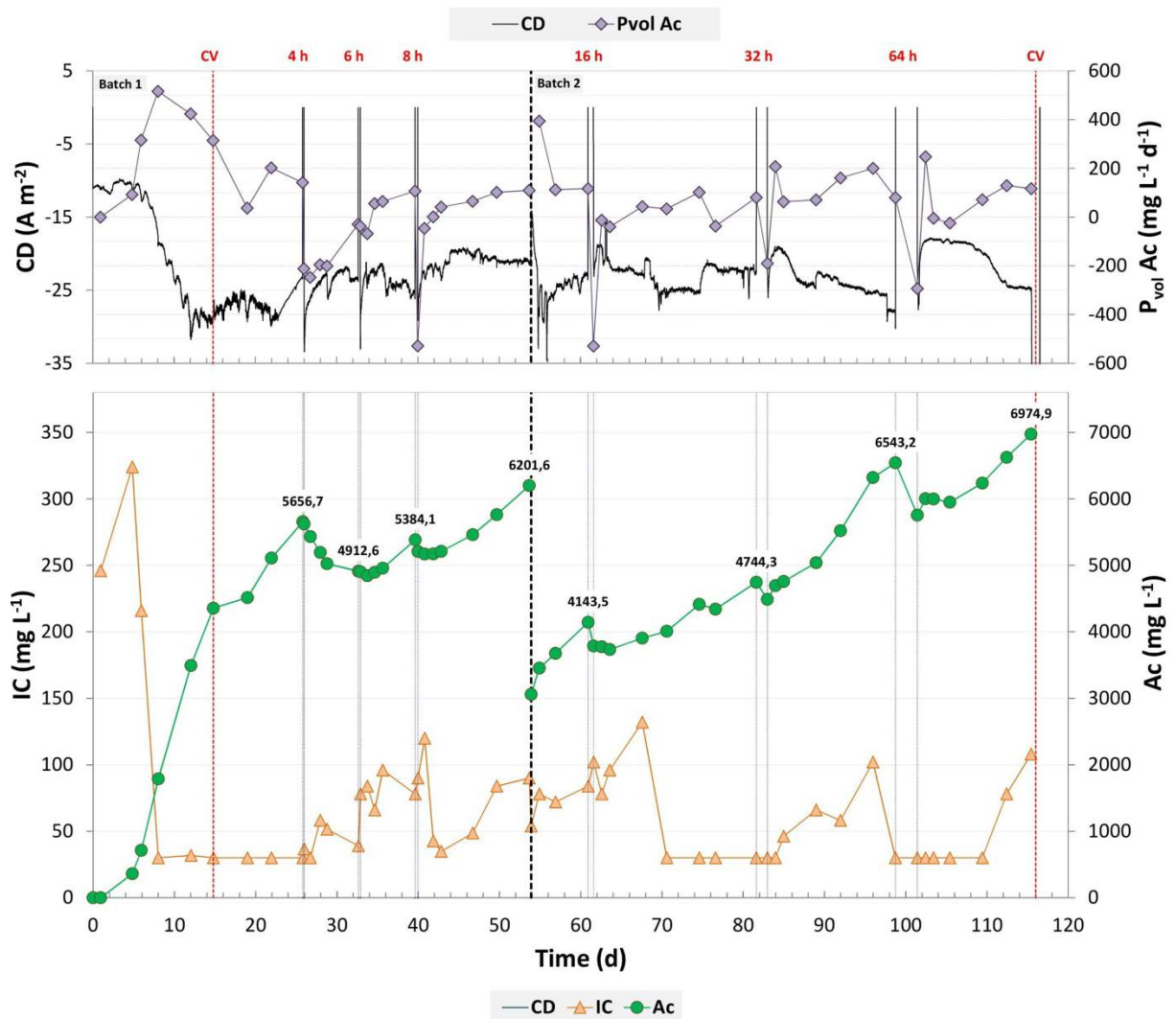


**Figure 7.2:** H-Cell MES reactor performance under different current supply interruptions: Current density (CD), Inorganic carbon (IC) and Acetate (Ac) concentration

The experimental power interruptions period was divided in two different batches replacing half of the culture medium in order to avoid any possible product inhibition during this study and assuring comparability between gaps at the beginning and end. After 4 h of power supply interruption, acetate started to be consumed with a decrease of the concentration up to 4912 mg·L<sup>-1</sup> in seven days. However, the acetate consumption rate, represented by negative acetate production rate, was decreasing after electricity reconnection from -212 to -29 mg L<sup>-1</sup>·d<sup>-1</sup> (-14.7 to -2.0 g m<sup>-2</sup>·d<sup>-1</sup>) during the same period. Such a behavior was an indication that, although the interruption of current supply affected the microbial community, microorganisms were able to gradually restore their electroautotrophic activity. After 6 h gap, the initial response was similar to the previous one; the concentration of acetate was reduced from 4912 to 4845 mg L<sup>-1</sup> in one day, but after that, it increased to 5384 mg L<sup>-1</sup>. The acetate production rate fell just to -68 mg L<sup>-1</sup>·d<sup>-1</sup> (-4.7 g m<sup>-2</sup>·d<sup>-1</sup>), and it recovered and reached 107 mg L<sup>-1</sup>·d<sup>-1</sup> (7.4 g·m<sup>-2</sup>·d<sup>-1</sup>) in five days. A similar behavior was found at the interruption of 8 h reaching a maximum acetate concentration of 6201 mg·L<sup>-1</sup> after 14 days of reconnection. This means that after 40 days of continuously feeding pure CO<sub>2</sub> and without any addition of bicarbonate, the mixed culture biofilm was well established despite the three increasing interruption durations. Microorganisms could recover their electroautotrophic activity even when the interruption of electricity implied the consumption of a part of acetate during a short period of time.

During the second batch, in which 50% of the mineral medium was replaced in order to avoid any product inhibition caused by high acetate concentration, the system was firstly left connected without interruption for 5 days. After this period, acetate concentration achieved was 4143 mg·L<sup>-1</sup> at 115 mg·L<sup>-1</sup>·d<sup>-1</sup> (8.1 g·m<sup>-2</sup>·d<sup>-1</sup>). During the interruptions of 16, 32 and 64 h, acetate concentration had a decrease of approximately 500 mg·L<sup>-1</sup> immediately after each disconnection. However, after each interruption the production rate was recovered, reaching an average of 128 mg L<sup>-1</sup>·d<sup>-1</sup> (8.8 g·m<sup>-2</sup>·d<sup>-1</sup>) (negative rates not taken into account) in all three cases, and achieving a maximum acetate concentration of 6975 mg·L<sup>-1</sup>. Such negative rates were observed just on the first day after electricity reconnection, time that microorganisms used for their recovery.

In a previous study, the microbial community producing acetate from bicarbonate (0.05 M) was showed to suffer some effects under different interruption

---



regimes of electricity supply [14]. In those experimental batches, during the time off, electroautotrophic active microorganism seemed to go through a lag phase or a lethargy state, changing to fermentation and optimizing the energy gain. In some cases, acetate was re-oxidized, using the organic carbon for microorganism survivability and, then releasing CO<sub>2</sub> gas. Table 7.1 shows average current density and recovery time observed after the interruptions, in both cases, fed with bicarbonate and CO<sub>2</sub> gas. It is noticeable that the current density in MES fed with CO<sub>2</sub> gas was around 10-fold higher compared with the MES fed with bicarbonate. As expected, this increase on the use of electrons by microorganisms resulted in acetate production improvement.

**Table 7.1:** Average current density and recovery time comparison between MES fed with bicarbonate and fed with CO<sub>2</sub> gas

Off period (h)	Fed with bicarbonate [14]			Fed with CO <sub>2</sub> gas		
	Average Current Density (A m <sup>-2</sup> )		Time recovery (h)	Average Current Density (A m <sup>-2</sup> )		Time recovery (h)
	Before off period	After off period		Before off period	After off period	
0	-1.78	-	-	-21.66	-	-
4	-2.39	-2.09	1.4	-26.79*	-23.99	5.17
6	-2.15	-1.40	7.2		-23.75	5.33
8	-2.35	-1.62	11.7		-21.02	9.67
16	-2.38	-1.71	12.5	-24.03**	-22.81	6.67
32	-2.44	-1.11	15.6		-23.71	7.50
64	-2.52	-1.49	15.6		-22.22	8.17

\* After Cyclic Voltammetry (CV), from 15<sup>th</sup> to 26<sup>th</sup> day of operation.

\*\* Start of the second batch; from 54<sup>th</sup> to 61<sup>st</sup> day of operation.

On the other hand, table 7.1 show that the recovery time after the interruptions was increasing in the first three gaps together with longer off periods similarly to MES fed with bicarbonate. However, in MES with CO<sub>2</sub> gas such an increase was not maintained between both batches. Although the first interruption in the second batch was 16 h, the recovery time was 3 h less than the recovery time observed after 8 h off. Therefore, recovery time could have been affected not only by the interruption period, as well as by the accumulation of acetic acid.

### 7.3.2 SEM

SEM images were used to visualize both the clean graphite electrode (figure 7.3: A and B) and the inoculated electrode (figure 7.3: C, D, E and F). These SEM images show irregular coverage of bacteria but confirmed clear biofilm formation on the electrode surface in the biofilm samples. In the control samples a smooth carbon material can be seen with a limited amount of impurities or dust. An overview of a graphite fiber can be seen in figure 7.3C flanked by other two fibers and covered by a biofilm. Interestingly, a bacterial accumulation can be seen in the center of the image from which a bacterial bridge is formed to connect this fiber with the next one. A detail of the microbial accumulation (D) and the bridge (E) can also be seen in this figure. Last image in this figure (F) corresponds to the detail of a rod-shaped cell that is physically connected to the surface of the graphite fiber via pilus-like appendages. This kind of pilli has been reported to play an important role in the bioelectrochemical mechanism for product generation [6,21]. These studies state that this type of connections are nanowires which favor electron transfer, however, in our study more specific analytical techniques would be necessary to ensure this fact [22]. These pilus-like appendages can also be seen in between microorganisms facilitating interspecies electron transfer [21]. Similar extracellular appendage (pili or flagella)-like structures as those described in *Geobacter* spp., have been also identified in some species of *Desulfovibrio* (identified as one of the main genus present in our biofilm (figure 7.4) and might also be involved in adherence to electrode [23]. In addition, some salt deposits can be seen over the carbon surface.

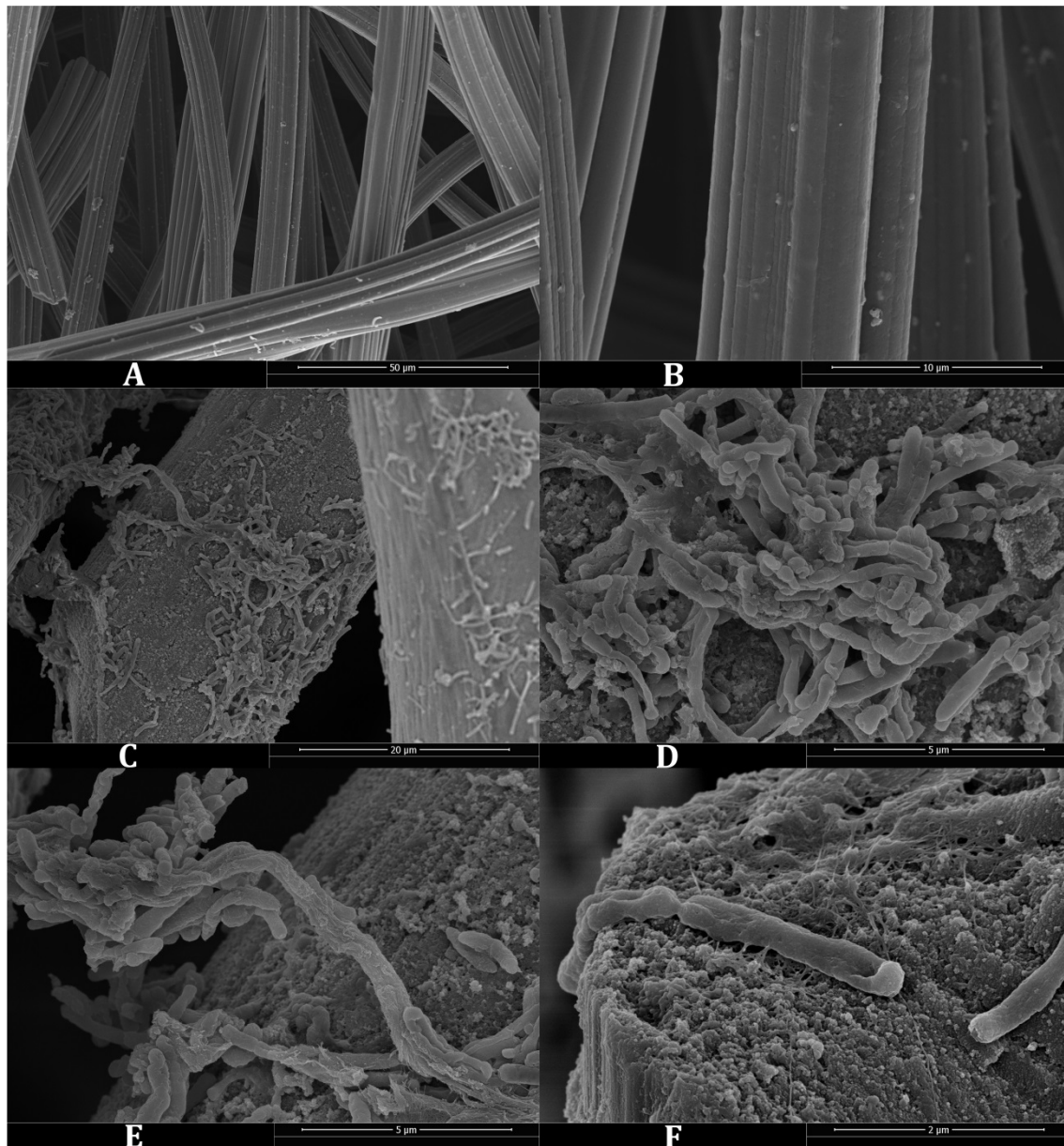


**Figure 7.3:** SEM at different magnification of control clean graphite felt (A and B) and enriched biofilm covering the electrode (C, D, E and F).

### 7.3.3 Microbial community analysis

#### 7.3.3.1 Microbial diversity assessment

High-throughput sequencing based on *16S rRNA* gene massive libraries was carried out in order to analyze the microbial community and structure both in the initial inoculum and in the final biofilm and supernatant. The alpha and beta-diversity analysis were performed in the three analyzed samples. The highest difference between the samples was the number of quality reads found for each one (table 7.2). The number of

sequences detected in the cathodic biofilm was 5-fold higher than in the supernatant, which means that the concentration of planktonic Eubacteria with respect to those attached on the electrode was low. Despite the difference between the number of sequences on each sample, the coverage values range was close to 100%, and therefore all diversity is represented on each sample. In general, these values show a great specialization in terms of Eubacterial populations due to the high number of sequences analyzed corresponding to low species richness, as it has been observed by the OTUs and Chao1 index (table 7.2). This could be due to the inoculum used, which came from an original electroautotrophic community previously enriched in another MES, as it has been described in material and methods section. On the other hand, the 1/Simpson index shows how the biofilm diversity index was reduced to less than half compared to the diversity represented in the inoculum. Moreover, the low bacterial concentration existing in the supernatant was, however, highly diverse approximately at the level of the biofilm (table 7.2).

**Table 7.2:** N° of sequences and OTUs, estimated richness (Chao1), diversity index (Shannon) and sample coverage values for Eubacterial operational taxonomic units (OTUs).

Sample	N° Seqs.	Sobs OTUs	Chao1		1/Simpson		Coverage (%)
			mean	c.i.*	mean	c.i.*	
<b>Inoculum</b>	63367	295	398	356-466	13.1	12-13	99.8
<b>Biofilm</b>	49899	234	356	295-476	4.9	4.8-5.0	99.8
<b>Supernatant</b>	9521	130	229	176-354	12.8	12.4-13.5	99.5

\*c.i.: 95% confidence intervals

### 7.3.3.2 Microbial community composition.

The evolution of the microbial communities from the inoculum to the Eubacterial population established in the biofilm is represented in figure 7.4. The phyla representation in the inoculum is 45.3% *Proteobacteria* and 36.4% *Firmicutes*. However, *Proteobacteria* decreased to 13% in the biofilm, while *Firmicutes* increased to 85%. Most part of *Firmicutes* (81%) in the biofilm is represented by two families, *Veillonellaceae* and *Clostridiaceae*. The third most dominant family enriched in the

biofilm is *Desulfovibrionaceae*, belonging to *Proteobacteria*. It should be noted that these three families are composed by only one genus, demonstrating again the high specialization of these populations. The family *Veillonellaceae* is strongly represented by *Sporomusa* (56.5%), *Desulfovibrionaceae* by genus *Desulfovibrio* (12%) and *Clostridiaceae* by *Clostridium* (24.5%). These three genera accounted for 93% of the total Eubacterial community attached to the electrode.

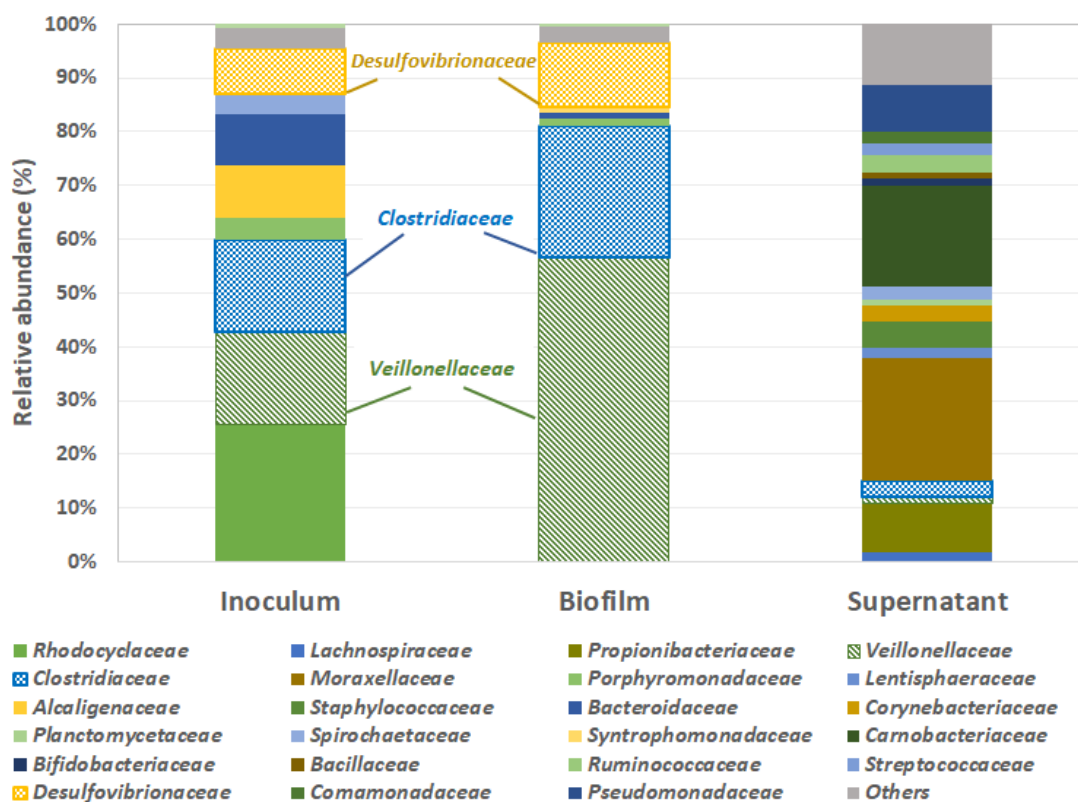


**Figure 7.4:** Taxonomic classification of *16S rRNA gene* from Eubacterial classification at a family level. Groups making up less than 1% of the total number of sequences per sample were classified as “others”.

An analysis of the microbial community composition in the supernatant (figure 7.4) revealed a dramatic difference with respect to those identified in the electrode. This population is not specialized and is composed of a high diversity community (table 7.2) in a low relative abundance. The highest relative abundance families were *Moraxellaceae* previously described as electrothrophic microorganism in cathodic communities (Semeneć and Franks, 2015), *Carnobacteriaceae*, *Propionibacteriaceae* and *Lachnospiraceae*, which may be involved in intermediary metabolic pathways. Moreover, *Pseudomonadaceae* was detected, which is usually more abundant in suspension, and it has physiological evidence for hydrogenase activity [25] and is

known for producing shuttles in bioelectrochemical systems, and hence plays a role in extracellular electron transfer [26].

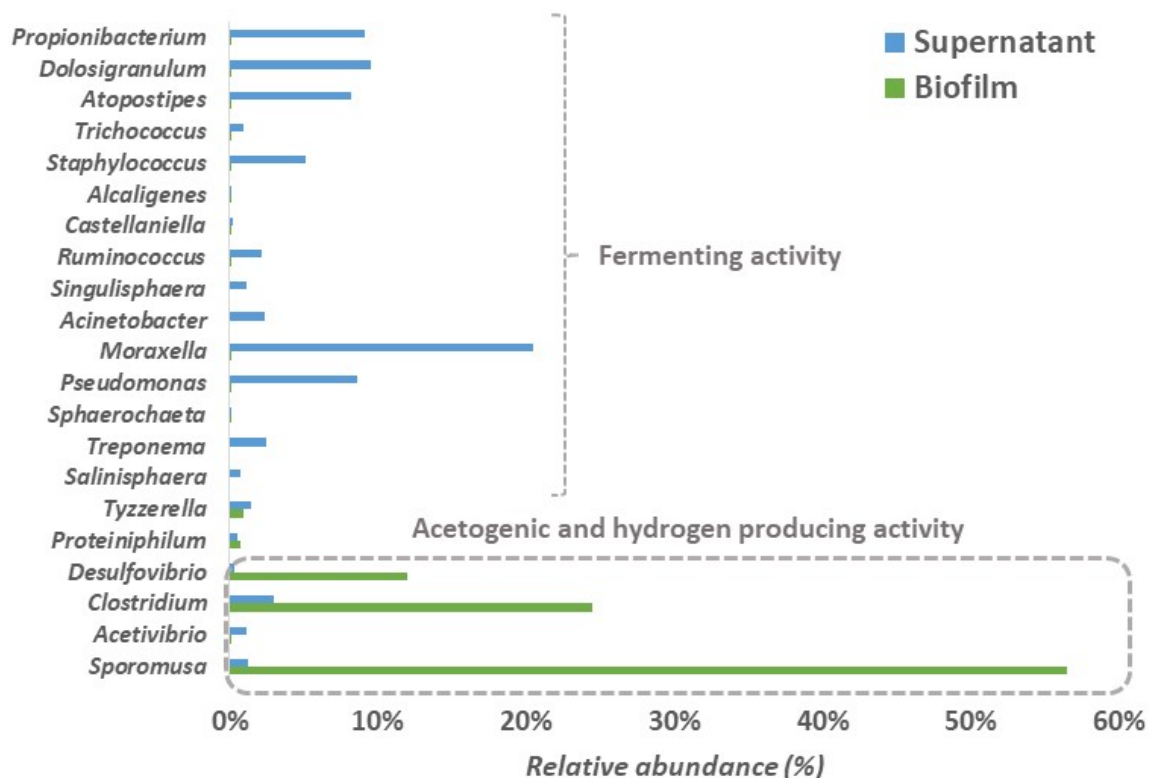


**Figure 7.5:** The most abundant genera identified in the supernatant and biofilm samples.

### 7.3.3.3 The role of main identified genera

The community attached on the electrode was absolutely dominated by microorganisms belonging to three genera namely *Sporomusa*, *Clostridium* and *Desulfovibrio* (figure 7.5). The potential function of the dominant genera can be classified as acetogenic and hydrogen producing activity. The OTUs belonging to *Sporomusa* and *Clostridium* genera could be responsible of the maximum production rate of 516 mg L<sup>-1</sup> d<sup>-1</sup> acetic acid reached in this experiment. Moreover, contrary to other well-known acetogenic bacteria as *Acetobacterium*, dominant in MES, both *Sporomusa* and *Clostridium* have been identified as acetogenic bacteria with bioelectrochemical activity [27]. In general, acetate is the primary product of these acetogenic bacteria but other intermediates as 2-oxobutyrate and formate are formed [28]. A syntrophic relationship can be established in the biofilm as *Desulfovibrio*

presents formate dehydrogenase activity to produce CO<sub>2</sub>, and this could explain that it was more abundant on the electrode compared to the supernatant [29,30]. Furthermore, the electrochemically active *Desulfovibrio* has been previously shown as being able to catalyze hydrogen production on biocathodes [23], and it also performs a combination of carbon-fixation and acetate utilization [30]. Therefore, *Desulfovibrio* could be responsible for acetic acid oxidation to CO<sub>2</sub> during the absence of power supply (figure 7.2).

Regarding the supernatant, the main genus observed is *Moraxella* (20.4%) and the rest of the community is composed by groups below 10% among which *Pseudomonas*, *Propionibacterium*, *Acinetobacter* or *Treponema* are present (figure 7.5). It is quite evident that both communities (biofilm and supernatant) are completely different (figure 7.5), however some bacteria are common to both. Phylotypes identified as *Sporomusa* have been found in the supernatant (1.2%), while this abundance increased up to 56.5% in the biofilm being the clear dominant bacteria. The same happens with *Clostridium* and *Desulfovibrio* which increased their abundance in the biofilm but are also identified in the supernatant although below 3%. Some minor OTUs belonging to *Proteiniphilum*, which has been also shown to generate acetate [30], are also present in both communities.

To sum up, it can be stated that apart from some similarities between biofilm and supernatant communities, the acetogenic activity was represented by members attached onto the biofilm, while the supernatant community was responsible of the fermentative metabolism.

#### 7.3.4 Technological and commercial perspectives

Here, we have shown how MES systems can withstand power supply interruptions without a significant deterioration in its performance, which allows for moderate optimism about its integration with renewable energy sources. Still, significant challenges lay ahead, making the journey for real-field implementation a demanding one. In a simplified techno-economic evaluation, ElMekawy et al. [31] situated MES, together with microalgae and photosynthetic systems, as equally promising and viable technologies for CO<sub>2</sub> conversion into chemicals, additionally showing a relatively large potential market for acetic acid (~12900 tonnes per year).

However, the production costs of pure acetic acid from CO<sub>2</sub> with a MES system as core reactor can be as high as 3.84-5.74 £/kg (~4.30-6.42 €/kg for a 1000 tonnes per year basis) [32], which is still one order of magnitude above its current market price. Improved titers and productivities are critical to make acetate production through MES competitive.

In addition to market barriers, MES need to face significant technological hurdles, most of which are common to all BES, but some others are intrinsic to MES. On the one hand, as renewable energy production is unpredictable and must be coupled to a CO<sub>2</sub> stream (that could also present fluctuations), suitable energy control systems and strategies will be critical to effectively combine both systems. The perturbation and observation method proposed by Tartakovsky et al. [33] for the optimization of a single microbial electrolysis cell, or the dynamically adaptive control system for stacked BES developed by Andersen et al. [34] can provide the basis for specific control systems for MES. Another obstacle of CO<sub>2</sub>-reducing MES systems has to do with the poor substrate availability to microorganisms, as CO<sub>2</sub> solubility kinetics are not fast enough in these culture media. In proof-of-concept and lab scale studies, MES are usually provided with an excess of CO<sub>2</sub> to improve mass transport and production rates. However, an important amount of substrate is lost in the process, making this approach unsuitable for real-field application. Recirculation or stirring systems to achieve higher mass transfer from the bulk to the biofilm could become relevant alternatives. Relatively high energy consumption rates represent another important drawback of MES that impact directly on its economic feasibility. Water oxidation (Standard reaction potential: +1.23V vs. SHE) is the reaction that usually takes place in the counter electrode to provide electrons and protons to the biocathode. Although pure oxygen can be recovered as a byproduct in the process, cell potential gets easily over 3V resulting in large energy usage per gram of acetic acid produced. Using bioanodes as counter-electrode could reduce cell potential to half as they can operate at around 0V vs. SHE [35]. However, this approach is not without difficulties since bioanodes would require an organic substrate (most probably a waste stream), which can give rise to contamination issues.



#### 7.4. CONCLUSION

This study explores for the first time the effect of electrical power interruptions on a MES system fed with gaseous CO<sub>2</sub>. Power supply interruptions affected the behavior of MES, causing the microbial community to reverse the acetogenic reaction for a period below one day and consume a part of the product for survivability. However after power interruptions, the system showed to recover with a maximum recovery time of 9.7 h after 8 h of power interruption. Such a recovery was associated with the robust population formed by bioelectrochemically active acetogenic bacteria, reaching production rates and current consumptions similar to the values found before the interruptions. Highest product titer was found at the end of the experiment (6975 mg·L<sup>-1</sup>) while highest production rate was achieved before power interruptions (516 mg·L<sup>-1</sup>·d<sup>-1</sup>). Cathodic biofilm was dominated by the well-known electroactive bacteria *Sporomusa*, *Clostridium* and *Desulfovibrio*, which showed to be resilient to frequent interruptions of electricity supply. Therefore, a MES system proved to be ready for renewable energy supply coupling withstanding power fluctuations. This fact opens the pathway to a profitable symbiotic relationship between renewable energy and MES systems, although extensive further work must be carried out to achieve real-field implementation of MES systems together with renewable energy power plants.

## 7.5. REFERENCES

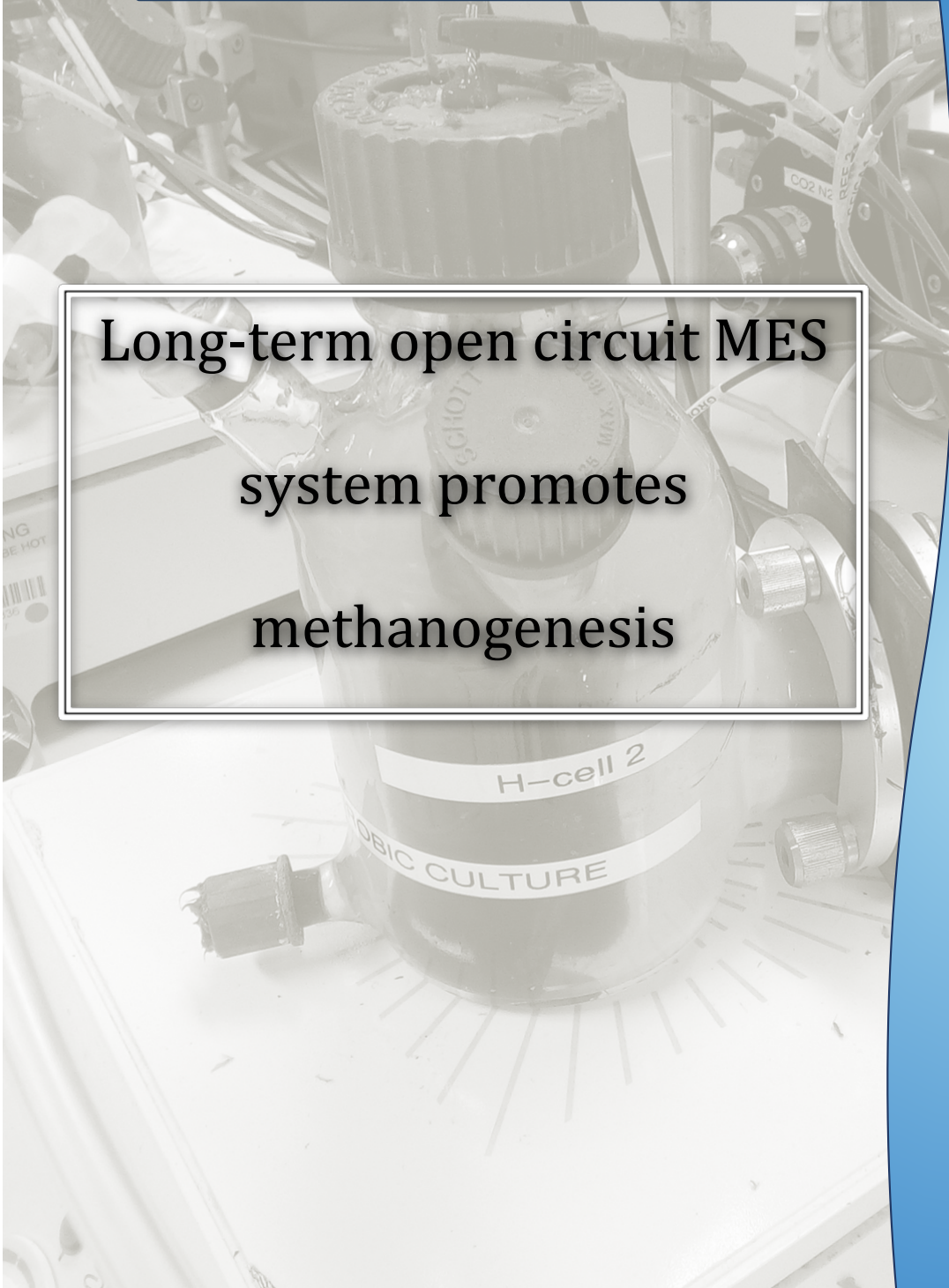
- [1] IEA. World Energy Outlook 2017. Organisation for Economic Co-operation and Development, OECD; 2017.
- [2] Hu X, Zou C, Zhang C, Li Y. Technological developments in batteries: a survey of principal roles, types, and management needs. *IEEE Power and Energy Magazine* 2017;15:20–31.
- [3] Bakelli Y, Hadj Arab A, Azoui B. Optimal sizing of photovoltaic pumping system with water tank storage using LPSP concept. *Solar Energy* 2011;85:288–94. doi:10.1016/J.SOLENER.2010.11.023.
- [4] Chi J, Yu H. Water electrolysis based on renewable energy for hydrogen production. *Chinese Journal of Catalysis* 2018;39:390–4. doi:10.1016/S1872-2067(17)62949-8.
- [5] Yekini Suberu M, Wazir Mustafa M, Bashir N. Energy storage systems for renewable energy power sector integration and mitigation of intermittency. *Renewable and Sustainable Energy Reviews* 2014;35:499–514. doi:10.1016/J.RSER.2014.04.009.
- [6] Rabaey K, Rozendal RA. Microbial electrosynthesis—revisiting the electrical route for microbial production. *Nature Reviews Microbiology* 2010;8:706–16.
- [7] Desloover J, Arends JBA, Hennebel T, Rabaey K. Operational and technical considerations for microbial electrosynthesis. *Biochemical Society Transactions* 2012;40:1233 LP-1238.
- [8] Nevin KP, Woodard TL, Franks AE, Summers ZM, Lovley DR. Microbial electrosynthesis: feeding microbes electricity to convert carbon dioxide and water to multicarbon extracellular organic compounds. *MBio* 2010;1:e00103--10.
- [9] Bajracharya S, Srikanth S, Mohanakrishna G, Zacharia R, Strik DP, Pant D. Biotransformation of carbon dioxide in bioelectrochemical systems: State of the art and future prospects. *Journal of Power Sources* 2017;356:256–73. doi:10.1016/j.jpowsour.2017.04.024.
- [10] Mateos R, Sotres A, Alonso RM, Escapa A, Morán A. Impact of the start-up process on the microbial communities in biocathodes for electrosynthesis. *Bioelectrochemistry* 2018;121:27–37. doi:10.1016/j.bioelechem.2018.01.002.
- [11] Sato K, Kawaguchi H, Kobayashi H. Bio-electrochemical conversion of carbon dioxide to methane in geological storage reservoirs. *Energy Conversion and Management* 2013;66:343–50. doi:10.1016/J.ENCONMAN.2012.12.008.
- [12] Abate S, Lanzafame P, Perathoner S, Centi G. New Sustainable Model of Biorefineries: Biofactories and Challenges of Integrating Bio-and Solar Refineries. *ChemSusChem* 2015;8:2854–66.
- [13] Perathoner S, Centi G. CO<sub>2</sub> Recycling: A Key Strategy to Introduce Green Energy in the Chemical Production Chain. *ChemSusChem* 2014;7:1274–82.

- doi:10.1002/cssc.201300926.
- [14] Anzola Rojas M del P, Zaiat M, Gonzalez ER, De Wever H, Pant D. Effect of the electric supply interruption on a microbial electrosynthesis system converting inorganic carbon into acetate. *Bioresource Technology* 2018;266:203–10. doi:10.1016/J.BIORTECH.2018.06.074.
- [15] Mohanakrishna G, Vanbroekhoven K, Pant D. Imperative role of applied potential and inorganic carbon source on acetate production through microbial electrosynthesis. *Journal of CO2 Utilization* 2016;15:57–64. doi:10.1016/j.jcou.2016.03.003.
- [16] Bajracharya S, ter Heijne A, Dominguez Benetton X, Vanbroekhoven K, Buisman CJN, Strik DPBTB, et al. Carbon dioxide reduction by mixed and pure cultures in microbial electrosynthesis using an assembly of graphite felt and stainless steel as a cathode. *Bioresource Technology* 2015;195:14–24. doi:10.1016/j.biortech.2015.05.081.
- [17] Bajracharya S, Yuliasni R, Vanbroekhoven K, Buisman CJN, Strik DPBTB, Pant D. Long-term operation of microbial electrosynthesis cell reducing CO<sub>2</sub> to multi-carbon chemicals with a mixed culture avoiding methanogenesis. *Bioelectrochemistry* 2017;113:26–34. doi:10.1016/j.bioelechem.2016.09.001.
- [18] Callaway TR, Dowd SE, Wolcott RD, Sun Y, McReynolds JL, Edrington TS, et al. Evaluation of the bacterial diversity in cecal contents of laying hens fed various molting diets by using bacterial tag-encoded FLX amplicon pyrosequencing. *Poultry Science* 2009;88:298–302. doi:10.3382/ps.2008-00222.
- [19] Reeder J, Knight R. Rapidly denoising pyrosequencing amplicon reads by exploiting rank-abundance distributions. *Nature Methods* 2010;7:668–9. doi:10.1038/nmeth0910-668b.
- [20] Schloss PD, Westcott SL, Ryabin T, Hall JR, Hartmann M, Hollister EB, et al. Introducing mothur: open-source, platform-independent, community-supported software for describing and comparing microbial communities. *Applied and Environmental Microbiology* 2009;75:7537–41. doi:10.1128/AEM.01541-09.
- [21] Malvankar NS, Lovley DR. Microbial nanowires for bioenergy applications. *Current Opinion in Biotechnology* 2014;27:88–95. doi:10.1016/J.COPBIO.2013.12.003.
- [22] Tan Y, Adhikari RY, Malvankar NS, Pi S, Ward JE, Woodard TL, et al. Synthetic biological protein nanowires with high conductivity. *Small* 2016;12:4481–5.
- [23] Croese E, Pereira MA, Euverink GJW, Stams AJM, Geelhoed JS. Analysis of the microbial community of the biocathode of a hydrogen-producing microbial electrolysis cell. *Applied Microbiology and Biotechnology* 2011;92:1083–93. doi:10.1007/s00253-011-3583-x.
- [24] Semenc L, E Franks A. Delving through electrogenic biofilms: from anodes to cathodes to microbes. *AIMS Bioengineering* 2015;2:222–48.

doi:10.3934/bioeng.2015.3.222.

- [25] Schwartz E, Friedrich B. The H<sub>2</sub>-Metabolizing Prokaryotes. 2006.
- [26] Rabaey K, Boon N, Höfte M, Verstraete W. Microbial phenazine production enhances electron transfer in biofuel cells. *Environmental Science and Technology* 2005;39:3401–8. doi:10.1021/es048563o.
- [27] Saheb-Alam S, Singh A, Hermansson M, Persson F, Schnürer A, Wilén B-M, et al. Effect of start-up strategies and electrode materials on carbon dioxide reduction on bio-cathodes. *Applied and Environmental Microbiology* 2017;AEM.02242-17. doi:10.1128/AEM.02242-17.
- [28] Nevin KP, Hensley SA, Franks AE, Summers ZM, Ou J, Woodard TL, et al. Electrosynthesis of organic compounds from carbon dioxide is catalyzed by a diversity of acetogenic microorganisms. *Applied and Environmental Microbiology* 2011;77:2882–6. doi:10.1128/AEM.02642-10.
- [29] Patil SA, Arends JBA, Vanwonterghem I, Van Meerbergen J, Guo K, Tyson GW, et al. Selective enrichment establishes a stable performing community for microbial electrosynthesis of acetate from CO<sub>2</sub>. *Environmental Science & Technology* 2015;49:8833–43.
- [30] Marshall CW, Ross DE, Handley KM, Weisenhorn PB, Edirisinghe JN, Henry CS, et al. Metabolic reconstruction and modeling microbial electrosynthesis. *Scientific Reports* 2017;7:1–12. doi:10.1038/s41598-017-08877-z.
- [31] ElMekawy A, Hegab HM, Mohanakrishna G, Elbaz AF, Bulut M, Pant D. Technological advances in CO<sub>2</sub> conversion electro-biorefinery: A step toward commercialization. *Bioresource Technology* 2016;215:357–70. doi:10.1016/j.biortech.2016.03.023.
- [32] Christodoulou X, Okoroafor T, Parry S, Velasquez-Orta SB. The use of carbon dioxide in microbial electrosynthesis: Advancements, sustainability and economic feasibility. *Journal of CO<sub>2</sub> Utilization* 2017;18:390–9. doi:10.1016/J.JCOU.2017.01.027.
- [33] Tartakovsky B, Mehta P, Santoyo G, Guiot SR. Maximizing hydrogen production in a microbial electrolysis cell by real-time optimization of applied voltage. *International Journal of Hydrogen Energy* 2011;36:10557–64. doi:10.1016/J.IJHYDENE.2011.05.162.
- [34] Andersen SJ, Pikaar I, Freguia S, Lovell BC, Rabaey K, Rozendal RA. Dynamically adaptive control system for bioanodes in serially stacked bioelectrochemical systems. *Environmental Science & Technology* 2013;47:5488–94.
- [35] Nam J-Y, Tokash JC, Logan BE. Comparison of microbial electrolysis cells operated with added voltage or by setting the anode potential. *International Journal of Hydrogen Energy* 2011;36:10550–6. doi:10.1016/J.IJHYDENE.2011.05.148.

## CHAPTER 8



Long-term open circuit MFC  
system promotes  
methanogenesis

*Chapter adapted from:*

**Mateos, R.,** Sotres, A., Escapa, A., Pant D. (n.a.)

Long-term open circuit MFC system promotes methanogenesis.

In preparation.



---

**ABSTRACT**

Microbial Electrosynthesis (MES) can potentially provide a means for storing renewable energy surpluses as chemical energy. However, the unstable nature of these energy sources may represent a threat to MES, as the microbial communities that develop on the biocathode rely on the existence of a polarized electrode. This work assesses how MES performance, product generation and microbial community evolution are affected by a long-period (6 weeks) power cut. Acetogenic and H<sub>2</sub>-producing bacteria activity recovered after reconnection. However, few days later syntrophic acetate oxidation bacteria and H<sub>2</sub>-consuming methanogens became dominant, consuming both the acetic acid and the hydrogen present in the cathode environment. Thus, although the system proved to be resilient to a long-term power interruption in terms of electroactivity, it also showed that it could extensively affect both the product generation and microbial communities.

## 8.1. INTRODUCTION

Renewable energy production is beating records year by year around the world. However, the unpredictable nature and the variability of renewable power represent the key hurdles for a widespread use of these technologies. Efficient storage systems, that allow to exploit the electricity surpluses can be part of the solution to this challenge [1].

Microbial electrosynthesis (MES) is a novel technology capable of converting a CO<sub>2</sub> stream and electricity into easily storable fuels and chemicals [2]. First studies were able to produce mainly acetate, although the spectrum of products has been enlarged during the last years enabling the production of longer chain fatty acids, alcohols and fuels like methane [3]. In MES, electrorophic microorganisms are capable of accepting electrons from a solid cathode and use inorganic carbon as the sole carbon source for their metabolism and growth [4,5]. This technology shows several advantages for CO<sub>2</sub> fixation and energy surplus exploitation [6] as it is independent from land use, require reduced nutrient and water consumption and can be installed next to CO<sub>2</sub> or renewable energy sources with minor instrumentation [7]. It is widely admitted that MES can only develop its full potential as a sustainable environmental technology when powered by renewable energy [2,6]. This integration between MES and renewable energy systems may bring additional advantages to the later, as MES can provide a means to store surpluses of electricity during peak production [8]. However, the unpredictable interruptions and fluctuations, typical of renewable power, can represent a potential threat to the stability of the microbial communities that thrive of the electrons that arrive at the cathode. The impact of short power interruptions have been examined in a previous study [9] showing that MES can be resilient to power interruptions in the range of hours, recovering its previous stable performance in 7-16 hours after power gaps.

The aim of the present work is to evaluate how longer (6 weeks) power disconnections affects the performance and microbial communities of a MES that has been producing acetate in a stable and efficient manner for a period over a year.



## 8.2. MATERIALS AND METHODS

### 8.2.1 MES reactors set up

A two-chamber H-cell type reactor was built consisting on a biotic cathode chamber and an abiotic anode chamber separated by a Nafion N117 cation exchange membrane (figure 8.1). In this case the cathode (working electrode (WE)) was made of graphite felt (67 cm<sup>2</sup>) attached to a graphite stick (Mast Carbon, UK) set at -1V vs. Ag/AgCl. On the other hand the anode (counter electrode (CE)) was a 37.5 cm<sup>2</sup> dimensionally stable electrode (DSA, Magneto Anodes, Netherlands). The reference electrode was a commercial Ag/AgCl reference electrode (Radiometer analytical, France) checked for potential stability before and after experiment, and the tip was placed as close to the cathode as possible. Both chambers had a working volume of 500mL, the liquid was continuously stirred at 200rpm, the temperature maintained at 30°C and the system was electrically controlled using a VMP3 Biologic potentiostat (Biologic, France).

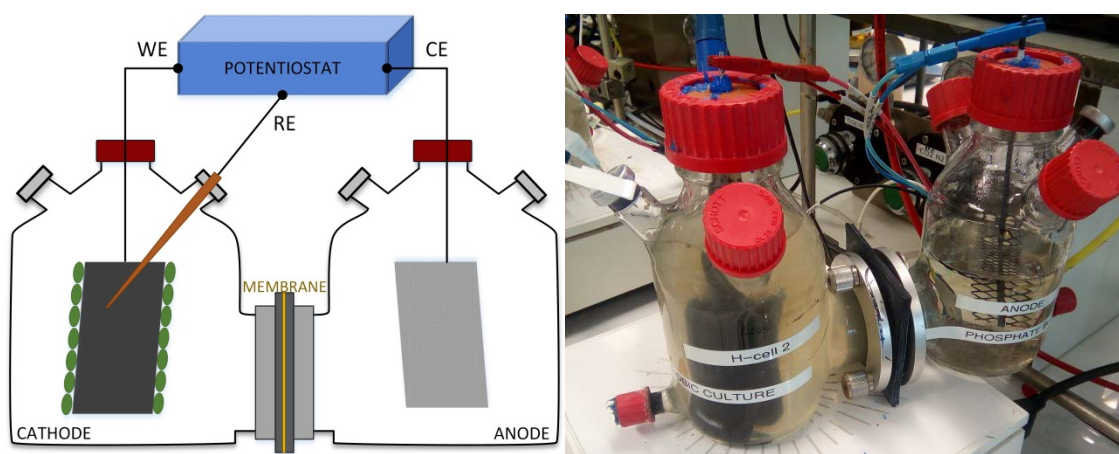


**Figure 8.1:** Schematic and image of cell assembly

### 8.2.2 Inoculum, influents and experimental procedure

The cathodic chamber was inoculated from the supernatant of an acetogenic biocathode originally grown from an enriched digested sludge [10] and the cell used for long term acetogenic experiments [9]. The cathodic chamber was filled at the beginning of this experiment with a fresh mineral medium containing: K<sub>2</sub>HPO<sub>4</sub> (0.45 g·L<sup>-1</sup>); KH<sub>2</sub>PO<sub>4</sub> (0.33 g·L<sup>-1</sup>); NH<sub>4</sub>Cl (1 g·L<sup>-1</sup>); NaCl (0.8 g·L<sup>-1</sup>); KCl (0.1 g·L<sup>-1</sup>); MgSO<sub>4</sub>·7H<sub>2</sub>O (0.2 g L<sup>-1</sup>); DSMZ 141 vitamin solution (1 mL·L<sup>-1</sup>), and DSMZ 141 trace

mineral solution ( $10 \text{ mL}\cdot\text{L}^{-1}$ ). The cathode chamber was then fed with sodium bicarbonate twice a week in order to raise the bicarbonate concentration up to 0.05M in the culture medium. The catholyte needed pH adjustment to 7 due to bicarbonate addition, which was solved by the addition of small quantities of concentrated HCl in order to disturb the working volume as little as possible. The anolyte was filled with the same mineral medium to avoid unnecessary ion gradient and migration through the membrane.

The catholyte was sampled twice a week right before being fed with fresh bicarbonate in order to determine dissolved TOC, IC, VFAs, ethanol and pH. The gas in the headspace was sampled at the same time. Produced gas flowrate was continuously measured along the experiment.

### 8.2.3 Analytical techniques

Ethanol and volatile fatty acids (VFA) were determined by an Agilent 1200 high-performance liquid chromatography (HPLC), using an Agilent Hi-Plex H column and an Agilent 1260 infinity refractive index detector. Organic and inorganic carbon of liquid phases were measured with a total carbon analyzer (TOC 5050A – Shimadzu). Gas composition (carbon dioxide ( $\text{CO}_2$ ), hydrogen ( $\text{H}_2$ ), methane ( $\text{CH}_4$ ), nitrogen ( $\text{N}_2$ ) and oxygen ( $\text{O}_2$ )) was determined by gas chromatography (CTC Analytics model HXT Pal), equipped with a thermal conductivity detector (TCD). Outlet gas flow rate was measured using a Milligascounter MGC-1 PMMA (Ritter, Germany). pH was determined with a HACH 5014T probe in a CRISON 20+ pH meter.

Electrical system control and operation was managed using a multichannel VMP3 Biologic potentiostat (Biologic, France).

### 8.2.4 Microbial community analysis

For the analysis of the microbial community on the electrode surface, supernatant and inoculum, genomic DNA was extracted with the Soil DNA Isolation Plus Kit<sup>®</sup> (Norgen Biotek Corp.), strictly following the manufacturer's instructions. The extracted DNA was utilized for the pyrosequencing of eubacteria *16S-rRNA* gene based massive library. The primer set employed for this purpose was 27Fmod (5'-AGRGTTTGATCMTGGCTCAG-3') /519R modBio (5'-

GTNTTACNGCGGCKGCTG-3') [11] and Arch 349F (5'-GYGCASCAGKCGMGAAW-3') / Arch 806R (5'-GGACTACVSGGGTATCTAAT-3') [12] for Eubacterial and Archaeal analysis respectively. The obtained DNA sequences were compiled for bioinformatics processing in FASTq files. The following steps were performed using QIIME: Denoising, using a Denoiser [13]. After that, Operational Taxonomic Units (OTUs) were taxonomically classified using Ribosomal Database Project (RDP) Bayesian Classifier (<http://rdp.cme.msu.edu>).

### 8.2.5 Scanning electron microscopy (SEM)

SEM images were taken to check microorganism attachment and structures on the surface of the graphite cathode. For this purpose, approximately 0.25 cm<sup>2</sup> of a thin layer of felt was taken from the biocathode surface at the end of the experiment and also a control new graphite felt sample was taken for comparison purposes. Samples were prepared as described in [14]. Microorganisms were fixed in 4% glutaraldehyde in a sterile solution consisting of phosphate buffer for 1 hour at ambient temperature, and then samples were rinsed in the same phosphate buffer and stored at 4 °C overnight. After that, samples were dehydrated by subsequent 10-minutes immersion in alcohol 20%, 30%, 50%, 70%, 90% and 100%. Eventually the samples were dried at CO<sub>2</sub> critical point for three hours, and gold coated.

## 8.3. RESULTS AND DISCUSSION

### 8.3.1 Previous operating history

The experimental cell was inoculated with the enriched supernatant of a long-term working acetogenic MES [10] around one year before the present study was carried out. That inoculum was analyzed for Archaea and Eubacterial composition, confirming that homoacetogenic and hydrogen producing microorganism were dominant at that point and Archaea were not present (See section 8.3.3). This inoculated cell was acclimated for 3 months with bicarbonate as carbon source in order to allow for the development of a robust biofilm. During this period the cell reached an average acetic acid production of 236 mg·L<sup>-1</sup>·d<sup>-1</sup> with a peak value of 550 mg·L<sup>-1</sup>·d<sup>-1</sup>. Maximum titers over 1 g·L<sup>-1</sup> and up to 78% bicarbonate conversion into acetic acid, together with

the previously mentioned production rates led to think that the biofilm was stable and ready to undergo a defined experimental plan.

At this point the cell was used in a 6 month experiment in which short power gaps (4 to 64 hours) were subsequently applied to assess how unexpected electrical disconnections affect MES performance [9]. The cell was resilient to these short power interruptions always restoring bioelectrochemical acetic acid production, although its production rate decreased by 77% after the longer gap.

After this experimental period, the cell was left in open circuit for 6 weeks and reconnected in the frame of the present study to evaluate the impact of this long power interruption on MES performance and on the microbial communities present in the cathode.

### 8.3.2 Biocathode evolution and performance

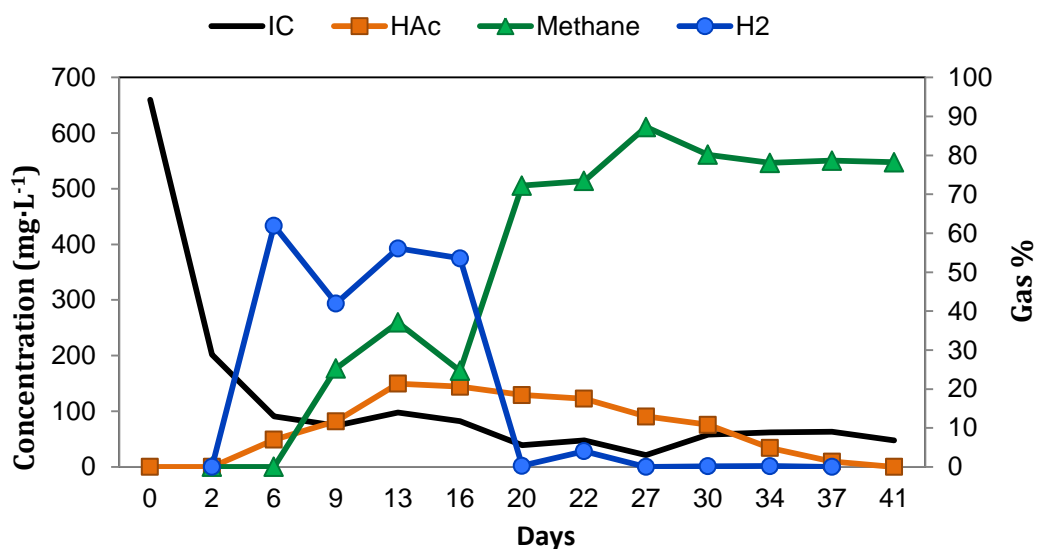


**Figure 8.2:** Substrate and acetic acid concentration in the liquid medium (Black and orange) and gaseous products proportion in the outlet gas (Blue and Green). Day 0 corresponds to power supply reconnection.

After replacing the catholyte by a fresh culture medium, the cell was reconnected by poisoning the WE (cathode) at -1 V vs. Ag/AgCl. Figure 8.2 shows substrate (IC) and products (Acetic acid, methane and hydrogen) evolution during the experimental time. At the moment of first sampling (day 2), and despite the sharp decrease in the substrate (inorganic carbon), no products were found in the gas headspace or the culture medium. This, together with the electrical charge consumption

measured during this period (863 C), suggests that microorganisms were using the available inorganic carbon source and energy to proliferate and adjust their metabolic pathways to the new conditions after the long power interruption. 6 days after reconnection, hydrogen and acetic acid began to appear although in low quantities: acetate reached only  $49 \text{ mg}\cdot\text{L}^{-1}\cdot\text{d}^{-1}$  and despite the percentage of hydrogen in the headspace was important (62%), negligible net gas production rate was measured. From day 6 to 16 the product profile diversified, adding methane to acetate and hydrogen. Acetate production grew slowly during this period and then decreased gradually until no net production was found by the end of the experiment. Importantly, total net gas production became measurable, growing up to  $75 \text{ mL}\cdot\text{L}^{-1}\cdot\text{d}^{-1}$ . Hydrogen concentration in the off gas was steady in the range between 40% and 60%, and methanogenic activity grew drastically boosting methane proportion from 0% to 37%. Between days, 16 and 20 methanogenesis clearly overtakes acetogenic activity and after day 20 methanogenesis is absolutely dominant, with most of the product formation corresponding to this gas and only small quantities to hydrogen and acetate. Methane percentage in the off-gas is consistently maintained around 80% reaching a peak of 87% corresponding to rates ranging from 30 to  $55 \text{ mL}\cdot\text{L}^{-1}\cdot\text{d}^{-1}$  of pure methane. Methane rates, after the methanogenesis becomes dominant, are shown in figure 8.3 together with methane cathodic efficiency.

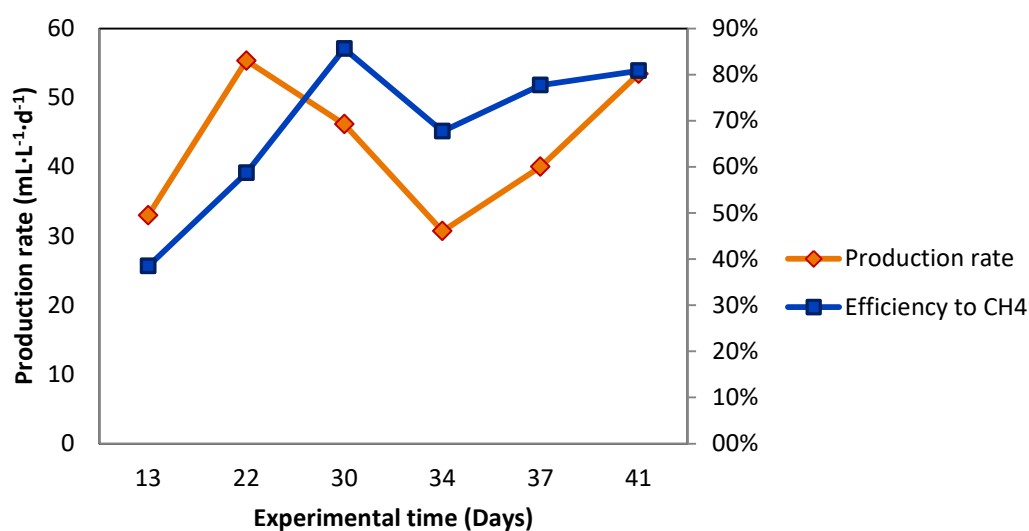


**Figure 8.3:** Methane production and efficiency.

### 8.3.3 Role of Microbial communities involved in the process

SEM images were taken to confirm microbial attachment on the electrode surface. Clean graphite electrode can be seen in figures 8.4 A and B at different magnification, while images corresponding to inoculated electrode are shown in figures 8.4 C, D, E and F. Biofilm coverage is not regular and it is scattered in clumps upon the electrode, showing thick biofilm formation in some regions together with areas in which the graphite surface is not covered.

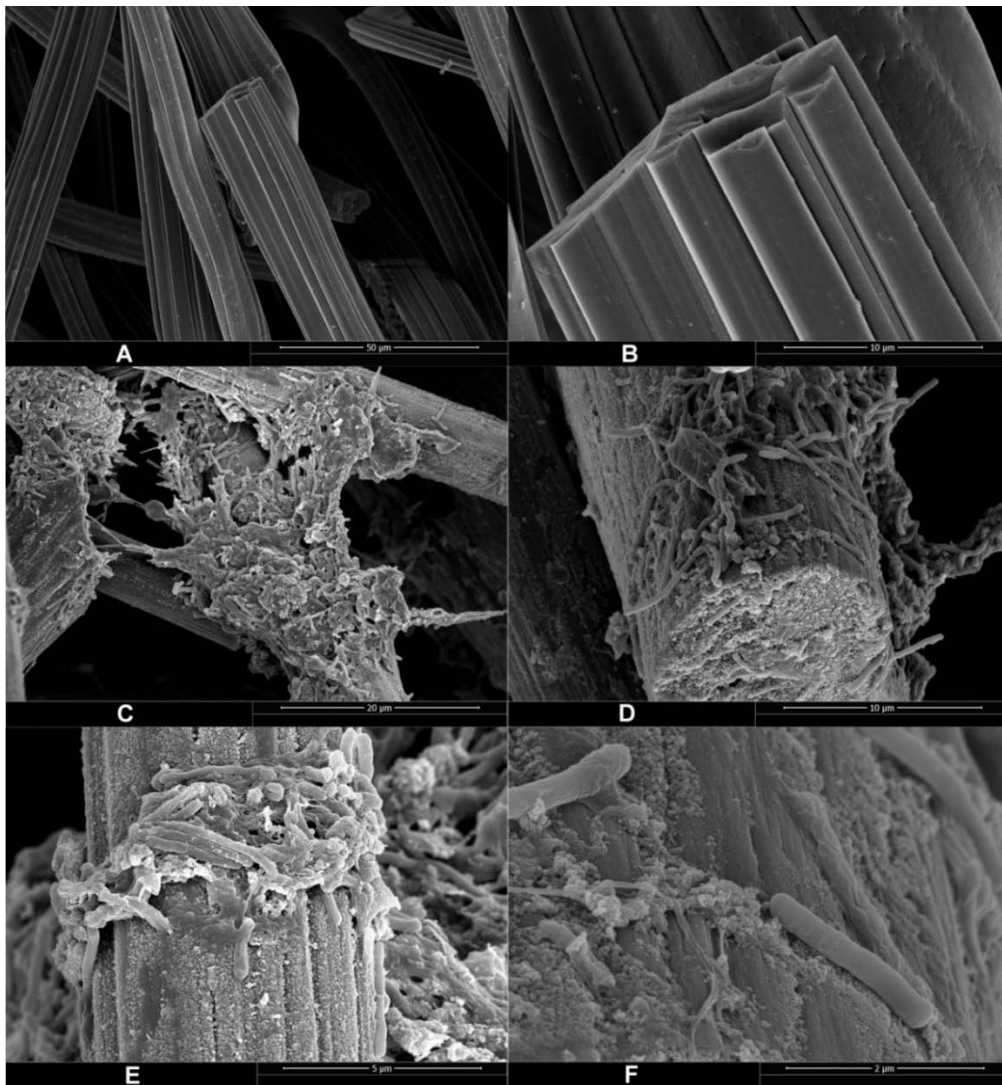


**Figure 8.4:** SEM images belonging to control graphite felt (A and B) and biofilm covered graphite electrode (C, D, E and F) at different magnification.

The microbial community analysis at family level (figure 8.5) shows differences among inoculum, biofilm and supernatant at the end of the experiment. Although main families are common, the relative abundance shows great difference in all the samples. As mentioned above, the inoculum was dominated mainly by homoacetogenic and  $H_2$ -producing bacteria. In contrast, the biofilm was enriched in a greater diversity of families. *Porphyromonadaceae* (a VFA producing family that shows an important increase in the biofilm) together with *Clostridiaceae* (already present in high proportion in the inoculum), could probably be the main responsible for the acetic acid production. *Desulfovibrionaceae* also increases in the biofilm sample and is widely described as electroactive in biocathodes, where they are able to catalyze hydrogen production [15,16]. Another hydrogen producing family found in all the samples in relevant proportion is *Rhodocyclaceae* also described in biocathodes [15]. *Veillonellaceae* family, which is one of the most important electroactive bacteria in bioelectrosynthesis [17] is also present in the biofilm and absent in the supernatant.

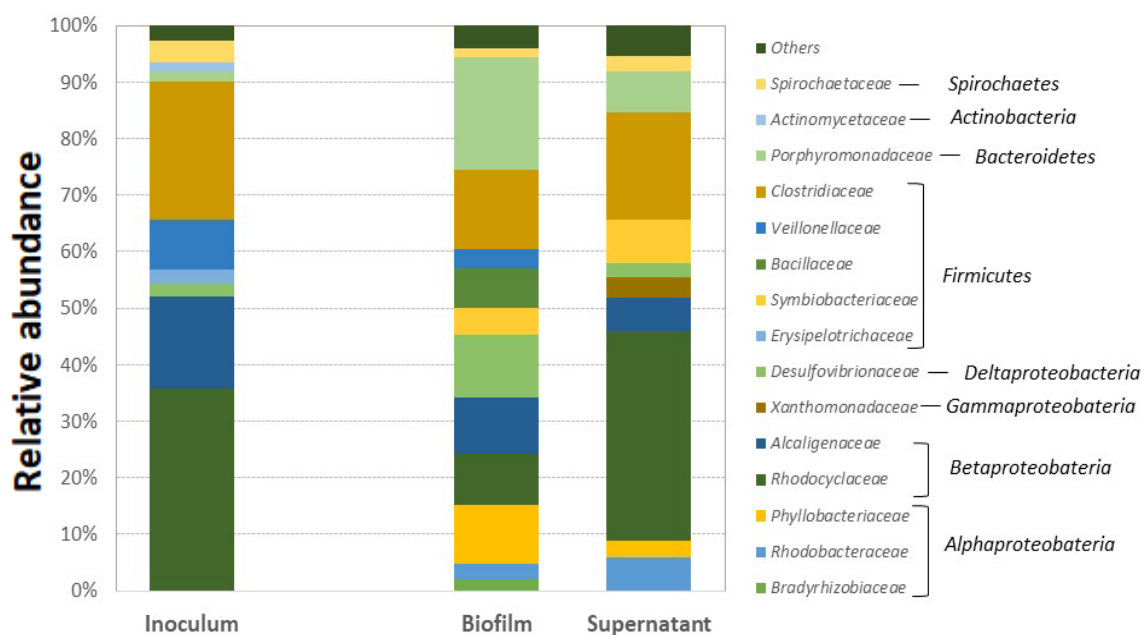


**Figure 8.5:** Inoculum, biofilm and supernatant Eubacterial composition at family level.

Around 90% of the present bacteria are represented by only 13 genera as shown in figure 8.6 for both biofilm and supernatant samples. The biofilm is composed mainly of acetogens, such as *Desulfovibrio*, *Clostridium* or *Sporomusa*, together with hydrogen producers such as *Symbiobacterium* [16] and *Azonexus*. In contrast, and despite

*Clostridium* is also abundant in the supernatant, this sample is composed mainly of hydrogen producers such as *Symbiobacterium* and *Azonexus*, and other fermentative bacteria.

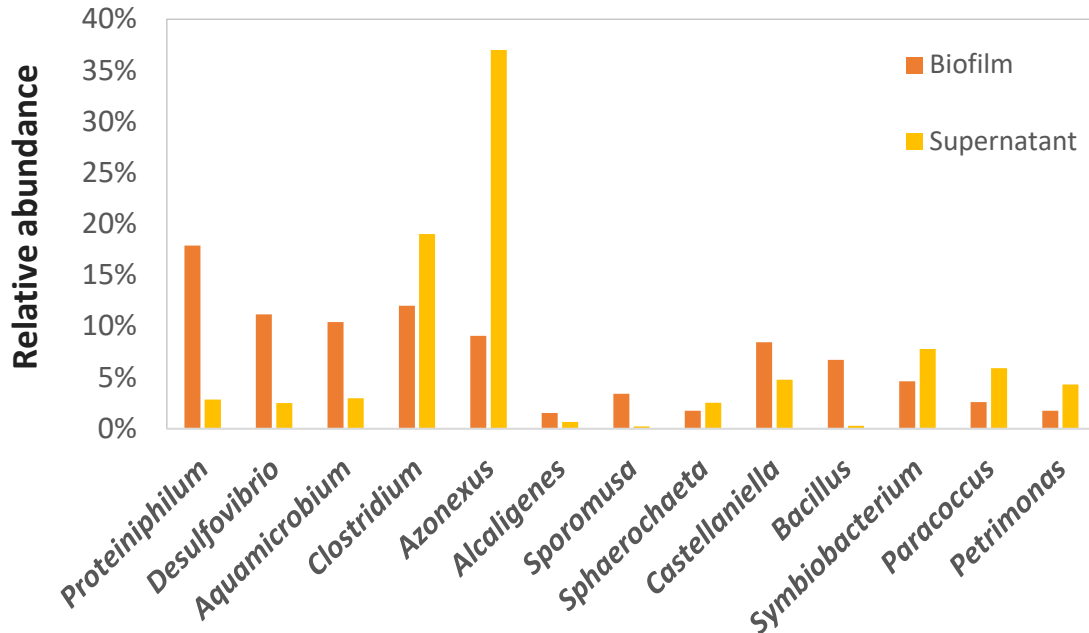


**Figure 8.6:** Biofilm and supernatant microbial community at genera level.

Archaea community analysis is also relevant to understand the behavior of MES systems in which methane is being produced. As shown in Table 8.1, Archaea is represented by almost only one family with one genus. *Methanobacteriaceae* is clearly dominant both in the biofilm and the supernatant, accounting for >99.4%, being represented by the genus *Methanothermobacter*. This is a hydrogenotrophic Archaea that produces methane from CO<sub>2</sub> and hydrogen, which could explain the methane production and hydrogen depletion observed during the experiment. The rest of the Archaeal families found in the MES are mainly acetoclastic, with *Methanosaetaceae* being predominant (See Table 8.1). Interestingly, no Archaea were found in the inoculum and therefore the sample is not shown in table 8.1. This fact, together with the absence of methane during the previous cell history (before power interruption), led us to hypothesize that open-circuit conditions might have favored the growth of residual Archaeal communities up to a dominant position during the unpowered period. Moreover, reconnection conditions with the strong presence of produced hydrogen during the first days also could favor *Methanobacteriaceae*. Nevertheless, further work



is required to identify the mechanism that would trigger this shift in the microbial community.

**Table 8.1:** Archaeal communities in the biofilm and supernatant at family level

Family	Biofilm	Supernatant	Role
<i>Methanobacteriaceae</i>	<b>99.45%</b>	<b>99.41%</b>	
<i>Nitrososphaeraceae</i>	0.00%	0.13%	
<i>Methanoregulaceae</i>	0.08%	0.06%	<b>Hydrogenotrophic</b>
<i>Methanospirillaceae</i>	0.02%	0.02%	
<i>Methanomassiliicoccaceae</i>	0.02%	0.02%	
<i>Methanosaetaceae</i>	0.42%	0.35%	<b>Acetoclastic</b>
<i>Methanosarcinaceae</i>	0.01%	0.01%	

To sum up, the presence of hydrogen and acetic acid producers in the microbial community of the biofilm and supernatant lead us to think that the acetic acid was being produced following two (widely described) pathways simultaneously: (i) direct Bioelectrosynthesis and (ii) hydrogen mediated bioelectrosynthesis [4]. During the first 2 weeks after reconnection, the appearance of hydrogen and acetic acid can be mainly attributed to the presence of microorganisms such as *Symbiobacterium*, *Azonexus*, *Desulfovibrio* and *Sporomusa*. However, after those 2 weeks, a quick hydrogen and acetic acid depletion was observed accompanied by simultaneous rise in methane production. It is important to note that the fact that methane was almost the unique product found from day 20 onwards does not mean necessarily that acetic acid and hydrogen was not being produced any more. It might be possible that Syntrophic Acetate Oxidizers (SAO) such as *Clostridium* [18] could be consuming acetic acid and producing hydrogen. Although hydrogen production from acetate is thermodynamically unfavorable, SAO bacteria are in a syntrophic relationship with the H<sub>2</sub>-consuming methanogens, making the whole process thermodynamically favorable [19]. Therefore, hydrogen and acetic acid might be acting as intermediates in the methane production observed in this study.

A tentative hypothetical diagram is shown in figure 8.7. Moreover, in the case of acetic acid, the presence of SAO promotes acetic acid depletion in the reaction medium (despite having important acetogenic communities in the biofilm and the supernatant), and also favoring hydrogenotrophic methanogens [20].

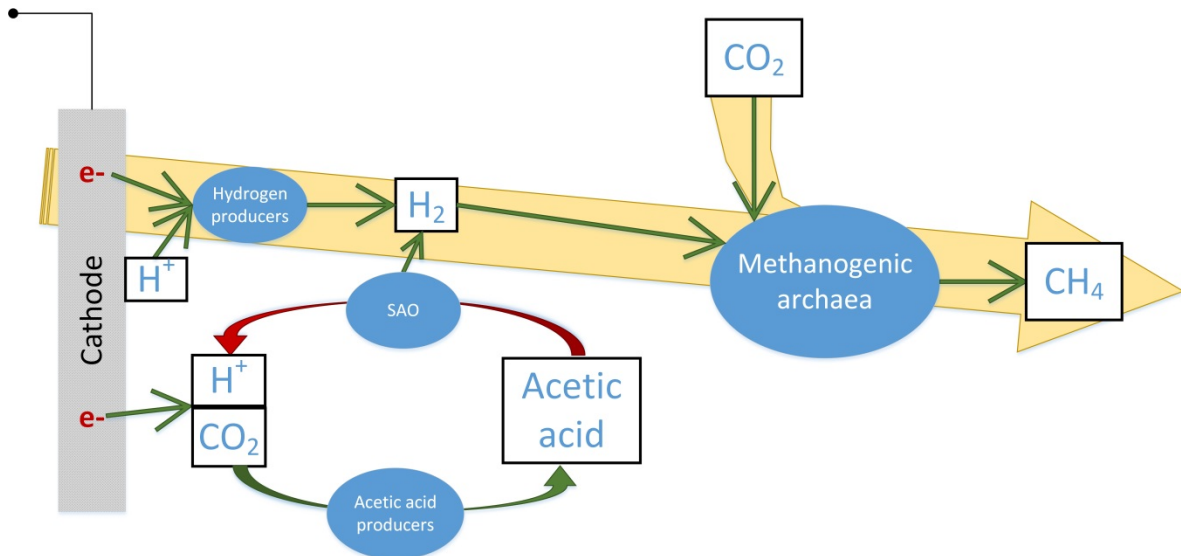


**Figure 8.7:** Tentative hypothetical mechanism. In yellow: main pathway suggested by physico-chemical and microbiological analyses.

#### 8.4. CONCLUSIONS

This study evaluates the influence of a long-term interruption of power supply on a MES system fed with inorganic carbon. After the disturbance, and following a lag period of 2 days, the MES recovered part of its previous acetate and hydrogen producing activity for about 20 days. However, after that, syntrophic acetate oxidation and  $H_2$ -consuming methanogenesis were the dominant pathways utilizing acetic acid and hydrogen as reaction intermediates to produce methane. Methane production rate reached  $55 \text{ mL} \cdot \text{L}^{-1} \cdot \text{d}^{-1}$  with a peak concentration of 87% in the outlet gas. Overall, our results suggest that a prolonged electrical disconnection extensively affects MES behavior, modifying the end-product.

## 8.5. BIBLIOGRAPHY

- [1] Olabi AG. Renewable energy and energy storage systems. *Energy* 2017;136:1–6. doi:10.1016/J.ENERGY.2017.07.054.
- [2] Nevin KP, Woodard TL, Franks AE, Summers ZM, Lovley DR. Microbial electrosynthesis: feeding microbes electricity to convert carbon dioxide and water to multicarbon extracellular organic compounds. *MBio* 2010;1:e00103-10. doi:10.1128/mBio.00103-10.
- [3] Bajracharya S, Srikanth S, Mohanakrishna G, Zacharia R, Strik DP, Pant D. Biotransformation of carbon dioxide in bioelectrochemical systems: State of the art and future prospects. *Journal of Power Sources* 2017;356:256–73. doi:10.1016/j.jpowsour.2017.04.024.
- [4] Rabaey K, Rozendal RA. Microbial electrosynthesis—revisiting the electrical route for microbial production. *Nature Reviews Microbiology* 2010;8:706–16.
- [5] Patil SA, Arends JBA, Vanwonterghem I, Van Meerbergen J, Guo K, Tyson GW, et al. Selective enrichment establishes a stable performing community for microbial electrosynthesis of acetate from CO<sub>2</sub>. *Environmental Science & Technology* 2015;49:8833–43.
- [6] Abate S, Lanzafame P, Perathoner S, Centi G. New Sustainable Model of Biorefineries: Biofactories and Challenges of Integrating Bio- and Solar Refineries. *ChemSusChem* 2015;8:2854–66. doi:10.1002/cssc.201500277.
- [7] Desloover J, Arends JBA, Hennebel T, Rabaey K. Operational and technical considerations for microbial electrosynthesis. *Biochemical Society Transactions* 2012;40:1233 LP-1238.
- [8] Escapa A, Mateos R, Martínez EJ, Blanes J. Microbial electrolysis cells: An emerging technology for wastewater treatment and energy recovery. From laboratory to pilot plant and beyond. *Renewable and Sustainable Energy Reviews* 2016;55:942–56. doi:10.1016/j.rser.2015.11.029.
- [9] Anzola Rojas M del P, Zaiat M, Gonzalez ER, De Wever H, Pant D. Effect of the

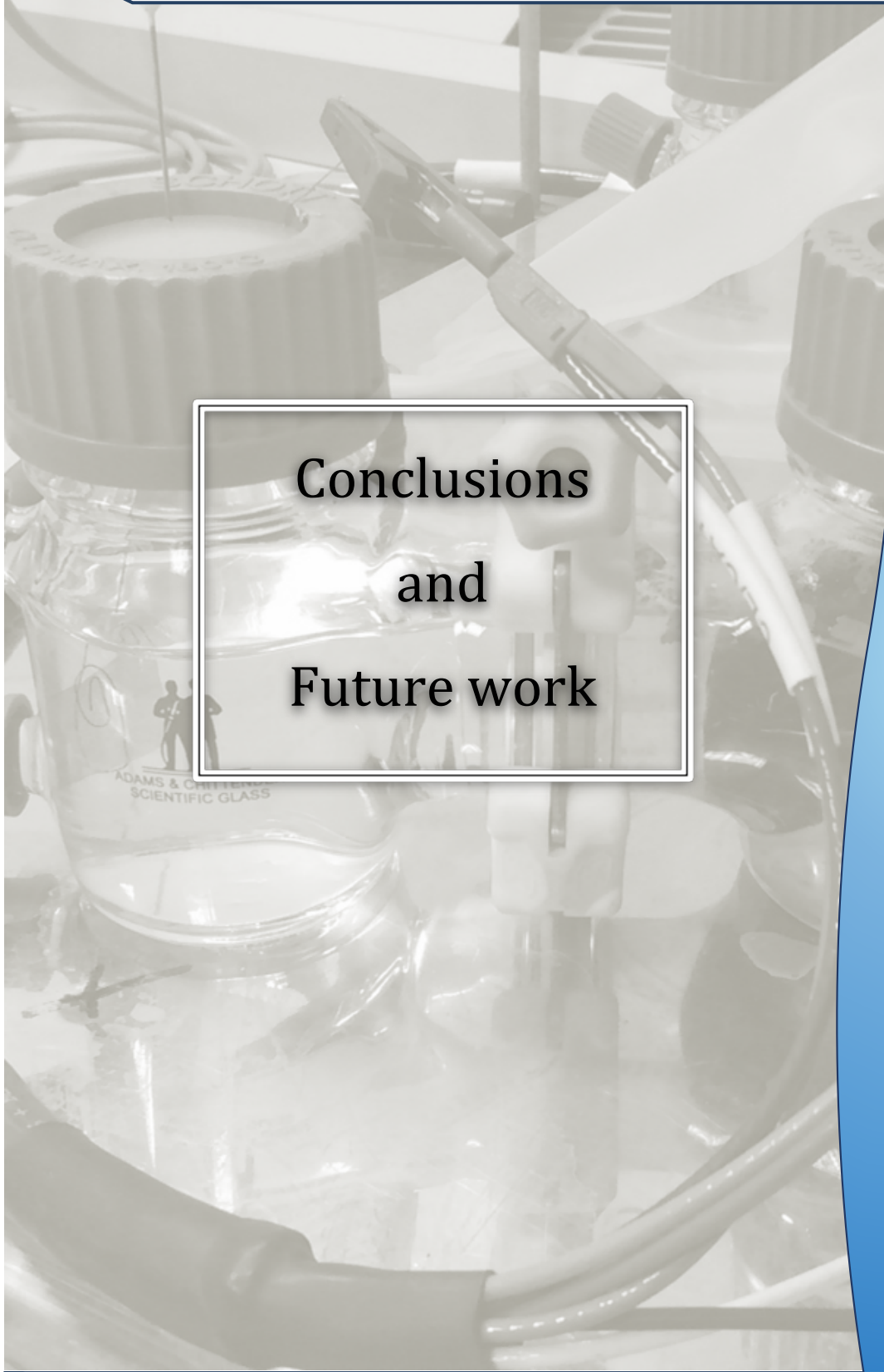
- electric supply interruption on a microbial electrosynthesis system converting inorganic carbon into acetate. *Bioresource Technology* 2018;266:203–10. doi:10.1016/J.BIORTECH.2018.06.074.
- [10] Bajracharya S, Yuliasni R, Vanbroekhoven K, Buisman CJN, Strik DPBTB, Pant D. Long-term operation of microbial electrosynthesis cell reducing CO<sub>2</sub> to multi-carbon chemicals with a mixed culture avoiding methanogenesis. *Bioelectrochemistry* 2017;113:26–34. doi:10.1016/j.bioelechem.2016.09.001.
- [11] Callaway TR, Dowd SE, Wolcott RD, Sun Y, McReynolds JL, Edrington TS, et al. Evaluation of the bacterial diversity in cecal contents of laying hens fed various molting diets by using bacterial tag-encoded FLX amplicon pyrosequencing. *Poultry Science* 2009;88:298–302. doi:10.3382/ps.2008-00222.
- [12] Takai KEN, Horikoshi K. Rapid detection and quantification of members of the archaeal community by quantitative PCR using fluorogenic probes. *Applied and Environmental Microbiology* 2000;66:5066–72.
- [13] Reeder J, Knight R. Rapidly denoising pyrosequencing amplicon reads by exploiting rank-abundance distributions. *Nature Methods* 2010;7:668–9. doi:10.1038/nmeth0910-668b.
- [14] Bajracharya S, ter Heijne A, Dominguez Benetton X, Vanbroekhoven K, Buisman CJN, Strik DPBTB, et al. Carbon dioxide reduction by mixed and pure cultures in microbial electrosynthesis using an assembly of graphite felt and stainless steel as a cathode. *Bioresource Technology* 2015;195:14–24. doi:10.1016/j.biortech.2015.05.081.
- [15] Mateos R, Sotres A, Alonso RM, Escapa A, Morán A. Impact of the start-up process on the microbial communities in biocathodes for electrosynthesis. *Bioelectrochemistry* 2018;121:27–37. doi:10.1016/j.bioelechem.2018.01.002.
- [16] May HD, Evans PJ, LaBelle E V. The bioelectrosynthesis of acetate. *Current Opinion in Biotechnology* 2016;42:225–33. doi:10.1016/j.copbio.2016.09.004.
- [17] Tremblay P-L, Zhang T. Electrifying microbes for the production of chemicals. *Frontiers in Microbiology* 2015;6:201. doi:10.3389/fmicb.2015.00201.
-

- 
- [18] Cai M, Wilkins D, Chen J, Ng S-K, Lu H, Jia Y, et al. Metagenomic Reconstruction of Key Anaerobic Digestion Pathways in Municipal Sludge and Industrial Wastewater Biogas-Producing Systems. *Frontiers in Microbiology* 2016;7:778. doi:10.3389/fmicb.2016.00778.
- [19] Dolfing J. Thermodynamic constraints on syntrophic acetate oxidation. *Applied and Environmental Microbiology* 2014;80:1539–41. doi:10.1128/AEM.03312-13.
- [20] Hattori S. Syntrophic acetate-oxidizing microbes in methanogenic environments. *Microbes and Environments* 2008;23:118–27.



## ***CHAPTER 9***

**Conclusions  
and  
Future work**







## 9.1 CONCLUSIONS

Microbial electrosynthesis (MES) is taking its first steps towards practical application. This thesis is aimed at gaining insight on the nature of some key challenges that need to be overcome before bringing MES out of the laboratory. Specifically, the studies gathered in this document focus on: (i) developing a methodology for a fast characterization of electrode materials, (ii) assessing the impact of different start-up strategies on biocathode formation, (iii) improving substrate availability to microorganisms and (iv) understanding how power fluctuations affect MES performance. The completion of this work has made it possible to achieve these main conclusions:

- A simple, fast and cost-effective methodology for electrode screening for biocathodes is possible by graphically integrating the information obtained from the electroactive area and the fractal dimension.
- The microbial structure that finally develops on the biofilms is highly dependent on the raw community present in the inoculum (because of its diversity and richness), as well as the start-up strategy carried out.
- High biofilm specialization is related to an improvement in acetic acid generation in MES. Moreover, the coupling of acetic acid bacteria with H<sub>2</sub> producing bacteria plays an important role in acetic acid production.
- Continuous recirculation of gas headspace in a CO<sub>2</sub> fed MES improves product generation. This thesis shows how headspace recirculation increases acetate production by up to 44%, while achieving acetate production rates of up to 261 mg HAc·L<sup>-1</sup>·d<sup>-1</sup>. Cathodic efficiencies up to 91% were found in this configuration.
- A group of microorganisms integrated by *Sporomusa*, *Sulfurospirillum*, *Arcobacter*, *Desulfovibrio*, *Pseudomonas* and *Clostridium* form the core microbial community of acetogenic MES reactors.

- MES proved to be resilient to short term power interruptions. Despite a short period where acetate concentration declined, the MES system recovered successfully after the power gap, reaching production rates similar of those observed before the gaps. This resilience could be attributed to *Clostridium*, *Desulfovibrio* and *Sporomusa* that accounted for 93% of the final total community in the cathodic biofilm.
- A biocathode obtained from a well-established acetogenic MES, recovered its electroactive capacity within two days after a prolonged electrical disconnection. However, this long-term power gap extensively affected the end-product generated after reconnection.

Overall, these results allow for some optimism about the future prospects of MES as an environmental technology. Relevant electroactive microorganisms and their interactions have been identified as responsible of product generation, which are commonly shared in all the reactors. Also substrate feed is a key factor and must be carefully provided to the system, as it has an important impact on current density and production rate. Finally, since the origin of biocathodes, MES has been considered as a very unstable and delicate technology; however these reactors show satisfactory resilience against fluctuations in one of the cornerstones of this technology, power supply.

### **9.1bis CONCLUSIONES (CASTELLANO)**

*La electrosíntesis microbiana (MES) está dando sus primeros pasos hacia la aplicación práctica. Esta tesis tiene como objetivo el conocimiento de la naturaleza de algunos factores clave que requieren ser solucionados para llevar la tecnología MES fuera del laboratorio. Específicamente, los estudios que recoge este documento tratan: (i) el desarrollo de una metodología para la caracterización rápida y sencilla de materiales para electrodos, (ii) la evaluación del impacto que tienen las estrategias de arranque sobre la formación del biocátodo, (iii) la mejora de la disponibilidad de sustrato por parte de los microorganismos y (iv) el conocimiento de cómo la fluctuaciones de suministro eléctrico afectan a un reactor MES. La ejecución de este trabajo ha hecho posible llegar a las siguientes conclusiones:*

- 
- *Es posible clasificar materiales para electrodos de una forma rápida, sencilla y efectiva en coste combinando gráficamente la información obtenida del área electroactiva y la dimensión fractal.*
  - *La estructura microbiológica que se desarrolla en los biofilms es muy dependiente de la comunidad original del inóculo (en cuanto a diversidad y riqueza), así como de la estrategia de arranque.*
  - *Una alta especialización del biofilm está relacionada con una mejora de la producción de ácido acético en MES. Además, las bacterias productoras de H<sub>2</sub> y ácido acético en combinación juegan un rol importante en la producción de acético.*
  - *La recirculación continua de la cabecera en una MES alimentada con CO<sub>2</sub> mejora la generación de producto. Esta tesis muestra como la recirculación mejora la productividad de acético hasta un 44% consiguiendo productividades de hasta 261 mg HAc·L<sup>-1</sup>·d<sup>-1</sup>. Se encontraron eficiencias culómbicas de hasta el 91% en esta configuración.*
  - *El grupo de microorganismos compuesto por Sporomusa, Sulfurospirillum, Arcobacter, Desulfovibrio, Pseudomonas y Clostridium forma la comunidad central en reactores MES acetogénicos.*
  - *La tecnología MES ha probado ser robusta frente a cortes breves de corriente. A pesar de un breve periodo en el que la concentración de ácido acético decaía, el sistema se recuperó con éxito tras los cortes, alcanzando productividades similares a las de antes de las interrupciones. Esta robustez se atribuye a Clostridium, Desulfovibrio and Sporomusa que representaban el 93% del biofilm catódico.*
  - *Un biocátodo acetogénico de un sistema MES bien establecido pudo recuperar su actividad electroactiva en dos días tras un periodo largo de desconexión eléctrica. Sin embargo, este corte afectó drásticamente al producto final tras la reconexión.*
-

*En resumen, los resultados permiten cierto optimismo sobre el futuro de la tecnología MES como tecnología medioambiental. Se han identificado microorganismos electroactivos relevantes y sus interacciones como responsables de la generación de producto, y que son comunes en todos los reactores. También la alimentación de sustrato es un factor clave y debe ser suministrado al sistema correctamente ya que tiene un impacto importante en la densidad de corriente y la productividad. Finalmente, desde el origen de los biocátodos han sido considerados una tecnología muy inestable y delicada, sin embargo estos reactores muestran una robustez satisfactoria frente a fluctuaciones en un punto clave como es el suministro de energía.*

## **9.2 FUTURE WORK**

MES systems represent a promising technology that are currently gathering merits and milestones to leave the laboratory bench and start to be applied in practice. The objective of this thesis was to contribute to it and, according to the obtained results, we all should be encouraged to think about MES as an applied technology rather than fundamental science. However, still a long journey must be covered as many obstacles remain unresolved.

Coupling MES with renewable energy could generate a profitable symbiosis, as MES could make use of electricity surpluses serving as an energy storage system in the form of chemicals. In this scenario, MES systems must be capable to endure the power interruptions derived from the unstable and unpredictable nature of renewable power sources. This thesis has evaluated the effects of a fluctuating power supply on MES systems, however only scheduled fluctuations have been tested. Coupling MES to an actual unpredictable renewable energy source will give valuable information for practical application.

The typical water-splitting chemical anode on MES systems is one of those issues that threaten real application, as they promote high cell voltages leading to high energy consumption in the system. Replacing them with bioanodes would hypothetically help to: (i) lower cell potential (also energy consumption) by a factor of 3, (ii) link MES with waste treatment in one single reactor and (iii) get rid of expensive noble metal counter electrodes. However, coupling a bioanode and a biocathode generates system control problems that must be faced in the near future.

---

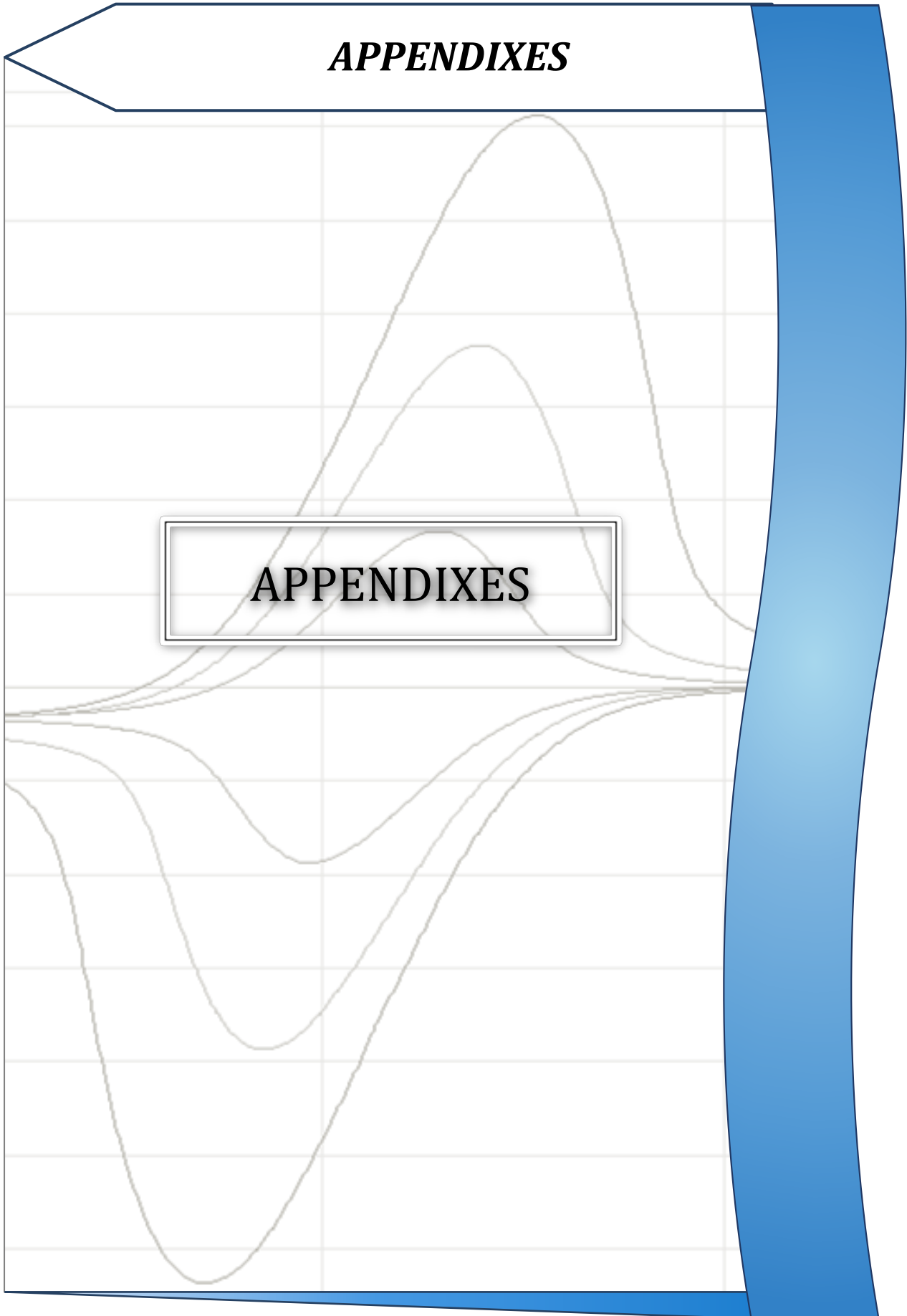
Another key factor for future research should be the use of real CO<sub>2</sub> rich exhaust gases as feed on MES systems. Here, main challenges are related to the biofilm survivability as biocathodes are usually very sensitive to impurities or oxygen content that may be present in the exhaust gas.

Microbiology is a fundamental factor on MES systems, and a wide range of microorganisms have been identified playing a key role in the overall performance. However there are uncertainties around how these microorganisms actually interact with the electrode, the media and among themselves. Moreover, and from my point of view, metabolic engineering of these microorganisms could probably boost MES production.



***APPENDIXES***

**APPENDIXES**







## APPENDIX I

### Chapter 4: Supporting information

#### S4.1. Ohmic drop determination

The current registered in the set of cyclic voltammetry experiments suggest the necessity to carry out ohmic drop compensation in order to obtain voltammograms suitable for data analysis [1].

The ohmic drop was determined using two different analytical techniques, current interrupt and electrochemical impedance spectroscopy, the final value used to compensate the cyclic voltammetry was the 85% of the average between both results. Mean value of 10 repetitions per technique.

The current interrupt technique consists in the measurement of ohmic drop by the application of Ohm's law once a known multi-step current signal is applied. The potential is measured immediately before and after the current has been interrupted, then the difference in the observed potentials is the ohmic drop. The ohmic drop divided by the known current,  $I$ , before the interrupt gives the ohmic resistance [2].

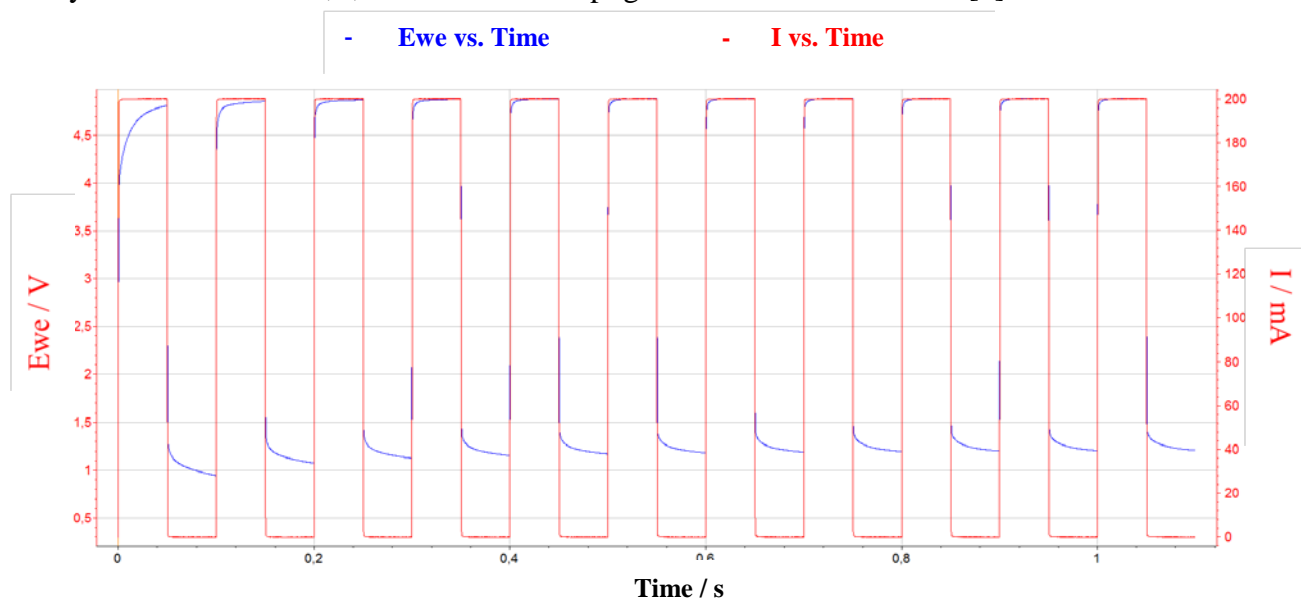


**Figure S4.1:** Example of current interrupt experiment performed in this study. (Ewe: Working Electrode Potential; I: Current)

Ohmic drop can also be determined by electrochemical impedance spectroscopy (EIS). This technique measures the impedance of a system over a range of frequencies by applying a variable frequency sinusoidal signal, superimposed to a fixed applied potential. In the Nyquist plot, the intersection of the impedance data with the real part of the axis at the high frequency end gives the ohmic resistance [2,3]. In our experimental procedure, the selected parameters are the following: Working electrode potential 0V vs. open circuit potential; Perturbation amplitude 20mV (root mean square value); Frequency range from 200kHz to 100mHz; 6 point per logarithmic decade; The first value of the EIS at high frequency is rejected to estimate EIS spectrum [3].

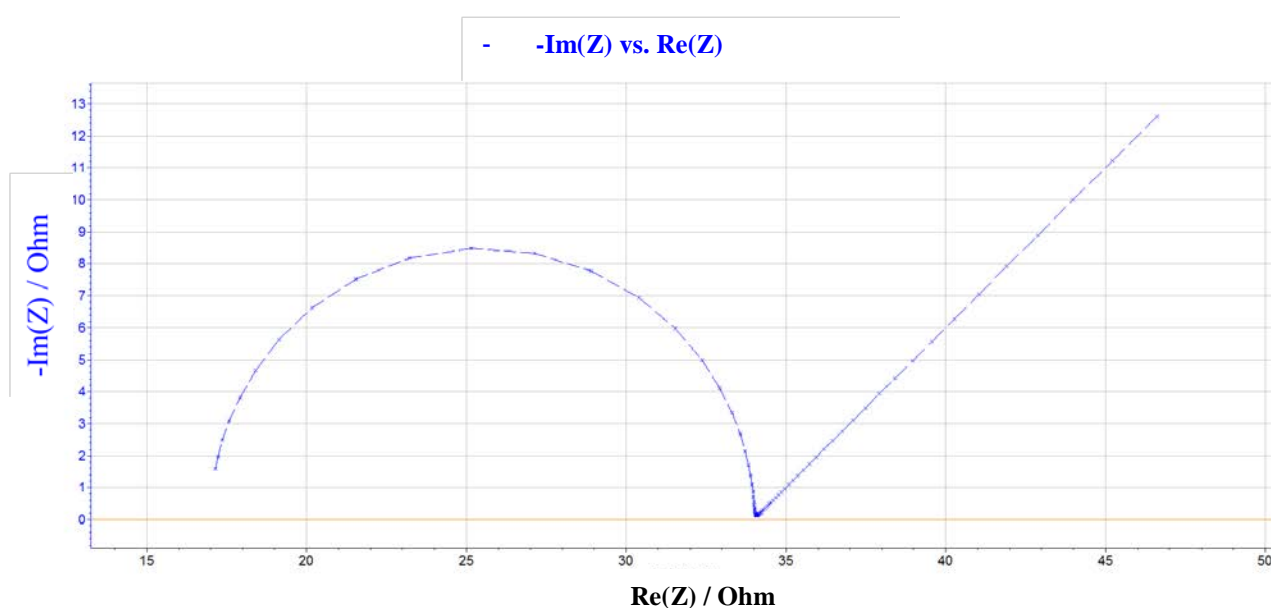


**Figure S4.2:** Model of a cell EIS experiment. (Z: Impedance)

## S4.2. Cyclic voltammetry experiments

Cyclic voltammetry experiments were performed in scan rates of 1, 2.5, 5, 10, 20, 50, 100 and 200 mVs<sup>-1</sup>. The highest scan rates (>50 mVs<sup>-1</sup>) showed a significant peak separation, which indicates process irreversibility due to sluggish electron transfer. The electrolyte was deaerated to avoid oxygen reactions artifacts in the CV experiments. Ohmic drop was compensated for each test. Three examples of subsequent voltammeteries on 1 cm<sup>2</sup> thick felt electrodes are shown below (Figure S4.3).

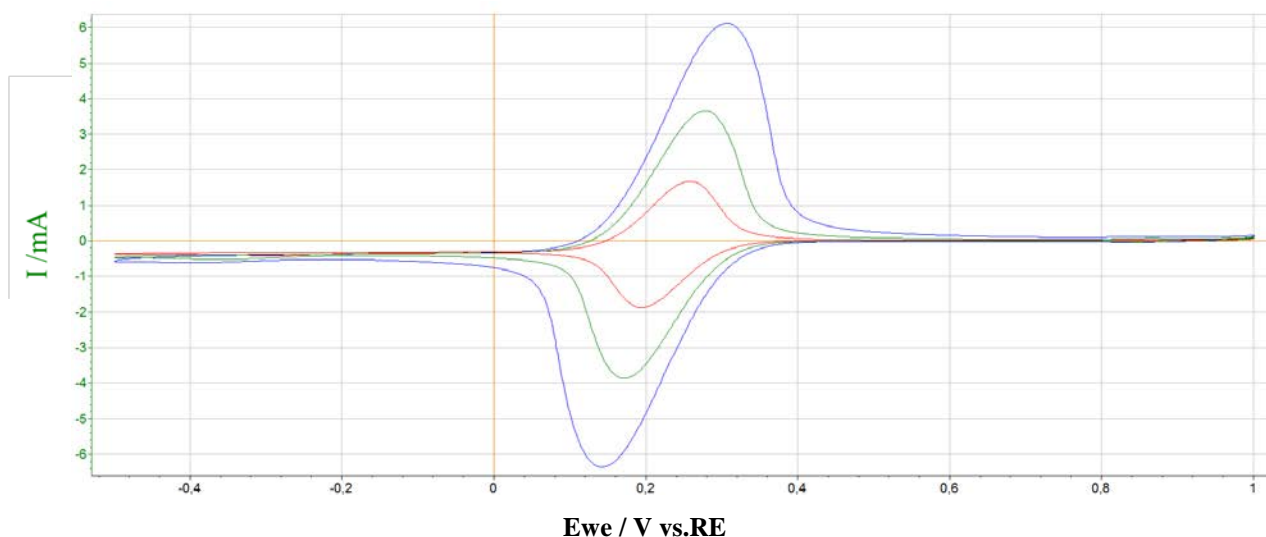


**Figure S4.3:** Example of voltammetries performed on 1 cm<sup>2</sup> thick felt

### S4.3 Projected brush electrode area determination

The projected area of the brushes was calculated as a coverage percentage in order to compare the obtained electroactive area per apparent area (Table 4.3 in the paper). In the case of these electrodes the procedure consists in taking a digital image of the electrode over a white background. The image file is introduced in R data analysis software, where it is processed from RGB model. The black pixels percentage is then distinguished from the background using a threshold value for each channel. The coverage area is inferred from the percentage of black pixels obtained.



**Figure S4.4:** Original brush image (a) and digitally treated brush image (b)

### S4.4. References

1. Zoski, C. G. C. *Handbook of Electrochemistry*; Elsevier, 2007; Vol. 5.

2. Cooper, K. R.; Smith, M. Electrical test methods for on-line fuel cell ohmic resistance measurement. *Journal of Power Sources* **2006**, *160*, 1088–1095.

3. Orazem, M. E.; Tribollet, B. *Electrochemical impedance spectroscopy*; John Wiley & Sons, 2011; Vol. 48.

## APPENDIX II

### Chapter 5: Supporting information

#### S5.1. Polymerase chain reaction (PCR)

After DNA extraction, a PCR was carried out with all samples. For amplification, 2  $\mu$ l of each DNA was used and a reaction was carried out in 50  $\mu$ l containing 0.4 mM of fusion primers, 0.1 mM of dNTPs, 2.5 U of Taq ADN polymerase (Qiagen), and 5  $\mu$ l of reaction buffer (Qiagen). The PCR amplification operated with the following protocol: 30 s at 95 °C, followed by 30 cycles at 94 °C for 30 s, annealing at 55 °C for 30 s, extension at 72 °C for 10 min; and the PCR was carried out in a PCR thermocycler GeneAmp PCRsystem 9700 (Applied Biosystems).

#### S5.2. MECs start-up behaviour

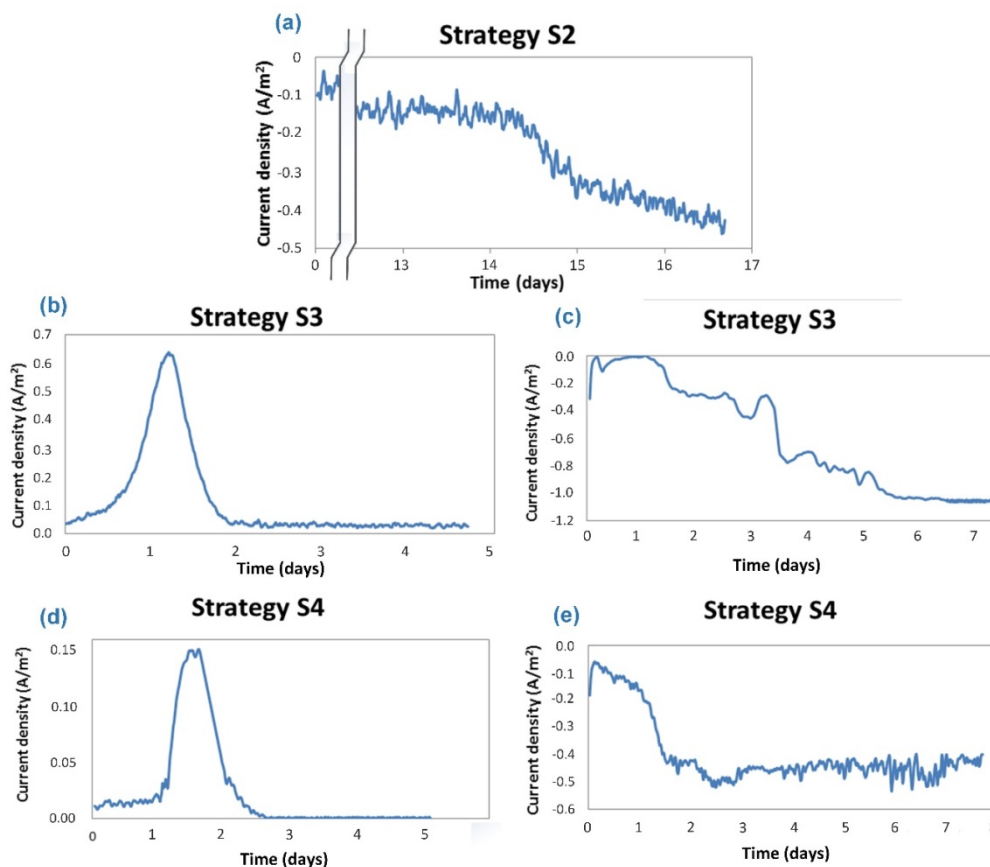


**Figure S5.1.** Current profiles of MECs start-up behaviour. (a) Cathodic start-up for strategy S2; (b) Anodic start-up for strategy S3; (c) Cathodic start-up for strategy S3 after inversion; (d) Anodic start-up for strategy S4; and (e) Cathodic start-up for strategy S4 after inversion.

We assume that the start-up process begins when there is a noticeable change in the slope of the current profiles. As we can see in figure S5.1 (a), strategy S2 took around 2 weeks begin to produce bioelectrochemical current showing a typical growing pattern for biocathodes at day 14. A quicker response was observed when the biocathodes were started-up inverting the potential from a running bioanode (strategies S3 and S4, figure S5.1 (b)-(e)). For both strategies S3 and S4, the bioanodes started to produce a positive current in around 24 hours (Figure S5.2 (b) and (d)). When inverted into biocathodes they required 2-4 days to produce cathodic current.

### S5.3. Archaeal community structure

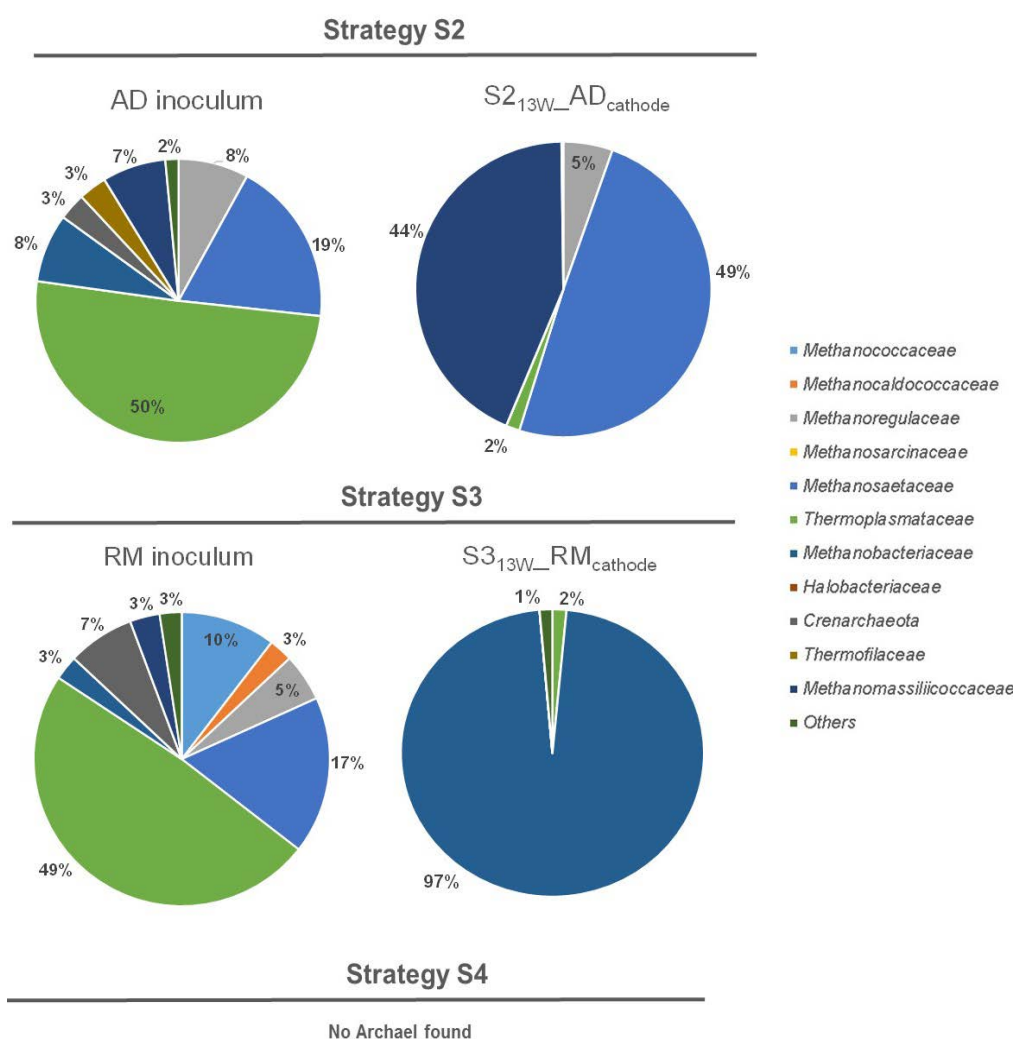


**Figure S5.2.** Taxonomic classification of high throughput sequencing at family level.

## APPENDIX III

## Chapter 6: Supplementary Information

## S6.1. MES1 and MES2 electrical and production behaviour

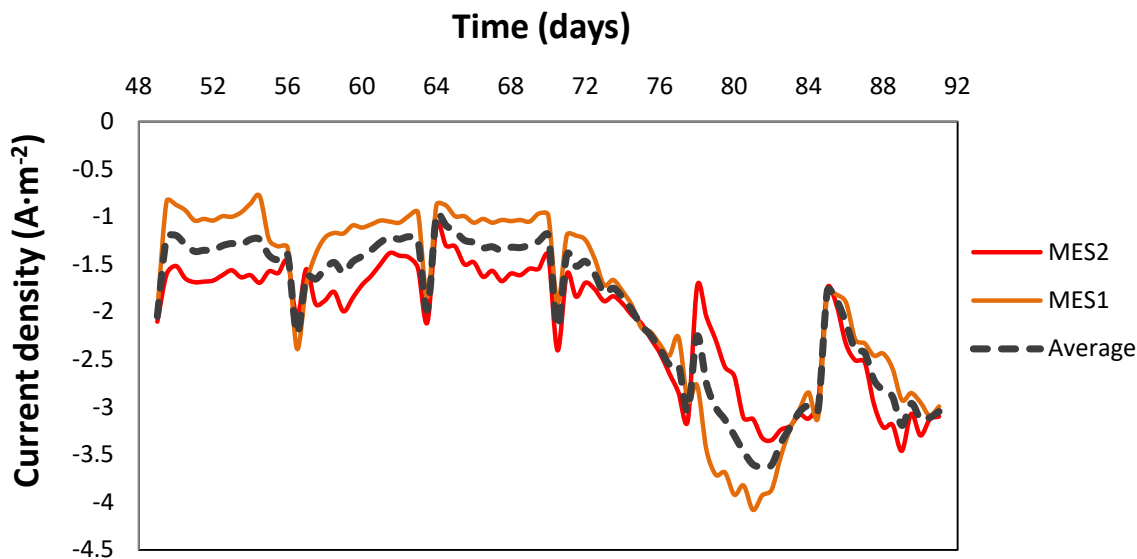
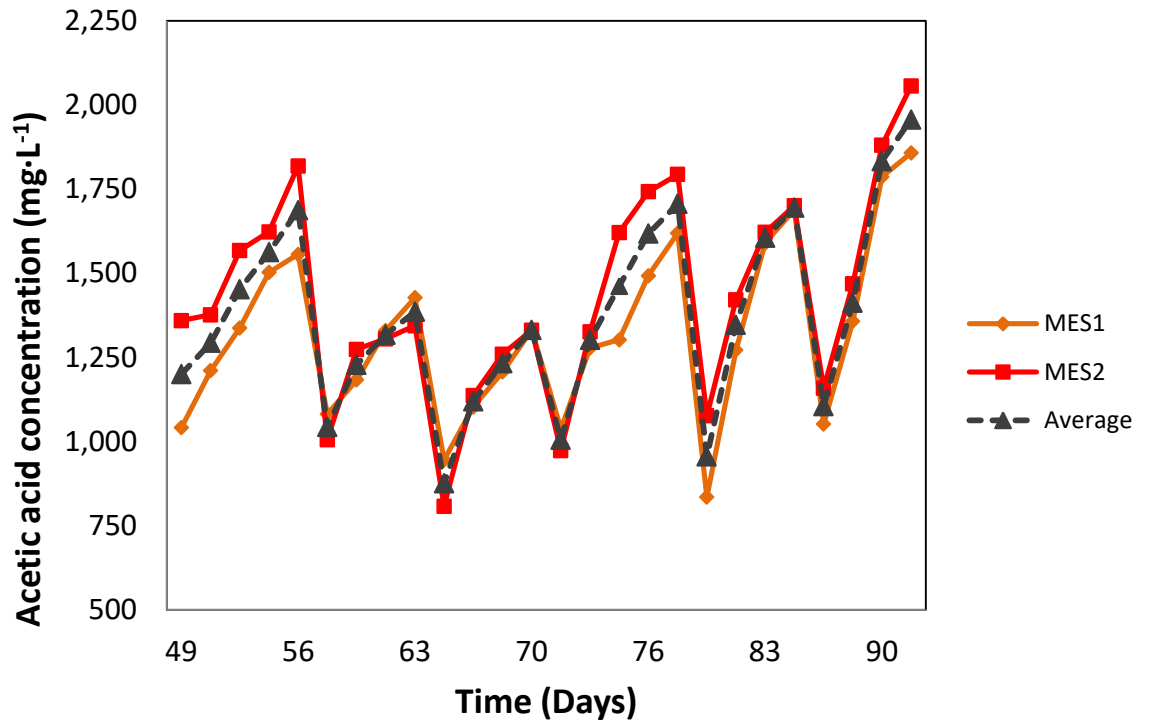


Figure S6.1. Current consumption for reactors MES1, MES2 and their average

Figure S6.1 shows current consumption in both replicate reactors and their average profile. It can be noticed that typical differences from mixed culture biological reactors are found, however figure S6.1 shows very similar trends in both reactors.



**Figure S6.2.** Acetic acid production for reactors MES1, MES2 and their average

Figure S6.2 shows acetic acid production for reactors MES1 and MES2 as well as their average values. These data show a very similar trend between both replicates which almost overlays in certain periods. Small noticeable differences are typical for mixed culture reactors.

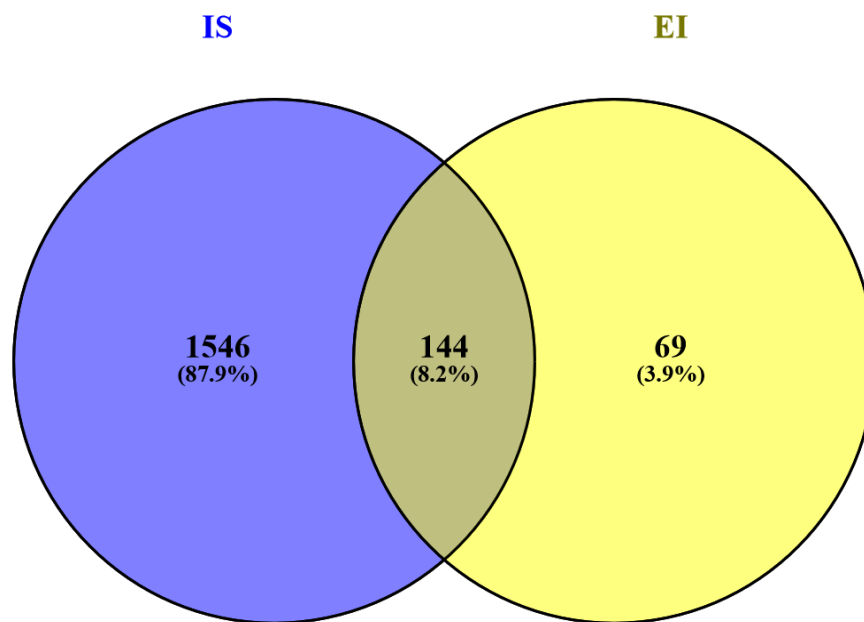


## S6.2. Microbial community analysis

**Table S6.1:** Number of sequences and total observed OTUs for IS and EI samples.

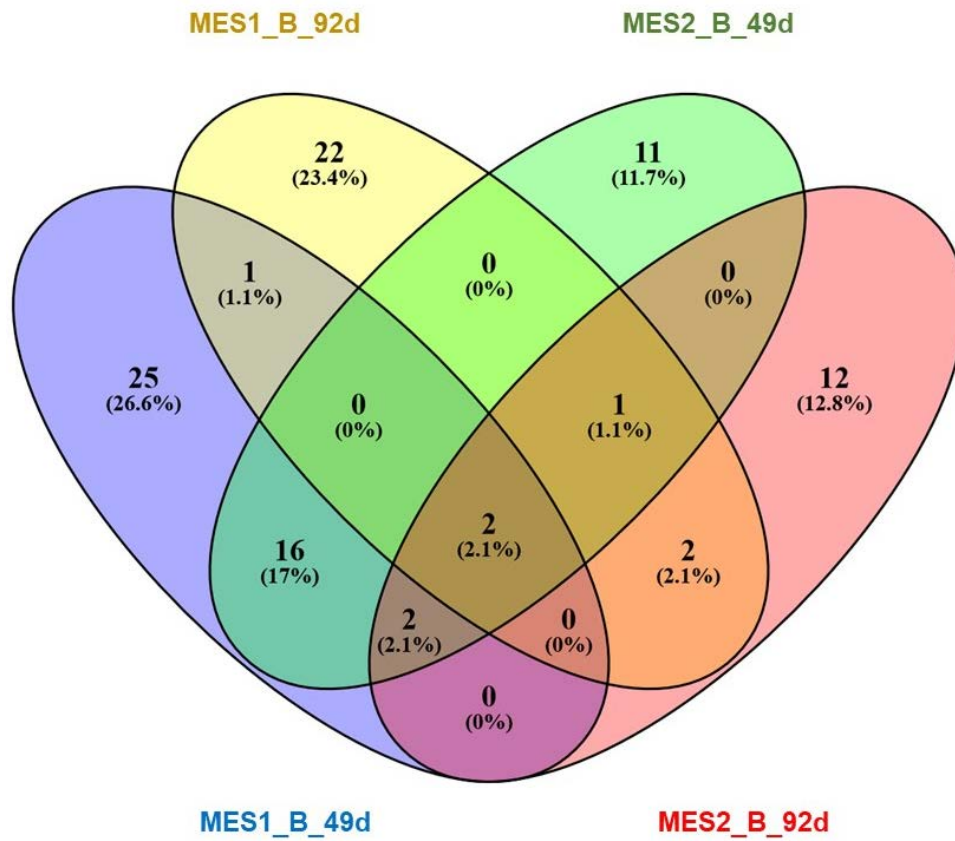
Sample	Number of sequences	OTUs observed
IS	67168	1690
EI	24387	213

Table S6.1 shows how the enrichment makes the microbial population more specific in terms of number of sequences and total observed OTUs.



**Figure S6.3.** Overlap bacterial communities from the initial sludge (IS) and for the enrichment inoculum (EI) based on the taxonomic identities of the shared OTUs.

Figure S6.3 shows which proportion of microorganisms are common or not in the IS and EI, and the number of OTUs that correspond to these proportions.



**Figure S6.4.** Overlap of the four biofilms communities and the taxonomic identities of the shared OTUs.

Figure S6.4 shows which microorganisms' proportion is common in all supernatant samples over 0.10% of the relative abundance, and the number of OTUs that correspond to these proportions.